ISSN 0257-3660

ACTA MINERALOGICA PAKISTANICA

Volume 1

1985

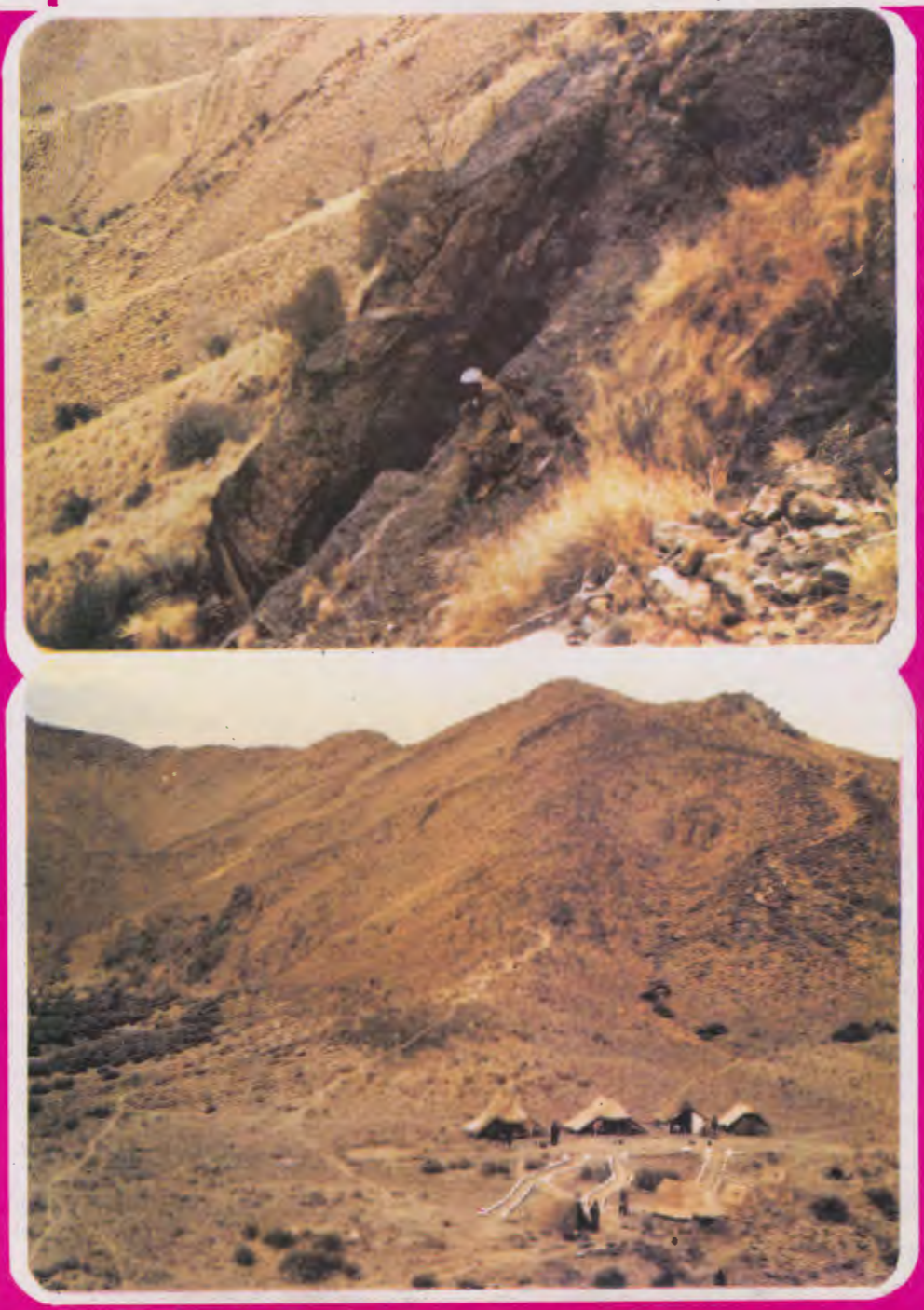

NATIONAL CENTRE OF EXCELLENCE IN MINERALOGY
(UNIVERSITY OF BALUCHISTAN), QUETTA, PAKISTAN

ACTA MINERALOGICA PAKISTANICA

VOLUME 1-1985

EDITOR: ZULFIQAR AHMED

REFEREES: *ROBERT A. HOWIE*
ANTHONY HALL
DUANE M. MOORE
GEORGE R. McCORMICK
R.G. DAVIES
AFTAB AHMAD BUTT

ISSN-0257-3660

PRICE

PAKISTANI RUPEES 50.00 OR U.S. $ 6.00 OR U.K. £ 4.00

(including airmail postage and handling charges)

Published in December each year.

Printed at KASHMIR OFFSET PRESS, SIRKI ROAD, QUETTA.

ACTA MINERALOGICA PAKISTANICA VOLUME 1, 1985.

CONTENTS

ON THE COVER : NEW VISITS OLD

Below : In December, 1985, the camping site of a geological field party was not far from the old time smelting plant located by black pieces of slag lying on the ground; and seen near the centre of this photograph as a small and round, black patch crossed by a footpath.

Above : A view of dark gossan covering the Jurassic age "Zidi Formation" limestone beds in Surmai area, near the Gunga barite deposit,Khazdar District, Baluchistan. Recent man sits at the entrance to a large mining cave dug in prehistoric times, parallel to bedding to exploit the now "newly found" zinc-lead bearing sulphide ore. Many dioritic pieces found at the locality are considered old time mining tools, as there is no diorite outcrop in the region.

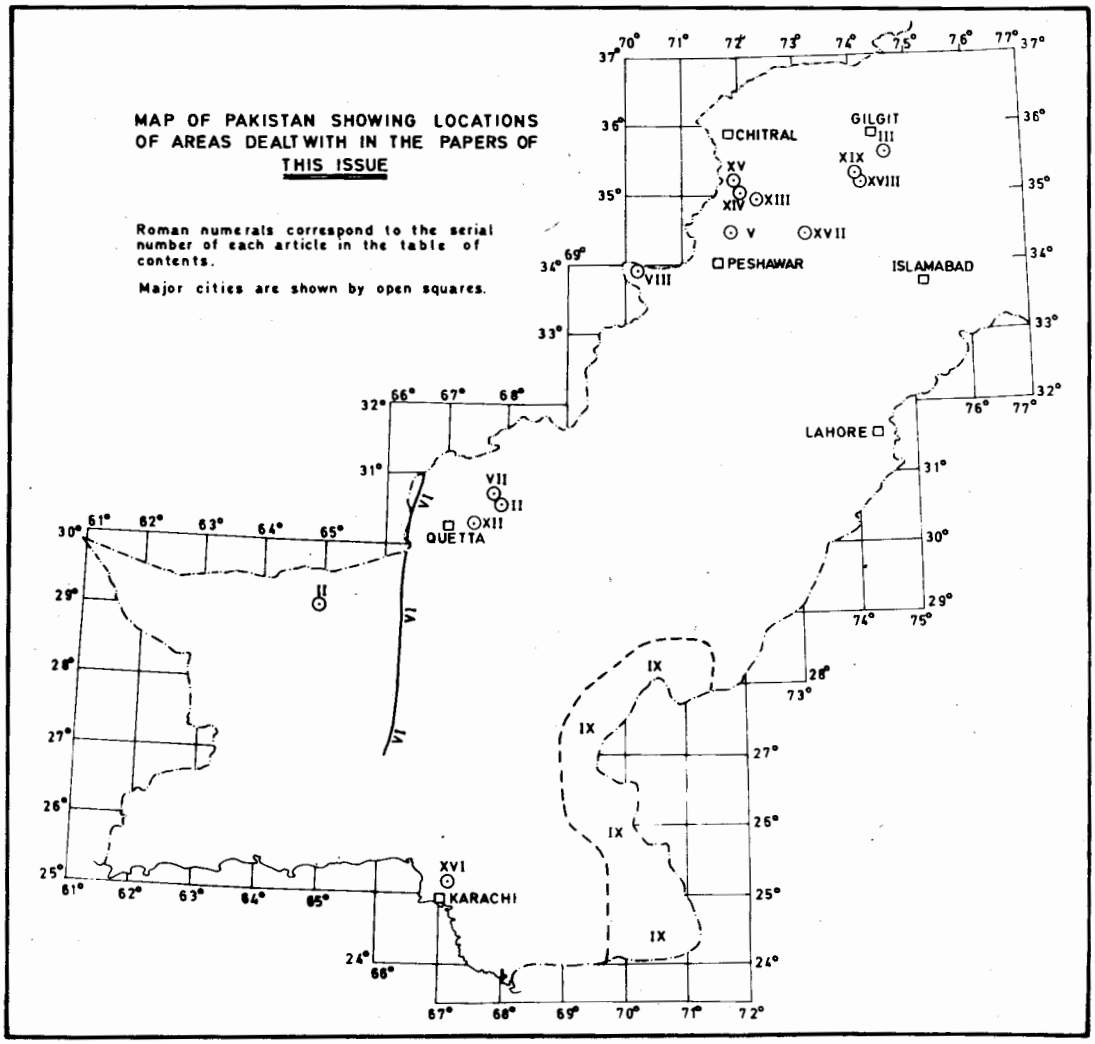
MAP OF PAKISTAN SHOWING LOCATIONS OF AREAS DEALT WITH IN THE PAPERS OF THIS ISSUE
Roman numerals correspond to the serial number of each article in the table of contents.
Major cities are shown by open squares.
CHITRAL
GILGIT
PESHAWAR
ISLAMABAD
LAHORE
QUETTA
KARACHI
III
XIX
XVIII
XV
XIV
XIII
V
XVII
VIII
VII
II
XII
VI
IV
IX
XVI
37°
36°
35°
34°
33°
32°
31°
30°
29°
28°
27°
26°
25°
24°
60°
61°
62°
63°
64°
65°
66°
67°
68°
69°
70°
71°
72°
73°
74°
75°
76°
77°

ACTA MINERALOGICA PAKISTANICA
VOLUME 1 (1985) pp. 2-9

PRELIMINARY STUDY OF THE VOLCANIC ROCKS OF THE SOUTH TETHYAN SUTURE IN BALUCHISTAN, PAKISTAN.

GEORGE R. McCORMICK

Centre of Excellence in Mineralogy, University of Bluchistan, Quetta, Pakistan.

Present Address: **Department of Geology, University of Iowa, Iowa city, Iowa 52242, U.S.A.**

Abstract: The South Tethyan suture zone in Baluchistan has two distinct tectonic segments. The north-south portion along the "Axial Belt" from Karachi to the Pamirs has primarily a strike-slip motion. Volcanic agglomerates, flows, and breccia in the Parh Formation of Maastrichtian age on which ophiolites are obducted are reported to be basaltic. Preliminary microprobe analyses of pyroxenes from agglomerates and flows indicate the volcanic rocks are "within plate alkali basalts".

It is proposed that this zone which is a landward extension of the Owen Fracture Zone is an old structural element, perhaps early Mesozoic, and was the site of oceanic islands during the Maastrichtian which were perhaps caused by motion of the Indian plate over a "hot spot" as has been suggested for the Ninetyeast Ridge to the east of India. Ophiolites were obducted onto the volcanic deposits on the westward twisting Indian plate in the Paleocene from fractures or perhaps incipient subduction zones near the volcanic islands.

The suture zone west of the Axial Belt in the Makran is the only remaining active subduction zone of the South Tethys that has not been involved in continent – continent collision. It has been proposed that the northern Makran represents an island arc system on the upper plate of the Afghan block accreted to the Eurasian plate. The Chagai Hills have been interpreted as the andesitic volcanic arc. It is now proposed that the Ras Koh range represents a collision mass of oceanic basaltic islands originally south of the Ras Koh with the outer arc of the island arc sequence and perhaps even with the volcanic arc itself.

INTRODUCTION

This paper is a preliminary report on observations made on a 6-week reconnaissance of the India-Eurasia suture zone and Makran region of Baluchistan (Pakistan) and on preliminary microprobe data on pyroxenes recently obtained from samples collected during that reconnaissance. This work was carried out in preparation for a proposed detailed three year investigation of the nature of the south Tethys margin in Baluchistan (Pakistan). A model is here proposed on the basis of the preliminary work but it is to be understood that it represents thoughts of the first approximation and is subject to much refinement and debate.

The nature of the suture line parallel to the trace of the Chaman-(Ornach-Nal) fault zone is distinctly different to that in the Makran region west of the Ornach-Nal fault. For purposes of discussion I will divide Baluchistan into an Eastern section to include the area between the Chaman-(Ornach-Nal) fault zone and the Sulaiman-Kirthar ranges to the east and a western section which will include the Makran region west of the Chaman-(Ornach-Nal) fault. (fig. 1).

Eastern Baluchistan *GEORGE R. McCORMICK*

The easternmost region of Baluchistan contains the Kirthar and Sulaiman ranges which are composed of Triassic, Jurassic, and Cretaceous sediments which have been folded and thrust onto the Indian plate by its collision with the Eurasian plate. The uppermost Cretaceous (Maastrichtian) on the westernmost flank of these ranges is the Parh Formation (Bakr, 1963; Kazmi, 1982). The Parh Formation is not continuous along these ranges. The majority of Parh sediments are limestones, however, marls and shales are locally abdundant. Bakr (1963), Kazmi (1982), and the Hunting Survey Corp. (1960) have described the Parh formation as containing volcanic ash, flows, tuff, breccia, and agglomerate in addition to the sediments but at a scale too small to be mapped. Kazmi (1979) described a volcanic sequence near Ziarat which he interprets as a part of a remnant island arc. He described the volcanic units as occurring in the uppermost Cretaceous unit which he named the Bibai Formation and which immediately overlies the Parh Formation.

De Jong (1979) has described a series of agglomerates in the Bela region which lie immediately on top of the Parh formation; he has named these the Porali agglomerates. The Porali agglomerates and Bibai formation are time equivalents and, indeed, they may also have originated in the same tectonic framework. Published data on mineralogy and chemistry of these volcanic units is negligible other than reference by Kazmi (1979) and the Hunting Survey Corp. (1960) that the flows are basaltic and the pyroxene phenocrysts in the flows and agglomerates are titaniferous augite.

During April of 1984, I spent several weeks with Mr. Wazir Khan of the Geological Survey of Pakistan making a reconnaissance survey of the Parh formation and associated volcanics from near Kach northwards past Chinjun, Bagh, and onto Qila Saifullah. I found excellent sections of pillow lavas, flows, agglomerates, ash, and tuff interbedded in the limestones and marls of the Parh formation. I found xenoliths of Parh limestone in agglomerates and fragments of lava and agglomerates in limestones. There is little doube that the volcanics were deposited simultaneously and/or alternately with limestone and marls.

Preliminary petrography of the volcanic rocks indicates that they are basaltic and that the augites are titaniferous. The matrix of the agglomerates and flows for the most part is highly altered, however, good unaltered phenocrysts of clinopyroxene are usually present. I performed electron microprobe analyses on 5 pyroxenes from one flow (sample GG1) and 5 pyroxenes from an adjacent agglomerate (sample GG3, table 1) both obtained at a large water gap in the Parh formation at Gwanda Gwazi which is located 10 miles southwest of Chinjun which is on the southern flank of the Jang Tor Ghar and Supplai Tor Ghar ophiolite massifs which are immediately southeast of Muslimbagh which is northeast of Quetta. These pyroxenes (table 1) plot (fig. 2) within the field of "within plate alkali basalt" on the MnO-Na_2O-TiO_2 pyroxene-diagram of Nisbet and Pearce (1977).

The band of volcanic units within the Parh formation seems to widen and narrow indicating centres of volcanism at about 30-40 kms separation. Immediately west of the Parh-volcanic sequences are small to large blocks of ophiolite always in tectonic contact. The major units are the Bela ophiolite that begins near Karachi and extends north to about Kalat and the Zhob Valley ophiolite bodies extending from near Kach north of Quetta northward along the valley to Waziristan (Fig. 1). It is important to note that the largest ophiolite masses in the north (Muslimbagh and Waziristan) are present where the fold ranges make a southwest lobe from the Sulaiman reentrant near Quetta to Waziristan (Fig. 1).

Abbas & Ahmad (1979) describe slices of metamorphic rocks beneath the north end of the Jangtor massif and along the west side of the Saplaitor massif at Muslimbagh. He describes the units as grading from amphibolite grade at

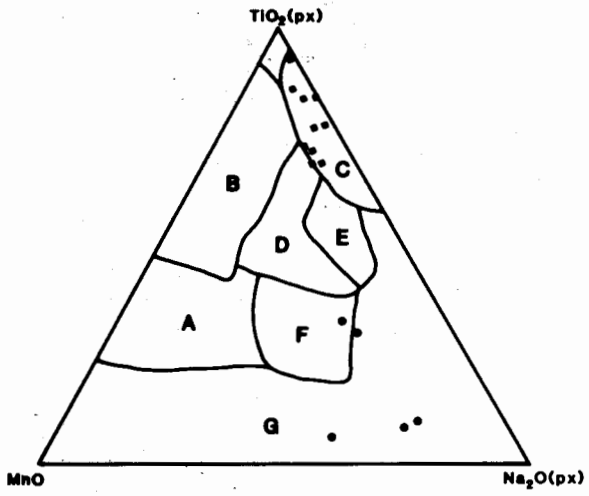

Fig. 2: Clinopyroxene compositon and tectonic setting (after Nisbet and Pearce, 1977). Key to fields: A = VAB, B = OFB, C = WPA, D = All, E = VAB+WPT+WPA, F = VAB+WPA, G = WPA. Key to magma types: OFB = ocean floor basalt, VAB = volcanic arc basalt, WPT = within plate tholeiite, WPA = within plate alkali.

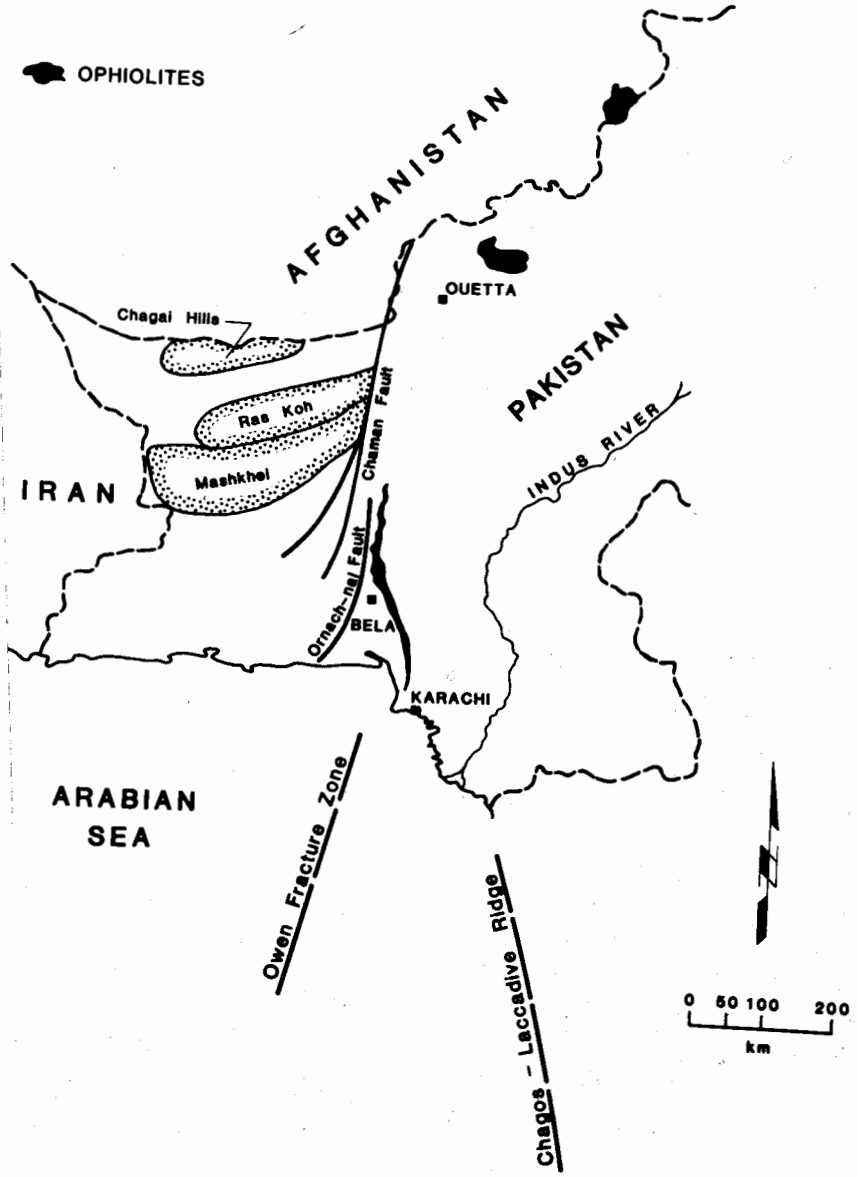

Fig. 1: Map of southern Pakistan showing location of major geographic and structural features and ophiolite massifs in Baluchistan.

the contact with the ophiolite to greenschist grade away from the contact but at a greater depth. Williams & Smyth (1973) has described a similar sequence in Newfoundland, and Lanphere (1981) in Oman. Williams & Smyth (1973) felt the metamorphic rocks in Newfoundland were greywackes metamorphosed by frictional heat by the obducting ophiolite. This accounted for the higher grade of metamorphism at the contact with the ophiolite and lower grades downsection away from the contact. Abbas & Ahmed (1979) attribute the metamorphism to either frictional or residual heat in the ophiolite. During late October of 1983 and late April of 1984, I recognized the contact zone around parts of the Jangtor and Saplaitor massifs. An excellent exposure of a sequence of metamorphic rocks approximately 1000 feet thick is exposed on the north side of Jangtor.

Hornblendite is at the contact followed by garnet gneiss, chlorite-garnet-schist, marble, garnet-schist, and farthest away is a two-mica schist. The marbles and aluminous schists and gneisses are indicative of a metamorphosed sedimentary sequence, perhaps flyschoid.

The hornblendite could well be a metamorphosed flow. I found some metamorphosed rock, usually chlorite schist exposed almost everywhere at the contact of the ophiolite massifs. I feel that much more metamorphic rock is associated with the massifs than previously reported. Part of the problem probably is that ophiolite, volcanics, mélange, and schists have not been accurately separated. For example, the 1:50,000 geologic map of the Nisai quadrangle shows a large area of ultramafic rocks and mélange near Bagh on the southeast side of Saplaitor. Field work revealed that the greater part of this mapped area was volcanic breccia and agglomerate. Additionally a band of chlorite and/or two-mica schist is present above a small melange and below a layered gabbro of the massif. In fact, I found that at least 500 feet of the east end of Saplaitor is schist and gneiss and not gabbro as mapped. It is important to note that I did not observe any andesitic rocks in the volcanic sequences nor have any been reported in the literature although, admittedly, published analytical data is meagre to non-existent. Shams (1976) did report calc-alkaline compositions for late dolerite dykes in the area.

Western Baluchistan

The major structural trends in western Baluchistan (Makran) are all east-west. From north at the Afghanistan border to the south they are the Chagai Hills - Saindak area composed of andesitic volcanics, sediments, and intrusives; the Dalbandin trough filled with Tertiary and Recent sediments; the Ras Koh range composed of andesitic volcanics, basaltic volcanics, intrusives and ophiolites; and the Hamun - i - Maskel depression filled with Tertiary and Recent sediments (fig. 1).

The Chagai Hills-Saindak area has been studied by a number of geologists (Bakr, 1963, 1964; Ahmed, et al., 1972; Hunting Survey Corp., 1960; Arthurton et al., 1979). The region consists of a sequence of late Cretaceous andesitic agglomerates, breccias, and flows together with limestones, shales, and sandstones. Dioritic to granitic intrusive rocks are present in a number of places and some of the granitic intrusives contain tourmaline (personal communication with Mohammad Munir at the University of Baluchistan).

Bakr (1964), Kazmi (1982), and the Hunting Survey maps (1960) report Sinjrani andesitic volcanics as present in the northeasternmost portion of the Ras Koh range. The remainder of the range is mapped as Bunap on the older maps and as Rakhshani formation on more recent ones. Ophiolitic masses, here called Bunap intrusions, are scattered but for the most part are present in the northern part of the Ras Koh range. Several dioritic intrusives are present in the north central and northwest part of the range (Bakr, 1963). Bakr (1963) in his study of the western Ras Koh describes the Bunap formation (Rakhshani) as being composed of basaltic flows, agglomerates, and breccia together with shaley limestones, shales

and sandstones. He mapped peridotite (ophiolite?) on the northernmost part and also mapped dioritic intrusions on the northern side.

I made a 6 day reconnaissance of the northern Makran from Nushki to Saindak in early May of 1984 and found two distinct volcanic types in the northeast Ras Koh Range which I interpret to be Sinjarani and Rakhshani. The Sinjarani specimens are all so altered it is difficult to tell whether they are andesitic or basaltic. The Rakhshani units make up the mass of the Ras Koh range; thin sections of 8 specimens collected are all basaltic. I performed electron microprobe analyses on 3 pyroxenes from one breccia (Sample RK-4) and 5 pyroxenes from one flow (Sample RK-6) (table 1). All pyroxenes plot in the field of "within plate alkali basalt" on the MnO-TiO_2-Na_2O diagram of Nisbet and Pearce (1977) (fig. 2). They do however plot in a different field than do the basalts from Gwanda Gwazi described previously in this paper. A number of andesitic breccias and flows were observed in the region from Saindak to Rabat and in the Saindak project area.

Much field work needs to be done in the Ras Koh in the light of new plate tectonic interpretations. It is crucial that all ophiolite blocks be looked at not only as to their chemistry and possible ore potential but as to their tectonic relationship to each other. Bakr (1963) describes schists and hornblendites in the western Ras Koh associated with ultramafics which in 1963 were interpreted as intrusive. I suspect that a restudy would show the ultramafics to be obducted ophiolites and the schist and hornblendites to be metamorphosed wedges under the ophiolites much as at Muslimbagh. Careful mineralogical and chemical study needs to be made of the volcanics in the Ras Koh range to determine if they are all basalt, andesite, or more likely, a mixture.

SUGGESTED MODEL FOR THE BALUCHISTAN SUTURE ZONE

Eastern Baluchistan

Field evidence reveals that basaltic lavas and agglomerates interspersed with Maastrichtian marine sediments are found immediately west of the folded Mesozoic sediments on the western side of the Indian plate (Kazmi, 1979; De Jong, 1979; McCormick, field work 1983-84). Ophiolites have been tectonically obducted onto these basalts and sediments from the west probably in mid to late Pliocene (Abbas & Ahmad 1979; DeJong, 1979). Tapponnier et al. (1981) report volcano-clastic material throughout the deposits in the Katawaz basin west of the ophiolite belt. They also report andesitic volcanics in the vicinity of Karandahar, Afghanistan.

This portion of the suture is distinctly different from that of northern Pakistan as described by Tahirkheli et al. (1979). If the Indian plate was subducted under the Afghan extension of the Eurasian plate and then collided with it we would expect to find India first colliding with an outer arc composed of flyschoid sediments and ophiolites which would be accreted and obducted onto the margin against the Mesozoic sediments. As subduction proceeded the volcanic arc would next be collided with and andesitic volcanics accreted onto the Indian plate westward of the ophiolites. Furthermore, it seems likely that in mid to late Paleocene the Indian plate was not yet close to the position where one would expect to find the outer arc of the island arc system on the subduction zone.

I submit that the within plate alkali basaltic volcanics associated with the Parh formation represent oceanic island basalts as described by Searle et al. (1980) for the Haybi volcanics of Oman.

Sclater and Fisher (1974) considered both the Ninetyeast Ridge and Chagos-Laccadive Ridge as scars of the northward movement of India after the breakup of Gondwanaland. Curray et al. (1980) put forth the hypothesis that the Ninetyeast Ridge was formed by passage of the Northward moving plate over a "hot spot" perhaps presently located under Kerguelen Island. If so. it is reasonable to assume that the Chagos-Laccadive Ridge also was formed by passage of the northward moving plate over a "hot spot" perhaps presently located under the Reunion-Mauritius-Rodriguez islands region.

TABLE 1. Microprobe analyses of clinopyroxenes from Gwanda Gwazi and Ras Koh Range, 10 km west of Padag.

	GG1-1	GG1-2	GG1-3	GG1-4	GG1-5	GG3-1 (core)	GG3-1 (rim)	GG3-2	GG3-3	GG3-4	GG3-5	RK4-1	RK4-2	RK4-3	RK6-1	RK6-2	RK6-3	RK6-4	RK6-5
Na_2O	0.23	0.50	0.48	0.51	0.27	0.31	0.12	0.24	0.31	0.45	0.33	1.09	1.19	1.29	1.17	1.42	1.35	1.41	1 45
MgO	11.35	11.32	11.49	13.02	11.25	14.60	15.22	15.42	15.26	15.16	14.27	12.77	12.58	13.49	13.99	13.77	13.44	14.55	13.46
Al_2O_3	0.09	8.75	8.46	6.46	8.98	3.86	2.98	2.96	3.07	3.76	3.87	9.94	9.27	9.76	7.70	7.26	8.29	7.75	8.50
SiO_2	44.65	45.09	45.19	47.71	44.66	50.43	51.06	51.44	50.92	50.58	50.46	48.35	49.04	48.07	49.28	48.27	48.00	49.66	47.60
CaO	23.49	22.79	23.19	23.11	23.06	22.16	22.03	21.97	22.00	22.06	22.06	12.13	12.56	11.88	12.42	11.91	12.04	12.43	12.11
K_2O	0.06	0.15	0.15	0.16	0.11	0.05	0.06	0.15	0.08	0.13	0.09	0.12	0.08	0.05	0.06	0.16	0.20	0.08	0.20
TiO_2	3.01	3.19	2.75	2.30	2.97	1.45	1.05	0.95	1.10	1.34	1.27	0.15	0.11	0.14	0.72	1.02	1.06	0.82	0.95
CrO_2	0.09	0.22	0.11	-	0.19	0.60	0.54	0.63	0.53	0.47	0.37	0.12	-	-	-	-	0.17	0.20	0.20
MnO	0.10	0.22	-	0.08	0.18	0.19	-	0.18	0.20	0.19	0.20	0.35	0.83	0.39	0.51	0.64	0.68	0.64	0.54
FeO	7.83	8.63	7.95	7.36	7.95	7.64	6.72	6.67	6.65	6.71	7.47	15.02	15.50	14.97	14.66	15.26	14.54	13.96	15.36
Sum	99.80	100.86	99.54	100.72	99.30	101.30	99.56	100.62	100.12	100.86	100.42	100.03	101.25	101.04	100.49	100.26	99.76	101.49	100.38
Numbers of ions on the basis of 24 atoms of oxygen																			
Na	0.07	0.15	0.14	0.15	0.08	0.09	0.03	0.07	0.09	0.13	0.10	0.13	0.34	0.37	0.34	0.42	0.39	0.40	0.42
Mg	2.55	2.53	2.59	2.89	2.54	3.22	3.37	3.39	3.37	3.33	3.16	2.84	2.78	2.99	3.09	3.09	3.00	3.18	3.00
Al	1.62	1.55	1.51	1.13	1.60	0.67	0.52	0.51	0.54	0.65	0.68	1.75	1.62	1.71	1.34	1.29	1.46	1.34	1.50
Si	6.74	6.76	6.83	7.10	6.76	7.42	7.58	7.58	7.55	7.45	7.48	7.21	7.26	7.15	7.30	7.27	7.19	7.28	7.12
Ca	3.80	3.66	3.76	3.68	3.74	3.49	3.50	3.47	3.49	3.48	3.50	1.94	1.99	1.89	1.97	1.92	1.93	1.95	1.94
K	0.01	0.03	0.03	0.03	0.02	0.02	0.01	0.03	0.02	0.02	0.02	0.01	0.01	0.01	0.01	0.02	0.02	0.01	0.02
Ti	0.34	0.36	0.31	0.26	0.34	0.16	0.12	0.11	0.12	0.15	0.14	0.02	0.01	0.02	0.08	0.12	0.12	0.09	0.011
Cr	0.01	0.03	0.01	-	0.02	0.01	0.06	0.07	0.06	0.05	0.04	0.01	-	-	-	-	0.02	0.02	0.02
Mn	0.01	0.03	-	0.01	0.02	0.03	-	0.02	0.03	0.02	0.03	0.04	0.10	0.05	0.06	0.08	0.09	0.08	0.07
Fe	0.99	1.08	1.00	0.92	1.01	0.94	0.83	0.82	0.82	0.83	0.93	1.87	1.92	1.86	1.82	1.92	1.82	1.71	1.92

It is not unreasonable to hypothesize that the alkali basalt volcanics associated with the Parh formation represent oceanic islands formed on the western side of India as the northward moving plate passed over a "hot spot". The trace of this path is presently seen as the Chagos-Laccadive Ridge, however, the northernmost part (volcanics in the Parh formation) has been tectonically wedged in the Indian - Eurasian suture zone.

Beginning in early Jurassic small fragments of the Arabian crust broke off and moved north, each colliding with Eurasia and accreting onto it. As this happened the subduction zone would move southward and by Maastrichtian time formed a southward lobe in the suture line. The principal motion along both the Owen Fracture Zone and Ninety East Ridge was strike-slip throughout Mesozoic time.

During the Paleocene - Eocene, fractures or even an incipient subduction zone might have formed in the region of the oceanic volcanic islands. When the Indian plate began its north-west twist in the Paleocene, chunks of the ocean floor near the volcanic islands, perhaps including them, were obducted onto the Indian plate from the west. Quite possibly much of the rock was from near conduits or the magma reservoir and was still hot. This would account for the metamorphosed sediments now formed below some of the ophiolite masses. As the westward movement proceeded the Indian plate should have collided with the outer arc as described by Mitchell and Garson (1981). Perhaps some of the smaller ophiolite masses belong to a second collision and some to the obducted floor in the vicinity of the islands. As migration proceeded the Indian plate collided with the volcanic arc represented by reported andesites in Afghanistan.

Western Baluchistan (Makran)

Beginning in early Jurassic small fragments of the Arabian crust broke off and moved north. By Maastrichtian time they had all been accreted into one mass, the Afghan block (Tapponnier, 1981). By this time the subduction zone had migrated southwards to its approximate position under the Makran of today. The Lut block projects farther south and most likely the subduction zone migrated farther south of the Lut block than the Afghan block either being drapped around the strike-slip faults between the blocks or offset by them. The present day subduction zone might well have a similar bend in it as indicated by the zone of Cenozoic volcanoes from Sultan to Taftan.

To the south of the continental blocks was an island arc system on the Eurasian plate as elsewhere along the suture. To the south of the island arc in the region of the Gulf of Oman and perhaps close to Oman was fracture zone along which were oceanic volcanic islands. The present Chagai Hills and Saindak area are the remnants of the volcanic arc which accounts for the andesitic rocks, dioritic intrusives, and mineralization, particularly of copper and iron. Perhaps magma generated in the subduction zone passed through a thin portion of the overlying Afghan block and thus accounts for some of the more silicic plutons and tourmaline-bearing granites in Chagai. Mitchell and Garson (1981) describe similar situations in Indonesia and Malaysia.

The subducting Arabian plate would ultimately carry the oceanic islands to where they would collide with the outer arc and thus create a basaltic island sequence with ophiolites obducted on the southern side much as is observed in Ras Koh today. At the time of this collision or soon after, motion on the subduction zone either slowed more than the spreading rate on the Carlsburg Ridge or other ridges pushing Africa-Arabia northward or stopped altogether. The Arabian plate was forced northward and the motion was countered by raising the Chagai arch and downfolding and/or faulting of the Dalbandin trough. This motion then brought the oceanic island - fore arc collision mass (Ras Koh) close to the andesitic volcanic arc (Chagai Hills). Within the Cenozoic, motion has resumed on the subduction zone with andesitic volcanism occurring at nearly the same geographical region as it did in the Cretaceous and Paleocene.

REFERENCES

AHMED, W., KHAN, S.N. & SCHMIDT, R.G. (1972) Geology and copper mineralization of the Saindak quadrangle, Chagai District, West Pakistan. U.S. Geol. Surv. Prof. Pap. 761-A, 12p.

ABBAS, S.G. & AHMAD, Z. (1979) The Muslimbagh ophiolites. In: Farah, A. & De Jong, K.A. (eds.) GEODYNAMICS OF PAKISTAN, Geol. Surv. Pak. Quetta, pp. 243-9.

ARTHURTON, R.S., ALAM, G.S., AHMED, S.A. & IQBAL, S. (1979) Geological history of the Almred-Mashki Chah area, Chagai District, Baluchistan. In : Farah, A. & DeJong, K.A. (eds.) GEODYNAMICS OF PAKISTAN, Geol. Surv. Pak. Quetta, pp. 325 - 31.

BAKR, M.A. (1963) Geology of the Western Ras Koh Range, Chagai and Kharan Districts, West Pakistan. Rec. Geol. Surv. Pak. 10 (12-A), 28p.

———— & JACKSON, R.D. (1964) Geological map of Pakistan. Pak. Geol. Surv. Scale 1:2,000,000.

CURRAY, J.R., EMMEL, F.J. & MOORE, D.G. (1980) Structure, tectonics and geological history of the northeastern Indian Ocean. In : Nairn, A.E.M. & Stehli, F.G. (eds.) THE INDEAN OCEAN. Plenum Press, New York.

DE JONG, K.A. & SUBHANI, A.M. (1979) Note on the Bela ophiolites, with special reference to the Kanar area. In: GEODYNAMICS OF PAKISTAN (op.cit.) pp. 263-9.

FARHOUDI, G. & KARIG, D.E. (1979) Makran of Iran and Pakistan as an active arc system. Geology 5, pp. 664 - 8.

HAMILTON, W. (1979) Geotectonics of the Indonesian region. U.S. Geol. Surv. Prof. Pap.

HUNTING SURV. CORP. LTD. (1960) RECONNAISSANCE GEOLOGY OF PART OF WEST PAKISTAN. Colombo Plan Cooperative Project, Toronto, canada.

JACOB, K.H. & QUITTMEYER, R.L. (1979) The Makran region of Pakistan and Iran: Trench-arc system with active plate subduction. In: GEODYNAMICS OF PAKISTAN (Op. Cit.), pp. 305 - 17.

KAZMI, A.H. (1979) The Bibai and Gogainappes in the Kach-Ziarat area of northeast Baluchistan. In: GEODYNAMICS OF PAKISTAN (op. cit.) pp. 333 - 9.

———— & RANA, R.A. (1982) Tectonic map of Pakistan. Geol. Surv. Pak, Scale 1:2,000,000.

LANPHERE, M.A. (1981) K-Ar ages of metamorphic rocks at the base of the Samail ophiolite, Oman. Jour. Geophys. Res. 86 (84), pp. 2777 - 82.

MITCHELL, A.H.G. & GARSON, M.S. (1981) MINERAL DEPOSITS AND GLOBAL TECTONIC SETTINGS, Academic Press, 405p.

NISBET, E.G. & PEARCE, J.A. (1977) Clinopyroxene composition in mafic lavas from different tectonic settings. Cont. Min. Pet. 63, pp. 149 - 60.

SCLATER, J.G. & FISHER, R.L. (1974) Evolution of the east-central Indian Ocean, with emphasis on the tectonic setting of the ninety east Ridge. Geol. Soc. Amer. Bull. 85, pp.683-70.

SEARLE, M.P., LIPPARD, S.J., SMEWING, J.D. & REX, D.C. (1980) Volcanic rocks beneath the Semail ophiolite nappe in the northern Oman mountains and their significance in the Mesozoic evolution of Tethys. Jour. Geol. Soc. London 137, pp. 589 - 604.

SHAMS, F.A. & AHMAD, S. (1976) Petrology of the Twin Sisters soda dolerite, southeast of Muslimbagh, Zhob District, Baluchistan, Pakistan. Pak. Jour. Sci. Res. 28, pp. 79 - 84.

TAHIRKHELI, R.A.K. (1979) The India-Eurasia suture zone in northern Pakistan: synthesis and interpretation of recent data at plate scale. In: GEODYNAMICS OF PAKISTAN (op. cit.) pp. 125 - 30.

TAPPONNIER, P., MATTAUER, M., PROUST, F. & CASSAIGNEAU, C. (1981) Mesozoic ophiolites, sutures and large-scale tectonic movements in Afghanistan. Earth Planet. Sci. Lett. 52, pp. 355 - 71.

ACTA MINERALOGICA PAKISTANICA
VOLUME 1 (1985) pp. 10-16

ORE–MINERAL COMPOSITIONS FROM GALENA MINES OF THELICHI VALLEY, GILGIT AGENCY, PAKISTAN.

ZULFIQAR AHMED
Centre of Excellence in Mineralogy, University of Baluchistan, Quetta, Pakistan.

Abstract: Microanalytical work on ore samples from small scale mines developed for galena at Thelichi Valley shows the presence of lead, silver, antimony, copper, and zinc. Mineralogical aspects are discussed. Mineralization probably occurred from low temperature hydrothermal solutions by fissure filling.

INTRODUCTION

Galena has been mined from at least three locations in the Thelichi Valley, Gilgit Agency, Pakistan. At these places small pits and mines exist from which galena has been mined intermittently in the past. From the present mineralogical study, the occurrence of many metals associated with galena ore is exhibited. This feature will enhance the mining prospects of the area.

The galena-bearing samples were collected from the mines and studied in thin sections and polished sections. The ore microscopic study was followed by microanalytical work using the electron probe microanalyzer.

MINERALOGY OF THE AREA

The general geology and petrology of Thelichi area has been described by Ahmed et al. (1977). The area exposes part of a bigger dioritic pluton and adjacent schistose metamorphic rocks, often garnetiferous. The field relations at mine-1 are shows in fig. 1. Galena ore is contained in thin layers in a 0.3 m thick fissure vein which strikes N30°W and dips 73°NE. The fissure vein has tectonic contacts with enclosing quartzite, and parallels the foliation in quartzite. The quartzite is partly of ferruginous type, and has massive, non-foliated diorite exposed towards southwest; and foliated diorite towards northeast. The foliated diorite displays banding due to alternate mafic and felsic layers. Further towards northeast, the foliated diorite is succeeded by exposures of massive diorite.

At mine-2, galena is contained in a quartz vein similar to that found at mine-1; and the country rock is diorite. Galena and associated sulphides are present in Surmabat Valley, 220 metres above the valley floor, in a 46 metres long quartz vein.

None of the mines is being worked at the present time. Galena is the principal ore mineral of the veins. The variety of associated minerals or metals can be seen in fig. 2 depicting the x-ray scanning pictures of a galena sample. The backscattered electrons picture (2A) shows euhedral pyramidal projections of quartz crystals (black) and probably later matrix-like galena (white) and other sulphides (greyish white).The polishing quality of the sample is not good enough to reveal perfectly the fine intergrowths in galena, as have been shown in some cases, e.g., Stanley & Vaughan, (1981). However, the energy dispersive x-ray spectrum of many galena samples showed presence of Sb also. The sulphur distribution picture shows filling of cracks in quartz crystals by sulphides. Also different sulphur concentrations are exhibited by different sulphides. Pb-distribution picture shows the galena; and copper concentration is highest over covellite area. The energy-dispersive microprobe analyses for covellite and argentite are given in table 1.

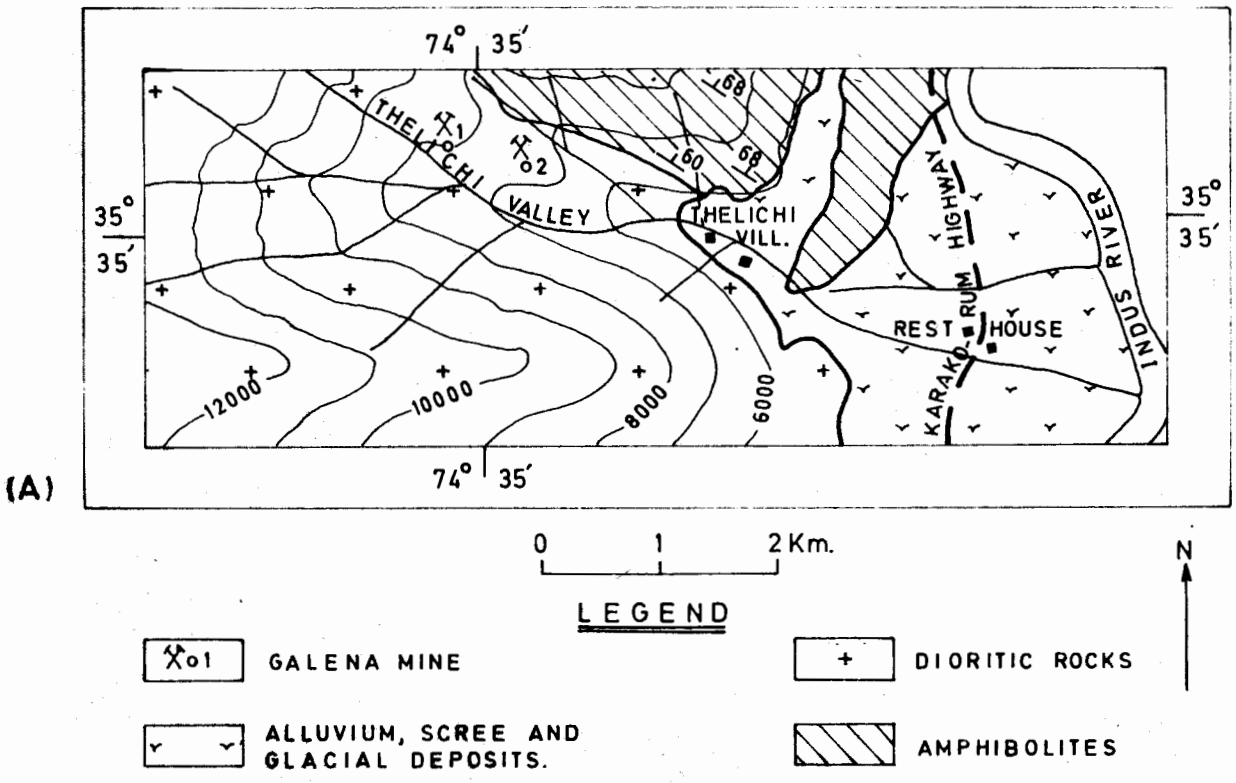

(A)

FIG. 1(A) GEOLOGICAL MAP OF THELICHI VALLEY (AFTER AHMED ET. AL., 1976) SHOWING LOCATION OF GALENA MINES.

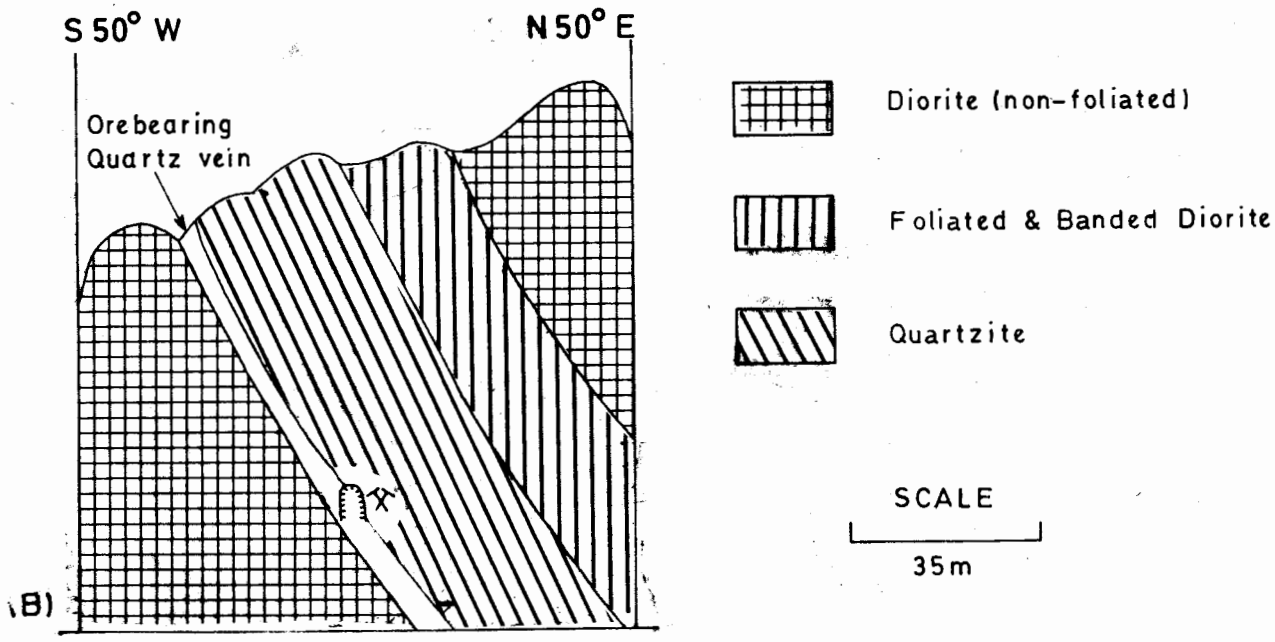

(B)

Fig.1 (B). Field sketch cross section showing field relations at galena mine-1.

Table 1. Microprobe analyses of covellite (1-4) and argentite (5-6) from the sample shown in fig. 2.

Anylsis No.	1	2	3	4	5	6
S	33.4	33.2	32.8	33.5	13.8	13.7
Cu	66.5	65.6	64.5	65.1	0.7	0.6
Ag	1.8	2.2	1.7	2.2	80.6	79.9
Sb	0.07	0.05	0.03	0.09	1.8	1.7
Pb	–	–	–	–	2.8	3.1
As	–	–	–	–	0.5	1.1
Fe	–	–	–	–	0.5	0.6
Zn	–	–	–	–	0.0	0.0
Total	101.77	101.05	99.03	100.89	100.7	100.7
Atomic	percents:-					
S	49.32	49.42	49.41	49.01	34.92	34.69
Cu	49.85	49.59	49.81	49.98	0.89	0.77
Ag	0.80	0.98	0.77	0.98	60.62	60.13
Sb	0.03	0.02	0.01	0.04	1.20	1.13
Pb	–	–	–	–	1.10	1.21
As	–	–	–	–	0.54	1.19
Fe	–	–	–	–	0.73	0.87

Fig. 3 illustrates another sample of galena ore showing the persence of discrete subhedral grains of sphalerite which appear dark grey in the back scattered electrons image.

SILVER OCCURRENCE

Fig. 4 illustrates concentration of silver just outside and along the boundary of galena grain which itself lacks silver. Discrete grains of argentite are present and their analyses are reported in table 1. This table also shows the presence of silver in covellite. Silver is present in high amounts in tetrahedrite as well.

The fahlore group sulphosalt solid solution also occurs. One grain was analyzed to give the following atomic percents:

$$(Cu_{32.8}\ Fe_{1.1}\ Ag_{1.9})\ (Sb_{7.9}\ As_{6.4})\ S_{49.9}$$

It also contains some Zn. In weight percents, this mineral contains 36 to 40% Cu, 4 to 7% Ag, 16.4 to 18% Sb and 27.6 to 30% S.

Fig. 5 shows the replacement of galena along cleavages by copper mineral covellite. Analyses from discrete grains of covellite are reported in table 1, which show the presence of around 2% silver and upto 0.1% antimony in covellite.

DISCUSSION

The lower depositional temperature of the deposit is indicated by comparison of the distribution of elements with evidence from other studies of galena. The absence of bismuith from Thelichi galena ores may indicate lower depositional temperature. According to Schroll (1955), bismuith content increases near the magmatic source. Malakhow's (1968) analyses of galenas from 84 different deposits suggest low bismuith and high antimony contents, as found in Thelichi samples (fig. 2) to indicate lower temperatures of formation.

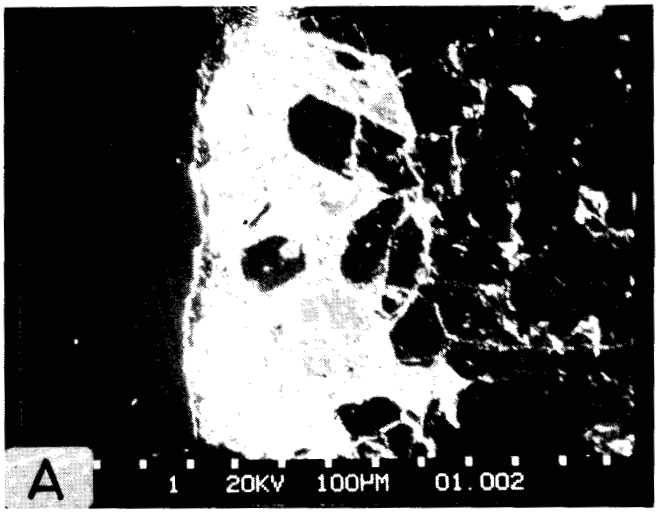
A
1 20KV 100HM 01.002

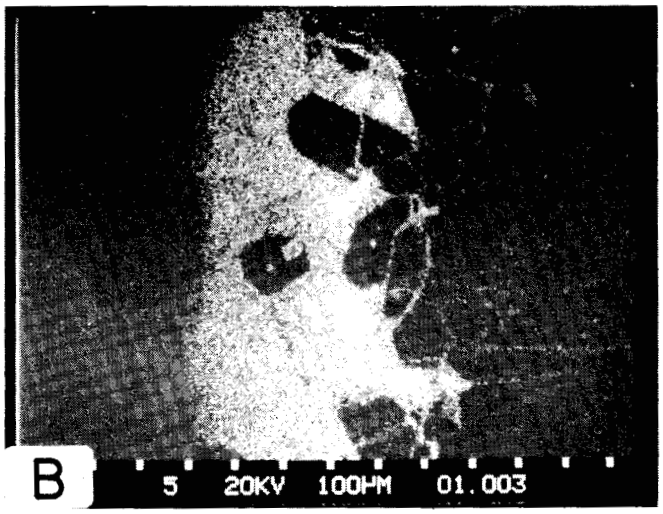
B
5 20KV 100HM 01.003

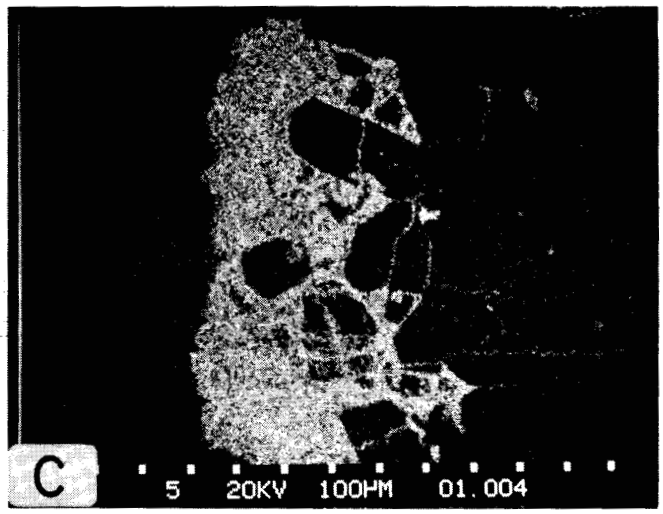
C
5 20KV 100HM 01.004

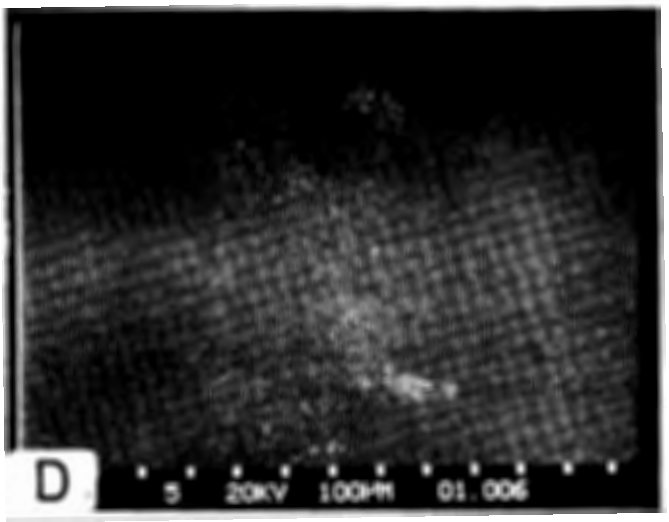
D
5 20KV 100HM 01.006

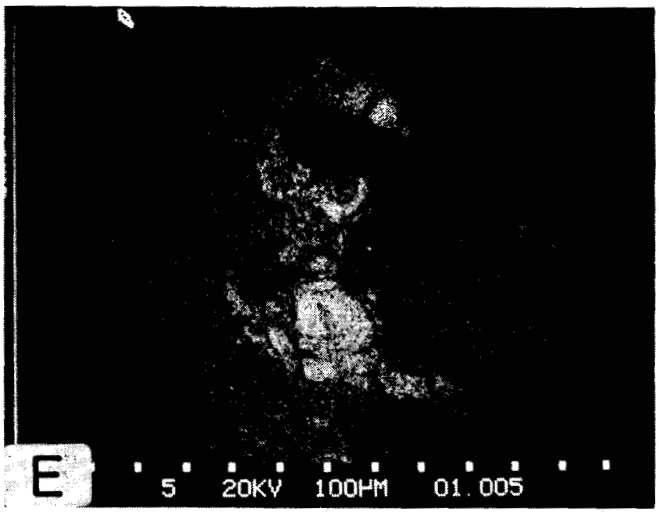
E
5 20KV 100HM 01.005

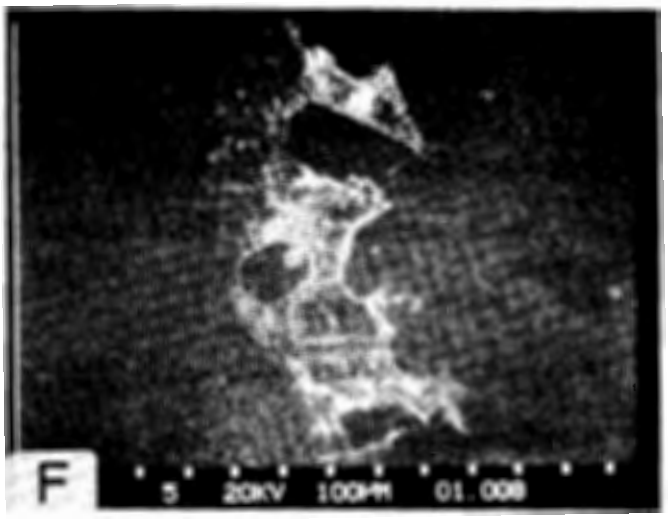
F
5 20KV 100HM 01.008

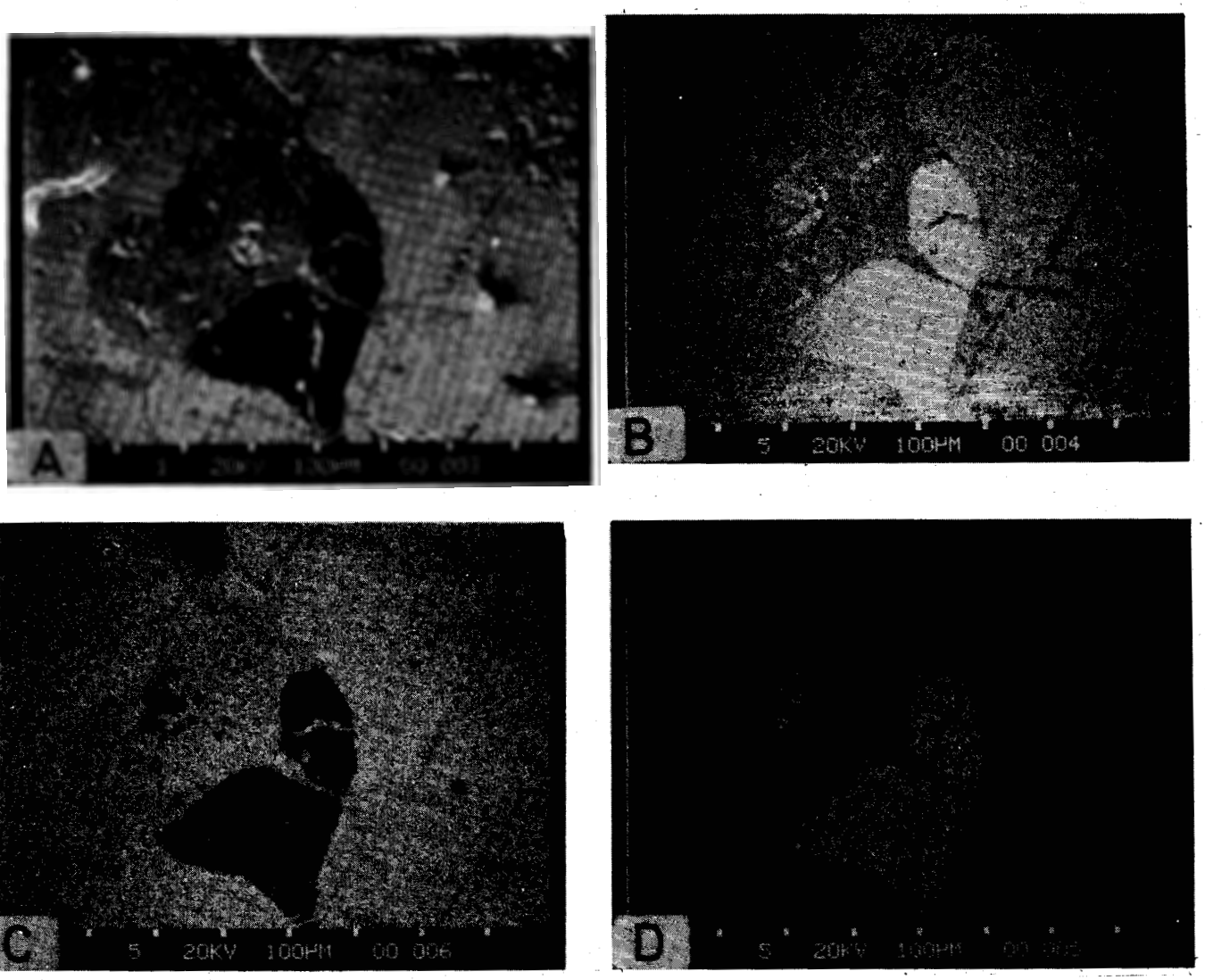

↑ Fig. 3 (Above). Discrete sphalerite grains (dark grey) set in galena (white) in a polished sample are seen in the back-scattered electrons image (A) and its scanning pictures for sulphur (B), lead (C) and zinc (D).

← Fig. 2 (Facing page). Euhedral quartz (black), galena (white) and associated sulphides (e.g., light grey) in a polished sample are seen in the back-scattered electrons image (A) and its scanning pictures for sulphur (B), lead (C), silver (D), copper (E) and antimony (F).

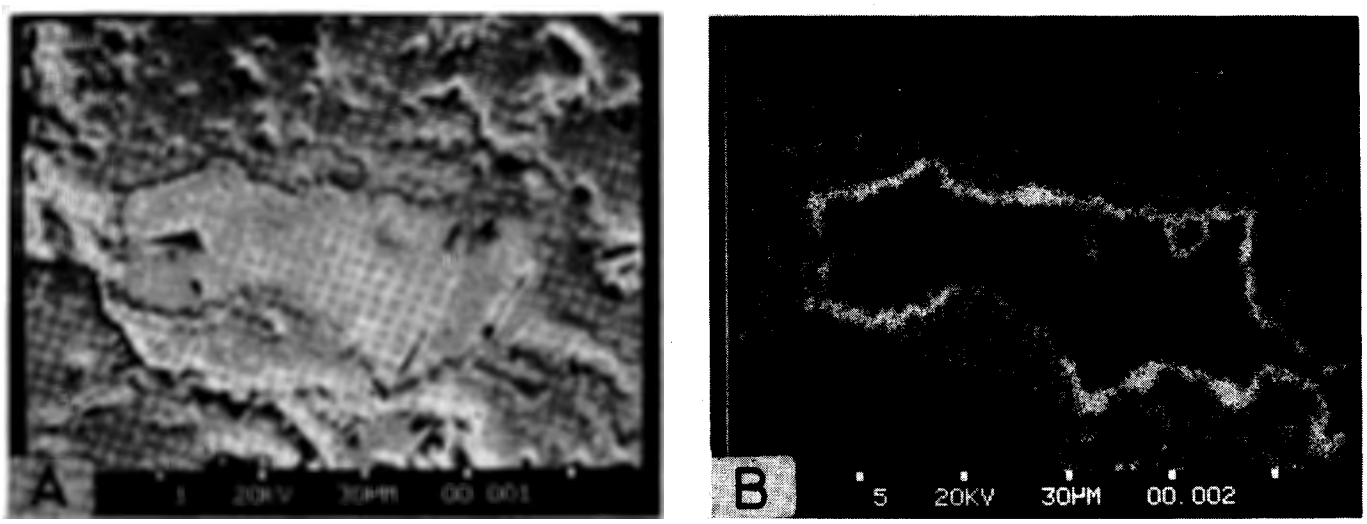

Fig. 4. A galena grain in the central portion of back-scattered electrons image (A) and its Ag-scanning picture (B) shows silver concentrated just outside margin of grain which lacks Ag content.

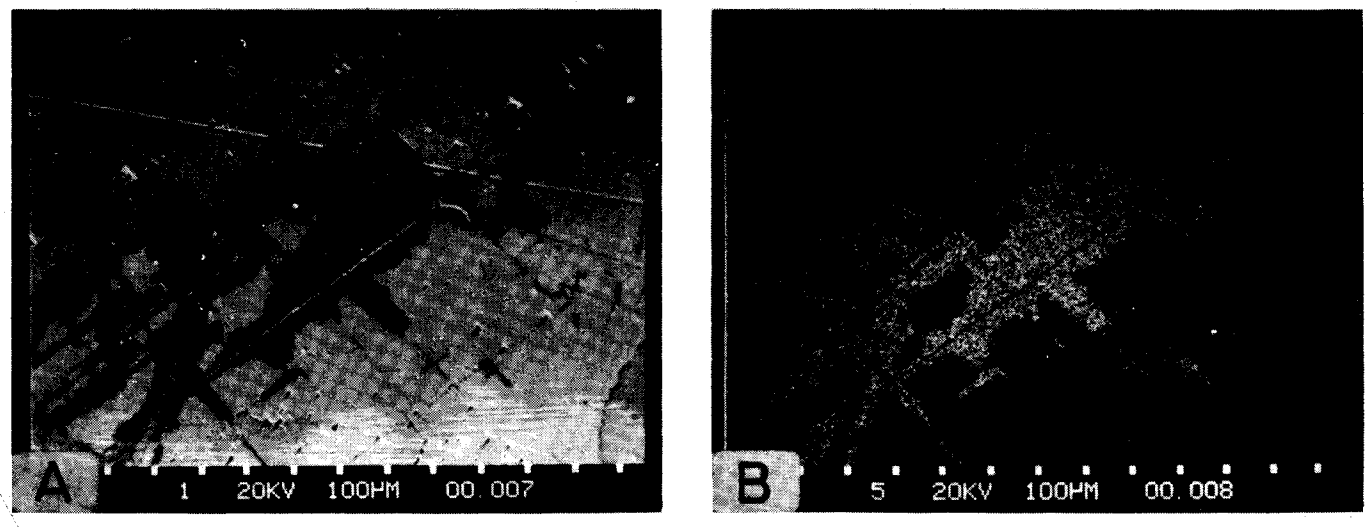

Fig. 5. (A) Back-scattered electrons image of polished galena ore sample shows development of covellite (dark grey) along cleavages.
(B) Copper distribution in the same area as in (A).

Fig. 5 exhibits a galena crystal with very little silver directly solved in it, although strong silver concentration marks the outside boundary of galena crystal. The presence of antimony observed in Thelichi ores (fig. 2) should have increased the solubility of silver in galena had it been crystallized at temperatures exceeding 400°C (Amcoff, 1976) especially when the stability of Ag dissolved in galena at higher temperatures is larger than its stability in discrete silver minerals. A comparison with the observations of Amcoff (1984) suggests higher solubility of silver in galena at higher temperatures, but subsequent fall in temperature led to the separation of silver from galena and its precipitation outside galena as well as in the sulphosalts. The former higher temperature solution is indicated by the presence of tetrahedrite - tennantite crystals.

Copper is more immobile relative to lead and zinc and is usually the first element to precipitate from ore forming solutions (e.g., Large, 1977). Thus covellite might have crystalized before galena and sphalerite. Thelichi ores also exhibit the pronounced affinity between silver and galena in the presence of significant amounts of antimony (Amcoff, 1984; Amcoff et al., 1985).

The cavity filling type of ore texture (fig. 2A) shows that the distribution of ore metals was probably little affected by post - or syn-depositional metamorphism or deformation. Such processes can cause distribution and movements of ore constituents which may overprint the primary distribution of elements. Thus, the Thelichi ores are better suited to study of primary elemental distributions.

CONCLUSIONS

Thelichi galena mines should be worked considering all the metals present which include lead, silver, zinc, copper, antimony, arsenic apart from sulphur. The ore minerals appear to have been generated by crystallization from low-temperature (epithermal) hydrothermal solutions, which may have remained at higher temperatures much before the ore deposition. Galena was crystallized after quartz. Argenitite developed after galena deposition. The primary ore minerals suffered later alteration and replacements along cleavages and grain boundaries.

ACKNOWLEDGEMENTS

The electron probe microanalyses were mad through co-operation by the Natural History Museum (Drs. R.F. Symes and Gary Jones) and the Queen Mary College (Mr. Archie Maclachlan) at London, U.K.

REFERENCES

AHMED, Z., HUSSAIN, SHABBIR & AWAN, A. (1977) Petrology of the Thelichi area, Geol. Bull. Punjab Univ. 14, pp. 27 - 38.

AMCOFF, Ö. (1976) The solubility of silver and antimony in galena. Neues Jahrb. Mineral. Monatsh. 6, pp. 247 - 61.

——(1984) Distribution of silver in massive sulfide ores. Mineralium Deposia 9, pp. 63 - 9.

——JEPPSON, M. & SELKMAN, S. (1985) Distribution and zoning of silver and associated elements in the complex sulfide deposit at Saxberget, central Sweden. Econ. Geol. 80, pp. 641 - 26.

LARGE, R.W. (1977) Chemical evaluation and zonation of massive sulfide deposits in volcanic terrains. Econ. Geol. 72, pp. 549 - 72.

MALAKHOW, A.A. (1968) Bismuith and antimony in galenas as indicators of some conditions of ore formations. Geo chemistry Int. 5, pp. 1055 - 68.

SCHROLL, E. (1955) Über des Vorkommen einiger Spureneiemente in Blei-Zink-Erzen der Ostalpinen Metallprovinz. Tscher Min Pet Mitt 5, pp. 183 - 208.

STANLEY, C.J. & VAUGHAN, D.J. (1981) Native antimony and bournonite intergrowths in galena from the English Lake District. Min. Mag. 44 (335), pp. 257 - 60.

ACTA MINERALOGICA PAKISTANICA
VOLUME 1(1985) pp. 17-26

A REVIEW OF THE SMECTITE–ILLITE TRANSFORMATION

DUANE M. MOORE

Centre of Excellence in Mineralogy, University of Baluchistan, Quetta.
Permanent Address: Knox College, Galesburg, Illinois 61401, U.S.A.

Abstract: Studies of burial diagenesis of Tertiary and Cretaceous shales and bentonites, of hydrothermal mineral assemblages from geothermal areas, and of Tertiary and Cretaceous shales and bentonites intruded by igneous dykes strongly indicate a transformation series from smectite to illite to muscovite through the following stages: smectite → randomly interstratified smectite/illite mixed-layer clay mineral → smectite/illite with IS ordering → smectite/illite with ISII ordering → illite → muscovite. These discrete changes seem to be controlled by several kinetic rate laws and involve times as short as 10^2 years for the high temperatures associated with dyke intruded systems, to 10^7 years for burial diagenesis at temperatures of 90 — 100 °C. These discrete changes are an extention into lower temperature ranges of the classical Barrovian sequence of isograds. They can serve as markers in the time-temperature analysis of basinal histories and can be particularly helpful in the temperature range in which petroleum is generated. The reaction characterizing this transition is:

SMECTITE + K-FELDSPAR → ILLITE + CHLORITE + QUARTZ.

The loss of K-feldspar and the formation of chlorite and quartz has important implications for mass balance changes, secondary porosity and cementing of reservoir rocks.

There is a discrepancy when this transition series is applied to studies of Paleozoic shales and bentonites. Whereas the apparent thermal history of Paleozoic shales on stable platforms where temperatures probably have not been higher than 50 °C and therefore should be characterized by smectite with small amounts of randomly interstratified illite, the smectite/illite that is present is the ISII ordered variety. This suggests that for lower temperatures, the kinetics of this transition series may involve times of $10^8 - 10^9$ years.

INTRODUCTION

Smectite and illite are two of the most common clay minerals. Geologists, but not necessarily engineers or soil scientists, define clay on the basis of particle size, and clay minerals on the basis of size, structure and composition. Most geologists take $< 2\ \mu m$ ($= 2 \times 10^{-6}$ metre) as the boundary for clay size material. Material of this size is dominated by hydrous aluminium silicates with structures and compositions similar to the macroscopic layer silicates. These are the clay minerals and non-clay minerals often occur with them; such minerals as quartz, feldspars, carbonates, pyrite, zeolites and other common minerals. Clay minerals can be formed from other minerals in the weathering zone; they can form during diagenesis; they can crystallize directly in pore spaces from fluids of appropriate composition; and they can form in geothermal and hydrothermal processes.

That there are changes in the clay mineral assemblages in fine grained detrital sediments with increasing depth, particularly the gradual disappearance of smectite, had been recognized by a number of workers (Burst, 1959, 1969; Dunoyer de Segonzac, 1965; Powers, 1959, 1967; Weaver, 1960). The generalized observation is that under the influence of burial diagenesis smectite is converted to illite through an intermediate mixed-layer phase, kaolinite decreases in abundance and is eventually lost while chlorite appears and then increases with depth. It was Hower, his students and his coworkers who explained the detailed mineralogical and chemical changes that took place and

emphasized their significance (Perry and Hower, 1970; Eslinger and Savin, 1973; Hower et al., 1976; Aronson and Hower, 1976; and Yeh and Savin, 1977).

In this review, the significance of and the mechanism of change of the smectite → illite transformation will be considered. In addition, other situations in which the smectite → illite transformation has been observed and used will be discussed. Some improved techniques for identifying and analyzing the clay minerals involved in this transformation series and a consideration of the mechanism responsible for ordering of layers will be discussed. And finally, the concept of clay minerals in the smectite → illite series as fundamental particles will be described.

TERMINOLOGY AND DEFINITIONS

Only two modules are needed to describe the structures of the clay minerals: a tetrahedral sheet and an octahedral sheet. The basic unit of the tetrahedral sheet is a cation, Si^{+4} or Al^{+3}, in 4-fold coordination with O^{-2} . Joining the centres of the oxygens makes a tetrahedron. Each tetrahedron shares 3 oxygens, the ones on the base, with 3 other tetrahedra. This makes a sheet of infinite extent in 2 dimensions with unshared apical oxygens. The basic unit of the octahedral sheet is a cation in 6-fold coordination with O^{-2} or OH^{-}. The most common cations here are Mg^{+2}, Fe^{+2}, Fe^{+3} and Al^{+3}. The octahedra share edges rather than corners, resting on a triangular face, and again making a sheet of infinite extent in 2 dimensions. The two major groups of clay minerals are: 1) those with one tetrahedral and one octahedral sheet joined by sharing; and 2) those with two tetrahedral and one octahedral sheet joined by sharing. (see fig. 1).

From fig. 1 it can be seen why these minerals are called layer silicates. There infinitely extending layers stack one on another. In the case of kaolinite there is one tetrahedral and one octahedral layer and all tetrahedral cations are Si^{+4} and and all octahedral cations are Al^{+3}. The layer is electrically neutral. In smectite and illite (and muscovite in the macromineral world) there are two tetrahedral sheets and one octahedral sheet. Here Al^{+3} can substitute for Si^{+4} in the tetrahedral position and/or a divalent cation may substitute for Al^{+3} in the octahedral position giving the layer a charge. This is neutralized by a cation between the layers, an interlayer cation. Muscovite has 1.0 units of charge per formula unit which is neutralized by 1.0 K^{+} per formula unit; illite has from 0.8 to 0.6 unit of charge which is neutralized by 0.8 to 0.6 K^{+} ; and

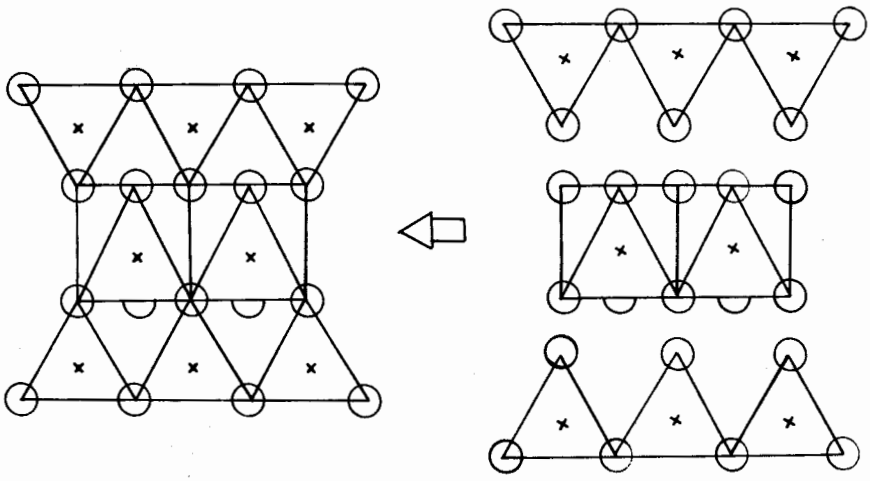

Figure 1. Joining of sheets by sharing oxygens. The unshared anions of the octahedral sheet are hydroxyls.

*Some workers prefer the term burial metamorphism.

smectite has 0.6 to 0.3 layer charge and 0.6 to 0.3 K^+, Na^+ or $Ca^{+2}/2$. These relations are shown in fig. 2. Chlorite has two tetrahedral and one octahedral sheet but is different from the clay minerals described above in that its layer charge is neutralized by an octahedral sheet in the interlayer space. (A detailed discussion of the structures of clay minerals may be found in Bailey, (1980a). The state of current terminology may be seen by referring to Bailey (1980b and 1982).

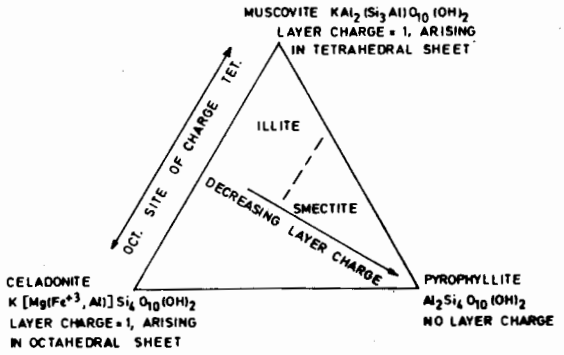

Figure 2. A comparison of the composition and origin of layer charge of three macro layer silicates with illite and smectite.

BURIAL DIAGENESIS*

An important axiom in the study of igneous and metamorphic rocks is that the mineral assemblage present is a consequence of: 1) the chemical composition of the rock and fluids present; 2) the pressure and temperature history; and 3) the extent to which reactions have gone to completion. Because metamorphosed argillaceous rocks have proved most useful in defining metamorphic grade, regional metamorphic facies generally are defined on the basis of mineral assmeblages in metamorphosed shales. This was the basis for the classical Barrovian sequence of isograds which is now known to cover the temperature range from about 300 to 600°C. Reactions taking place between 300°C and earth surface conditions were not amenable to analysis until the smectite — illite — muscovite sequence has come to be understood.

The change from smectite to illite involves adding potassium and aluminium, and, though not apparent from the preceding discussion, taking away magnesium, iron and calcium. Hower et al. (1976) give the overall reactions as:

K-feldspar + smectite → illite + chlorite + quartz

Their evidence was x-ray diffraction analysis of the whole rock and the $< 0.1\,\mu$m fraction and chemical analysis of the whole sample, the $> 2\ \mu$m and the $< 0.1\ \mu$m fractions. They showed that the total K-content did not change as a function of depth but that the $> 2\,\mu$m fraction lost K while the $< 0.1\ \mu$m fractions. gained K as a function of depth. This corresponded closely with the increasing proportion of illite in the smectite/illite mixed–layer clay mineral. Because K-feldspar disappeared with depth, they concluded that K was shifting from the coarse fraction to the fine fraction; from K-feldspar to illite. The decomposition of mica may provide K under some circumstances, also.

This reaction is important for at least four reasons. As a consequence of this reaction pore water chemistry is changed, and all the major chemical components in the shale are mobilized. Most of these are consumed in the reaction but part will be transported in some circumstances to adjacent sandstone units where they will be involved in cementation, replacement and diagenetic clay mineral formation in potential reservoir rocks (Boles and Franks, 1979; Hower, 1983). The development of secondary porosity in both the shale bed in which the reaction has taken place and in adjacent reservoir beds is due, in part to components mobilized by this reaction.

A second reason for its importance is that the smectite → illite transformation takes place within the same volume of shale that develops greater than hydrostatic pressures. Bruce (1983) suggests there is a close relation between high fluid pressure buildup and this reaction. He suggests that SiO_2 released in the smectite → illite reaction can be deposited in the shale reducing its permeability. A third reason is this reaction also takes place within the volume of shale and within the temperature range in which petroleum is generated from kerogen. This

relation has been considered by a number of workers. Burtner and Warner (1983) note that for a sandstone-shale pair of early Cretaceous age in the Great Plains, U.S.A. region, the sandstone produces petroleum only where the smectite → illite reaction has proceeded in the adjacent shale and furthermore, only where this reaction has occurred the shale is lower in organic content than where smectite remains unreacted. Johns (1983) has discussed the role of smectite as a catalytic agent in petroleum generation. Davis (1983) found that when kerogen is pyrolyzed (heat treated) in the laboratory in the presence of smectite, relatively low molecular weight hydrocarbons, similar to those of petroleum, are produced whereas kerogen pyrolyzed by itself or in the presence of other clay sized material produced long chain aliphatic hydrocarbons. Another more mechanical relation between petroleum and the smectite → illite transition is that as smectite is collapsed, water is expelled. This can amount to 15% of the volume of the shale. When this water moves out of the shale into paths of less resistance, i.e., adjacent reservoir sandstones, it is quite possible it carries with it petroleum.

And the fourth and last reason that will be considered is that the various stages in the transition smectite → illite → muscovite offer the potential for establishing the equivalent of Barrovian isograds in the temperature range from near surface conditions to 300 – 350°C. This potential is of interest because rections proceed so slowly at low temperatures that very few promise to serve this purpose. There have been developed in recent years several other methods of estimating temperatures in the diagenetic zone. For example, there are the reflectivity of organic matter, usually phytoclasts, (see Bostick 1971) and the darking of conodonts. Smectite is more common than phytoclasts and conodonts and could, correspondingly, be more widely applicable.

The lower temperature part of this scale depends on the manner in which smectite and illite layers in the mixed-layer are stacked. But, illite does not begin to form until a temperature of about 50°C. (Środoń and Eberl, 1984). (See below the fourth qualification of the validity of the scale). When illite does appear, the lowest temperature conditions correspond to random stacking of the two components. The next step is the transition to ordered stacking of the two components. Then there is the transition to ordered stacking in a 1:1 ratio of smectite: illite, IS mixed-layering. At still higher temperatures, more illite is formed and an ordered arrangement of 3 illites to 1 smectite is observed, ISII mixed-layering. The transition to illite without smectite is the next step. Hower and Altaner (1983) conclude that these reactions are kinetically controlled. Given long periods of time ($> 10^7$ years), the step from disordered to 1:1 ordered stacking takes place at 90–100°C. If temperatures are higher, this step can occur at 130–150°C for reaction times of $< 10^6$ years. The IS state persists to about 175°C. Above this temperature reaction to the IISI state proceeds.

On the higher temperature side of this scale, the differences from one step to another depend on, first, how one illite layer is stacked on another (different stackings give different polytypes M = monoclinic, T = trigonal, the number = the number of layers involved: 1M, 2M, 3T, etc.) and second, the amount of potassium per formula unit with the limite = 1.0. At this limit the mineral is muscovite. From data from hydrothermal mineral assemblages associated with geothermal areas, Hower and Altaner (1983) suggest that above about 260°C, illite without smectite is the stable phase and that above about 310°C, muscovite is the stable phase. Illite apparently exhibits the same polytypes as muscovite and, using data from serveral workers, the sequence $1M_d$ - 1M-1M/3T-3T-$2M_1$ has been suggested as correlating with conditions of increasing temperature from the line of several arguments, most presuasive being that of Carman (1974), pressure does not seem to effect the state of reactions throughout the transition.

From a study of a metamorphic sequence in the southern Appalachian Mountains, U.S.A., Weaver and Broekstra (1984) extend this scale from the diagenetic zone into the two lowest metamorphic zones and they show approximate agreement with Hower and Altaner (1983).

Weaver and Broekstra (1984) conclude that the highest temperature diagenetic zone is characterized by the absence of the two layer polytype $2M_1$ of illite. The appearance of the $2M_1$ polytype coincides with the beginning of the lowest temperature metamorphic zone, the anchizone, at about 280°C. As temperature increases across this zone, more and more illite changes to the $2M_1$ polytype until at about 360°C, all illite is converted and the mineral is more properly called muscovite. In addition, across this zone the amount of smectite layers goes from 10% to 0%. This is the boundary to the next metamorphic zone, the epizone.

Before this temperature scale can be rigorously applied there are at least four problems that need to be pushed closer to solution. First, it is generally agreed that the reactions in the smectite → illite transition are kinetically controlled but there is lack of agreement on the details (Eberl and Hower, 1976; Roberson and Lahann, 1981; Pytte, 1982). Second, the degree to which smectite is converted to illite may be a function not of kinetic conditions but of availability of K^+ and the absence of Na^+, Ca^{+2}, Mg^{+2} (Środoń and Eberl, 1984; Roberson and Lahann, 1981). Altaner et al. (1984) present evidence suggesting that at least in some cases the smectite → illite transition is controlled by the rate of diffusion for K^+ moving into the reacting system. Third, Morton (1985) uses RB-Sr data to argue that the diagenetic change from smectite to illite occurs suddenly at relatively shallow depths, the different degrees of conversion to illite being a function of different temperatures at different depths.

The fourth reason is more involved. There is a general inconsistency when the clay mineral assemblage of shales of Cenozoic and Mesozoic age are compared with those of Paleozoic and Pre-Cambrian shales. Paleozoic shales and bentonites from stable platforms, rocks that almost certainly have never been at temperatures >80°C, have smectite/illite of the IS II variety. In an effort to explain this apparent inconsistency, Moore (1978, 1982, 1984) has studied the bulk chemical composition, the clay minerals and the silt sized feldspars and micas of the Pennsylvanian Purington Shale. Conventional interpretation of the setting of this shale on the northwest corner of the Illinois Basin suggests it has not been burried more than 850 metres nor heated to more than 40°C. The <0.1 μm clay minerals show smectite/illite mixed-layering with about 90% illite layers. There is not enough detail in the diffraction tracing to tell if it is the ISII ordering. The feldspars show chemical compositions almost identical to those of Land and Milliken (1981) from depths of 11,500 feet in the Frio Formation (Oligocene), a formation with a well documented smectite → illite transition. Their feldspars have been albitized. Mass balance calculations for the Purington Shale (Moore, unpublished data) indicate that, given an ordinary range of feldspar compositions in the initially deposited material, approximately the same amount of K^+ has been freed by the albitization of the feldspars as would be needed to change original smectite to smectite/illite with 90% illite layers. This suggests two conclusions: that the smectite → illite transition process has operated at least through Phanerozoic time; and, that the smectite → illite reaction may proceed at lower temperatures given long enough times ($>10^8$ - 10^9 years). This latter conclusion must apply to the albitization process as well though Milliken et al. (1981) suggest the zone of most rapid albitization is near 130°C.

SMECTITE → ILLITE IN OTHER SETTINGS

Evidence of the smectite → illite transition in metamorphic and hydrothermal-geothermal environments has been noted above. Work, for example by Horton (1983), has shown that ore deposits may be zoned with respect to the smectite → illite → muscovite sequence. McDowell and Elders (1980) show that parts of the sequence can be found in boreholes in the Salton Sea Geothermal Field, California, U.S.A. Another setting in which parts, or potentially all, of the series may be found is in dyke intruded shale systems. Ideally, for shales containing unaltered smectite, the thermal energy from an intruded dyke can cause the changes associated with the series. An ideal setting has not yet

From Figure 3A, see that the dipole axis from the centre of the oxygen to the centre of the hydrogen points into the interlayer space. When layer 2 and 3 collapse in 3B, see that the dipole axis, the hydrogen being repulsed by the approaching sodium cation, has shifted away from the interlayer space and toward the octahedral site M1 (which would be vacant for dioctahedral layer silicates and almost all illites are dioctahedral). This shift brings the hydrogen of the upper hydroxyl of layer 2 in 3B closer to the hydrogen of the lower hydroxyl. Because they are both positive charges, if the lower hydroxyl tries to shift toward the M1 site it will be repulsed by the hydrogen from the upper hydroxyl. For this reason the interlayer space between layer 2 and layer 1 will tend to stay hydrated while the interlayer space immediately below can more easily collapse because the lower hydroxyl of layer 1 can rotate away from the interlayer space without meeting resistance from the hydrogen of the upper hydroxyl. This may seem like a small difference but Giese (personal communication) calculated the electrostatic bonding energies for random stacking and for ordered stacking of dehydrated and hydrated Na-smectite layers and found the ordered stacking more stable, in agreement with this model.

Moore and Hower (1985) suggest that the same mechanism may apply to ordered smectite/illite interlayering. The additional K^+ added in the interlayer space during the formation of illite would exaggerate the effect of re-orienting hydroxyl dipole axes. One major difference is that hydration-dehydration reactions are rapid and reversible and the conversion to illite from smectite is neither of these. In the process of dehydration, any "mistakes" in the ordered sequence can be "corrected". This difference explains, perhaps, the observation that smectite/illite does not change to an ordered state until more than hlaf of the layers are illite.

INTERSTRATIFIED CLAY MINERALS AS FUNDAMENTAL PARTICLES

X-ray diffraction by sedimented oriented aggregates is the common analytical technique used to investigate clay minerals. A fundamental problem is to understand what the diffracted beam is telling us about the structure of the clay mineral particles. The introduction of new technology often brings observations or interpretations that conflict with conventional understanding. This has been the case as transmission electron microscopy (TEM) has been used to examine smectite, illite and smectite/illite. The conventional understanding is that diffraction peaks are sharp and intense if there are $>$ 20 layers in the clay mineral particles causing diffraction.

Nadeau et al. (1984), on the basis of examination of these minerals with TEM, suggest smectite and regularly interstratified smectite/illite, IS, consist primarily of particles 10 Åand 20 Å thick respectively. They suggest that the ability shown by smectite to expand is, in reality, the interface between particles which is capable of absorbing water, ethylene glycol, etc. Therefore, particles that are 10 Å thick will behave like smectite and those 20 Å thick will behave like IS, the plane between the two layers being unable to expand. They propose to reconcile the conventional view that about 20 layers are needed to have a structure that gives a sharp diffraction peak and their conclusion that smectite and IS are 10 and 20 Å thick by suggesting that there is an interparticle diffraction effect so that the effective number of layers diffracting coherently is about 9.

They measured the thickness of these particles by spraying Pt at an angle across very dilute, dried suspensions, then, knowing the angle of the spray, they measured the length of the shadows cast by the particles. As is so often the case, an early paper (Yoshida, 1973) suggested smectite behaves as an elementary layer, but, at the time, it did not attract attention. This concept of single and double layers, if confirmed by other workers, will cause rethinking of many concepts about clay minerals.

SUMMARY

There are five common discrete clay minerals·

chlorite, illite, kaolinite, smectite and vermiculite. In addition to occurring as discrete minerals, they often occur as mixed-layer minerals in which two (very common) or more (apparently uncommon) of these five are interstratified in a random manner or in one of several patterns of ordering. There seems to be a strong tendency for mixed-layer clay minerals to be ordered rather than random. The discrete and the mixed-layer clay minerals are probably the most abundant group of minerals at the surface of the earth. Smectite, illite and smectite/illite are the most common of the clay minerals. Smectite and smectite/illite can be found as both detrital and diagenetic material, but discrete illite seems to occur only as detrital material in sedimentary rocks.

There is a mass of evidence supporting the conclusion that smectite is transformed to illite through an intermediate stage of interstratified smectite/illite. This transformation can take place in a number of settings: in response to burial; in response to an intrusion; in response to hydrothermal-geothermal processes; and in response to tectonic activity. It is not yet clear what the precise roles of time and temperature are in this transformation. It does seem clear that pressure is not an important variable. The transformation can take place relatively quickly (about 10^2 years) in an environment of very high temperature (dyke intruded shale systems) but it also seems to take place at much lower temperatures (about 40°C) over longer periods of time (10^8-10^9 years).

Potentially (once the controls on and rate of reaction questions are satisfactorily answered) the smectite → illite → muscovite transformation offers an extension of the classical Barrovian-type isograds into the diagenetic environment. The illite → muscovite part of this temperature scale is in the lowest two zones of the metamorphic enviornment.

REFERENCES

ALTANER, S.P., Hower., J., WHITNEY, G. & ARONSON, J.L., (1984) Model for K-bentonite formation: evidence from zoned K-bentonites in the disturbed belt, Montana. Geology 12, pp. 412-5.

ARONSON, J.L. & HOWER, J. (1976) Mechanism of burial metamorphism of argillaceous sediments: 2, Radiogenic argon evidence. Geol. Soc. Am. Bull. 87, pp. 738-44.

BAILEY, S.W. (1980) Structures of layer silicates. In: Brindley, G.W. and Brown, G. (eds.) CRYSTAL STRUCTURES OF CLAY MINERALS AND THEIR X–RAY IDENTIFICATION. Min. Soc. London, pp. 1-124.

——(1980 b) Summary and recommendations of AIPEA Nomenclature Committee. Clays & Clay Minerals 28, pp. 73-8.

——(1982) Nomenclature for regular interstratifications: Am. Mineral. 67, pp. 394-8.

BOLES, J.R. & FRANKS, S.G. (1979) Clay diagenesis in Wilcox sandstones of Southwest Texas: implications of smectite diagenesis on sandstone cementation. J. Sed. Pet. 49, pp. 55-70.

BOSTICK, N.H. (1971) Thermal alteration of clastic organic particles as an indicator of contact and burial metamorphism in sedimentary rocks. Geoscience and Man, 3, pp. 83-93.

BRADLEY, W.F. (1950) The alternating layer sequence of rectorite. Am. Mineral. 35, pp. 590-5.

BRUCE, C.H. (1983) Relation of illite/smectite diagenesis and development of structure in the northern Gulf of Mexico Basin. Am. Assoc. Petroleum Geolog. Program of Abstracts, April 17-20, p. 44.

BURST, J.F. (1969) Post diagenetic clay mineral-evironmental relationships in the Gulf Coast Eocene in clays and clay minerals. Clays & Clay Minerals 6, pp. 327-41.

——(1969) Diagenesis of Gulf Coast clayey sediments and its possible relation to petroleum migration. Bull. Am. Assoc. Petroleum Geol. 53, pp. 73-93.

BURTNER, R.L. & WARNER, M.A. (1983) Smectite diagenesis and hydrocarbon generation in the Cretaceous Mowry and Skull Creek Shales of the Northern Rocky Mountains-Great Plains region. Am. Assoc. Petroleum Geolog. Program of Abstracts. April 17-20, p. 46.

CARMAN, J.C. (1974) Synthetic sodium phlogopite and its two hydrates: stabilities, properties and mineralogic implications. Am. Mineral, 59, pp. 261-73.

DAVIS, J.B. (1983) Catalytic effect of smectitic clays in hydrocarbon generation. Am. Assoc. Petroleum Geolog. Program of Abstracts, April 17-20, p. 59.

DUBA, D. & WILLIAMS–JONES, A.E. (1983) The application of illite crystallinity, organic matter reflectance, and isotopic techniques to mineral exploration: A case study in south western Gaspé, Quebec. Econ. Geol. 78, pp. 1350-63.

DUNOYER DE SEGONAZ, G. (1965) Les argiles du Cretace superieur clans le bassin de Douala (Cameroun): Problems de diagenese. Bull. Serv. Carte Geol. Alsace-Lorraine, 17, (4), pp. 287-310.

EBERL, D.D. & HOWER, J. (1976) Kinetics of illite formation. Geol. Soc. Am. Bull. 87, pp. 1326-30.

ESLINGER, E.V. & SAVIN, S.M. (1973) Oxygen isotope geothermometry of the burial metamorphic rocks of the Precambrian Belt Supergroup, Glacier National Park. Montana. Geol. Soc. Am. Bull. 84, pp. 2549-60.

GIESE, R.F., JR. (1971) Hydroxyl orientation in muscovite indicated by electrostatic energy calculations. Science 172, pp. 263-4.

——(1977) The influence of hydroxyl orientation, stacking sequence, and ionic substitution on the interlayer bonding of micas. Clays & Clay Minerals 25, pp. 102-4.

——(1979) Hydroxyl orientations in 2:1 phyllosilicates. Clays & Clay Minerlas 27, pp. 213-23.

——(1980) Hydroxyl orientations and interlayer bonding in amesite. Clays & Clay Minerals 28, pp. 81-6.

GRUNER, J.W. (1934) The structure of vermiculites and their collapse by dehyration. Am. Mineral. 19, pp. 557-78.

HOFFMAN, J. & HOWER, J. (1979) Clay mineral assemblages as low grade metamorphic geothermometers: application to the thrust faulted distrubed belt of Montana, USA. In: Scholle, P.A. and Schluger, P.R. (eds.), ASPECTS OF DIAGENESIS, SEPM Spec. pub. 26, pp. 55-79.

HORTON, D. (1983) Argillitic alteration associated with the amethyst vein system, Creede Mining District, Colorado. Ph.D. Dissertation, University of Illinois at Urbana-Champaign.

HOWER, J. (1983) Clay mineral reactions in clastic diagenesis. Am. Assoc. Petroleum Geolog. Program of Abstracts, April, 17-20, p. 98.

——ESLINGER, E.V., HOWER, M.E. & PERRY, E.A. (1976) Mechanism of burial metamorphism of argillaceous sediments: 1, Mineralogical and chemical evidence. Geol. Soc. Am. Bull. 87, pp 725-37.

——&ALTANER, S.P (1983) The petrologic significance of illite/smectite. Program of Abstracts, 20th Annual Mtg. Clay Minerals Soc. p. 40.

ISLAM, S. & HESSE, R. (1982) Zonation of diagenesis and low-grade metamorphism in Cambro-Ordovician flysch of Gaspé Peninsula, Quebec Appalachians. Can. Minerals. 20, pp. 155-67.

JOHNS, W.D. (1983) Clay mineral catalysis and petroleum generation. Am. Assoc. Petroleum Geolog. Program of Abstract, April, 17-20, p. 102.

LAND, L.S. & MILLIKEN, K.L. (1981) Feldspar diagnesis in the Frio Formation, Brazoria country, Texas, Geology 9, pp. 314-18

MATTHEWS, J.C. (1983) The alteration of smectite-rich Cretaceous shales by dike intrusion in Chouteau county, Montana. B.A. Honors thesis, Knox College, Galesburg, Illinois.

MCDOWELL, D.S. & ELDERS, W.A. (1980) Authigenic layer silicate minerals in borehole Elmore 1, Salton Sea Geothermal Field, California, USA. Cont. Min. Pet. 74, pp. 293-310.

MILLIKEN, K.L., LAND L.S. & LOUCKS, R.G. (1981) History of burial diagenesis determined from isotopic geochemistry, Frio Formation, Brazoria county, Texas. Bull. Am. Assoc. Petroleum. Geolog. 65, pp. 1397-1413.

MOORE, D.M. (1978) A sample of the Purington shale prepared as a geochemical standard, J. Sed. Petrol. 48, pp. 995-8.

(1982) Shallow burial diagenesis of the Pennsylvanian Purington shale. Program of Abstracts 19th Annual Mtg. Minerals Soc. p. 73.

——(1984) Modal analysis and mineral chemistry of the Pennsylvanian Purington Shale. Geol. Soc. Amer. Program of Abstracts, Northcentral-Southeastern Sections.

——& HOWER, J. (1985) Ordered interstratification of dehydrated and hydrated Na-Smectite. Clays & Clay Minerals 33, (in press).

MORTON, J.P. (1985) Rb-Sr evidence for punctuated illite/smectite diagenesis in the Oligocene Frio Formation, Texas Gulf Coast. Geol. Soc. Am. Bull. 96, pp. 114-22.

NADEAU, P.H. & REYNOLDS, R.C., JR.(1981) Burial and contact metamorphism in the Mancos Shale. Clays & Clay Minerals 29, pp. 249-59.

——TAIT, J.M., McHARDY, W.J. & WILSON, M.J. (1984) Interstratified XRD characteristics of physical mixtures of elementary clay particles. Clay Minerals 19, pp. 67-76.

PERRY, E. & HOWER, J. (1970) Burial diagenesis in Gulf Coast Pelitic sediments. Clays & Clay Minerals 18, pp.165-77.

POWERS, M.C. (1959) Adjustments of clays to chemical change and the concept of the equivalence level. Clays and Clay Minerals 6, pp. 309-26.

——(1967) Fluid-release mechanisms in compacting marine mud-rocks and their importance in oil exploration. Bull. Am. Assoc. Petroleum. Geolog. 51, pp. 1240-54.

PYTTE, A.M. (1982) The kinetics of the smectite to illite reaction in contact metamorphic shales. M.A. thesis, Dartmouth College, Hanover, New Hampshire.

REYNOLDS, R.C. JR. (1980) Interstratified clay minerals. In: Brindley, G.W. and Brown, G. (eds.) CRYSTAL STRUCTURES OF CLAY MINERALS AND THEIR X—RAY IDENTIFICATION. Min. Soc. London, pp. 249-303.

——& HOWER, J. (1970) The nature of interlayering in mixed-layer illite-montmorilonites. Clays & Clay minerals 18, pp. 25-36.

ROBERSON, H.E. & LAHANN, R.W. (1981) Smectite to illite conversion rates: effect of solution chemistry. Clays and Clay Minerals 29, pp. 129-35.

SRODON, J. (1980) Precise identification of illite/smectite interstratifications by x-ray powder diffraction. Clays & Clay Minerals 28, pp. 401-11.

——(1984) X-ray identification of illitic materials. Clays & Clay Minerals.

——& EBERL, D.D. (1984) Illite. In: Bailey, S.W. (ed.) MICAS, REVIEWS IN MINERALOGY VOL. 13 Min. Soc. Amer., pp. 495-571.

WEAVER, C.E. (1960) Possible use of clay minerals in the search for oil. Bull. Am. Assoc. Petroleum Geolog. 44, pp. 1505-18.

——& BROEKSTRA, B.R. (1984) Illite-mica. In: Weaver, C.E. et al., SHALE SLATE METAMORPHISM IN SOUTHERN APPALACHIANS. Elsevier, Amsterdam, pp. 67-199.

YEH, H.W. & SARIN, S.M. (1977) The mechanism of burial metamorphsm of argillaceous sediments: 3, Oxygen isotopic evidence. Geol. Soc. Am. Bull. 88, pp. 1321-30.

YOSHIDA, T. (1973) Elementary layers in the interstratified clay minerals as revealed by electron microscopy. Clays & Clay Minerals 21, pp. 431-20.

ACTA MINERALOGICA PAKISTANICA
VOLUME 1 (1985) pp. 27-33

A NEW OCCURRENCE OF URANIUM–BEARING THORIAN MONAZITE, NORTHWESTERN PAKISTAN.

ZULFIQAR AHMED
Centre of Excellence in Mineralogy, University of Baluchistan, Quetta, Pakistan.

Abstract: **A new type of occurrence of uranium - and thorium - bearing monazite is described from a chloritic rock from near Musa Mena in Malakand Agency. The locality is being reported for the first time and may prove an economically viable mining area for uranium, thorium, rare earth elements such as lanthanum, cerium, neodymium, in addition to titanium-mineral rutile. Monazite forms euhedral porphyroblasts which appear zoned and occur alongwith euhedral rutile in a schist of low metamorphic grade. Microprobe analyses of rutile, monazite, apatite and chlorite are presented. The chlorites of monazite-bearing and adjacent monazite-lacking schists are chemically different. Zoned monazite crystals display increased Th and Ca and decreased Ce, Nd, Sm, Gd and Dy towards the rims. This is different from the usual trends.**

INTRODUCTION

Monazite, $REE^{3+}(PO_4)^{3-}$, is considered economically important mineral because of its rare-earth elements and its thorium content which is usually upto 5%. Monazite occurs widespread as an accessory mineral in granitic rocks, syenites and granitic pegmatites. These may weather to concentrate monazite in the commercially exploitable placers and sands, especially the beach sands which are a major world source of rare-earth elements and thorium. Uraninite and thorite may also occur associated with monazite. Metamorphic rocks seldom contain monazite. Only recently a metamorphic monazite was described by Mohr (1984) from black graphitic metashales of North Carolina. Mohr (1984) states that monazite occurs widespread at sillimanite and higher grades and is common in staurolite and kyanite zones. At garnet or lower grades, monazite is rare and its place is taken by allanite or sphene. During the course of present investigations, a new kind of the monazite occurrence was located near Dargai town. The monazite - bearing rock is a talcose chlorite schist and contains a U-Th bearing monazite and rutile. Furthermore, the question of zoning of these monazite crystals is also addressed while reporting the microanalyses of monazite porphyroblasts, as most of the previously published analyses of monazite are bulk analyses.

MODE OF OCCURRENCE

This new type of occurrence is located near Musa Mena village (71°53′ E, 34°29′ N) which lies a few km westward from Dargai town of Malakand Agency, Pakistan. In the area around this occurrence, regionally metamorphosed sediments occur in contact with the northeastern tip of the Sakhakot - Qila ophiolite (Ahmed, 1984). The metasediments include a variety of petrographic types such as the chlorite schist, pyritous chlorite schist, graphite mica schist, mica schist, quartzofeldspathic schist, sericite schist, marble, calcareous schist, quartzite and phyllite. Quartz veins or lenses are not uncommon in these schistose rocks. Bright emerald-green coloured muscovite (fuchsite) is developed interbedded in schists at an outcrop exposed west of Musa Mena. Because of its shine and colour, it has been quarried for use as dimension stone. Along their strike, the schists extend for many kilometres and form part of regionally widespread Precambrian-Cambrian metamorphic rocks.

The ophiolitic rock in contact with the metasedimentary rocks is a metagabbro which belongs to the middle level out of the three levels of gabbroic rocks recognized in the Sakhakot-Qila ophiolite (Ahmed, 1982, 1984.) This

Table 1. Chlorite analyses by microprobe from the monazite-bearing rock. All Fe is expressed as FeO.

SiO_2	28.75	28.66	28.86	28.17	28.89
TiO_2	0.09	0.01	0.05	0.10	0.1
Al_2O_3	20.01	20.41	19.69	19.72	20.24
Cr_2O_3	0.01	0.00	0.00	0.00	0.05
FeO	11.43	11.45	11.44	11.30	11.39
MnO	0.27	0.22	0.24	0.21	0.19
MgO	25.78	25.53	25.33	24.96	25.50
NiO	0.00	0.14	0.07	0.06	0.01
CaO	0.02	0.00	0.05	0.04	0.02
Na_2O	0.67	0.52	0.37	0.13	0.24
K_2O	0.00	0.02	0.01	0.03	0.02
P_2O_5	n.d.	n.d.	n.d.	n.d.	0.04
Total	87.03	86.96	86.11	84.72	86.60
Cations based on 28 oxygens ignoring H_2O^+:–					
Si	5.672	5.657	5.747	5.698	5.711
Al^{iv}	2.238	2.343	2.253	2.302	2.289
Al^{vi}	2.326	2.406	2.370	2.401	2.426
Ti	0.014	0.000	0.007	0.014	0.001
Cr	0.002	0.000	0.000	0.000	0.008
Fe	1.886	1.890	1.905	1.912	1.882
Mn	0.045	0.036	0.039	0.035	0.031
Mg	7.582	7.514	7.519	7.528	7.513
Ni	0.000	0.022	0.010	0.009	0.001
Ca	0.004	0.000	0.011	0.008	0.003
Na	0.255	0.196	0.141	0.050	0.093
K	0.000	0.004	0.003	0.007	0.003
P	–	–	–	–	0.006

n.d. = Not determined. The formulae are calculated by a computer online with microprobe, whereas the oxide percentages are reduced to the second decimal.

Table 2. Representative microprobe analyses of chlorites from metasedimentary schists lacking monazite.

Anal. No.	6.	7.	8.	9.	10.	11.	12.	13.	14
Sample No.	Z267	Z355	Z355	Z385	Z385	Z391	Z392	Z392	Z401
SiO_2	29.85	28.64	24.99	25.76	30.75	24.97	25.53	26.02	25.87
TiO_2	0.11	0.23	0.24	0.12	0.27	0.30	0.17	0.17	0.37
Al_2O_3	22.01	23.52	21.45	20.30	22.89	20.89	21.06	22.00	24.18
Cr_2O_3	0.02	0.00	0.04	0.17	0.13	0.02	0.27	0.03	n.d.
FeO	25.97	23.30	26.03	24.28	19.73	29.75	21.39	21.84	24.91
MnO	1.93	0.67	0.93	0.16	0.28	0.04	0.19	0.18	0.06
MgO	12.76	11.44	13.01	15.23	12.46	11.36	16.08	16.88	12.06
NiO	0.30	0.00	0.00	0.09	0.09	0.06	0.08	0.07	n.d.
CaO	1.27	0.07	0.08	0.03	0.04	0.23	0.40	0.15	0.14
Na_2O	0.74	0.17	0.00	0.22	0.00	0.39	0.00	0.00	0.39
K_2O	0.21	1.01	0.12	0.04	1.98	0.04	0.00	0.04	0.12
Total:	95.17	89.05	86.89	86.31	88.62	88.05	85.17	87.38	88.10
Cations based on 28 oxygens ignoring H_2O:									
Si	5.819	5.845	5.364	5.482	6.185	5.382	5.440	5.394	5.386
Al^{iv}	2.181	2.155	2.636	2.518	1.815	2.618	2.560	2.606	2.614
Al^{vi}	2.877	3.503	2.792	2.593	3.612	2.690	2.731	2.771	3.918
Ti	0.016	0.035	0.039	0.019	0.040	0.048	0.028	0.027	0.058
Cr	0.003	0.000	0.007	0.029	0.020	0.003	0.045	0.004	n.d.
Fe^{2+}	4.234	3.977	4.674	4.338	3.319	5.363	3.812	3.787	4.336
Mn	0.319	0.116	0.169	0.028	0.047	0.007	0.035	0.032	0.010
Mg	3.707	3.480	4.164	4.849	3.736	3.652	5.109	5.218	3.741
Ni	0.047	0.000	0.000	0.015	0.014	0.009	0.014	0.012	n.d.
Ca	0.265	0.015	0.018	0.008	0.009	0.054	0.091	0.033	0.031
Na	0.280	0.067	0.000	0.090	0.000	0.163	0.000	0.000	0.159
K	0.052	0.263	0.033	0.011	0.507	0.012	0.000	0.010	0.032

Z267= Schistose, green coloured rock with spessartine, quartz, chlorite, muscovite, and accessory sphene and magnetite; from grid reference 4150-8332 of toposheet No. 38 N/15.

Z355= Quartzitic schist with chlorite, muscovite, biotite, apatite, sphene and Mn-ilmenite; located 30 m northwards uphill from the Musa Mena fuchsite-marble mine.

Z385= Phyllite with graphite, quartz, albite, muscovite and chlorite.

Z391= Schist with chlorite, biotite, muscovite, albite, ilmenite and siderite from near fuchsite marble outcrop at grid reference 4625-8655 on toposheet 38 N/15.

Z392= Schist with fuchsite, quartz, hematite, muscovite, chlorite, calcite and magnetite from grid reference 4605-8655 on toposheet 38 N/15.

Z401= Schist with chloritoid, quartz, muscovite, chlorite and magnetite from grid reference 4605-8310 on toposheet 38 N/15.

---

metababbro forms an east-west elongated outcrop parrallel to the general trend of the ophiolite. The metagabbro contains abundant tremolite in addition to albite, clinozoisite, epidote, chlorite, quartz and rarely sphene. The norm shows presence of 'ab' molecule. A higher level "hornblende gabbro" outcrops in the western part of this gabbroic outcrop.

South of Musa Mena village, ultramafic section of the ophiolite is exposed.

Chlorite Schists

The chlorite schists exposed in the area are low-grade regionally metamorphosed pelitic rocks of greenschist facies or chlorite grade. The pelitic rocks were deposited long before the tectonic emplacement of the ophiolite. The rocks are thin bedded and individual layers may be only a few cms thick. Graphite is often present and many places are pyritic. Graphite content is economically exploitable from the lateral extensions of the same rock unit elsewhere. Chlorite abundance is conspicuous from the green colouration of the rock.

Monazite-bearing Chlorite Schist:

At the northeastern contact of the gabbroic rocks of Sakhakot-Qila ophiolite, a soapstone deposit is present in the chlorite schist.

Monazite is contained in a chlorite schist which is present at immediate contact of the Musa Mena soapstone quarry at grid reference 463-865 on topographic sheet no. 38 N/15 of the Survery of Pakistan. The rock actually hosts the soapstone. The rock is composed of chlorite, apatite, rutile and monazite which is rich in rare-earth elements, uranium and thorium. Monazite forms euhedral porphyroblasts. The green colour of the monazite-bearing rock is much deeper than that of other chloritic schists.

The chlorite analyses from the monazite-bearing chlorite schist are reported in table 1. The chlorite analyses from the adjacent schistose rocks which do not contain monazite are given in table 2. A comparison of the two tables shows that the monazite-bearing schist contains chlorite with conspicuously lower FeO and higher MgO than the rest of the schist samples. The chlorite in the monazite-bearing rock also shows lower TiO_2 and Al_2O_3 contents compared to the rest of chlorite schists. The chlorite from the adjacent ophiolitic rocks was also analyzed (Ahmed, 1982) and shows comparatively much smaller FeO. The chlorite of most non-monzonitic schists is generally ripidolite, although brunsvigite and pycnochlorite compositions are also encountered. The within-sample variations in these schists are large. For example, sample Z355 contains a brunsvigite associated with

ripidolite. Sample Z385 shows occurrence together of ripidolite and pycnochlorite.

The monazite-bearing rock also contains apatite whose analyses are reported in table 3. The Mn and Cl contents of the apatite are below the detection level of the microprobe.

Table 3. Apatite analyses.

FeO	0.46	0.30
MnO	0.00	0.06
MgO	0.22	0.08
CaO	55.50	55.60
Na_2O	0.05	0.06
K_2O	0.03	0.00
P_2O_5	42.35	42.30
Total	98.61	98.40

This chlorite schist is also different from the adjacent schists as it contains acicular rutile. Rutile is rare in other metamorphic rocks of the area, and its presence in this rock may indicate different P, T conditions. Rutile analyses are reported in table 4.

Table 4. Rutile analyses.

Anal. no.	1	2	3
SiO_2	0.41	0.30	0.70
TiO_2	94.76	98.75	96.24
Al_2O_3	0.97	0.00	0.50
Cr_2O_3	b.d.	b.d.	b.d.
FeO	1.54	1.05	1.25
MgO	1.10	0.00	0.68
MnO	0.23	0.00	0.04
CaO	b.d.	b.d.	0.00
NiO	b.d.	0.00	0.00
Na_2O	b.d.	0.00	0.00
K_2O	b.d.	0.00	b.d.
Total	99.01	100.10	99.41

Monazite

The monazite present in the rock was analyzed by electron microprobe (table 5). The mineral shows zoning and the core-rim pair analyses are also given in table 5. Distinctly strong uranium peak was observed during analyses of all the monazite grains. However, it could not be quantitatively measured. All REE were present in most of the spots, in some HREE were below detection limit. Ce and Nd are higher in cores, whereas Th is higher in the margins. Also, Sm, Gd and Dy are slightly higher in cores and Ca slightly higher in the rims. Low Totals of the analyses indicate the amounts of other elements and uranium that were not measured.

CONCLUDING REMARKS

Monazite is the principal ore mineral for rare earth elements and thorium, and is usually mined from beach sands and detrital sands derived from weathering of granitic rocks that often contain accessory amounts of monazite. Another common host of monazite are granitic pegmatites, which may also bear uranium and thorium minerals (Traill, 1983). A metamorphic monazite has been described only recently (Mohr, 1984) from highly graphitic metashales from North Carolina.

The present account describes a new occurrence of uranium and thorium-bearing monazite from chloritic schist. However, monazite does not seem to have formed with the chlorite schist, as its occurrence is in its restricted part only. Cullers et al. (1974) analyzed REE of

Table 5. Monazite analyses.

Anal. No.	1	2	3	4	5	6	7
Core/rim	core	rim	core	rim	core		
P_2O_5	29.86	29.56	30.38	30.32	29.56	29.94	30.15
La_2O_3	20.05	18.83	17.38	18.25	19.93	19.62	19.71
Ce_2O_3	31.07	29.61	29.93	28.82	30.95	31.18	31.25
Pr_2O_3	1.92	2.34	2.50	1.88	1.92	3.43	3.40
Nd_2O_3	12.24	10.98	14.84	11.01	12.18	12.37	12.45
Sm_2O_3	1.93	1.15	1.36	0.38	1.93	0.71	0.65
Gd_2O_3	0.32	0.28	0.51	0.41	0.32	0.28	0.27
Dy_2O_3	0.20	0.07	n.d.	n.d.	0.20	n.d.	n.d.
ThO_2	1.44	2.83	1.91	2.48	1.44	2.11	2.12
U	Present	Present	Present	Present	Present	Present	Present
CaO	0.48	0.60	0.58	0.59	0.00	0.60	0.50
Y_2O_3	0.00	b.d.	b.d.	b.d.	b.d.	b.d.	0.00
Total	99.51	96.25	99.39	94.14	98.43	100.24	100.50

pelitic schists of the greenschist and amphibolite facies from Maine, U.S.A. They concluded that REE content does not vary with metamorphic grade; rather it depends on the original protolith composition. It may have resulted from later metasomatic changes. The co-occurrence of a soapstone deposit in the monazite-hosting rock; and more magnesian composition of its chlorite (table 1) may point to possible effects of magnesium-rich solutions. However, since monazite genesis is often linked with granitic rather than magnesian rocks, and acicular rutile crystals are also developed in the same rock; probably more acidic solutions might be involved.

A review of the monazite paragenesis by Deer et al. (1962) does not mention its occurrence in chloritic schists. In this respect, the present occurrence of monazite is of a new type.

Metamorphic monazite only recently came to limelight with the work of Mohr (1984) on monazite from staurolite-kyanite grade metashales of North Carolina. From analyses, the monazite seems to be zoned with Ce and Nd being higher in the cores and Th higher in the rims. The uranium peak was not analyzed quantitatively but a distinctly high peak was observed in the energy-dispersive spectrum. The zoning observed in Musa-Mena monazite contrasts with that found in monazite from high-grade metamorphic shales of North Carolina by Mohr (1984). In the monazite of present study Th and Ca are higher in the rims than in the cores whereas in North Carolina both these elements are lower in the rims of monazite and higher in the cores. A Th- and U-lacking monazite from a quartz vein in North Carolina exhibits impove-

rishment of La and Ce but enrichment of Nd, Sm, Gd and Y in the rims (Bernstein, 1982). In Musa Mena, zoning is most marked for Nd, Ce (enriched in the cores) and Th (enriched in the rims).

The monazite bearing chlorite schist rock described here should be economically exploitable. Soapstone mining has already been done. The rock also has titanium mineral, rutile. It contains sufficient quantity of monazite which contains uranium, thorium and rare-earth elements such as lanthanum, cerium, praseodymium, neodymium, samarium, etc., which form a phosphate compound. The rock is sufficiently softer to be mined out by routine blasting operations and can yield a variety of products besides uranium. More search is likely to lead to more finds of the same mineralization in the nearby areas.

ACKNOWLEDGMENTS

The author is grateful to Ds. J.V.P. Long and P.J. Treloar of the Cambridge University, UK, and Ian Young and Dr. R.M.F. Preston of the University College, University of London, for providing the electron microprobe facilities at these institutions to carry out this study.

REFERENCES

AHMED, Z. (1982) Chromite deposits of the Sakhakot - Qila ultramafic complex, Pakistan, Unpub. Ph.D. thesis University of London, UK, 344 p.

— (1984) Petrology and mineralization of the Sakhakot - Qila ophiolite, Pakistan. In Gass, I.G., Lippard, S.J. and Shelton, A.W. (eds.) OPHIOLITES AND OCEANIC LITHOSPHERE. Spec. Pub. Geol. Soc. London 13, pp. 241 - 52.

MOHR, D.W. (1984) Zoned porphyroblasts of metamorphic monazite in the Anakeesta Formation, Great Smoky Mountains, North Carolina. Amer. Mineral. 69, pp. 98 - 103.

DEER, W.A., Howie, R.A. & Zussman, J. **(1962)** ROCK FORMING MINERALS: Vol. 5. Longmans, London, 371 p.

BERNSTEIN, L.R. (1982) Monazite from North Carolina having the alexanderite effect. Amer. Mineral. 67, pp. 356 - 9.

CULLERS, R.L., YEH, L—T., Chaudhuri, S. & Guidotti, C.V. (1974). Rare earth elements in Silurian pelitic schists from N.W. Maine. Geochim. Cosmochim. Acta 38 (3), pp. 389 - 400.

TRAIL, R.J. (1983) Catalogue of Canadian minerals: Revised 1980. Geol. Surv. Canada Paper 80-18, 432 p.

ACTA MINERALOGICA PAKISTANICA
VOLUME 1 (1985) pp. 34-37

A PROPOSAL TO STUDY THE CHAMAN NUSKHI FAULT ON THE PATTERN OF SAN ANDREAS FAULT

ABDUL HAQUE

Department of Geology, University of Baluchistan, Quetta, Pakistan.

Abstract: Based partly on bibliographical work and partly on laboratory and field observations, the results of study of Nushki-Chaman fault in Pakistan are compared to the San Andreas fault in the United States, in view of the importance of involved concept of tectonic plates. However, proposed studies will restrict to simple features explaining the model experiments such as: strain ellipsoid method; microstructural analysis; fault plane solution; history of earthquakes data and field mapping, etc. as compared to the types of studies already done over San Andreas fault.

INTRODUCTION

Both, the San Andreas fault in the United States and Nuskhi-Chaman fault in Pakistan are of regional importance. The latter one was discovered by Griesbach (1893), after (1892) earthquake.

San Andreas fault is situated at the limit of western Pacific plate and North-American plate; while Nuskhi-Chaman fault shows the suture line between two plates, Indo-Pakistani plate in the east, and Eurasian plate in the west. The former one is oriented NW–SE with dextral horizontal movement, having length 900 km; while the latter one has N–S to NE–SW orientation with both horizontal and vertical sinistral movements measured 1100 km with its southern branch Ornach-Nal fault, having 1000 km radius of curvature (Auden, 1974).

Both faults are considered as capable of producing destructive earthquakes. These include incidents of 1906 and 1971 earthquakes, associated with the San Andreas fault and the intense earthquakes of 1892, 1935 produced by Nuskhi-Chaman fault.

CHARACTERISTICS

Both faults are of regional importance. San Andreas fault is oriented NW–SE with dextral horizontal displacement having zero pitch; whereas Nuskhi-Chaman fault has NS & SW directions, having both horizontal and vertical sinistral movements, and of variable pitch.

The attitude of San Andreas fault is nearly vertical while for Nushki-Chaman fault, is probably vertical in the depth and becomes inclined with vergeance towards west at the surface. The width for both the fault zones varies from few metres to several km.

From the earthquake data, the depth of the San Andreas fault is 25 km and at the time of 1892 earthquake, the vertical displacement calculated over the Nushki-Chaman fault, by Griesbach has been 0.75 m.

Both the faults have a long geological history regarding their origin. San Andreas fault, at present, is the product of expansion and subduction zones, while Nushki-Chaman fault has resulted purely through the collision of two

plates.

On both sides, the abrupt termination of geological deposits, on the one hand, and recently the discovery of gravity anomaly (Mc-Ginis, 1971) on the other hand, show the megatectonic importance of Nushki-Chaman fault which thus fall in the category of Eyzincan fault in Turkey and Toktogai fault in Russia (Auden, 1974).

SENSE OF DISPLACEMENT

The velocity over San Andreas fault has been calculated as 4 to 6.5 cm per year since several million years ago. Such determination is still required for Nushki-Chaman fault. However it is hypothetically proposed that the velocity over Nushki-Chaman fault is 3 to 4 cm per year (Paul Tapponnier, personal communication).

During violent earthquake of San Francisco intensity of 8.3 Mercalli scale, in April 1906, the horizontal displacement measured over San Andreas fault had been upto 6.5 m. and in 1971 earthquake of San Fernando, this fault has registered only a displacement vector of 1.8 m. Moreover, the velocity calculated through magnetic anomalies method for the ocean shows the expansion rate of upto 6.5 cm per year. At present, the displacement rate varies from 1 to 3 cm per year.

Regarding Nushki-Chaman fault, the work of Griesbach in 1893, on the 1892 earthquake shows a vertical displacement of 0.75 m. A lot of work remains to be done regarding the historical earthquakes data, which should lead us to evaluate the intensity of historical destruction and future seismic prevention: such as economically exorbitant construction in the Chaman-Quetta-Nushki-Bela areas. Such constructions would not be apocalyptic to the national economy as that of 1935 earthquake, as we know this megafault is geologically active, because it cuts the recent deposits and piedmonts, as observed visible over aerial photographs, which can be easily verified through proper geological field mapping. In addition, with the Ornach-Nal fault are associated the most recent and the most active faults visible in the eastern side, which show that the Indian plate is still in motion towards north (Powell, 1979).

ORIGIN

All previously mentioned geological and geophysical data, regarding San-Andreas fault have a direct relation to the relative motion of the corresponding involved plates. Hence, the absence of magnetic anomalies in the eastern coast of California indicates that an oceanic dorsal has been forced into collision with the North-American plate roughly 30 million years ago (Atwater, 1970).

Generally, the rate of expansion over mid-oceanic ridges can be compensated reciprocally with the rate of subduction, which in fact, leads to the concepts of sea-floor spreading and eventually plate tectonics. In the case of San Andreas fault, the expansion velocity has never been the same as that of subduction. Consequently, the dorsal reaches nearer to the North-American plate, the geometry and dynamics of interaction between the corresponding two plates would have been changed. The absence of magnetic anomalies over the Farallon plate (situated between Pacific and American plates), indicates they have been eaten by the subduction zone. This scenario began in Tertiary, thus showing the first tectonic meeting dates 20 to 30 million years ago. Present limits between the mid-oceanic ridge and subduction zone define the actual orientation of San Andreas fault, which facilitate the dextral movement between Pacific and North-American plates.

On the contrary, the Nushki-Chaman and Ornach-Nal fault is purely due to the collision of Indo-Pakistani plate on the east and Eurasian plate to the west and defines a major suture line. This 1100 km long fault has been active throughout the Tertiary period after Eocene and since then it shows a displacement of 300 km (Powell, 1979). Before the collision of

Indian plate against the Eurasian plate, the present Makran-Kirthar-Sulaiman chains had E–W direction. The actual meridional orientation of these chains is due to the collision of these two plates, which produced a tectonic transport towards Indian foreland (Andrieu & Brunel, 1977; Stöcklin, 1977; Powell, 1979).

As we go far from the fault zone towards east, the associated minor faults become more and more recent in age. Thus near the main fault the age of these faults is Plio-Pleistocene and toward Indian foreland their age becomes Pleistocene-Recent.

ORIGIN OF STRESSES

San Andreas Fault

The collision of the two corresponding involved plates has generated the stress system which has, by consequence fabricated the actual tectonics of the region.

Northern California has been divided into several blocks, each has its own stress system. Amongst these blocks the Majove block has two parts, eastern and western, each of them has again a tectonics designed by the morphology of the region. Thus the eastern part has been active throughout the Holocene period and still continues, being characterized by the NW–SE strike slip faults over which displacements are in the direction of dip. On the contrary, the morphology of the western part of Majove block suggests that in the Holocene period, it was tectonically inactive, however, with few sporadic earthquakes (Bull, 1977).

The result obtained successively from different methods namely: mechanics of epicentre suggests the stress orientation is N-S; the strain ellipsoid method shows NW–SE direction; triangulation method in the north of "Transverse Range" gives N-S compression; the seismic, geodetic and deformational analysis in the region of California and in Nevada permit us that the regional stress is oriented N-S, while near the fault, this orientation slightly changes its direction.

In the region of central California the orientation of San Andreas fault is N40W, but the limit between San Andreas and Majove block is N 70° W, while the relative movement between them is in the direction N 40° W. Thus the region has gone through N-S compression verified by the folds and inverse faults of E-W direction and the E-W orientation of eastern and western "Transverse Ranges" (Minister et al., 1974). Moreover, the thrust mechanism of "Kern country" and the recent earthquake of San Fernando also suggests N-S compression with horizontal dip. This orientation of stresses is again compatible with the deformation of Neogene geology (Marc.L.Shar, 1979).

The pole of rotation for the boundary of corresponding two plates (i.e. San Andreas fault) is situated at 50° 9' and 66° 3' E. Therefore, the two circles of rotation are compatible with the direction of San Andreas fault (Minister et al., 1974). Moreover, on both sides of this limit several geological and structural features, which have been called "the system of San Andreas fault" such as: earthquakes of 1836, 1906, 1971; the presence of volcanoes; the coastal mountain chains, and the multiple fracture pattern of California verify the megatectonic importance of San Andreas fault.

Zaback (1979) has calculated that the shear stress increases over San Andreas fault from 17±4 bars to 54±4 bars with the augmentation of distance from 2 to 20 km and the shear stress augments slowly upto 100 bars with varying depth from 15 to 20 km. Moreover, compressive stress obtained from Well's method being dugged on both sides of the San Andreas fault, show that it is horizontal of direction N10°W±10° which makes an angle of 45° with the San Andreas fault.

Nushki-Chaman Fault

After the collision of Indo-Pakistani plate

with the Asian plate, which has created the present orographical features of Baluchistan geology, in which one can apply all the above mentioned methods to study in detail this regionally important fault, to get the proper stress orientation. For example, with strain elliposid method on the one hand, and by analyzing the microstructures associated with the main fault on the other hand, one can get regional direction of stress axes.

My unpublished data of fracture analysis through different methods, over seven different maps, on a scale 1 inch to 4 miles, shows the following results; the number of fractures measured only in the Axial Belt of Baluchistan geosyncline area is 4295, among them 224 faults having dip angles, in which 139 faults dip toward Afghan plate; 61 faults towards Indian shield and 24 faults are vertical. Moreover, through the results of strike-frequency and density diagrams we can say that from Bela to Sibi (4 maps) the Nushki-Chaman fault behaves like strike-slip fault, while from Quetta to Zhob (3 maps) this fault has both horizontal and vertical components, with direction roughly E-W. Amongst the thrust faults in these regions 62 faults are dipping towards north, 14 faults are dipping towards south and only 8 faults are vertical.

ACKNOWLEDGEMENTS

I am extremely grateful to Messieurs J. Mercier and P. Tapponnier, Professors in the Universities of Paris XI and Paris VI, for their worthy discussions over the given problem, during my studies in France. My gratitudes go equally to Professor Dr. Zulfiqar Ahmed, Director C.E.M., Baluchistan University both for his useful suggestions in the preparation of this paper and for his corrections of the manuscript.

REFERENCES

ANDRIEUS, J., & BRUNEL, M. (1977) L' evolution des chaines accidentales du Pakistan. Mem. H.Ser., Soc. Geol. France. 8 pp. 189 - 207.

ATWATER. T. (1970) Implications of the plate tectonics for the Cenozoic tectonic evolution of western North America. In: Cox, A. (ed) PLATE TECTONICS & GEOMAGNETIC REVERSALS, pp. 583 - 609.

AUDEN, J.B., (1974) Afghanistan-West Pakistan. In: Spencer. A.M. (ed) MESOZOIC—CENOZOIC OROGENIC BELTS. Geol. Soc. London Spec. Pub. 4, pp. 235 - 53.

BULL, W.B. (1977) Tectonic geomorphology of the Majave Desert. U.S. Geol. Surv., office Earthq. Stud., Semi-annual grant report, 200 p.

GRIESBACH, C.L. (1893) Notes on the Central Himalyas. Rec. Geol. Surv. India, **26** (1), pp. 19 - 25.

MARC, L.S. (1979) Stress pattern near San Andreas fault, Palmadale, California, from near-surface in situ measurements. Jour. Geophys. Res. **84** (B 1), pp. 156 - 64.

MARK, O.Z., & JOHN, C.R. (1979) Magnitude of shear stress on the San Andreas Fault, implications of shear measurements profile at shallow depth. Science **206** (4417), pp. 445 - 7.

MC—GINIS, L.D. (1971) Gravity fields and tectonics in the Hindu Kush. Jour. Geophys. Res. **76**, pp. 1894-904.

MINISTER, J.R., JORDAN, T.H., MOLNAR, R. & HAINES, E. (1974) Modelling of instantaneous plate tectonics. Geophys. Jour. Roy. Astron. Soc. **36**, pp. 541 - 76.

POWELL, C. McA. (1979) A speculative tectonic history of Pakistan and surroundings: some constraints from the Indian Ocean. In: Farah, A.& De Jong, K.A. (eds) GEODYNAMICS OF PAKISTAN, Geol. Surv. Pak. Quetta, pp. 5 - 24.

STÖCKLIN, J. (1977) Structural correlation, of the Alpine ranges between Iran and central Asia. Mem. Ser. Geol. Soc. France. 8, pp. 333 - 53.

ACTA MINERALOGICA PAKISTANICA
VOLUME 1 (1985) pp. 38-48

PETROCHEMISTRY OF THE CONTACT ROCKS FROM NORTHWESTERN JUNGTORGARH SEGMENT OF THE ZHOB VALLEY OPHIOLITE, PAKISTAN

MUHAMMAD MUNIR & ZULFIQAR AHMED
Centre of Excellence in Mineralogy, University of Baluchistan, Sariab Road, Quetta, Pakistan.

Abstract: **The results of whole-rock chemical and modal analyses of metasedimentary, metaigneous and ophiolitic rock samples from the northwestern portion of the outer contact of Jungtorgarh massif are reported. The metamorphic envelope rocks were sampled along traverses perpendicular to the contact to observe the effects and intensity of metamorphism as the basal ophiolitic contact is approached. The contact bears a thin parallel sheet composed of garnet orthoamphibolite and garnetiferous pelitic schists, both of which retain chemical differences of their protoliths. Beyond these, greenschist facies metasediments unmetamorphosed sediments occur with a parallel contact. A satellitic basaltic outcrop enclosed by metasediments possesses tholeiitic nature and is probably lesser factionated compared to average MORB composition.**

INTRODUCTION

The Zhob Valley ophiolite, spread over more than 2000 sq. miles area around the valley formed by Zhob River, is composed of five major segments. These segments were probably together and formed an overthrust sheet which presumably lost its coherence during emplacement (Abbas and Ahmad, 1979). One of these segments is the Jungtorgarh massif which outcrops over 150 km² area located south of Muslimbagh town. This massif is considered to be a tectonic klippe underlain by slivers of metamorphic rocks, serpentinite and mélange. Its lower contact is a thrust which trends across the structures in the interior of the massif.

The northwestern contact of Jungtorgarh carries a special significance as it shows the development of garnet amphibolites and other metamorphic rocks at the ophiolitic contact. A decrease in metamorphic grade away from the ophiolitic contact has also been reported at this locality. Older accounts of the Zhob Valley igneous complex regarded these rocks as representing a part of the contact aureole around the intrusion. Although the ophiolites are emplaced without a contact aureole, sequences of metamorphic rocks associated with the basal parts of ophiolites are reported from various parts of the world (e.g., Williams & Smyth, 1973,; Searle and Malpas, 1982) where these often form thin sheets displaying greenschist to amphibolite facies metamorphism that increases towards the ultramafic rocks. These rocks are important in ophiolite emplacement models.

This study was conducted to understand the nature of mineralogical and petrological changes across the contact along five different traverses at nearby places. The rock samples collected include metasedimentary rocks, garnet amphibolites, basalts and ophiolitic ultramafic rocks. They include the subophiolitic metamorphic rocks as well.

GENERAL GEOLOGY

The Jungtorgarh ophiolitic rocks probably originated at a spreading centre and got obducted on the western margin of the Indo-Pakistan plate during Palaeocene or early Eocene. The massif tectonically overlies the Maastrichtian age Parh Formation composed of limestones and shales; and older sedimentary rock formations. The massif is mainly composed of ultramafic tectonites (Moores et al., 1980). Rock types include harzburgite, chromitite, dunite, a few dolerite dykes and pillowed basalt.

The geological map of the northwestern part of Jungtorgarh is given in fig. 1. The map projects the outer contact of ultramafic rock massif composed of harzburgite and dunite. Successively outwards from the massif are found outcrops of garnet-bearing amphibolite, garnetiferous biotite schist, biotite-schist, muscovite-chlorite schist with marble bands. Next come the limestones and subordinate shales of Loralai Member of early Jurassic age; and shales and limestones of Alozai Group of Triassic age. A very small tectonic segment of volcanic rocks and breccias occurs separated from the main igneous mass. Various schistose lithologies have subparallel outcrops along the contact which displays some faults at high angle.

ANALYTICAL METHOD

The whole-rock chemical analyses reported in tables 1 through 4 were performed at the labortories of Chemistry Department, University of Paris 7 in France.

Al_2O_3 and SiO_2 were determined gravimetrically. FeO was determined by the Wilson's method, H_2O^+ by modified Penfield method and rest of the major element oxides were determined by spectrochemical methods.

PETROCHEMISTRY

Ultramafic Rocks

In table 1, chemical and normative compositions of one harzburgite and two dunite samples are listed. Their "mg" values (=MgO/(MgO+FeO)) are 0.86 for dunite and 0.85 for harzburgite. Compositions resemble those of typical ophiolitic rocks (Coleman, 1977, tables 1, 2) and fall within the variation ranges shown by corresponding unaltered rock types. The table also reports their mineral contents. The harzburgite probably belongs to the basal part of the ophiolite.

Basalts

An isolated basalt outcrop without pillow structures lies enclosed in metasedimentary rocks with its outer contact concealed under alluvium. Chemical and modal compositions and normative constituents for three samples are given in table 1. Their alkalis vs silica weight percentages plot (fig.2A) brings out their tholeiitic nature and their nearness to MAR basalt. Tholeiitic nature of the basalt liquid is indicated in some other plots as well. The basalt analyses (tabel 1), show high CaO probably due to calcite amygdules. The basalts are richer in soda compared to potash. The MnO content of these basalts is distinctly higher than most known ophiolitic basalts (cf. Coleman, 1977, table 7; Siroky et al., 1985).

CIPW norms show 'di' content of 14 to 21%. Normative quartz is present in one rock. Plagioclase of basalts has An content of 28 to 30%.

In the TiO_2 versus FeO (total)/MgO diagram, these three basalts plot within or near the major MORB trend and away from the Troodos glasses, island arc tholeiites and other thoeiitic magmas found in island arcs. But since there are only three samples included in this study, analyses of more samples, especially of those with higher TiO_2 content, will be needed to establish this trend. A comparision of the basalt analyses with the mean chemical composition of Mid-Atlantic Ridge basalt shows that the Jungtorgarh samples are not much different, except their smaller TiO_2 content. The three samples have lower TiO_2 and total iron and higher MgO and CaO (except lower lime in one sample) than the MORB. It may probably be due to their fractionated nature. With the three samples, variation range is not large, and so is probably their difference in fractionation.

Amphibolites

Amphibolites with about 2% garnet are developed at immediate contact of the ultramafic rocks. Modal and chemical whole-rock compositions of three samples are given in table 2. Their plagioclase composition varies from albite to andesine. Their plots in the ACF diagram (fig. 3) match the orthoamphibolites derived from basic volcanic rocks rather than

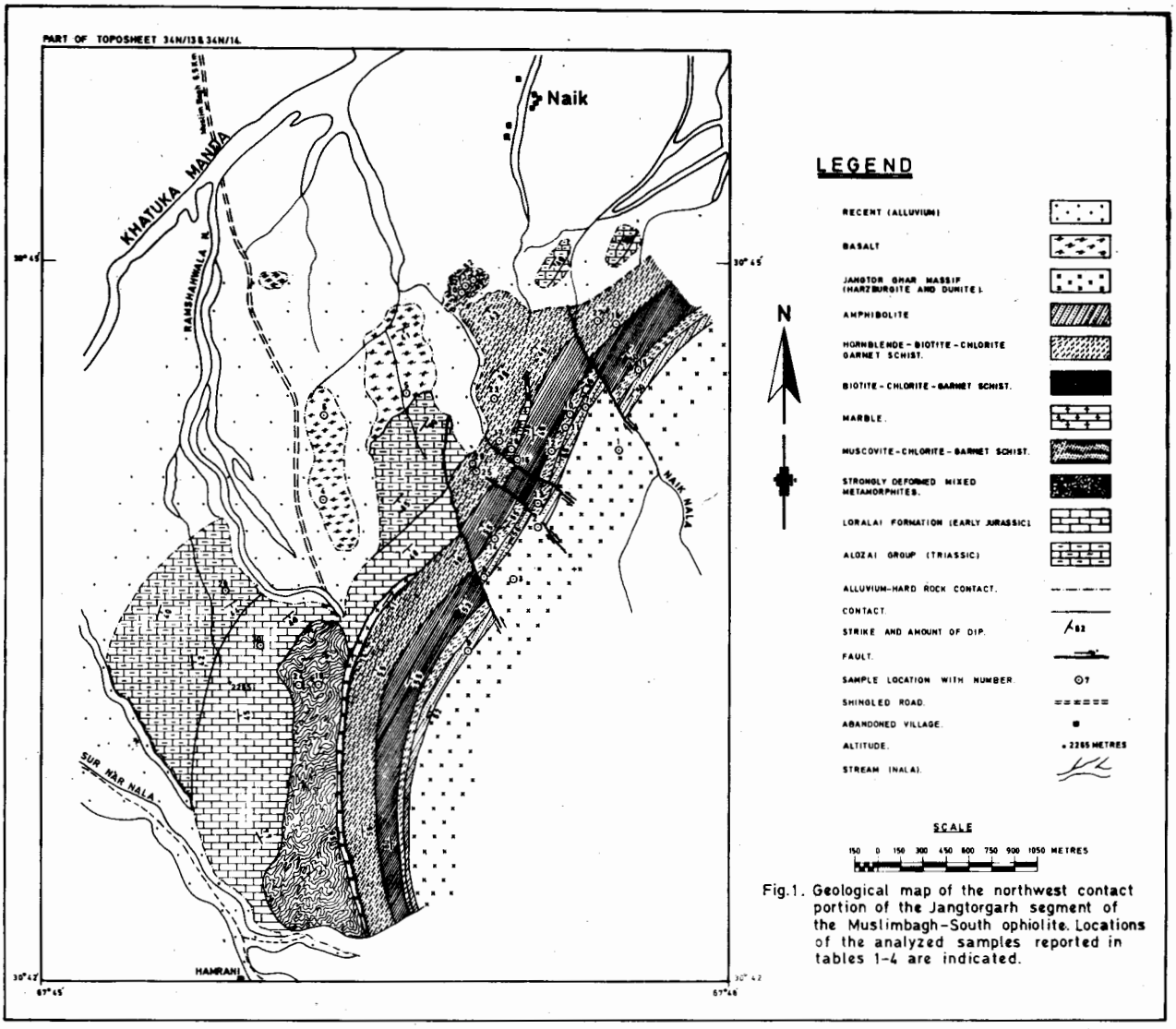

Fig.1. Geological map of the northwest contact portion of the Jangtorgarh segment of the Muslimbagh-South ophiolite. Locations of the analyzed samples reported in tables 1-4 are indicated.

sediments. Quartz abundance may be due to tholeiitic parentage. Epidote is especially abundant in one rock, whereas plagioclase is more in another. Field relations exclude the possibility of these amphibolites being derived from the gabbroic parts of the ophiolite. The amphibolite zone is very thin (fig. 1); and the ophiolitic rock in all the NW Jungtorgarh massif is mostly tectonitic harzburgite which probably represents the basal portion of ophiolite. Individual chemical analyses do not display significant differences amongst the garnet amphibolites.

Garnet rich schists

The composition of these rocks is shown by samples 10 to 15 in table 2. Compared to the associated amphibolites, these schists have distinctly higher SiO_2, Al_2O_3, FeO and K_2O; and have lower MgO, Fe_2O_3, CaO and Na_2O.

In their mineral assemblages, quartz, garnet, biotite and chlorite are higher and feldspar and hornblende are lower than the associated amphi bolites. These schists are different mineralogi

Table 1. Chemical, normative and modal compositions of Jungtorgarh harzburgite (1) dunite (2,3) and basalts (4–6). The mean composition of mid-ocean ridge basalt, from mid-Atlantic ridge (Melson & Thompson, 1971) is given under MORB.

Sp. No.	1	2	3	4	5	6	MORB
SiO_2	44.50	38.20	39.09	48.56	49.61	49.81	49.21
TiO_2	–	0.11	0.10	0.78	0.61	0.25	1.39
Al_2O_3	1.80	1.00	1.62	16.32	15.25	15.75	15.81
Fe_2O_3	3.15	3.75	2.00	3.64	3.29	3.00	2.21
FeO	4.29	4.98	4.75	5.33	5.07	5.25	7.19
MnO	0.10	0.06	0.05	2.16	2.20	1.25	0.16
MgO	42.50	47.48	47.69	8.69	10.68	10.43	8.53
CaO	0.60	0.25	0.22	13.22	9.95	11.53	11.14
Na_2O	0.10	0.03	0.05	1.04	2.84	2.21	2.71
K_2O	0.30	0.21	0.25	0.36	0.50	0.50	0.26
Cr_2O_3	0.15	2.35	2.69	–	–	–	–
H_2O^+	2.51	1.56	1.49	–	–	–	–
Total	100.00	99.98	100.00	100.10	100.00	99.98	–
C.I.P.W. Norms:–							
Q	–	–	–	1.29	–	–	
C	0.22	0.265	–	–	–	–	
or	1.78	1.225	1.503	2.11	2.95	2.95	
ab	0.83	0.262	0.420	8.81	24.01	18.72	
an	2.97	1.252	1.085	38.86	27.45	31.63	
di wo	–	–	–	11.16	9.15	10.67	
di en	–	–	–	7.22	3.83	7.28	
di fs	–	–	–	3.17	1.39	2.53	
hy en	22.70	1.351	2.476	14.41	3.12	8.59	
hy fs	1.39	0.45	0.097	6.33	1.12	0.30	
ol fo	54.76	81.918	81.495	–	13.76	7.06	
ol fa	3.03	2.992	3.522	–	5.49	5.44	
mt	4.56	5.441	2.894	4.64	4.76	4.35	
il	–	0.212	0.197	1.48	1.15	0.47	
cm	0.223	3.470	3.962	–	–	–	
Modal Compositions:							
Olivine	86.0	95.0	92.0	—	2.0	—	
Enstatite	8.0	—	—	—		—	
Pyroxene	—	—	—	35.5	36.5	35.0	
Serpentine	2.5	2.0	4.2	—	—	—	
Opaques	3.5	3.0	3.8	5.0	—	4.0	
Hornblende	—	—	—	—	—	6.0	
Plagioclase	—	—	—	49.9	46.6	47.0	
Epidote						1.0	
Amygdules:							
Quartz				2.6	3.9	–	
Calcite				6.0	6.0	6.0	
Natrolite				1.0	1.0	1.0	

Table 2. Analyses of garnet-rich metamorphic rocks at immediate contact of ultramafic rocks. Analyses 7 to 9 are of amphibolites; rest are metasedimentary schists.

Sp. No.	7	8	9	10	11	12	13	14	15
SiO_2	53.33	55.13	53.67	59.60	59.80	59.15	60.15	59.25	58.17
TiO_2	0.98	0.59	0.31	—	—	—	—	—	—
Al_2O_3	14.09	14.07	14.00	19.85	18.49	20.26	19.86	19.79	21.25
Fe_2O_3	4.37	2.50	4.50	2.35	4.79	2.57	3.75	3.89	2.60
FeO	3.00	2.50	2.50	4.40	6.31	5.05	4.25	4.05	3.50
MnO	1.09	3.02	1.03	1.25	1.24	0.75	1.75	1.25	0.75
MgO	8.01	8.38	8.31	1.97	2.25	2.75	2.13	2.95	1.95
CaO	8.52	6.06	7.69	1.33	0.93	2.85	1.00	2.49	2.05
Na_2O	5.15	5.49	5.59	1.80	1.07	1.50	1.06	1.15	1.30
K_2O	0.08	0.19	0.14	5.75	4.13	5.25	5.05	4.15	6.59
P_2O_5	0.33	1.21	0.36	—	—	—	—	—	—
H_2O^+	1.07	1.25	1.91	1.73	1.00	1.88	1.65	1.05	1.88
Total	100.02	100.39	100.01	100.03	100.01	100.01	100.60	100.02	100.04
Mineral assemblages (%):									
Quartz	2.5	2.5	8.2	42.0	40.4	38.7	42.5	39.6	49.5
Feldspar	4.5	8.6	14.5	6.4	6.5	6.5	10.5	10.6	12.0
Garnet	1.0	2.0	2.0	6.6	6.0	6.5	8.5	5.5	6.4
Hornblende	60.0	82.5	65.5	6.5	7.0	6.1	9.5	10.5	8.5
Actinolite	—	—	6.0	—	—	—	—	—	—
Biotite	—	—	3.4	22.5	19.7	18.8	12.5	10.0	10.9
Muscovite	—	—	—	—	2.9	2.8	—	2.5	—
Chlorite	—	—	—	9.5	7.9	8.0	6.5	7.9	8.8
Epidote	30.0	2.4	—	—	4.9	5.0	6.5	8.5	—
Sphene	0.5	1.0	0.3	—	—	—	—	—	—
Apatite	0.5	1.0	0.1	—	—	—	—	—	—
Calcite	1.0	—	—	4.0	—	3.8	1.5	2.0	—
Opaques	—	—	—	2.5	4.8	4.0	2.0	3.0	4.0

cally and chemically from the spatially associated garnetiferous amphibolites. The former may be derived from a sedimentary protolith in contrast to the mafic volcanic protolith of the latter.

The modal garnet content of the schists (table 2) varies from 5.5 to 8.5% as against the 1 to 2% garnet of associated amphibolites; and is probably due to difference in the source materials. The schists contain much lower hornblende, 6 to 11%, as compared to the amphibolites with 60 to 83% hornblende. Quartz is significantly lower in the amphibolites (table 2).

Their chemical compositions are comparable to typical pelitic schists (Mueller & Saxena, 1977) except their slightly higher SiO_2, MnO, CaO and K_2O and a little lower MgO and Al_2O_3.

Low-garnet schists

The modal and bulk-rock chemical compositions of these rocks, as given in table 3, suggest derivation from sediments rather than basic igneous rocks. They are chemically very close to the garnet-rich schists of table 2; and are drastically different from the orthoamphibolites of

Table 3. Whole-rock analyses of low-garnet schists located outwards from garnet-rich rocks.

Sp. No.	16	17	18	19	20	21	22
SiO_2	59.25	58.29	60.24	61.60	61.33	59.79	58.60
Al_2O_3	20.85	20.03	21.61	19.35	17.51	20.06	20.56
Fe_2O_3	3.40	3.29	2.25	2.65	4.49	3.01	2.99
FeO	4.71	6.00	3.25	4.41	6.43	2.79	3.98
MnO	0.69	1.25	0.61	1.24	0.13	1.60	1.75
MgO	1.75	2.11	2.02	2.50	2.11	2.93	2.07
CaO	0.90	1.10	2.06	0.95	0.97	1.15	1.85
Na_2O	1.35	2.05	1.10	1.10	1.69	1.62	1.55
K_2O	5.35	4.89	6.25	5.23	4.05	5.35	4.95
H_2O^+	1.85	1.03	1.60	1.08	1.69	1.85	2.08
Total	100.10	100.04	100.99	100.03	100.40	100.15	100.08
Modal Compositions:							
Quartz	40.3	46.6	56.7	71.9	55.1	44.5	43.0
Plagioclase	2.0	2.9	3.4	—	2.0	4.6	2.3
Orthoclase	4.2	2.0	2.3	—	2.0	2.3	2.0
Garnet	4.0	2.0	2.0	3.0	2.0	2.5	3.0
Biotite	15.0	2.0	—	—	16.8	—	—
Chlorite	5.5	8.0	10.0	6.5	12.3	15.0	20.5
Muscovite	25.6	30.5	19.6	12.7	5.9	28.6	25.0
Epidote	—	—	5.0	3.5	—	—	—
Calcite	—	—	2.2	—	3.0	—	—
Opaques	3.5	6.0	—	2.4	1.1	2.3	4.3

Table 4. Whole-rock analyses of schists without granet (23 to 26), enclosed marble beds (27, 28) and unmetamorphosed illitic shales (29,30).

Sp. No.	23	24	25	26	27	28	29	30
SiO_2	61.75	58.75	61.27	60.00	10.06	9.86	52.65	51.89
TiO_2	–	–	–	–	–	–	0.21	0.19
Al_2O_3	19.20	20.35	20.21	21.75	7.82	6.65	24.33	24.25
Fe_2O_3	2.65	2.08	2.60	2.90	0.25	0.10	3.21	3.59
FeO	4.25	6.25	3.25	3.40	0.16	0.50	2.10	2.69
MnO	0.15	1.07	1.15	0.63	–	–	–	–
MgO	2.10	2.11	2.15	2.15	5.50	4.00	2.14	1.15
CaO	0.86	1.02	2.05	2.10	49.58	50.95	2.25	2.35
Na_2O	1.44	1.15	1.10	1.09	0.02	0.06	1.36	1.79
K_2O	5.80	5.25	4.89	4.69	1.16	1.88	6.25	6.39
H_2O^+	1.77	1.32	1.39	1.30	0.50	1.00	5.50	5.14
CO_2	–	–	–	–	20.09	25.60	–	–
Total	99.97	100.30	100.06	100.01	100.09	100.60	100.25	100.03
Modal Compositions:								
Quartz	22.0	22.8	61.0	66.0	6.5	7.3		
Feldspar	6.5	3.8	–	4.6	–	–		
Biotite	–	–	–	–	–	0.5		
Chlorite	45.0	54.0	3.4	2.5	–	–		
Muscovite	5.0	12.5	18.4	16.5	3.2	4.7		
Phlogopite	–	–	–	–	1.0	2.4		
Talc	–	–	8.3	7.0	–	–		
Epidote	18.0	4.5	3.3	3.4	1.5	1.9		
Calcite	–	2.5	–	–	87.4	82.3		
Opaques	3.5	–	–	–	–	–		

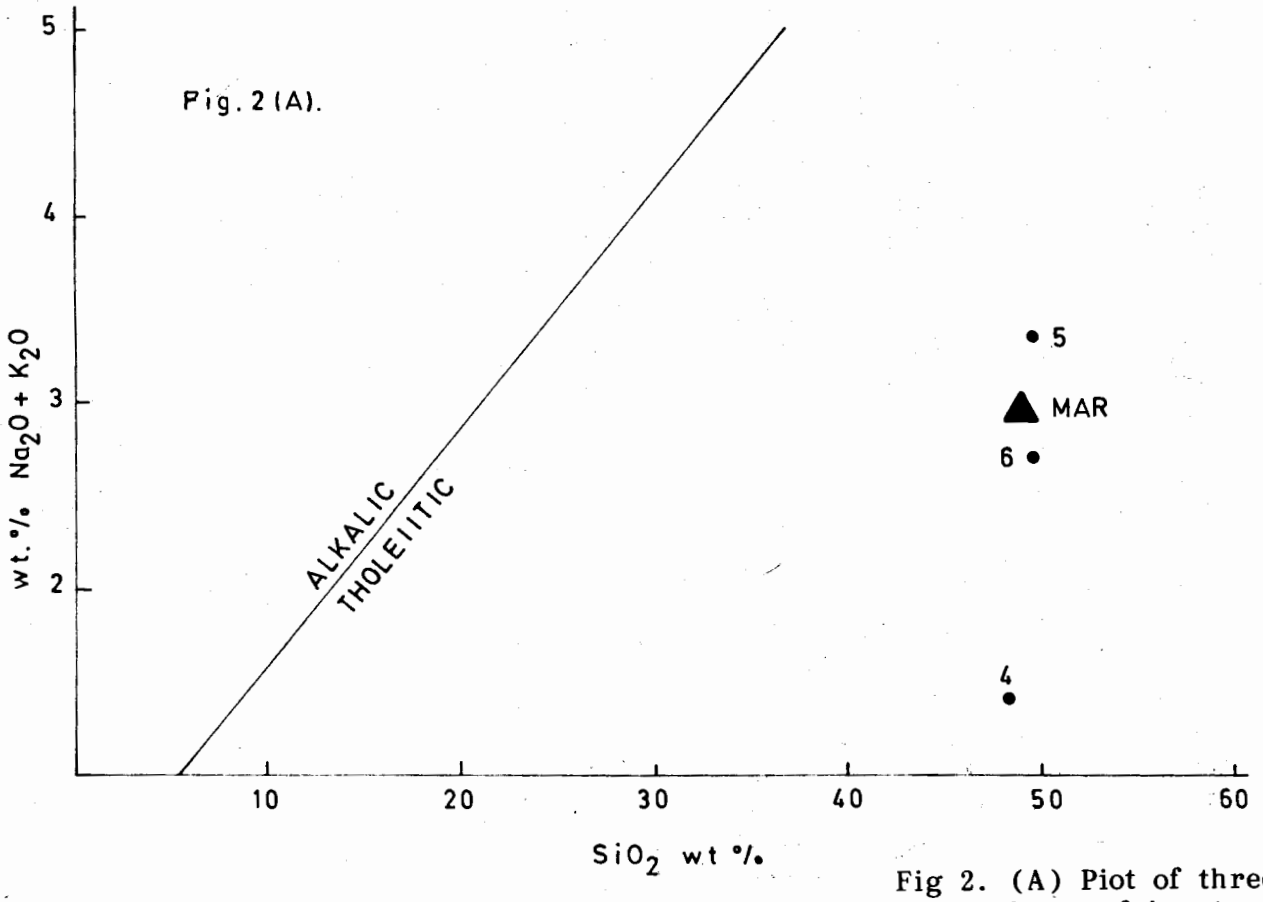

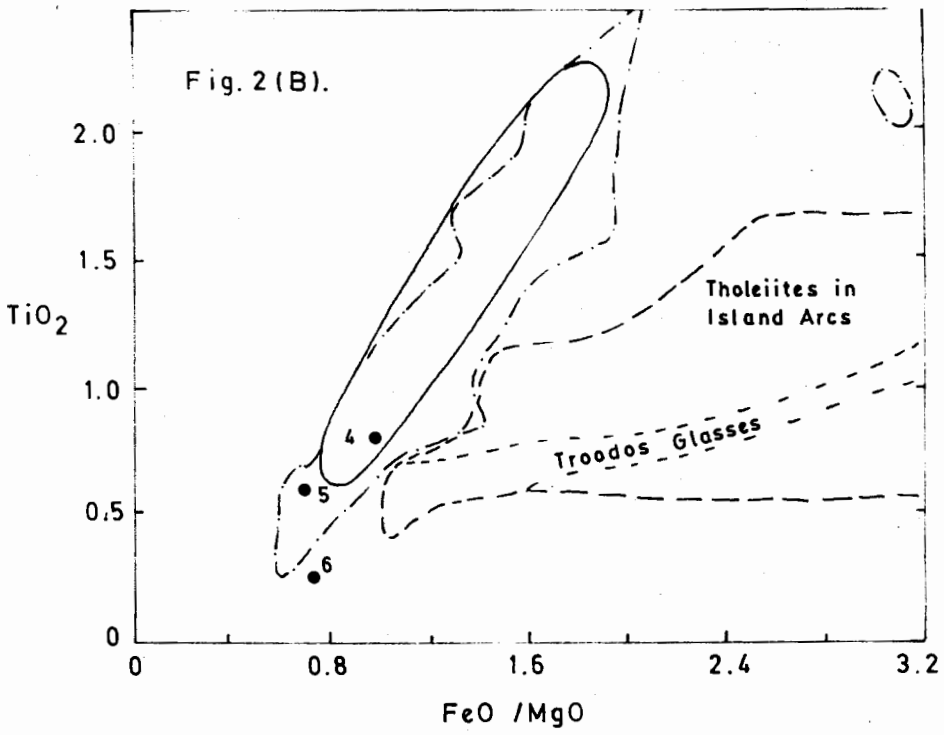

Fig 2. (A) Piot of three analyses of jungtorgrah basalts and MAR basalt on the diagram after Vallance (1974) Showing tholeiitic nature of basalts.

(B) TiO_2 Versus FeO/MgO variations in the Jungtorgarh basalts (numbered dots) compared to mid-ocean ridge basalts (solid line), tholeiites in island arcs (longerdash line) glasses from the Troodos ophiolite, Cyprus (short-dash line), and diabases from the Bay of Islands ophiolite, Newfoundland, Canada (dash & dot line). Drawn after Caseyetal 1985.

table 2. They also resemble metasedimentary schists without garnet, reported in table 4. Their high potash (4.05 to 6.25%) and relatively low soda (1.10 to 2.05%) and lime (0.90 to 2.06%) contents suggest pelitic sedimentary derivation. The plots on A'KF diagram (fig. 3) also indicate their resemblance to the metasedimentary schists of fig. 2 and not the orthoamphibolites in the same plot. Modal compositions show abundant quartz (43 to 72%), chlorite (6 to 21%) and muscovite (6 to 31%). Garnet varies from 2 to 4%. Compared to typical pelitic schists (Mueller & Saxena, 1977) they have only slightly higher SiO_2, MnO, CaO and K_2O and very slightly lower MgO and Al_2O_3.

Garnet-Lacking Metasediments

The chemical and mineralogical compositions of rocks from the outermost flank of the contact zone including the no-garnet schists, and associated marble bands and outer unmetamorphosed shale are given in table 4. The schists are chemically close to the unmetamorphosed shale. The presence of marble bands also indicates a metasedimentary origin of schists. Chemically these schists are similar to the garnet-bearing schists as reported in tables 2 and 3; and are similarly different from the amphibolites. They are chemically comparable to typical pelitic schists in the same way as are the schists of tables 2 and 3.

DISCUSSION

Emplacement of ophiolite nappes may result in their cooling and supply of heat to the

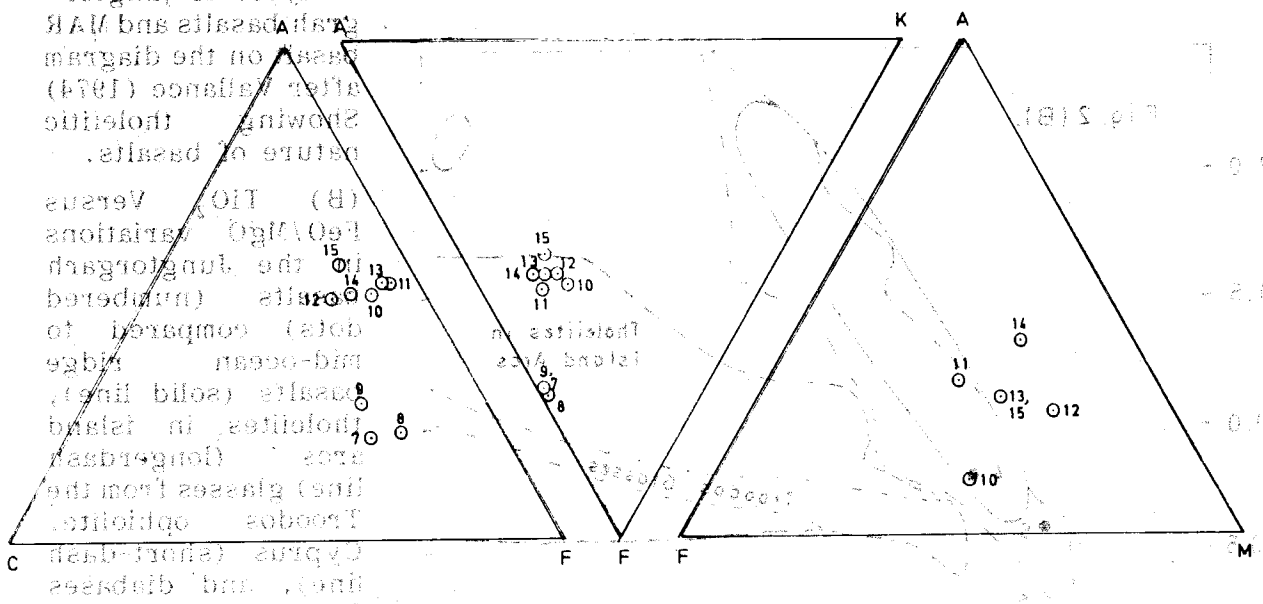

Fig. 3. ACF, AKF and AFM diagrams of garnetiferous amphibolites (7–9) and schists (10–15) at immediate contact. For chemical analyses, see table 2.

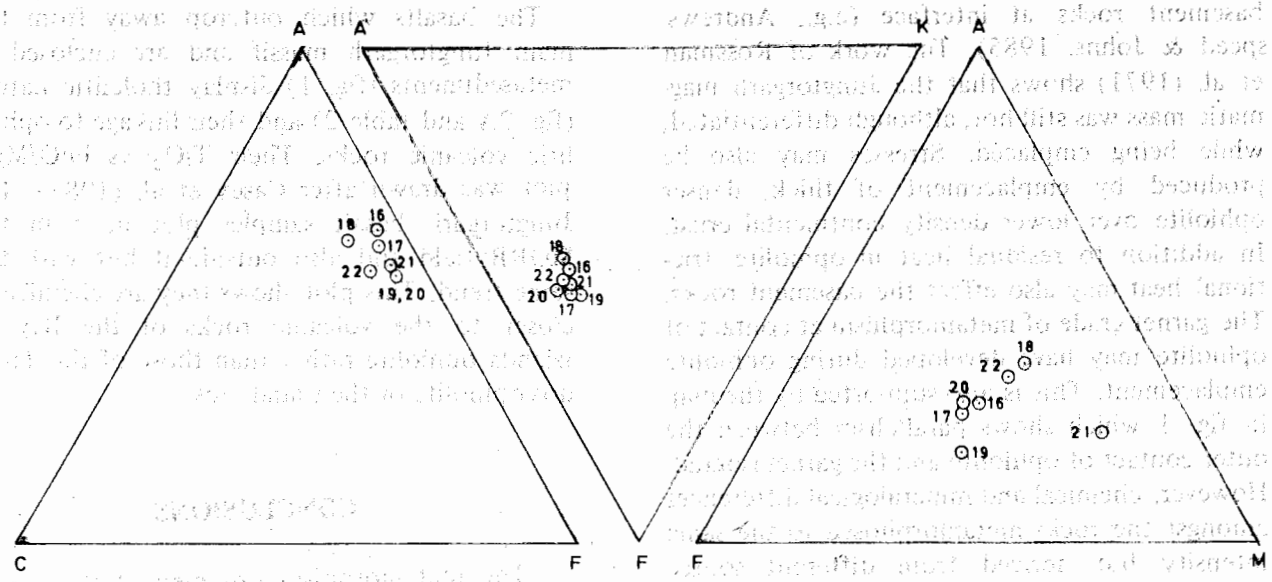

Fig. 4. ACF, AKF and AFM diagrams of low-garnet schists. Analyses are reported in table 3.

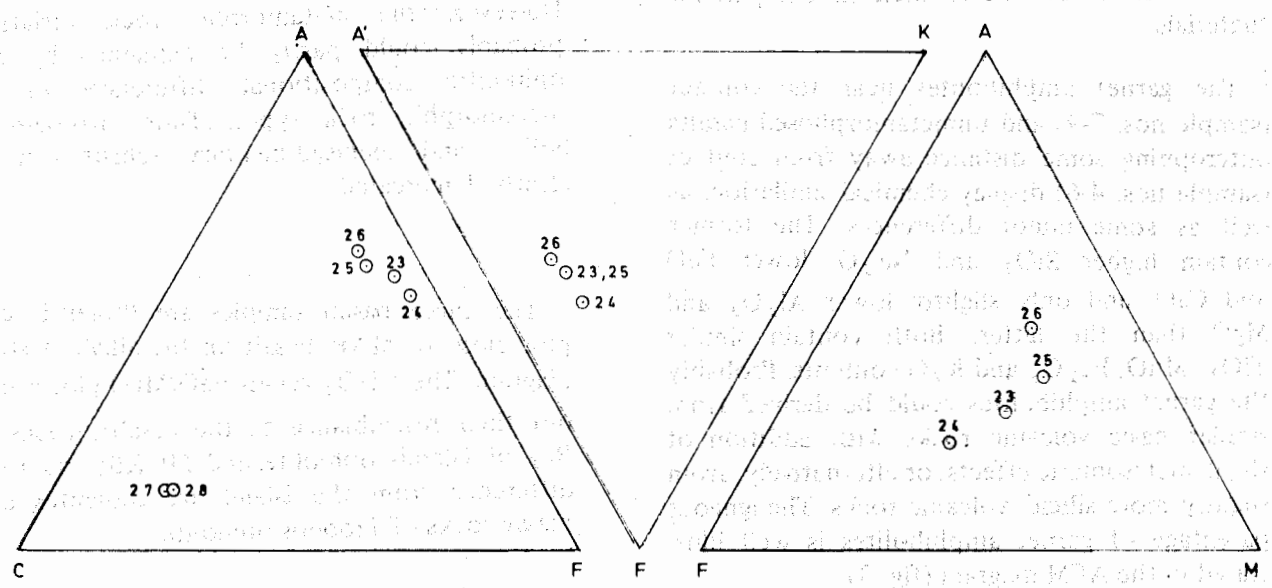

Fig. 5. ACF, AKF and AFM diagrams of no-garnet schists tabulated in table 4.

basement rocks at interface (e.g., Andrews-speed & Johns, 1985). The work of Rossman et al. (1971) shows that the Jungtorgarh magmatic mass was still hot, although differentiated, while being emplaced. Stresses may also be produced by emplacement of thick, denser ophiolite over lower density continental crust. In addition to residual heat in ophiolite, frictional heat may also effect the basement rocks. The garnet grade of metamorphism at contact of ophiolite may have developed during ophiolite emplacement. This is also supported by the map in fig. 1 which shows parallelism between the outer contact of ophiolite and the garnet isograd. However, chemical and mineralogical differences amongst the rocks metamorphosed to the same intensity but derived from different source rock compositions are also clearly noticeable. For example, in table 2, such petrochemical differences between orthoamphibolites and metasedimentary schists are obvious. The chemical analyses numbered 10 through 26 representing metasedimentary schists do not exhibit much noticeable variations, whether they have abundant garnet or no garnet at all. This seems to be due to their similar parental materials.

The garnet amphibolites near the contact (sample nos. 7-9) and unmetamorphosed basalts outcropping some distance away from contact (sample nos. 4-6) display chemical similarities as well as some minor differences. The former contain higher SiO_2 and Na_2O; lower FeO and CaO; and only slightly lower Al_2O_3 and MgO than the latter. Both contain similar TiO_2. MnO, Fe_2O_3 and K_2O contents. Probably the garnet amphibolites could be derived from similar basic volcanic rocks with addition of slight metasomatic effects; or alternatively, from slightly more silicic, volcanic rocks. The igneous parentage of garnet amphibolites is well illustrated in the AFM diagram (fig. 3).

The basalts which outcrop away from the main Jungtorgarh massif and are enclosed in metasediments (fig. 1) display tholeiitic nature (fig. 2A and table 2) and their linkage to ophiolitic volcanic rocks. Their TiO_2 vs FeO/MgO plot was drawn after Casey et al. (1985). The Jungtorgarh basalt samples plot in it in the MORB field and also outside it but with the same trend. This plot shows they are chemically closer to the volcanic rocks of the Bay of Islands ophiolite rather than those of the Troodos ophiolite or the island arcs.

CONCLUSIONS

The metamorphism observed at the contact seems to have occurred during the tectonic emplacement of ophiolite. The required heat might have been supplied from emplacement process from either or both of the two sources: frictional heat and the residual heat of the ophiolite slab. The outcrop pattern of metamorphic rocks shows parallelism with the contact of ultramafic rocks exposed in this area. However, the metamorphic rock variations probably could partly be explained by pre-ophiolitic compositional differences in the metamorphic rock types. Thus, orthoamphibolites and metasedimentary schists can be clearly demarcated.

The three basalt samples are tholeiitic and plot close to MAR basalt on the alkali vs silica diagram. Their TiO_2 versus FeO/MgO plot brings out their resemblance to the basaltic rocks of Bay of Islands ophiolite and MORB; and their difference from the island arc tholeiites and glassy rocks of Troodos ophiolite.

REFERENCES

ABBAS, S.G. & AHMAD, Z. (1979) The Muslim bagh ophiolites. In: Farah, A. & De Jong, K.A. (eds) GEODYNAMICS OF PAKISTAN. Geol. Surv. Pakistan Quetta, pp. 243-9.

ANDREWS–SPEED, C.P. & JOHNS, C.C. (1985) Basement diapirism associated with the emplacement of major ophiolite nappes: some constraints. Tectonophys. 118, pp. 43-59.

CASEY, J.F., ELTHON, D.L., SIROKY, F.X., KARSON, J.A. & SULLIVAN, J. (1985) Geochemical and geological evidence bearing on the origin of the Bay of Islands and Coastal Complex ophiolites of western Newfoundland. Tectonophys. 116, pp. 1-40.

COLEMAN, R.G. (1977) OPHIOLITES–ANCIENT OCEANIC LITHOSPHERE? Springer-Verlag, New York, 229 p.

MELSON, W.G. & THOMPSON, G. (1971) Petrology of a transform fault zone and adjacent ridge segments. Phil. Trans. Roy. Soc. London A-268, pp. 423-41.

MOORES, E.M. ROEDER, D.H., ABBAS, S.G. & AHMAD, Z. (1980) Geology and emplacement of the MuslimBagh ophiolite complex. In: Panayiotou, A. (ed). OPHIOLITES, Proc. Internat. Ophiolites Symp., Cyprus Geol. Surv. Deptt., pp. 424-29.

MUELLER, R.F. & SAXENA, S.K. (1977) CHEMICAL PETROLOGY. Springer-Verlag, New York, 394p.

NOCKOLDS, S.R. (1954) Average chemical composition of some igneous rocks. Geol. Soc. Amer. Bull. 65, pp. 1007-32.

ROSSMAN, D.L., AHMAD, Z. & REHMAN, H. (1971) Geology and economic potential for chromite in the Zhob Valley ultramafic complex (Jungtorgarh) Hindubagh, Quetta Division, West Pakistan. Pakistan Geol. Surv. & U.S. Geol. Surv. Interim Rept. PK–50, 63 p.

SEARLE, M.P. & MALPAS, J. (1982) Petrochemistry and origin of subophiolitic metamorphic and related rocks in the Oman Mountains. Jour. Geol. Soc. London 139, pp. 235-48.

SIRKOY, F.X., ELTHON, D.L., CASEY, J.F. & BUTLER, J.G. (1985) Major element variations in basalts and diabases from the North Arm Mountain massif, Bay of Islands ophiolite: implications for magma chamber processes at mid-ocean ridges. Tectonophy. 116, pp. 41-61.

VALLANCE, J.G. (1974) Spilitic degradation of a tholeiitic basalt. Jour. Petrol. 15, pp. 79-86.

WILLIAMS, H. & SMYTH, W.R. (1973) Metamorphic aureoles beneath ophiolite suites and alpine peridotites: tectonic implications with west Newfoundland examples. Amer. Jour. Sci. 273, pp. 594-621.

ACTA MINERALOGICA PAKISTANICA
VOLUME 1(1985) pp. 49-63

MINERAL CHEMISTRY OF SMALL INTRUSIVES FROM MULLABAGH AREA, KOHI SAFAID, KURRAM AGENCY, PAKISTAN.

ZULFIQAR AHMED

Centre of Excellence in Mineralogy,
University of Baluchistan, Quetta, Pakistan.

Abstract: **By geological mapping small sized intrusives and hypabyssal rocks were located in the Safaid Koh range, north of Parachinar in Kurram Agency. Constituent mineral analyses employing electron microprobe are reported for a variety of these rocks. The igneous suite exhibits a wide compositional spectrum from basic to acidic, within small dimensions. Pyroxene in diabase is diopside to magnesian augite. Plagioclase and amphibole compositions gradationally change for basic to acidic rocks. The pegmatite contains quartz, potash feldspar, epidote, apatite, green amphibole and sphene. Ilmenite is Mn richer in both the igneous rocks and the schists.**

INTRODUCTION

The area included in this study is a remote area that lies in the mountain range called "Kohi Safaid' in Kurram Agency close to the Afghanistan border. Previous geological studies of this area (e.g., Afridi et al., 1968; Meissner et al., 1975) mention the occurrence of some intrusive rocks. The mineralogy, petrography or mineral chemistry were not studied, and this is the main task of present study. The present work was initiated by sampling the large variety of igneous, sedimentary and metamorphic outcrops located north of the Zeran Dam and along various tributaries of the stream valley called Zeran Tangi. All these tributaries originate from the crest of Kohi Safaid. Geological mapping of a small area revealed many small outcrops of intrusive and hypabyssal rocks. Samples of these rocks and surrounding metamorphic rocks were studied microscopically and under the electron microprobe to characterize these rocks and their mineral assemblages especially by their mineral chemistry.

GENERAL GEOLOGY

On the 1:250,000 scale map by Meissner et al. (1975), the north-south stretch along Zeran Valley from Afghan border to the alluvial deposits of Kurram Valley is composed mainly of a lower Cretaceous quartzite which is partly conglomeratic, and many kms beyond the area towards west contains a few mafic intrusions. However, the intrusives described in the present study were not reported. Below the quartzite are the Jurassic formations whose undifferentiated outcrops were mapped in eastern part. In the western part they were divided into a grey coloured, partly oolitic, fossiliferous Samana Suk Limestone and a grey limestone with interbeds of marl, shale and sandstone that comprises the Datta Formation.

The 1:25,000 scale map, prepared from air photos and an inch to a mile toposheets, by Afridi et al. (1968) gives more detailed geology of the above described stretch in the following

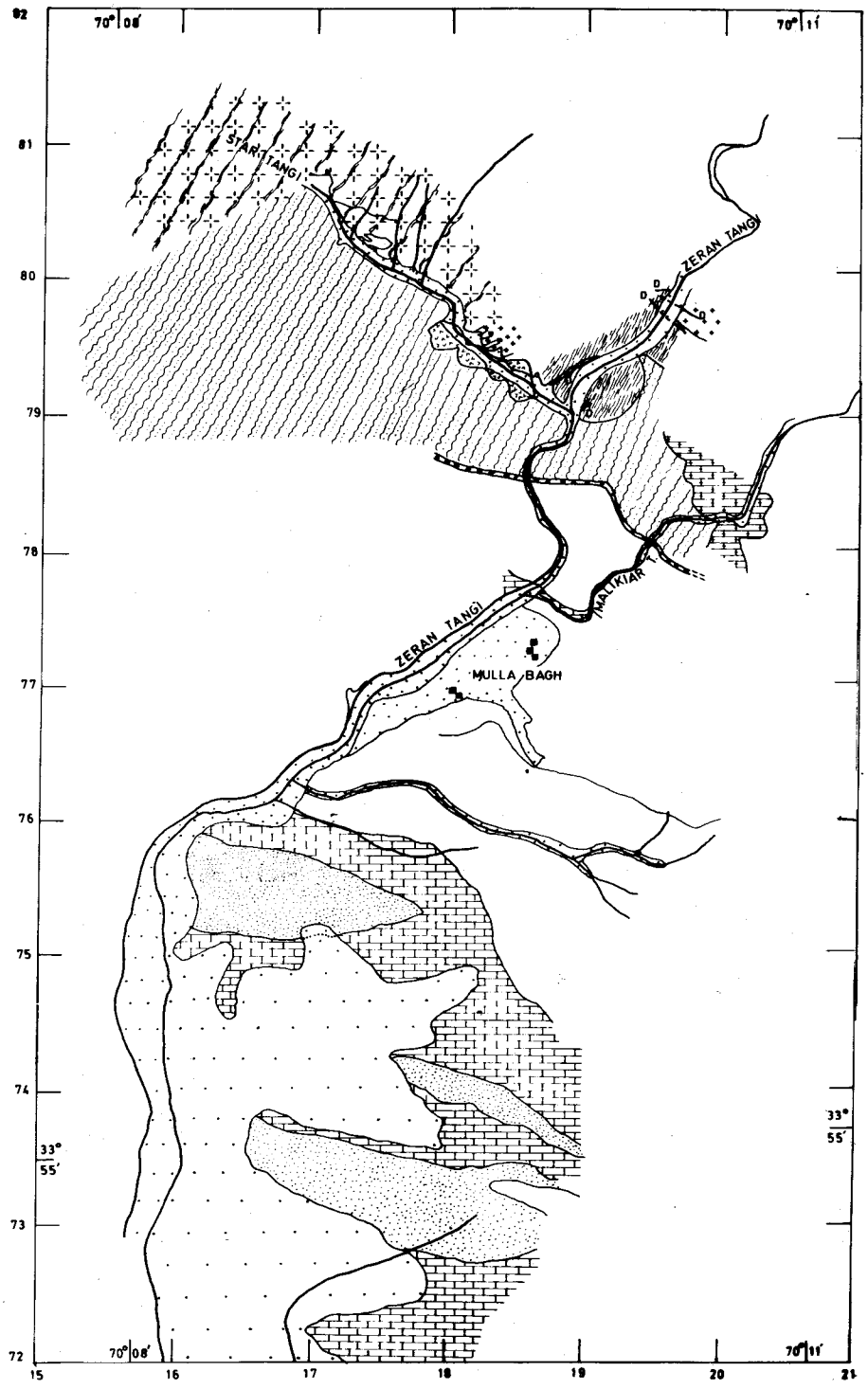

Fig. 1. Geological sketch map along a part of Zeran Tangi and its tributaries near Mulla bagh, Kurram Agency.

sequence exposed between Parachinar town and Kohi Safaid Afghan border.

Parachinar

9. Kurram Valley Quaternary alluvial deposits of silt, sand and gravel.

8. Greyish, hard, partly nodular and fossiliferous limestone with intercalcations of sandstone, shale and marl.

7. Red and greenish brown sandstone of probable Triassic age.

6. Calcareous schist

5. Grey, thin-bedded, compact limestones and dolomites intercalated with shale, sandstone, siltstone; with fossils and intrusives.

4. Bedded quartzite of white to dark colour; with basal conglomerate and grit which are at places ferruginous and hosts iron deposits. This conglomerate marks an unconformity.

3. Marble, dolomites, calcareous sediments and silicated rocks with some dolerite sills and dykes. Quartz veins contain copper minerals deposited by hydrothermal cavity filling. Some graphitic schists are present. Dolomite contains soapstone adjacent to basic intrusions.

2. Phyllites (Palaeozoic), equivalents of Hazara Slate Formation.

1. Pre-Palaeozoic Igno-metamorphic zone comprising schist, gneiss, migmatites with various later intrusions of pegmatite, granite, basic intrusions and some feldspar deposits.

Afghanistan Border (Kohi-Safaid Sector)

In this cross-section, sedimentary rocks lie southwards, towards the Kurram Valley; whereas the metamorphic rocks lie northwards, in an east-west trending zone that hosts small igneous bodies as well. The rock samples included in the present study of mineral chemistry come mainly from this latter part.

LITHOLOGY AND PETROGRAPHY

The sedimentary rocks are dominated by limestones. Just south of the conglomerate bed, a compact limestone outcrops near the Zeran Dam in Zeran Tangi (Valley). Shear planes are seen at a few places in this limestone. Mostly the limestone is light to dark grey, unfossiliferous, thickly bedded and weathers to dark grey or creamy brown colour. Veins of secondary calcite are abundant. Chopboard weathering and solution effects are seen at some outcrops. Southwards from this limestone, beds of clastic sediments are present. Splintry shales of dark brown colour and green sandstone are frequent. These and another thick limestone horizon form a thick succession of strata southwards till the Kurram Valley alluvium.

The metamorphic rocks are developed in an east–west zone along the crest and southern slopes of Kohi Safaid. The conglomerate bed with brownish red matrix forms the southern limit of metamorphic rocks. Compactness of this conglomerate is exceptionally high. Its matrix is often dark brownish red and highly ferruginous. It lies at the base of quartzite. Below the conglomerate bed is limestone as described above.

The quartzite is well-bedded and often greyish white. Calcareous quartzite contains abundant quartz and dolomite with small amounts of iron

Fig. 2. (Facing Page) Photographs showing field relations of rocks from the described area. (A) Typical chopboard weathered surface of quartzite. (B) The ferruginous matrixed compact conglomerate bed marking the unconformity alongwith its boulders and pebbles. (C) A granite gneiss outcrop occur farther eastwards in the Dradar Valley, outside the described area. (D) The sediments farther south of the igno-metamorphic zone, about 10 km east of Parachinar show cross-bedding in sandstone. (E) In the igno-metamorphic zone, in the Star Tangi (valley), schists enclose small bodies of silicified basalt; their sharp contact is illustrated here. (F) The marble beds occur on both sides of a steep dyke of dolerite. (G) A small stock-like gabbro outcrop in faulted and sheared contact with quartzite to the right. The contact appears turning around from the position of seated man upwards. (H) Sharp contact of migmatite with granite on left side. The hammer is placed right at the contact.

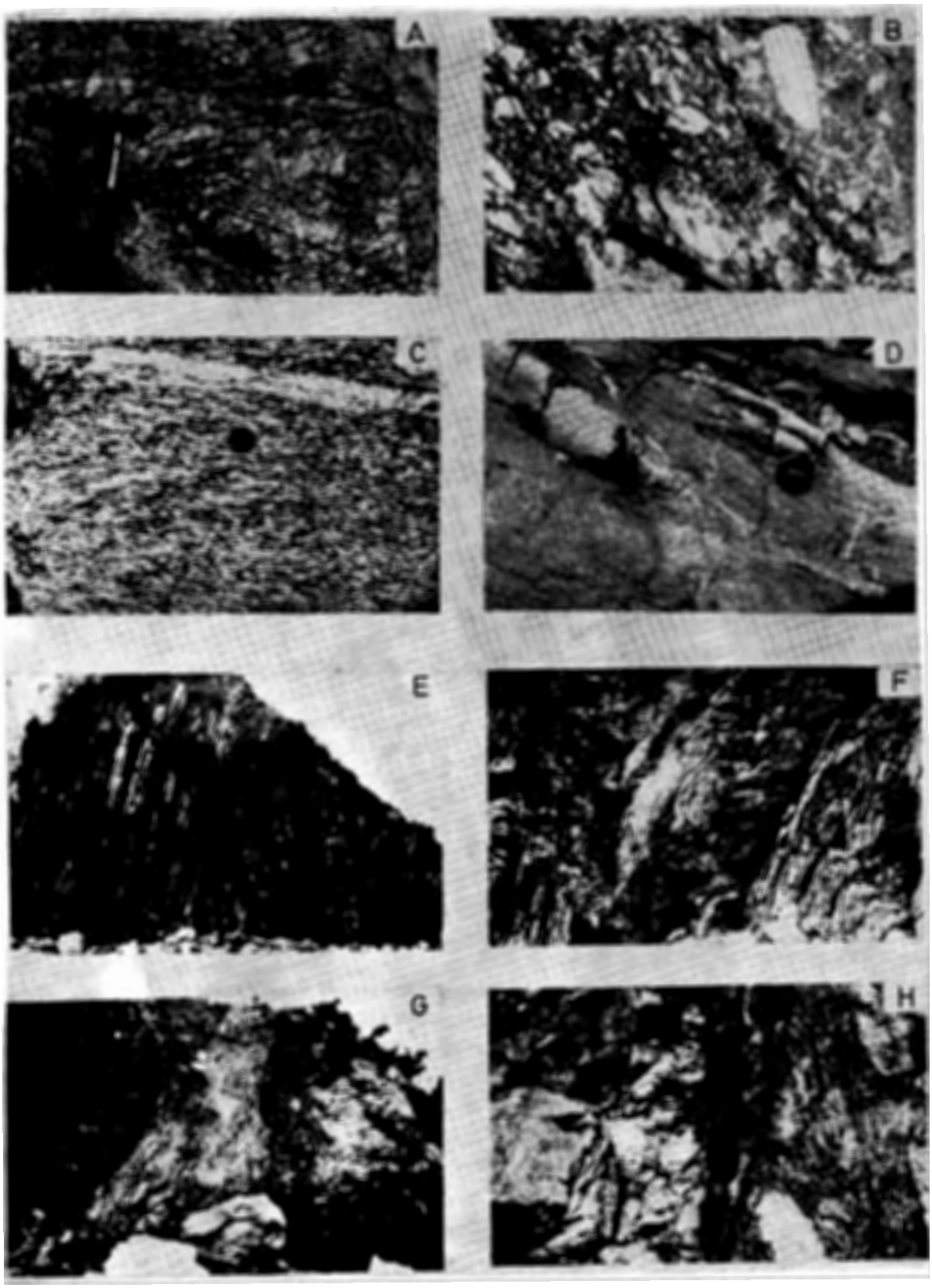
A
B
C
D
E
F
G
H

oxides and chlorite. Calcareous schist of grey colour weathers to white. It may contain interbeds of pelitic schists.

Marble beds occur adjacent to quartzite beds. Marble is white to greyish white coloured and often banded in shades of grey, but weathering colour is often brownish yellow. Small quartz veins intersect marble beds at places. Micaceous schists may be intensely folded and crenulated. At certain places, schists appear highly ferruginous and bear hematite and limonite. Some pegmatitic veins, lenses and dykes occur in mica schists. The doleritic sills and dykes are also present in schists. A few dolerite dykes are seen cutting across the mica schists as well as the enclosed pegmatite. The biotite schist contains abundant quartz with biotite, muscovite, chlorite and manganous ilmenite. The muscovite quartz schists contain abundant quartz and muscovite, with lesser amounts of biotite, sodic feldspar, hematite, and manganous ilmenite which is often intergrown with quartz or other silicates. Titanium oxide mineral also occurs. Garnet-mica schist is also widely developed. Small igneous bodies and pegmatites occur at some places surrounded by the garnet-mica schist.

Slates also occur, often rendered black by their carbon content. Slaty cleavage is also seen in phyllites which show interlayered greyish green and reddish brown weathering colours. They also contain calcareous and siliceous interbeds. Migmatites occur widely distributed northwards. Ptygmatic folding is frequent in them.

The igneous rocks grade from basic to acid pegmatitic.

Dolerites may occur as sills and discordant dykes in schists and quartzite and show ophitic texture. Some small basalt outcrops are also found in the schists zone. Basalts appear silicified and show no contact metamorphism. The diabases contain clinopyroxenes and two kinds of coexisting amphiboles; one being Al-richer green coloured and the other colourless in thin sections and poor in Al content. Recrystallized albite and epidote also occur. Ilmenite lamellae are found intergrown with amphibole and epidote; magnetite is absent. Some dolerite dykes cut across the granitic rocks and pegmatites. The iron containing minerals have imparted reddish brown weathering colour to the basic rock outcrops.

Microdiorites contain plagioclase of oligoclase-andesine range $An_{23.5}$ to $An_{35.7}$ which is more abundant than the associated potash feldspar; and may form long vein-shaped areas. Albite and perthite are also rarely seen. Both green and microscopically colourless amphiboles occur together; although greenish one is much more abundant. Amongst its opaque ore minerals, most abundant is ilmenite, exceeding 5% modally. Also present are the magnetite rims on pyrite cores, and individual magnetite grains, which are modally about 1% or less. Quartz is not present. Apatite needles are present.

The dioritic rocks may show sheared and faulted contacts. Diorites are often without quartz. Plagioclase is common and some potash feldspar is also present. Amphiboles are abundant. Epidote is also present. Pyrite may be the sole opaque mineral. Quartz is not found in diorites, but becomes abundant in granodiorites.

The granodiorites are rich in biotite which may be as abundant as plagioclase. Plagioclase are zoned in some samples. Alkali feldspar could not be seen and is almost absent. Accessory apatite often forms rounded grains in feldspar grains. Quartz may be abundant in some samples, but usually less than the biotite. Amphibole is not present.

Small stocks of granitic rocks are frequently found. Some micro-granites also occur in quartzite. Biotite flakes are abundantly developed in the granites. Microcline - granites may contain upto about 70% cross-hatched microcline, some albite and oligoclase. Muscovite flakes are rare and bent. Quartz may be abundant. Chlorite and ilmenite are accessories. Biotite is

a minor accessory. Quartz-rich leucogranites may contain oligoclase and abundant potash feldspar, some of which is perthitic. Muscovite and hydromuscovite also occur. Pegmatites occur widely distributed in the metamorphic and igneous rocks. One scanned pegmatite contained abundant potash feldspar and quartz; green, prismatic amphibole; sphene, as coarse grains and small rhombs; abundant epidote and euhedral, fresh apatite. Acicular tourmaline is also developed in pegmatites. Aplites are also rarely developed and contain hornblende and biotite in addition to quartz, feldspar and muscovite. Quartz veins occur commonly in schistose rocks and granites.

MINERAL CHEMISTRY

Clinopyroxene

The clinopyroxene analyzed from diabase (table 1) is a magnesian augite similar in composition to tholeiitic pyroxenes. Zoning or within-grain variation is not conspicuous. Fig. 3 shows their plot in the pyroxene quadrilateral.

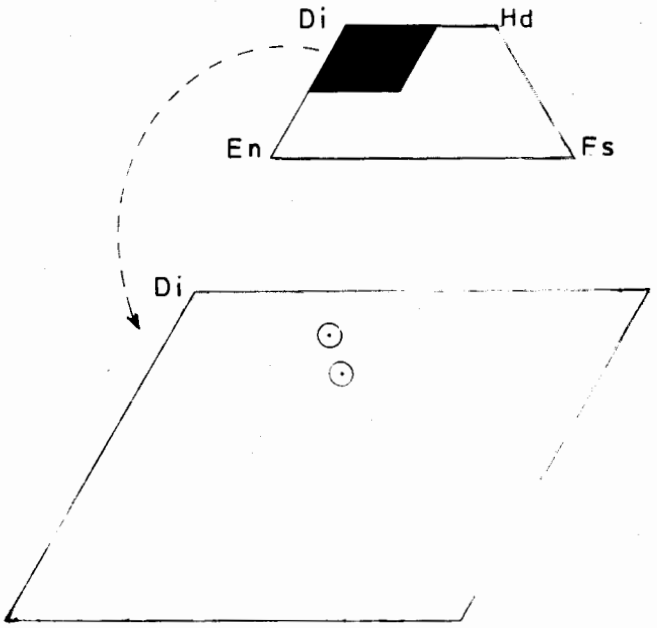

Fig. 3. Compositions of pyroxenes from diabase plotted on pyroxene quadrilateral.

Amphibole

Amphiboles are present in basic and intermediate rocks such as diabase and diorite. No amphibole could be analyzed from the granodiorites and granites which are exceptionally enriched in biotite. Amphibole is also present in pegmatite in high modal percentage and chemically (table 2) it seems quite different from the rest of the analyzed amphioles. Within each rock type amphiboles vary widely in composition. Probably more than one type of amphibole are present in each of the samples analyzed, especially in diabase and diorites. Optically distinctly green cloured amphiboles are marked with letter 'g' in table 2. These coexist with optically different amphiboles in each sample. Even within each optic type of amphibole, large chemical variations are noticed. However, a general pattern of variation of major elements in amphiboles especially those marked 'g' is observed. From diabase towards more acidic rocks, gradual decrease of TiO_2, Al_2O_3, FeO, Na_2O and K_2O and increase of SiO_2, MgO, CaO is noticed with a few and only minor discrepencies. The extreme end member of this trend is the pegmatitic green amphibole.

Plagioclase

Plagioclase feldspar from intermediate to acidic rocks (table 3) displays a general trend of becoming less calcic and more sodic with increasing silica content of the rocks. A parallel decrease in Al_2O_3 and increase in SiO_2 content is also observed. This trend of enrichment in soda and impoverishment in lime is normally expected in the case of simple igneous rock suites undergoing crystallization differentiation. Such a variation in the plagioclase compositions points to the probable primary linkage between the rock types.

In addition to plagioclase, albite has been analyzed from basic, intermediate and acid rocks, as shown in table 4. The albite composition does not vary significantly in these rocks. It seems that this albite might have been produced secondarily or by low grade metamorphism.

Table 1. Electron microprobe analyses of clinopyroxenes from diabase sample (no. 17746). Total iron is counted as Fe O. Cations on the basis of 6 oxygens.

	1	2		1	2		1	2
SiO_2	49.74	50.65	Si	1.875	1.878	Wo	43.676	46.691
TiO_2	0.47	0.60	Al^{iv}	0.125	0.122	En	43.521	42.962
Al_2O_3	3.84	4.10	Al^{vi}	0.046	0.057	Fs	12.803	10.347
Cr_2O_3	0.34	0.45	Ti	0.013	0.017			
Fe O	7.79	6.21	Cr	0.010	0.013			
Mn O	0.11	0.15	Fe	0.245	0.192			
Mg O	15.00	16.09	Mg	0.843	0.889			
Ca O	20.95	20.41	Mn	0.003	0.005			
Ni O	0.05	0.00	Ca	0.846	0.818			
Na_2O	0.35	0.46	Ni	0.001	0.000			
K_2O	0.00	0.01	Na	0.025	0.033			
Total	98.64	99.13	K	0.000	0.001			

Table 2. Electron microprobe analyses of amphiboles from diabase (1–5), microdiorite (6–9), diorite (10–14) and pegmatite (15–19). Total iron is expressed as Fe O.

Anal. No.	1	2	3	4	5	6	7	8	9	10	11	12
Sp. No.	17746	17746	17746	17746	17746	17779	17779	17779	17779	17737	17737	17737
SiO_2	39.32	44.01	48.49	53.34	53.40	45.63	47.88	43.48	41.39	46.93	53.59	49.11
TiO_2	0.42	0.52	0.85	0.53	0.36	0.35	0.47	0.64	0.56	0.29	0.70	0.59
Al_2O_3	15.73	10.59	4.86	3.06	2.62	8.03	6.45	11.16	14.34	6.73	3.23	4.75
Cr_2O_3	0.04	0.00	0.13	0.27	0.03	0.00	0.00	0.02	0.07	0.01	0.08	n.d.
Fe O	20.98	18.57	19.85	9.26	11.41	18.58	18.73	20.01	20.90	21.01	15.53	19.97
Mn O	0.31	0.23	0.52	0.15	0.29	0.26	0.34	0.24	0.24	0.41	0.39	0.31
Mg O	6.36	9.32	11.40	16.75	15.93	8.78	10.19	7.93	6.47	9.03	11.63	9.71
Ni O	0.02	0.00	0.03	0.08	0.00	0.00	0.04	0.13	0.04	0.06	0.05	0.00
Ca O	11.33	11.62	9.49	12.96	12.72	11.73	11.87	11.58	11.73	12.18	11.70	12.28
Na_2O	1.99	1.05	0.59	0.40	0.48	1.06	0.69	1.01	1.62	0.70	0.27	0.60
K_2O	0.62	0.31	0.48	0.01	0.05	0.35	0.51	0.65	0.66	0.25	0.11	0.22
Total	97.12	96.22	96.69	96.81	97.29	94.77	97.17	96.85	98.02	97.60	97.28	97.54

Anal. no.	13	14	15	16	17	18	19
Sp. no.	17737	17737	17732	17732	17732	17732	17732
SiO_2	49.96	50.49	55.01	53.82	53.96	53.50	53.31
TiO_2	1.57	1.95	0.19	0.13	0.01	0.01	0.10
Al_2O_3	4.59	4.80	1.50	1.69	2.13	2.80	1.97
FeO	16.45	15.15	8.36	8.79	8.92	9.41	9.10
MnO	0.43	0.25	0.38	0.38	0.49	0.45	0.45
MgO	11.20	11.60	18.14	16.79	16.96	16.76	16.77
NiO	0.03	0.09	0.00	0.05	0.09	0.06	0.00
CaO	12.87	13.02	13.22	12.92	12.92	12.88	12.98
Na_2O	0.26	0.71	0.37	0.23	0.59	0.27	0.29
K_2O	0.13	0.16	0.13	0.17	0.28	0.27	0.17
Total	97.49	98.22	97.30	94.97	96.35	96.41	95.14

Table 3. Electron microprobe data for plagioclase. Total iron is expressed as Fe_2O_3.

Sr. No.	Sample No	SiO_2	TiO_2	Al_2O_3	Fe_2O_3	MnO	MgO	CaO	Na_2O	K_2O	Total	An%
DIORITE												
1.	17737	50.79	0.11	29.01	1.43	0.00	0.55	12.97	3.87	0.15	98.88	64.368
2.	17737	54.20	0.14	27.06	1.08	0.00	0.22	10.64	4.97	0.25	98.56	53.381
3.	17737	56.74	0.12	26.27	0.90	0.00	0.19	8.55	6.26	0.26	99.29	50.548
MICRODIORITE												
4.	17779	59.68	0.10	24.81	0.27	0.02	0.12	7.04	6.93	0.09	99.06	35.745
5.	17779	61.48	0.02	23.49	0.31	0.00	0.24	5.05	8.24	0.08	98.91	25.182
6.	17779	62.80	0.00	23.00	0.08	0.00	0.00	4.88	8.22	0.02	99.00	24.676
7.	17779	60.95	0.01	23.24	0.25	0.05	0.20	4.93	8.52	0.12	98.27	24.067
7B.	17779	62.68	0.00	22.98	0.21	0.00	0.08	4.65	8.24	0.15	98.99	23.569
BIOTITE GRANODIORITE												
8.	17838	59.91	0.00	25.16	0.21	0.05	0.17	6.99	7.61	0.09	100.10	33.501
9.	17838	60.59	0.00	24.54	0.25	0.00	0.00	6.37	7.51	0.08	99.34	31.762
10.	17838	61.89	0.00	23.38	0.03	0.00	0.06	4.82	8.63	0.03	98.84	23.535
11.	17838	63.03	0.01	22.90	0.18	0.02	0.08	4.15	8.86	0.20	99.43	20.319
12.	17735	62.13	0.02	23.21	0.03	0.00	0.05	5.21	8.29	0.07	99.01	25.663
13.	17735	62.20	0.02	23.17	0.09	0.03	0.00	5.06	8.59	0.09	99.25	24.487
14.	17735	61.76	0.01	23.25	0.00	0.01	0.00	4.95	8.45	0.08	98.51	24.335
15.	17735	61.33	0.00	23.04	0.43	0.09	0.04	4.76	8.34	0.08	98.11	23.872
16.	17735	61.10	0.00	23.11	0.14	0.02	0.13	4.83	8.73	0.09	98.15	23.294
17.	17735	61.67	0.00	23.26	0.32	0.02	0.12	4.72	8.69	0.08	98.88	22.977
18.	17735	62.35	0.03	23.25	0.05	0.01	0.00	4.78	8.90	0.10	99.47	22.760
ALKALI GRANITE												
19.	17741	63.30	0.00	22.21	0.17	0.07	0.06	3.85	8.82	0.12	98.60	19.304
20.	17741	63.64	0.06	22.13	0.00	0.02	0.11	3.51	8.57	0.08	98.12	19.302
21.	17741	63.80	0.01	22.17	0.05	0.00	0.16	3.57	8.76	0.19	98.71	18.163
QUARTZ–RICH GRANITE												
22.	17742	62.54	0.05	22.51	0.05	0.00	0.00	3.26	10.68	0.02	99.11	14.422
23.	17742	62.49	0.00	22.48	0.08	0.00	0.00	3.48	10.81	0.08	99.42	15.037
24.	17742	62.55	0.01	22.35	0.00	0.00	0.00	3.61	10.84	0.14	99.50	15.415
25.	17742	62.24	0.00	22.58	0.00	0.00	0.00	3.53	10.39	0.09	98.83	15.736
26.	17742	62.24	0.00	22.54	0.07	0.00	0.00	3.50	11.40	0.09	99.84	14.436
27.	17742	63.47	0.00	23.22	0.00	0.00	0.00	3.55	11.01	0.03	101.28	15.107

Table 4. Electron microprobe data for albite.

Sr. No.	Sp. No.	SiO_2	TiO_2	Al_2O_3	Fe_2O_3	MnO	MgO	CaO	Na_2O	K_2O	Total
METADOLERITE											
1.	17746	67.99	0.00	19.16	0.33	0.00	0.00	0.29	11.21	0.04	99.02
2.	17746	67.51	0.06	20.15	0.23	0.00	0.00	0.82	10.36	0.09	99.22
MICRODIORITE											
3.	17779	67.28	0.00	19.11	0.67	0.06	0.00	0.12	11.18	0.11	98.53
GRANITE											
4.	17741	66.36	0.07	20.74	0.14	0.00	0.14	1.52	10.53	0.09	99.59
5.	17742	65.43	0.05	20.10	0.00	0.00	0.00	1.00	12.19	0.14	98.91
6.	17742	66.05	0.01	20.21	0.11	0.00	0.00	0.34	12.65	0.36	99.73

Table 5. Electron microprobe data for potash feldspars.

Anal. No.	Sp. No.	SiO_2	TiO_2	Al_2O_3	Fe_2O_3	MnO	MgO	CaO	Na_2O	K_2O	P_2O_5	Total
MICRO–DIORITE												
1.	17779	63.24	0.07	17.81	1.11	0.01	0.00	0.08	0.06	16.76	n.d.	99.14
2.	17779	64.39	0.12	18.02	0.07	0.03	0.00	0.00	0.00	16.61	n.d.	99.35
3.	17779	63.80	0.06	17.75	0.06	0.09	0.06	0.00	0.14	16.58	0.16	98.70
4.	17779	63.53	0.17	17.92	0.26	0.03	0.00	0.14	0.24	16.65	0.14	99.08
DIORITE												
5.	17737	62.73	0.12	18.33	1.31	0.03	0.64	0.06	0.56	16.10	n.d.	99.88
6.	17737	63.92	0.07	17.88	0.46	0.00	0.00	0.00	0.46	16.28	n.d.	99.07
MICROCLINE–GRANITE												
7.	17741	64.02	0.02	18.06	0.05	0.00	0.13	0.13	0.83	15.80	n.d.	99.04
8.	17741	64.19	0.07	18.11	0.06	0.00	0.00	0.00	1.88	14.09	n.d.	98.40
9.	17741	63.86	0.05	17.81	0.02	0.03	0.00	0.00	0.37	16.75	n.d.	98.89
10.	17741	64.67	0.09	18.46	0.00	0.02	0.14	0.00	0.97	15.18	n.d.	99.53
11.	17741	63.72	0.07	17.70	0.15	0.02	0.03	0.06	0.31	16.54	n.d.	98.60
12.	17741	63.59	0.14	18.14	0.03	0.04	0.13	0.04	0.45	16.72	n.d.	99.64
QUARTZ–RICH GRANITE												
13.	17742	63.73	0.18	18.39	0.00	0.01	0.16	0.01	0.86	14.89	n.d.	98.23
14.	17742	64.01	0.10	18.73	0.11	0.00	0.00	0.11	0.51	15.37	n.d.	98.94
15.	17742	63.98	0.11	18.44	0.00	0.06	0.00	0.07	0.15	15.57	n.d.	98.38
16.	17742	63.95	0.12	19.96	0.00	0.01	0.18	0.00	0.65	15.00	n.d.	98.87
17.	17742	64.22	0.28	18.90	0.10	0.00	0.00	0.04	1.08	15.45	n.d.	100.07
PEGMATITE												
18.	17732	63.62	0.09	18.14	0.05	0.02	0.00	0.00	0.68	15.69	n.d.	98.29
19.	17732	63.99	0.12	17.79	0.05	0.00	0.00	0.00	0.35	16.55	n.d.	98.85
20.	17732	63.79	0.09	18.00	0.03	0.08	0.00	0.00	0.38	16.39	n.d.	98.76
21.	17732	63.94	0.18	18.00	0.14	0.00	0.18	0.00	0.70	16.58	n.d.	99.72

Probably it developed independent of the plagioclase which coexists in many samples.

Potash Feldspar

Potash feldspar is present in microdiorite, diorites, granites and pegmatites. The biotite granodiorite contains very little potash feldspar. Its microprobe composition (table 5) does not vary significantly. Abundance of microcline twinning is obvious in one type of granite represented by sample 17741. Its potash feldspar has slightly higher Na_2O.

Epidote

Epidote compositions are set out in table 6. The four epidotes from the same sample of pegmatite resemble each other and inter-grain variation is small. The epidote from diabase is different from the rest, chiefly in Fe^{3+}: Al relationship.

Biotite

Biotite is abundant in the granodiorite and in some samples (e.g., 17838) its amount is nearly equal to that of plagioclase. Biotite analyses (table 8) are reported from the biotite granodiorite and metamorphic schists. The schists contain biotite with distinctly lower MgO than the granodiorite. The K_2O is also somewhat lower in the schists. This lower MgO is compensated in one schist by increased Al_2O_3; and in the other schist by increased FeO in the biotite. One analysis from a granite (sample 17742) also shows biotite with lower MgO, K_2O and higher Al_2O_3 and FeO. This biotite is different from the granodioritic biotites and resembles that of the schists. The Ti content of most biotites is a little less than 2%, except around 0.5% content in a quartz-rich schist. Ti has an

Table 6. Probe analyses of epidotes from diabase (1), diorite (2) and pegmatite (3-6). All Fe is assumed to occur as Fe^{3+} and all analyses summed to 100 on basis of assumed H_2O; structural formulae calculated on basis of 13(O,OH).

Anal. No.	1	2	3	4	5	6
Sample No.	17746	17737	17732	17732	17732	17732
SiO_2	38.02	37.94	37.47	37.82	36.92	37.32
TiO_2	0.02	0.14	0.03	0.07	0.15	0.12
Al_2O_3	25.80	22.26	23.83	23.59	22.81	22.64
Fe_2O_3	9.30	14.33	12.79	12.72	13.33	13.12
Mn_2O_3	0.24	0.45	0.27	0.31	0.47	0.45
MgO	0.17	0.57	0.30	0.24	0.14	0.20
NiO	0.00	0.03	0.00	0.00	0.10	0.00
CaO	24.37	23.05	23.75	23.73	23.64	23.66
Na_2O	0.00	0.08	0.00	0.00	0.36	0.00
K_2O	0.00	0.00	0.03	0.03	0.05	0.09
H_2O^+	2.08	1.15	1.53	1.49	2.03	2.40
Si	2.982	3.052	2.991	3.018	2.949	2.961
Al	0.018	0.000	0.009	0.000	0.051	0.039
ΣZ_4	3.000	3.052	3.000	3.018	3.000	3.000
Al	2.367	2.110	2.233	2.218	2.096	2.078
Ti	0.001	0.008	0.002	0.004	0.009	0.007
Fe^{3+}	0.549	0.867	0.768	0.764	0.801	0.783
Mn^{3+}	0.014	0.028	0.016	0.019	0.029	0.027
ΣY	2.931	3.013	3.019	3.005	2.935	2.895
Ni	0.000	0.002	0.000	0.000	0.006	0.000
Mg	0.020	0.068	0.036	0.029	0.017	0.024
Ca	2.048	1.987	2.031	2.029	2.023	2.011
Na	0.000	0.012	0.000	0.000	0.056	0.000
K	0.000	0.000	0.003	0.003	0.005	0.009
ΣX	2.068	2.069	2.070	2.061	2.107	2.044
H_2O	1.088	0.617	0.815	0.793	1.082	1.270

Table. 7 Electron microprobe analyses of apatites. Total iron is expressed as FeO.

	MICRO-DIORITE		BIOTITE-GRANITE		PEGMATITE
Sample	17779	17779	17735	17735	17732
FeO	0.07	2.00	0.08	0.22	0.00
MnO	0.03	0.00	0.03	0.14	0.00
MgO	0.00	0.85	0.00	0.02	0.08
CaO	54.93	50.91	55.84	54.92	55.62
NiO	0.00	0.00	0.09	0.07	0.01
Na_2O	0.00	0.08	0.08	0.11	0.07
K_2O	0.00	0.00	0.00	0.05	0.06
P_2O_5	40.60	38.19	41.43	41.17	41.29
Total	95.63	92.03	97.55	96.88	97.13

Table 8. Electron microprobe analyses of biotite from granite (1), biotite granodiorite (2–11), mica schist (12–13) and quartz muscovite schist (14-15). n.d. = not determined.

Anal. No.	1	2	3	4	5	6	7	8	9	10	11	12	13	14	15
Sample No.	17742	17838	17838	17838	17838	17838	17735	17735	17735	17735	17735	17734	17734	17736	17736
SiO_2	33.30	37.68	36.76	36.68	36.68	36.60	36.40	36.38	36.34	36.37	36.87	35.09	35.47	38.17	42.64
TiO_2	1.24	1.71	1.75	1.57	1.68	2.06	1.59	1.68	1.63	1.90	1.91	1.85	1.90	0.59	0.42
Al_2O_3	19.76	17.11	17.31	17.02	16.81	17.36	19.16	18.45	18.85	18.91	18.46	17.86	18.88	23.41	27.47
Cr_2O_3	0.08	n.d.	n.d.	n.d.	n.d.	n.d.	0.13	0.12	0.09	0.06	0.11	0.12	0.02	0.11	0.00
FeO	25.60	17.76	16.90	17.13	18.07	16.93	16.00	16.31	16.11	16.50	16.35	21.30	20.34	16.24	9.49
MnO	0.34	0.15	0.17	0.21	0.31	0.12	0.37	0.36	0.38	0.44	0.34	0.20	0.19	0.20	0.10
MgO	9.76	11.18	11.76	11.66	11.40	11.35	11.59	11.85	11.61	10.91	10.82	9.52	8.74	6.76	4.52
NiO	0.03	n.d.	n.d.	n.d.	n.d.	n.d.	0.00	0.00	0.12	0.01	0.00	n.d.	n.d.	0.05	n.d
CaO	0.06	0.03	0.00	0.05	0.00	0.00	0.00	0.06	0.03	0.06	0.08	0.00	0.00	0.08	0.17
Na_2O	0.40	0.09	0.00	0.00	0.13	0.18	0.00	0.17	0.40	0.16	0.21	0.15	0.00	0.06	0.37
K_2O	5.88	10.02	10.04	9.81	10.14	9.88	9.49	9.48	9.43	9.66	9.44	8.74	9.18	8.40	8.48
Total	96.45	95.73	94.69	94.13	95.22	94.48	94.73	94.86	94.99	94.98	94.59	94.83	94.72	94.07	93.66

inverse correlation with Al in the octahedral positions (Al^{vi}). Among metamorphic rocks, the biotite schist (sample no. 17734) has higher Ti and lower Al contents than the quartz-muscovite schist (sample 17736). This trend of increasing Ti and decreasing Al^{vi} with increasing metamorphic grade has also been observed in other areas (e.g., Schreurs, 1985). Biotite in schists is also associated with ilmenite.

Muscovite

Muscovite is abundantly present in the metamorphic schistose rocks. Granites also contain muscovite flakes, some of which are bent. Rare muscovite is also reported from diabase. Inspite of the wide compositional variations, mean FeO and MgO contents are quite compatible with normal muscovite. Differences between igneous and metamorphic muscovites are not clearly seen. MgO is slightly higher in the latter. K_2O in muscovites varies from 8.76 to 11.41, and Na_2O from 0.00 to 1.49.

Chlorite

Chlorite is present as accessory mineral in the microcline-granite in addition to the schists. Within each rock sample, the variations are small. A comparision of the chlorite from both rocks (table 10) shows higher SiO_2, FeO and CaO; in the former and higher Al_2O_3 and MgO in the latter (table 10). The former chlorite is brunsvigite and the latter is ripidolite. In igneous rocks, generally the chlorites form by hydrothermal alteration of ferromagnesian minerals (Deer et al., 1962). The analyzed brunsvigite from granite (table 10) may not be primary. Its Fe/(Mg+Fe) ratio is around 0.73, whereas in the chlorite from schists, it is around 0.55. In other chemical parameters also, the two types of chlorite exhibit differences (table 10). Comparing with the common chlorite compositions (Foster, 1962), the metamorphic chlorites fall well within the expected range, but the granitic chlorites fall slightly outside. Both types of chlorite are rich in Fe and Si. There is no gradation between the two chlorite types.

Sphene

Sphene contained in a pegmatite gave the analytical data reported in table 11. Sphenes from such host rocks usually contain rare-earth elements, and niobium and tantalum (Deer et al., 1982). Because of fewer analyses, the possibility of the presence of rare-earths in the sphene from these granitic pegmatites still remains to be checked. In the Y (octahedral) sites, Al predominates over Fe^{+3}. All Al and Fe

Table 9. Electron microprobe analyses of muscovites from diabase (1), microcline granite (2-3), quartz-rich granite (4-5), mica schist (6-9) and quartz-muscovite schist (10-13). Total Fe is expressed as FeO.

Anal. No.	1	2	3	4	5	6	7	8	9	10	11	12	13
Sp. No.	17746	17741	17741	17742	17742	17734	17734	17734	17734	17736	17736	17736	17736
SiO_2	48.53	45.31	46.34	47.92	48.27	44.92	47.69	46.36	46.92	46.73	47.26	47.20	46.50
TiO_2	0.27	1.50	0.49	0.81	0.72	0.60	0.35	0.46	0.48	0.53	0.62	0.30	0.52
Al_2O_3	30.21	31.89	31.63	33.27	33.67	32.23	32.11	32.20	32.15	31.67	28.32	26.60	32.24
Cr_2O_3	0.00	0.00	0.00	n.d.	n.d.	0.05	0.07	0.00	0.01	0.13	0.00	0.00	0.07
FeO	3.09	4.15	3.34	2.28	2.31	3.83	2.03	2.67	1.77	1.99	5.46	6.12	2.14
MnO	0.03	0.08	0.02	0.00	0.06	0.00	0.07	0.00	0.02	0.00	0.11	0.08	0.00
MgO	1.11	1.12	1.40	1.55	1.73	2.19	1.31	1.79	1.74	1.49	2.63	3.18	1.66
CaO	0.85	0.05	0.04	0.10	0.00	0.00	0.02	0.00	0.08	0.03	0.34	0.38	0.05
Na_2O	1.49	0.00	0.13	0.23	0.40	0.35	0.35	0.43	0.60	0.04	0.77	1.49	0.01
K_2O	9.38	10.57	11.12	10.95	10.99	10.54	10.36	10.71	10.70	11.41	9.16	8.76	10.65
Total	94.96	94.67	94.51	97.11	98.15	94.71	94.36	94.62	94.47	94.02	94.67	94.31	93.84

Table 10. Electron microprobe analyses of chlorite from microcline-granite (1–2) and mica schist (3–5).

Anal. No.	1	2	3	4	5
Sp. No.	17741	17741	17734	17734	17734
SiO_2	25.76	27.43	24.82	25.31	24.41
TiO_2	0.43	0.24	0.21	0.23	0.29
Al_2O_3	17.83	18.13	21.61	21.67	21.77
Cr_2O_3	0.00	0.03	0.06	0.05	0.04
FeO	35.34	35.08	27.76	26.73	27.27
MnO	0.51	0.45	0.47	0.42	0.41
MgO	7.45	7.31	12.95	12.68	12.25
CaO	0.17	0.13	0.01	0.01	0.00
Na_2O	0.00	0.34	0.18	0.20	0.03
K_2O	0.04	0.14	0.17	0.45	0.00
Total	87.53	89.28	88.24	87.75	86.47

Cations on the basis of 28 oxygens:–

	1	2	3	4	5
Si	5.773	5.978	5.288	5.392	5.289
Al^{iv}	2.227	2.022	2.712	2.608	2.711
Al^{vi}	2.481	2.636	2.711	2.835	2.849
Ti	0.071	0.038	0.033	0.037	0.047
Cr	0.000	0.006	0.010	0.008	0.006
Fe	6.622	6.394	4.945	4.763	4.941
Mn	0.096	0.082	0.085	0.073	0.075
Mg	2.488	2.375	4.111	4.027	3.955
Ca	0.039	0.029	0.002	0.002	0.000
Na	0.000	0.143	0.074	0.082	0.012
K	0.011	0.040	0.047	0.121	0.000
$\frac{100xFe}{(Fe+Mg)}$	72.689	72.916	54.605	54.187	55.542

Table 11. Electron microprobe analyses of sphene from pegmatite sample no. 17732. Total iron is expressed as Fe_2O_3.

Anal. No.	1	2		Formula to 4 silicons: 1	2
SiO_2	30.58	30.18	Si	4.000	4.000
TiO_2	37.07	36.08	Ti	3.646	3.596
Al_2O_3	2.45	2.66	Al	0.377	0.415
Fe_2O_3	0.73	1.04	Fe^{3+}	0.072	0.104
MnO	0.02	0.10	Mn	0.002	0.011
MgO	0.04	0.03	Mg	0.007	0.006
NiO	0.01	0.00	Ni	0.001	0.000
CaO	29.25	28.92	Ca	4.099	4.106
Na_2O	0.20	0.25	Na	0.051	0.064
K_2O	0.00	0.02	K	0.000	0.003
Total	100.35	99.28	O	20.10	20.13

Table 13. Electron microprobe analyses of pyrite from microdiorite (1) and diorite (2-4) n.d. = not determined.

Anal. No.	1	2	3	4
Sp. No.	17779	17737	17737	17737
Fe	44.08	47.71	47.81	48.13
S	53.64	53.98	54.89	54.24
Ti	0.18	0.18	0.14	0.16
Mn	0.06	0.00	0.00	0.00
Ni	n.d.	0.00	0.01	0.05
Cu	0.04	0.15	0.05	0.09
Si	0.12	n.d.	n.d.	n.d.
Total	98.12	102.02	102.90	102.67
ATOMIC PERCENTS:				
Fe	31.928	33.582	33.283	33.673
S	67.678	66.179	66.563	66.104
Ti	0.153	0.148	0.117	0.132
Mn	0.046	0.000	0.000	0.000
Ni	n.d.	0.000	0.005	0.033
Cu	0.024	0.092	0.032	0.058
Si	0.171	n.d.	n.d.	n.d.

Table 12. Electron microprobe analyses of ilmenite from diabase (1) microdiorite (2–3) alkali granite (4) and metamorphic rocks (5–9). All Fe is expressed as FeO.

	1	2	3	4	5	6	7	8	9
Sp. No.	17746	17779	17779	17741	17734	17734	17734	17736	17736
TiO_2	53.72	54.03	53.62	52.87	52.71	53.22	51.54	53.92	52.04
Al_2O_3	0.05	0.13	0.05	0.25	0.03	0.19	1.40	0.31	0.49
Cr_2O_3	0.00	0.12	0.05	0.00	0.00	0.00	0.03	0.04	0.01
FeO	43.86	44.18	44.36	38.89	41.83	43.09	41.80	40.00	40.64
MnO	3.47	2.98	3.18	6.24	4.54	4.44	4.32	5.47	4.83
MgO	0.16	0.00	0.00	0.06	0.00	0.36	0.51	0.00	0.62
CaO	0.31	0.28	0.08	2.56	0.09	0.06	0.08	0.68	0.18
Total	101.57	101.72	101.34	100.87	99.20	101.36	99.68	100.42	98.81
Formulae to 6 oxygens:–									
Ti	2.002	1.993	1.993	1.978	1.998	1.967	1.886	1.962	1.939
Al	0.003	0.007	0.003	0.015	0.002	0.011	0.081	0.017	0.028
Cr	0.000	0.005	0.002	0.000	0.000	0.000	0.001	0.001	0.000
Fe	1.818	1.814	1.837	1.618	1.763	1.771	1.694	1.619	1.684
Mn	0.145	0.123	0.132	0.263	0.194	0.185	0.180	0.224	0.203
Mg	0.012	0.000	0.000	0.004	0.000	0.026	0.037	0.000	0.046
Ca	0.017	0.015	0.004	0.137	0.005	0.003	0.004	0.035	0.009

The formulae are calculated by the online computer attached to the probe using oxide percentages upto third decimal and including some below detection limit values of certain elements as well.

has been assigned to the octahedral site, and tetrahedral sites are assumed to be filled by Si alone (Higgins and Ribbe, 1976).

Ilmenite

Ilmenite in the diabase sample occurs mostly as thin lamellae intergrown with amphibole and epidote. Ilmenite analyses (table 12) are quite consistent and all have relatively high MnO content which varies from 2.98 to 6.24 percent by weight. This high MnO content is observed from igneous as well as metamorphic ilmenites. In the mica schist sample 17736, some TiO_2 mineral occurs associated with ilmenite grains. Highest MnO content is observed in a granite which contains approximately double the amount present in ilmenites from intermediate and basic rocks. The calcareous quartzite does not contain ilmenite but it contains magnetite. The quartz-rich muscovite schist contains hematite together with ilmenite. The impurities in ilmenite are not large: $Si\ O_2$ is below the detection level of the microprobe experimental conditions, whereas Al_2O_3 is below 0.5% in all samples except one in which it is 1.4%.

Pyrite

Pyrite analyses are set out in table 13. Pyrite is seen only in intermediate rocks, and is of magmatic origin. Other often associated metals such as Ni and Co are negligible. However, presence of Ti is noteworthy. In microdiorite, pyrite cores are surrounded by magnetite rims. Some magnetite grains lack pyrite cores. In the diorite sample, pyrite is the only opaque ore mineral; and magnetite is absent.

CONCLUDING REMARKS

The Kohi Safaid igneous rock bodies are of relatively small size, and show a variety of rock types from basic to acidic. They show complex field relations and belong to more than one episodes of magmatic activity. Hybridization may have occurred. Many of the igneous bodies show tectonic contacts. The dolerite dykes are probably of tholeiitic nature.

A hard and compact conglomerate bed, frequently with ferruginous matrix serves as a stratigraphic marker horizon below the metamorphic rocks.

The igneous suite exposed in the Kohi Safaid range consists of geologically complex and compositionally diverse mixture of rocks including gabbro, diabase, microdiorites, diorite, quartz diorite, biotite granodiorite, granite, leucogranite, microcline granite and pegmatite. A large compositional spectrum is exhibited inspite of smaller size of igneous bodies. This is unlike other igneous localities of Pakistan where granitic and granodioritic rocks form large batholitic bodies which are compositionally restricted and homogeneous over wide areas. The heterogeneity on outcrop and larger scales combined with contemporaneity suggests hybridization and/or multiple injection. The mafic rock-types are mainly of finer grain-size, e.g., diabase, microdiorite. Gabbro outcrops are not observed. One reason might be the mixing of mafic and felsic magmas in which chilling of mafic magma of a higher temperature occurred in contact with lower temperature felsic magma.

Afridi et al. (1968) regard the igneous-metamorphic zone as of pre-Palaeozoic age. Meissner et al. (1975) noted that the basaltic sills intrude Jurassic and Cretaceous sediments in the westward extensions of the rocks under consideration.

ACKNOWLEDGEMENTS

The field work was done with the major efforts provided by Messrs Abdul Rehman and Abdul Rashid Khan who accompanied the author. The mineral analyses were done at the Department of Earth Sciences, Cambridge University, England, through the cooperation of Drs. J.V.P. Long and P.J. Treloar.

REFERENCES

AFRIDI, A.Z.K., MEMON, A.S. & YELDOZ, O. (1968) Geologic investigations in the upper Kurram Agency of West Pakistan, Unpublished Report, Mineral Development Wing, West Pakistan Industrial Development Corporation, 32 p.

DEER, W.A., HOWIE, R.A. & ZUSSMAN, J. (1962) ROCK-FORMING MINERALS. Vol. 3, Sheet Silicates. Longman, London, 170 p.

— (1982) ROCK—FORMING MINERALS Vol. 1A: Orthosilicates; Second Edition. Longman, London 919 p.

FOSTER, M.D. (1962) Interpretation of the composition and a classification of the chlorites. U.S. Geol. Surv. Prof. Pap. 414-A, pp. 1-33.

HIGGINS, J.B. & RIBBE, P.H. (1976) The crystal chemistry and space groups of natural and synthetic titanites. Amer. Mineral. 61 (9-10), pp. 878-88.

MEISSNER, C.R., HUSSAIN, M., RASHID M. A., AND SETHI, U.B. (1975) Geology of Parachinar quadrangle, Pakistan. U.S. Geol. Surv. Prof. Pap. 716-F, F1-F24.

SCHREURS, J. (1985) Prograde metamorphism of metapelites, garnet-biotite thermometry and prograde changes of biotite chemistry in high-grade rocks of West Uusimaa, southwest Finland. Lithos 18, pp. 69-80.

ACTA MINERALOGICA PAKISTANICA
VOLUME 1 (1985) pp. 64-67.

GEOLOGY OF THE THAR DESERT, PAKISTAN

ALI HAMZA KAZMI
Geological Survey of Pakistan
42/R, Block 6, PECHS, Karachi, Pakistan.

Abstract: **The Thar desert is located along the eastern borders of Pakistan and it covers an area of over 30,000 sq. miles.. It comprises one of the significant geomorphic features of Pakistan and may be divided into four main zones, which from south to north are (1) zone of stabilized longitudinal dunes (2) zone of barchan dunes, (3) zone of transverse sand ridges and mixed dunes and (4) the desert fringe zone. The aeolian sand is fine to medium (grain size ≃ 0.21 mm), contains less than 5% silt, some of the sand is bimodal and contains more than 50% coarse grains. It is commonly well sorted (s = 1.1) and contains mica (below 5%), quartz (80% +) and small amounts of dark minerals. It is concluded that most of the surficial desert sand has been derived from the late Pleistocene to early Holocene braided stream sediments of the Indus Plain, mainly from the lower reaches of the Indus and from the coastal region.**

INTRODUCTION

The Thar desert is one of the significant geologic and geomorphic features of Pakistan and is located along its eastern borders. It extends eastward across the international border into India. In Pakistan it covers an area of approximately 30,000 sq. miles and comprises an area of considerable economic significance. It constitutes the main hinterland along the margins of the thickly populated Indus Plain and nurtures a substantial portion of the cattle wealth of Pakistan. Unfortunately until recently geologically speaking, this fascinating desert had remained a "tera incoghita". Search for oil and gas and problems of waterlogging and salinity have necessitated geological investigations of this interesting area in recent years. The author has been associated with some of these investigations and a summary of the geological information gathered by the author pertaining to the Thar desert is presented in the following pages.

The Thar desert contains a variety of sand dune types and is mainly comprised of longitudinal, transervse, barchan as wess as more complex dune forms, which are probably transitional between these three main forms. Based on the dune morphology, their relative stability and dimensions, the desert may be divided into four main zones, which from south to north are (1) zone of stabilized longitudinal dunes, (2) zone of barchan dunes, (3) zone of transverse sand ridges and mixed dunes, and (4) the desert fringe zone (Fig. 1). These zones are described below.

ZONE OF STABLIZED LONGITUDINAL DUNES

This zone covers the southern part of the desert and contains large longitudinal sand dunes. These dunes have a northeast-southwest trend. Most of them are in the form of ridges 4 to 10 miles long. Frequently these ridges occur in en echelon fashion and overlap or coalesce to form ridges as much as 20 miles long. They are relatively narrow features and at the base barely exceed a width of about 600 to 800 feet. They have steep slopes and the relief varies from about 50 to 300 feet. Between the ridges are small, narrow elongated, flat depression or basins. In the northern part of this zone, these basins contain a thin veneer of loamy sand type of soil. In the southern part of this zone, the inter-dunal depressions are filled with playa type of sediments, salt deposits, or contain saline lakes and marshes.

ZONE OF BARCHAN DUNES

Along the margin of the zone of longitudinal dunes, there is a relatively small zone of active and moving barchan dunes (fig. 1). Swarms of

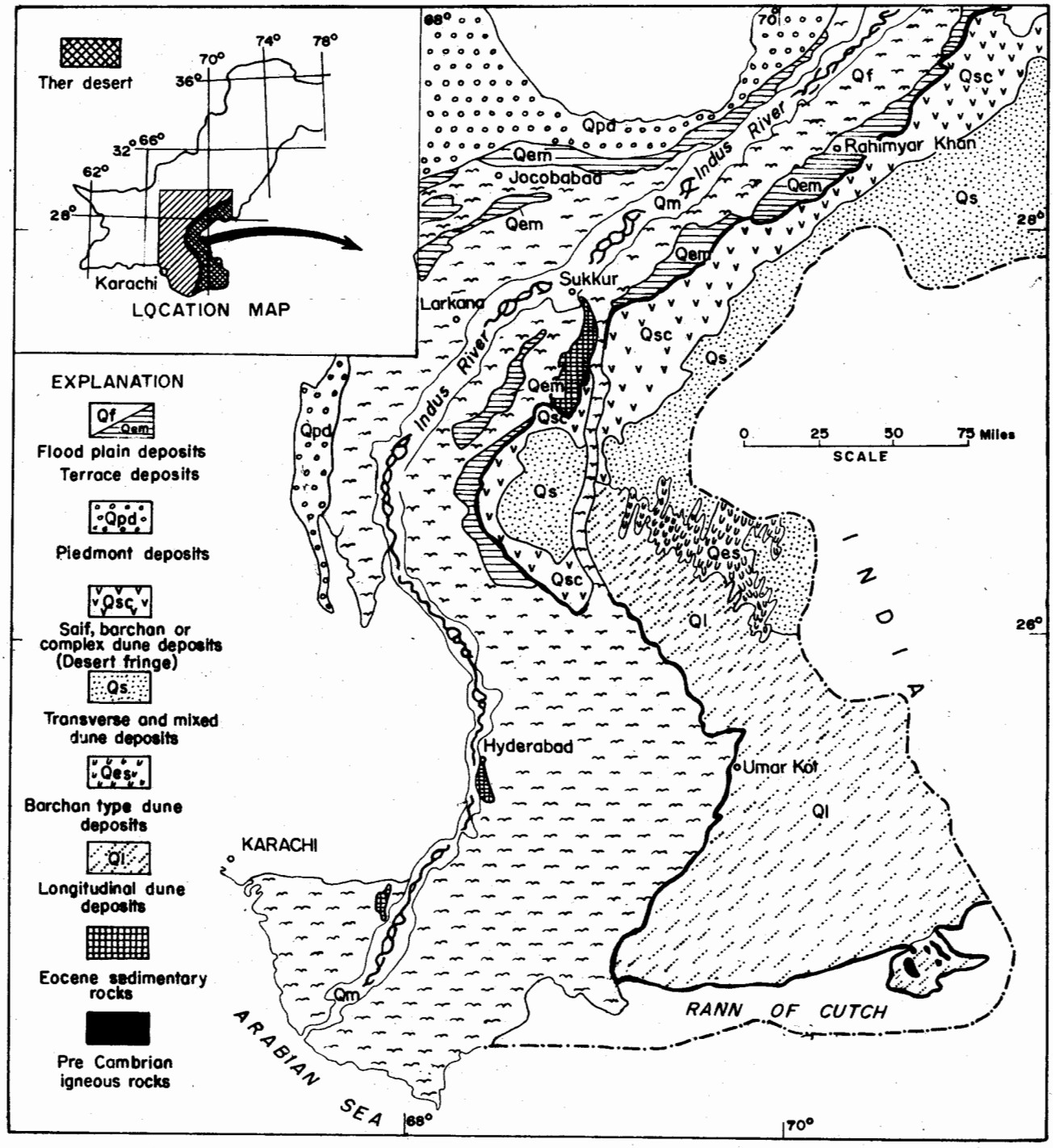

FIG. I– GEOLOGICAL SKECH MAP OF THAR DESERT.

barchan dunes, with their two pointed crescentic ends directed northeastwards, are arranged along narrow sand ridges. Their height varies from 10 to 50 feet and the larger ones are as much as 100 to 200 feet across. Southwestwards, these moving dunes are directly in contact with the longitudinal dunes which appear to be stabilized. It is interesting to note that the southern margin of this zone of barchans is in the form of a straight line parallel to the margin of the Indus flood plain and this line runs more or less at a constant distance from the edge of the plain (fig. 1). Formation of barchan dunes in an area where the longitudinal dunes had been formed earlier, clearly indicates a change in the meteorological conditions, particularly changes in the intensity and direction of prevailing winds. At present this region has a steady southwesterly wind and this, no doubt, formed the Recent barchans. In the past, at the time of the formation of the longitudinal dunes, this southwesterly wind may have been less strong and it may be expected that there were in addition strong, relatively short cross-winds from the northwest. The northwesterly wind at present affects the northern part of the desert, but does not reach as far south as the Lower Thar Desert. This wind may be expected to have been stronger during glacial periods and early parts of interglacials and it is likely that the longitudinal dunes grew during such climatic conditions.

ZONE OF TRANSVERSE RIDGES AND MIXED DUNES

This zone extends from near Nawabshah, northeastward up to Bahawalpur. It is characterised by sand dunes in the form of parallel transverse ridges. Along their crests these ridges frequently have a beaded or serrate appearance. They have a long gently windward slope and a narrow near vertical leeward slope. On their leeward side there is usually a small depression, occupied by mud flat. The ridges are about 2 to 4 miles long and 10 to 50 feet high. Most of these dune ridges are stabilized or in various stages of stabilization. The continuity of the transverse ridges is frequently broken by the influx of moving sand, in the form of barchan dunes or at some places in the form of small longitudinal dunes (fig. 1). Northeastward the dunes become more complex. In general, this zone of the desert is the most inhospitable, with little vegetation, no sizeable tracts of flat ground free from loose sand, a very confusing featureless "basket of egg" type of topography, without habitation and water.

THE DESERT FRINGE ZONE

This zone occupies a large area in the northern part of the Thar desert, along the margins of the Central Alluvial Plain. This zone has been invaded by the desert in relatively recent times. Numerous traces of the old extinct streams which must have once flowed in this region, indicate that originally this zone was part of a flood plain. Near Fort Abbas, its eastern part, there is a large, narrow depression, which has been recently reclaimed and is now under cultivation. This depression contains the bed of the old Hakra River, which according to historical records flowed through the region as late as the seventeenth and eighteenth centuries. However, recent investigations by the author have brought to light numerous extinct channels which suggest that the early drainage of the zone must have been quite complex.

With the gradual desiccation of the region and drying up of the streams such as the Hakra, the sand from the dry river beds and from adjacent areas blew across the old flood plain, filling in the old channels, burying the old flood plain and forming the various types of sand dunes. In recent times most of these dunes have become stabilized and are covered with thorny scrub vegetation. The dunes form only intermittent patches and in between them there are large irregularly shaped mud flats. Every monsoon season these flats get flooded. As a result of modern cultivation in some of the areas, the supply of sand from the ploughed fields has once again become available and fresh barchan dunes have begun to form and move in this region.

DESCRIPTION AND AGE OF AEOLIAN SAND DEPOSITS

The aeolian sand which forms the longitudinal dunes is commonly well sorted and the average coefficient of sorting is about 1.1. It is a fine to medium sand, with an average medium grain size of about 0.21 mm. The silt content of these sediments is less that 5 percent. Some of the sand is bimodal and contains more than 50 per cent coarse sand grains. The coarse fragments are up to 2 mm in diameter. The sand grains are well rounded. Mineralogically the desert contains less mica (less than 5 percent as compared with 5 to 30 percent in alluvial sediment), more quartz (80 percent or more as compared with 50 to 75 percent in alluvial sediments) and relatively smaller quantities of dark minerals. The sand in the barchan and transverse dunes is relatively finer and more micaceous than the sand in the longitudinal dunes. The former has been derived from the flood plain sediments.

CONCLUSIONS

The coarse nature of the sand in the longitudinal dunes is significant in view of the fact that the alluvial sediments in the lower Indus Plain do not contain fragments coarser than 0.5 mm. Therefore, the presence of coarse to very coarse sand grains in the desert near Umerkot indicates that these coarse sediments have not been derived from the Recent meander stage sediments of the Indus and may have been derived from the Early Recent braided stage sediments of the Tandojam Formation (Kazmi 1977, 1984). The northeast-southwest orientation of these dunes indicates that the dominant wind direction must have been from the southwest as at present. This precludes the possibility of the sand having originated from any region other than the Indus Plain. With the exception of a small patch of dune southeast of Badin which have been grown in Recent times and which cover the delta of the earliest exposed course of the Indus, most of the longitudinal dunes are probably late Pleistocene in age. The desert has grown in stages during the Quaternary period. Its eastern part is probably the oldest. During each successive glacial period, as the sea level fell and large tracts of coastal region were exposed to weathering and erosion, sediments were blown away by wind and deposited on the margins of the ever-expanding desert. This process may have been accelerated during the earlier part of interglacial periods when great quantities of sediments were brought down by the braided streams.

REFERENCES

KAZMI, A.H. (1977) Review of the Quaternary Geology of the Indus Plain, Presidential address, Earth Science Section, 18th Annual Conference, Multan, Scientific Society of Pakistan (in Urdu), 26 p.

KAZMI, A.H. (1984) Geology of the Indus Delta. In: Haq, B.U. & Milliman, J.D. (eds.) MARINE GEOLOGY AND OCEANOGRAPHY OF ARABIAN SEA AND COASTAL PAKISTAN. Van Nostrand Reinhold Co., pp. 71-84.

ACTA MINERALOGICA PAKISTANICA
VOLUME 1 (1985) pp. 68-70

SOURCE AREA DETERMINATION FROM COMPOSITION OF CLINOPYROXENES OF GALA AREA GREYWACKES, SCOTLAND

AKHTAR MOHAMMAD KASSI
Geology Department, University of Baluchistan, Quetta.

Abstract: Electron probe microanalyses of the pyroxenes of the lower Palaeozoic rocks (greywackes) of the Gala area, Southern Uplands, Scotland, show non-alkaline affinities and have been derived from a volcanic arc outside the basin of deposition. If found in coarse clastic sediments the clinopyroxenes may be useful source indicators.

INTRODUCTION

Clinopyroxene compositions vary in mafic lavas of different tectonic settings (Kushiro, 1960; LeBas, 1962; Nisbet & Pearce, 1977). An attempt was made to apply the methods used by the above writers to coarse grained greywackes to determine the origin of clinopyroxenes. The Ordovician and Silurian rocks of the Southern Uplands of Scotland consist of a flysch succession with greywackes and alternate shales and mudstone beds. In the Gala area of the Southern Uplands the Ordovician succession has been divided into a lower unit - the Falahill Formation, and upper unit - the Heriot Formation (fig. 2). Likewise the Silurian succession has been divided into four units. The Falahill Formation of the Ordovician and the Hazelbank Formation of Silurian succession are of basic-clast nature and bear plenty of clinopyroxenes. Apart from quartz and feldspar they are also rich in basic igneous rock fragments (andesite / basalt) and ferromagnesian minerals (clinopyroxene and amphibole). Other rock fragments of sedimentary and metamorphic origin are also present in subordinate amounts.

ANALYSIS AND RESULTS

Detrital clinopyroxenes both from the Falahill Formation and the Hazelbank Formation were analysed by electron microprobe. Their chemical compositions show that 22 out of 26 are calcic augite, two are salite and two diopsidic augite (fig. 3). The pyroxenes of both formations are comparable compositionally and have been derived from a similar source area. Results of the analyses were plotted on TiO_2–Al_z covariation diagram (after LeBas, 1962, and on a plot of discriminant functions, F1 against F2 (after Nisbet & Pearce, 1977). The TiO_2 - Al_z covariation plot (after LeBas, 1962) of the clinopyroxenes of the Gala area (fig. 4-b) show that 22 out of 26 grains fall into the non-alkaline field. The plot of discriminant functions F1 and F2 after Nisbet & Pearce (1977) suggest that the pyroxenes have been derived from a volcanic arc region. It can be concluded that the detrital pyroxenes of the Falahill and Hazelbank Formations are of non-alkaline nature and may have been derived most likely from a volcanic arc. There are other evidences which support the above conclusions, and are given below.

1) Basic clast greywackes extend across the south of Scotland and Ireland for more than 300 km, pointing to the presence of a laterally extensive source area - more likely a volcanic arc across the south of Scotland and Ireland.

2) Biotite is rich in MgO and Al_2O_3 and resembles the biotite of the calc-alkaline igneous rocks (Nockolds 1947; Kassi, 1984).

Fig. 1. Map of the Southern Uplands showing location of the Gala area.

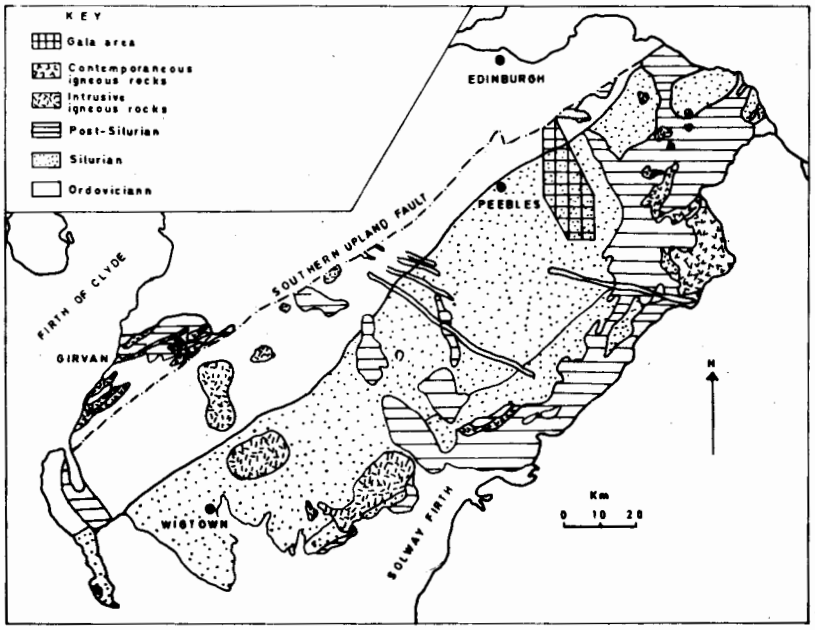

Fig. 2. Geological map of the Gala area.

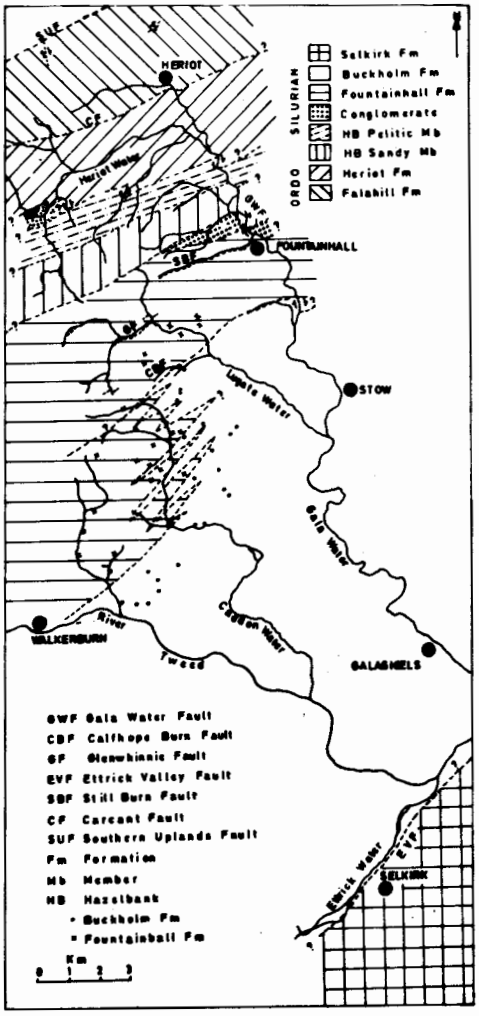

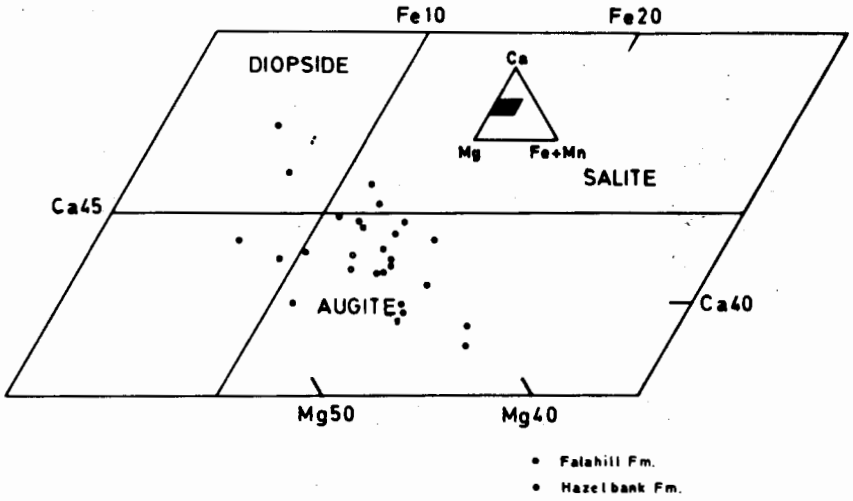

Fig. 3. Pyroxene analyses plotted on part of the pyroxene quardrilateral (inset).

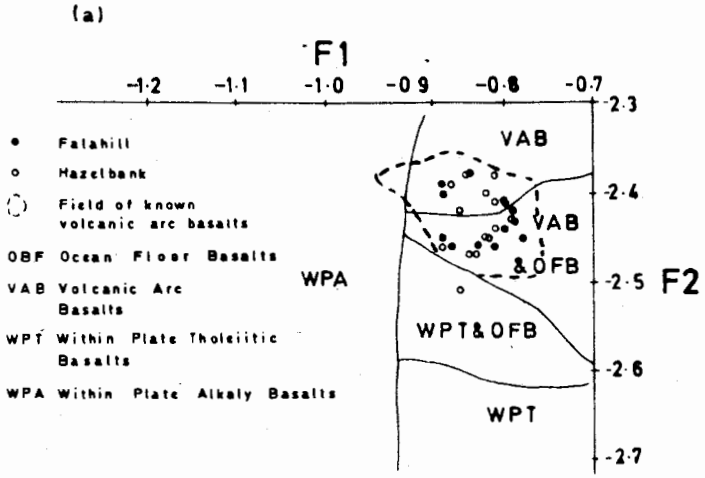

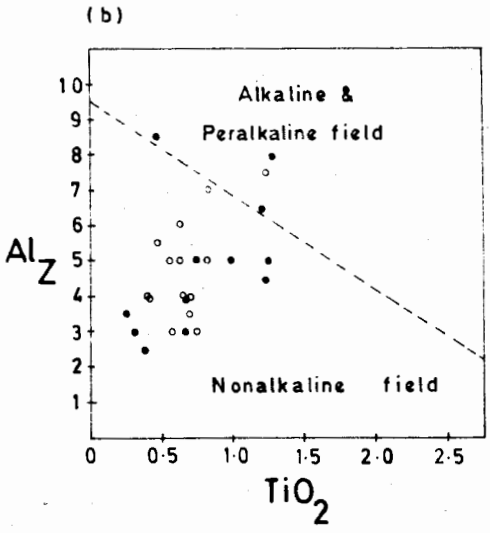

Fig. 4. Pyroxene analyses (a) Plot of discriminant functions, F1 against F2 (after Nisbet & Pearce 1977). (b) Plot of Al_Z against TiO_2 (after Le Bas 1962).

3) The presence of glaucophane blueschist, chrome spinel and other mafic and ultramafic rock fragments like gabbro, andesite and serpentine (Kelling, 1962; Floyd, 1975; Hepworth, 1981; Kassi, 1984) point to the presence of a subduction complex in the source area which in turn necessitates the presence of a volcanic arc.

REFERENCES

FLOYD, J.D. (1975) The Ordovician rocks of West Nithsdale. Unpub. Ph. D. thesis, University of St. Andrews.

HEPWORTH. B.C. (1981) Geology of the Ordovician rocks between Leadhills and Abington, Lanarkshire. Unpub. Ph. D. thesis, University of St. Andrews.

KASSI, A.M. (1984) Lower Palaeozoic geology of the Gala area, Borders Region, Scotland, Unpub. Ph. D. thesis, University of St. Andrews.

KELLING, G. (1962) The petrology and sedimentation of upper Ordovician rocks in the Rhinns of Galloway, Southwest Scotland. Trans. Roy. Soc. Edinburgh **65**, pp. 107-37.

KUSHIRO, L.(1960) Si - Al relation in clinopyroxenes from igneous rocks. Amer. Jour. Sci. **258**, pp. 548-54.

LeBAS, M.J. (1962) The role of alumina in igneous clinopyroxenes with relation to their parentage. Amer. Jour. Sci. **260**, pp. 267-88.

NISBET, G. & PEARCE, A. (1977) Clinopyroxene composition in mafic lavas from different tectonic settings. Cont. Min. Pet. **63**, pp. 149-60.

NOCKOLDS, S.R. (1947) The relation between chemical composition and paragenesis in the biotite micas of igneous rocks. Amer. Jour. sci. **245**, pp. 401-20.

ACTA MINERALOGICA PAKISTANICA
VOLUME 1 (1985) pp. 71-73

OVERLAPPING TURBIDITE FANS REVEALED BY LATERAL VARIATIONS IN LITHOLOGY AND MINERALOGY OF GALA AREA, SCOTLAND

AKHTAR MOHAMMAD KASSI
Geolgoy Department, University of Baluchistan, Quetta.

Abstract: **The lower Palaeozoic rocks (turbidites) of upper Llandovery age in the Gala area of the Southern Uplands of Scotland show drastic lateral variations in lithology and mineralogical composition. The lithlogies (units) were named as the Buckholm Formation and Fountainhall Formation. Study of lateral variations show that the lower part of the Fountainhall Formation interdigitate with the upper part of the Buckholm Formation, suggesting the overlapping of two turbidite fans, drawing sediments from partly contrasting sources. This interpretation is also supported by structural, sedimentological and faunal evidence.**

INTRODUCTION

The lower Palaeozoic succession of the Southern Uplands of Scotland comprises turbidite (greywackes) sediments. The area has been interpreted as an accretionary prism (Leggett et al. 1979) and has been divided into fault blocks bounded by a series of major strike faults leading to contrasting sequences within successive fault blocks (Hepworth, 1981). The blocks display successively younger flysch sequences to SE, whilst strata within each block young to NW. This particular structural style showing prolonged and continued deformation is comparable with accretionary prisms which form on active continental-oceanic margins by the subduction of oceanic plates (Kerig & Sharman, 1975). The area has been divided into various lithostratigraphic units (Walton, 1955; Kelling, 1961; Floyd, 1975; Kassi, 1984) based on the lithology and petrology of greywackes.

The Silurian succession of Gala area was subdivided (Kassi, 1984) into four units, namely the Hazelbank, Fountainhall, Buckholm and Selkirk Formations. Field evidence and petrology of the rocks studied show drastic lateral variations across Caddon Water whereby characters of the Buckholm Formation (to the east) are replaced by the Fountainhall Formation (to the west), showing evidence of interdigitation.

DESCRIPTION

Full description of stratigraphy and petrology of rock units of the Silurian succession have already been described (Kassi, 1984). However, for the present purpose it is necessary to go into details of the Fountainhall and Buckholm Formations (Kassi, 1985, fig. 2).

Fountainhall Formation

The Fountainhall Formation consists of medium to coarse grained, medium-grey greywackes, sporadic conglomerates and dark grey and light olive to olive-grey mudstones, siltstones and greyish black graptolitic shales. The greywackes and conglomerates are typified by quartz, acid igneous fragments and feldspars. Basic igneous, metamorphic and sedimentary rock fragments are present in subordinate amounts. The QMF-plot (fig. 1) based on point counting clearly differentiates the Fountainhall Formation from the underlying Buckholm Formation.

The pelitic sequences which represent pelagic/hemipelagic, black graptolitic shales (the Moffat Shales, Lapworth, 1878) of Llandovery age represent zones of prolonged and continued deformation (thrusts and imbricate zones). Faunal evidence shows that these shales vary from Parakidograptus accuminatus to Mono-

graptus maximus zones of Llandovery age (Peach & Horne 1899; Kassi 1984). It has been concluded on the basis of regional structure, nature of shale outcrops and faunal evidence that the Fountainhall Formation represents at least three fault blocks (Kassi, 1985, fig. 2), whilst the zone of interdigitation and the Buckholm Formation jointly represent another enormously wide block.

Buckholm Formation

The formation consists of thick and massive, medium dark grey and dark grey greywackes. In places these are conglomeratic and in others interbedded with thick to thin (3 cm to 40 cm) horizons of greyish grey, brownish grey mudstones and medium grey shales, mudstones and siltstones. The greywackes are silicic, being notably rich in quartz in association with acid igneous and metamorphic rock fragments (fig. 1). Garnet is commonly visible megascopically and is valuable as a horizon index. Feldspar, and sedimentary and basic igneous rock fragments are subordinate. The prevalence of quartz imparts a vitreous lustre to freshly fractured surfaces. The profusion of garnet and silicic fragments readily distinguishes the Buckholm Formation from the otherwise apparently comparable Fountainhall Formation. The interbedded mudstones are profilic in trace fossils, mostly burrows of Dictyodora (Benton, 1982).

The outcrop of the formation is enormously wide, carrying a cross strike width in excess of 15 km. This width is considered to reflect folding and imbrication rather than enormously large stratigraphical thickening.

Buckholm - Fountainhall contact

The lower contact of the Fountainhall Formation is faulted in the vicinity of the Calfhope Burn (Kassi, 1985, fig. 2) and the fault continues southwestwards across the high reaches of Ewes Water. The fault may be inferred to continue beyond the Caddon Water. Relationship between the Fountainhall Formation and Buckholm Formation becomes complicated in the vicinity of Caddon Water. The contact roughly follows the course of the river on a N-S trend and is highly irregular, the two formations appear to interdigitate. Southwards the contact again resumes its NE-SW trend. This relationship suggests the overlapping of turbidite fans in the vicinity of Caddon Water, carrying sediment from partly contrasting source areas, potentially far removed. This interpretation is supported by the following supplementary observations:

(a) Although the Caddon Water represents the trend of strike-slip faults, there is no evidence of major faulting along the Caddon Water, yet a strike-slip displacement of nearly 4 km would be necessary if the interdigitation were not responsible. Moreover, the northern boundary of the Fountainhall Formation with the Hazelbank Formation is not offset and a large strike-slip movement would have to be accomodated by thrusting and or differential buckle folding in each formation. There is no evidence of differential deformation on appropriate scale.

(b) The strata across the Caddon Water represent comparable facies associations (Kassi, 1984).

(c) Divergence of erosional currents by as much as 90° (Kassi, 1984) in successive turbidite sequences are most logically explained by overlapping fans.

(d) The occurrence of comparable faunas (Peach & Horne, 1899; Kassi, 1984) within the strata on both side of the Caddon Water.

CONCLUSION

Lateral variations in mineralogical composition have revealed that two overlapping turbidite fans have drawn sediments from partly contrasting source areas.

REFERENCES

BENTON, M.J. (1982) Trace fossils from the lower Palaeozoic ocear floor sediments of the Southern Uplands of Scotland. Trans. Roy. Soc. Edinburgh: Earth Science 73, pp. 67-87.

FLOYD, J.D. (1975) The Ordovician rocks of west Nothsdale. Unpubl. Ph. D Thesis, University of St. Andrews.

HEPWORTH, B.C. (1981) Geology of Ordovician rocks between Leadhills and Abington, Lanarkshire Unpubl. Ph. D. thesis University of St. Andrews.

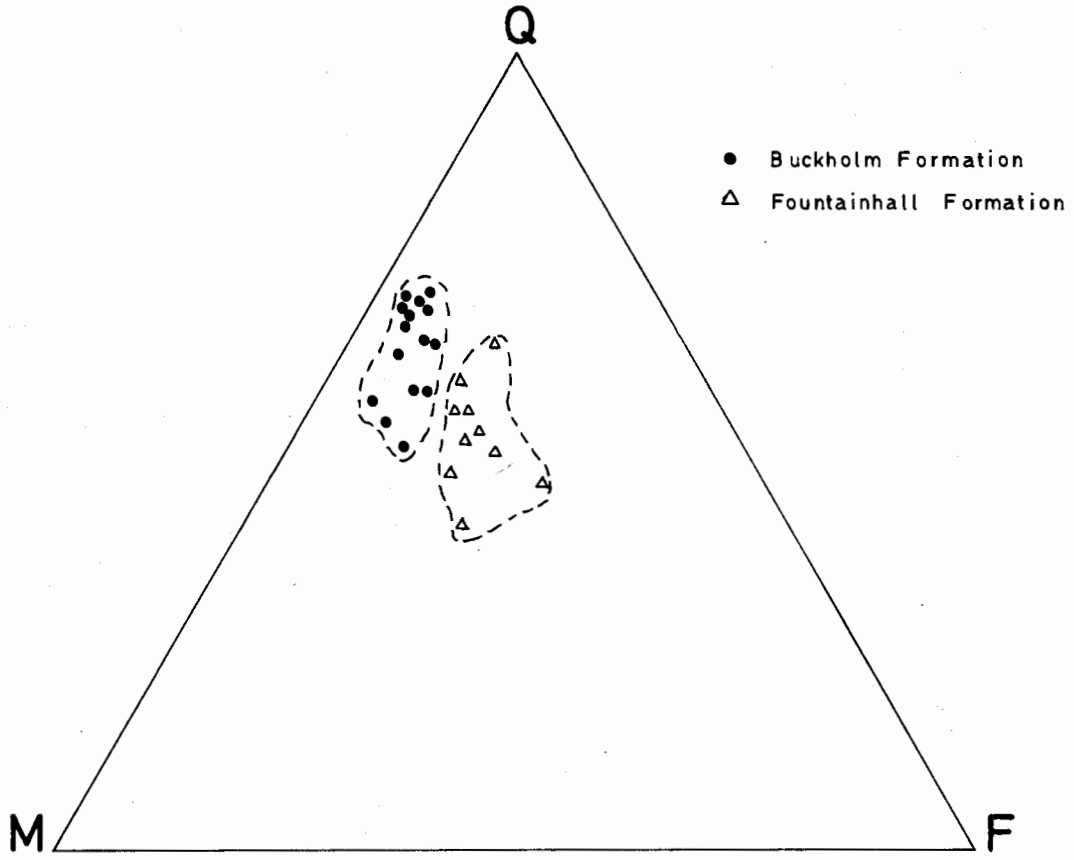

Fig.1. QMF plot based on point counting results.

Q = Quartz + acid igneous rock fragment + metamorphic fragments.

M = Matrix + sedimentary fragments.

F = Feldspar + basic igneous rock fragments + ferromagnisian fragments.

KARIG, D.E. & SHARMAN, G.E. (1975) Subduction and accretion in trenches. Bull. Geol. Soc. Amer. 86, pp. 377-89.

KASSI, A.M. (1984) Lower Palaeozonic geology of the Gala area, Borders Region, Scotland. Unpubl. Ph. D. thesis, University of St. Andrews.

— (1985) Source area determination from composition of clinopyroxenes of Gala area, Scotland, This volume.

KELLING, G. (1961) The stratigraphy and structure of the Ordovician rocks of the Rhinns of Galloway. Quart, Jour. Geol. Soc. London 177, pp. 37-45.

LAPWORTH, (1878) The Moffat Series. Quart. Jour. Geol. Soc. London 34, pp. 240-346.

LEGGETT, J.K. McKERROW, W.S. & EALES, M.H. (1979) The Southern Uplands of Scotland: A lower Palaeozoic accretionary prism. Jour. Geol. Soc. London 36, pp. 755-70.

PEACH, B.N. & HORNE, J. (1899) The Silurian Rocks of Britain. Vol. 1 Scotland. Mem. Geol. Surv. Scotland.

WALTON, E.K. (1955) Silurian greywackes in Peeblesshire. Proc. Roy. Soc. Edinburgh B-65, pp. 327-57.

ACTA MINERALOGICA PAKISTANICA
VOLUME 1 (1985) pp. 74-77

THE NATURE OF CLAY MINERALS FROM A SECTION OF GHAZIJ SHALE FORMATION IN CHAPPAR VALLEY NEAR MANGI KACH, BALUCHISTAN.

JAWED AHMED, DUANE M. MOORE* & ZULFIQAR AHMED
Centre of Excellence in Mineralogy, University of Baluchistan, Quetta, Pakistan.

***Present Address: Department of Geology, Knox College, Galesburg, Illinois 61401, U.S.A.**

Abstract: Across a section of the shaley Ghazij Formation of middle Eocene age exposed in the Chappar Valley near Mangi Kach area of Sibi District, twenty samples of clayey material were collected. Their clay mineral content has been characterized by means of XRD and DTA. The clay minerals identified are illitic clay, mixed layer clay and magnesium rich chlorite. The rock is generally composed of illitic clay (50-60%) mixed-layer clay (26%) and chlorite (14%).

INTRODUCTION

The Ghazij formation of middle Eocene age is exposed in the Kirthar Range, part of the Sulaiman Range and the Axial Belt regions of Pakistan. It consists dominantly of shale with subordinate claystone, sandstone, limestone, alabaster and coal. The outcrop colours are pale greenish grey, brown and light grey. The shale is calcareous, hard, flaky and in some places grades into marl.

The purpose of the present study is to charaterize the clay mineral content, because previously little mineralogical data exists on the clay minerals of this formation.

FIELD DESCRIPTION

The Ghazij shale section sampled for the purpose is located at Chappar Valley (latitude 30° 21′ N, longitude 67° 26′ to 29′ E), northeast of Quetta, Pakistan (fig. 1). Profile along the sample line gives a stratigraphic thickness of 3200 feet which was sampled at sampling interval of 160 feet measured using an Abney level. The formation is well-exposed. The shale is greenish grey to light grey coloured, soft, flaky and at some places blocky. Base of the Formation is well marked because the underlying strata of early Eocene Dunghan Limestone dip 30° SW and show an excellent dip slope. Chappar Valley cuts in right at the Dunghan–Ghazij contact. Top part of Dunghan Limestone is thin bedded. There were probably movements which were absorbed by movement along bedding planes. Wherever the lower part of Valley is occupied by more massive Dunghan limestone; many cross-cutting veins are present indicating accommodation to tectonic movements which, in the case of shale, would have been absorbed in more plastic manner. Therefore, a clear even bedding aligned with 30° dip of the Dunghan Limestone below and 30° dip of Spintangi Limestone above, is not expected.

Twenty samples were collected along a line across the strike, at a regular interval of 5% of the total thickness. Offset but stratigraphically equivalent samples were collected 100-200 feet in both directions from the main sampling line. The samples were taken from an average depth of one foot below the surface.

ANALYTICAL METHOD

X-ray diffractogram patterns were obtained for the clay-size ($< 0.5\ \mu$) fraction of each sample. About 8 gram material from each sample was crushed in the porcelain mortar, and kept in distilled water for 24 hours. This was treated with 5mg of sodium meta-hexaphosphate as dispersion agent. Then after one hour, this dispersed sample was split into three

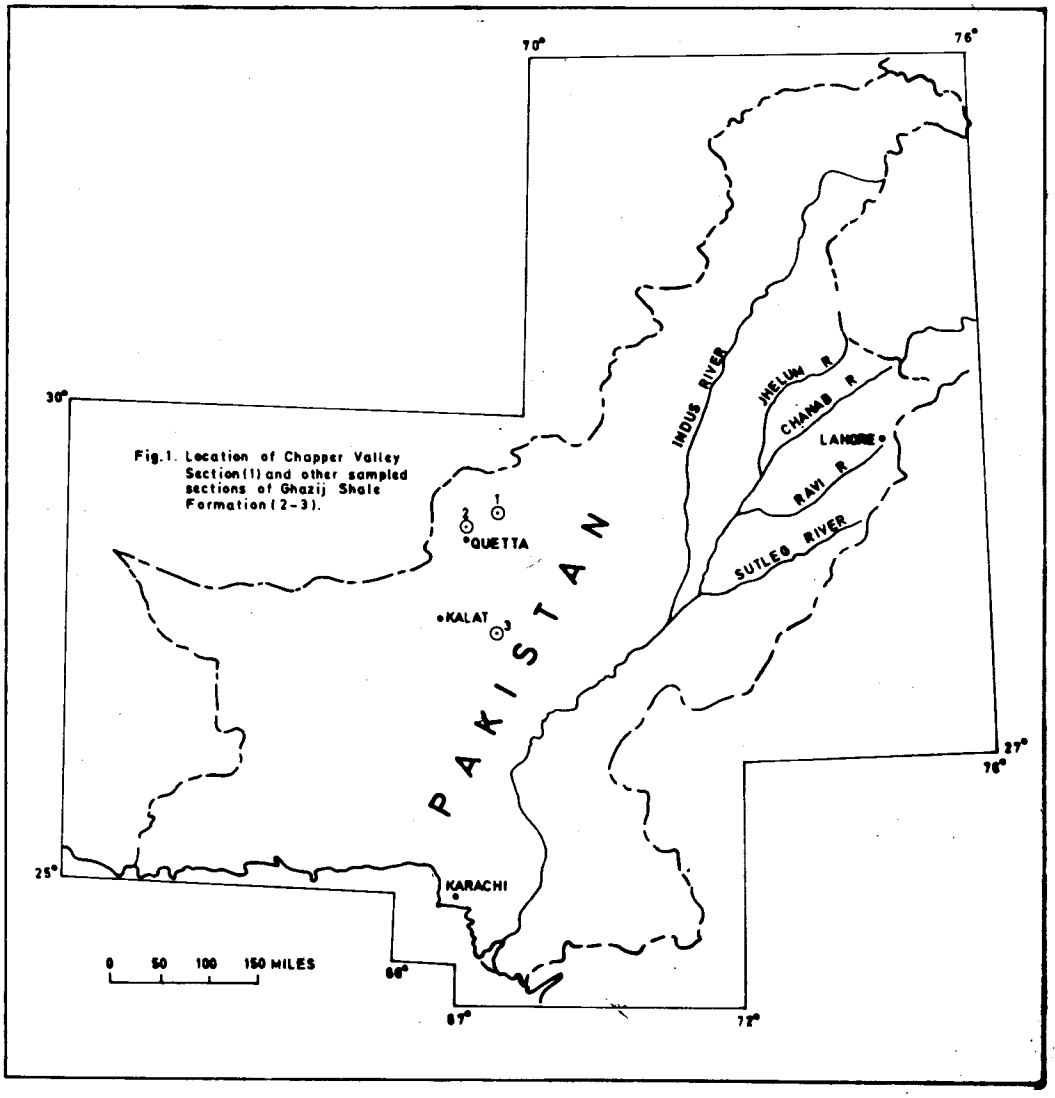

Fig.1. Location of Chapper Valley Section(1) and other sampled sections of Ghazij Shale Formation(2-3).

fractions for centrifuging. Glass slides were then prepared from each supernate suspended material. Thus, three slides of each sample were made representing (a) air dried oriented aggregates (b) ethylene glycolated aggregates and (c) fired oriented aggregates. These slides were run on XRD unit. All sample were treated for the removal of organic material and iron oxide. Several samples contained chlorite which was removed by heating in 1 N dilute HCL at 80°C for one hour.

For differential thermal analysis, 100 mg of each sample was crushed in a porcelain mortar and run on the DTA unit for 50 minutes. The DTA pattern was obtained on photographic film which was compared with the DTA card.

DISCUSSION AND RESULTS

X-ray diffraction data compare well with those of the illite. The basal spacing of 10 Å reflection shows no significant change when mineral is subjected to mild thermal treatment. With chemical treatment, the peak shapes are improved slightly. In the Chappar Valley clays, the 10 Å reflection displays an appreciable asymmetry. The intensity of this reflection is decreased and the shape is improved to a more symmetrical one by glycerol or ethylene glycol treatment as shown in figure 2.

To distinguish between kaolinite and chlorite structure the samples were heated to 550° to

Table 1. Clay minerals from individual samples of the Chapper Valley Section. "H" represents the height of each sample, in feet, above the base of Ghazij Formation.

Sample No.	H	Minerals present	Percentage by Peak-height method
20	3040	Chlorite	–
19	2880	Chlorite	–
18	2720	Chlorite	–
17	2560	Illite	–
16	2400	Illite	–
15	2240	Illite, chlorite	70, 30
14	2080	Mixed layer illite-smectite	80-20
13	1920	Illite, chlorite	75, 25
12	1760	Mixed layer illite-smectite	80, 20
11	1600	Illite, magnesian chlorite	80, 20
10	1440	Mixed layer illite-chlorite	78-22
9	1280	Mixed layer illite-smectite	80-20
8	1120	Mixed layer chlorite-smectite	80-20
7	960	Illite, magnesian chlorite	80,20
6	800	Illite	–
5	640	Illite, chlorite	75, 25
4	480	Illite	–
3	320	Illite, chlorite	80, 20
2	160	Illite	–
1	0	Illite	–

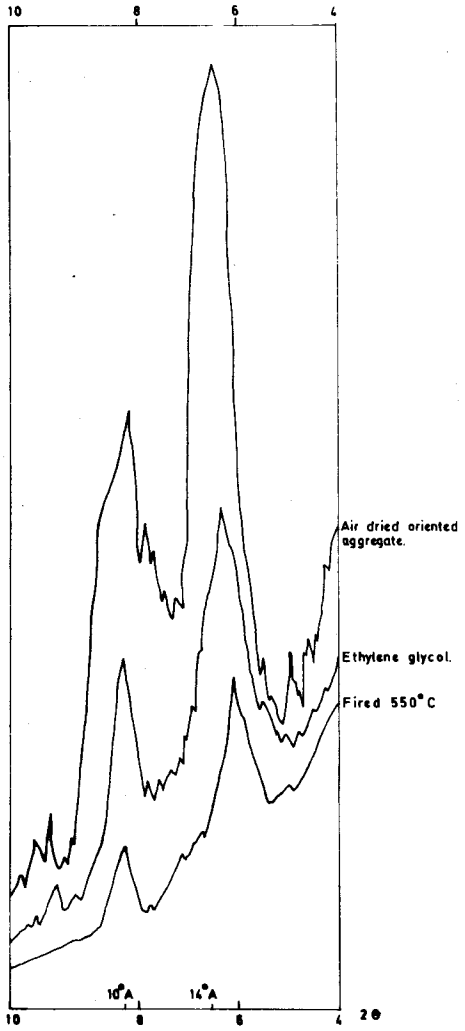

Fig. 2. X-ray diffraction pattern of clay sized fraction of sample No.7 from Chapper Valley.

600° C for half an hour. This should decompose kaolin minerals, but not chlorite (Brindley & Robinson, 1951). Heat treatment produces a partial dehydration which enharces 14 Å reflection and weakens the 7 Å layer peak. Another method is to use warm dilute HCl to dissolve chlorite and leave kaolinite. In Chapper Valley samples, the basal spacings of 14.1 to 14.3 Å of magnesium rich chlorite are present. In the mixed-layer clay minerals, individual layers of the crystal have different composition and proportions. In the minerals, individual layers of the crystals have different composition and proportions. In the mixed-layer clay of Chappar Valley, the layers are of illite/smectite and chlorite/smectite types. Two organic liquids commonly used to expand the smectite to known thickness are : ethylene glycol which produces 17 Å thickness; and glycerol which produces 18 Å layer thickness. The characteristic feature of illite layers is that they are non-expanding and have fixed layer thickness of 10 Å. Peak height method described by Schultz (1978) was used to indicate the amount of expandable clay. In figure 4, the the heights of the 17 Å and 10 Å reflections in arbitrary units are 100 and 30 respectively. A clay having 30 units peak height when heated, if it were entirely expanding smectite, should give 135 unit (30x4.5) peak height at 17 Å when treated with ethylene glycol. The observed 100 unit peak height is 74% of the expected height. Thus, 74% of the expanding clay was

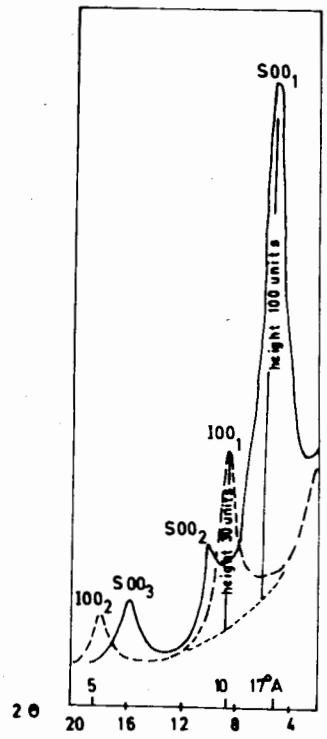

Fig.3. X-ray diffraction pattern of mixed layer illite-smectite from Chapper valley. Solid line- Ethylene glycol, Long dashed line- Glycerol, Short dashed line-heated.

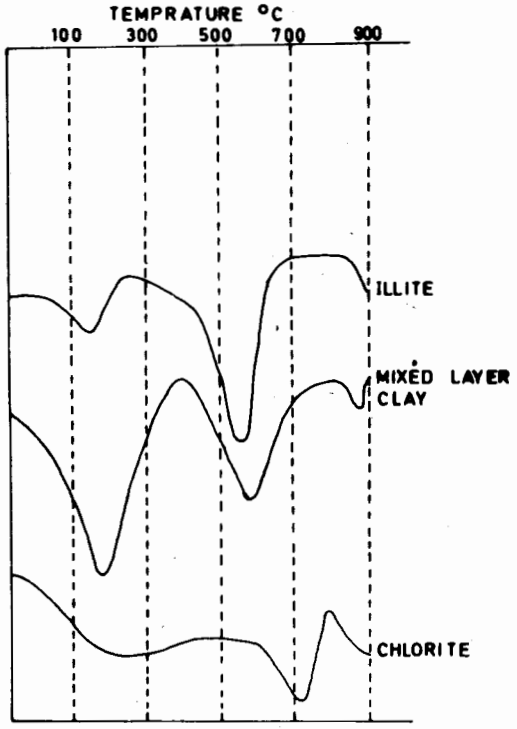

Fig.4. D.T.A curves of clay minerals from Chapper valley.

attributed to smectite and remaining 26% to mixed layer clay (fig. 3).

In the DTA curve for illite of Chappar Valley, endothermic peaks occur at 180° C, 550° C and 780° ± 20° C and exothermic peak at 830°C. Usually a broad endothermic peak occurs at 550° C. In chlorite the peak temperatures for the major endothermic reactions caused by loss of crystalline water are 720° ± 10° C or 610° ± 10° C and exothermic peak occurs at 810° C.

The clay minerals and their relative proportions as found in twenty samples are listed in table 1. The mixed layer minerals occur only in the middle part of the Formation. The lower part is mainly illite. The upper part has chlorite -rich horizons above the illite horizon.

CONCLUSION

In Chappar Valley, clay minerals of Ghazij Shale Formation are illitic clay, mixed layer clay and chlorite. The rock is generally composed of illitic clay (50-60%), mixed layer clay (26%) and chlorite (14%). Similar work to characterize the clay size fractions of the Ghazij shale Formation sections exposed at Degari, Kach and Mardan Valley near Khuzdar, is in progress.

REFERENCES

BRINDLEY, G.W. & ROBINSON, K. (1951) The chlorite minerals. In: Brindley, G.W. (ed) X-RAY IDENTIFICATION AND CRYSTAL STRUCTURES OF CLAY MINERALS. Mineralogical Society, London, pp. 173-98.

SCHULTZ, L.G. (1978) Mixed layer clay in the Pierre Shale and equivalent rocks of northern Great Plains region. U.S. Geol. Surv. Prof. Paper 1064-A, pp. 1-28.

ACTA MINERALOGICA PAKISTANICA
VOLUME 1 (1985) pp. 78-82

PETROGRAPHY OF HORNBLENDITES AND ASSOCIATED ROCKS AT MAHAK, UPPER SWAT.

M.U.K. KHATTAK[1], M. LATIF KHAN[2], M. IDRESS BANGASH[1] AND M. QASIM JAN[1]

1. NCE in Geology, University of Peshawar, Peshawar, Pakistan.
2. FATA Development Corporation, Warsak Road, Peshawar, Pakistan.

Abstract: An 8 km^2 area around Mahak consists of amphibolites, metamorphosed gabbros and pyroxenite, hornblendites, and minor dykes and veins of horblende-plagioclase pegmatite and quartzo-feldspathic rocks. These are described here petrographically, with a brief discussion on their origin. The amphibolites are meta-igneous and essentially composed of amphibole, plagioclase and/or epidote; the gabbros and pyroxenites are relictual and partially amphibolitized; the hornblendites are essentially monomineralic, variable in grain size and may grade into amphibolites through a plagioclase-bearing variety.

INTRODUCTION

The southern amphibolite belt of Kohistan consists of homogeneous to banded amphibolites with subordinate calcareous, pelitic and siliceous metasediments, and a spectrum of plutonic rocks ranging from ultramafites to gabbros, norites, diorites, tonalites, granites and trondhjemites (cf. Bard, 1983; Coward et al., 1982; Jan, 1979). The ultramafic bodies are generally small and include peridotites, pyroxenites, and hornblendites.

Several occurrences of hornblendites have been reported from the amphibolite belt, especially in Dir district, and different hypotheses of origin (igneous, metamorphic, metasomatic) have been proposed by previous workers (for a review, see Banaras and Ghani, 1983). The occurrence of hornblendites near Mahak (34° 53′ N, 72° 17′ F), about 20 km NW of Mingora, was first reported by Ahmed et al. (1980).This paper presents the petrography of the hornblendites and their associated rocks investigated in an 8 km^2 area around Mahak, Upper Swat. The area comprises amphibolites, hornblendites, metamorphosed gabbro/norite, pyroxenite, hornblende pegmatite, and quartzofeldspathic dykes and veins (fig. 1).

PETROGRAPHY

Amphibolites

These host the rest of the rocks and are homogeneous to locally banded. The bands may be uniform or variable in thickness, pinched and swollen, and in some cases are clearly produced due to shearing (fig. 2) The foliation in the amphibolites trends NE–SW and dips NW. The amphibolites can be classified into epidote amphibolites (up to 60% epidote), epidote-plagioclase amphibolites (up to 50% epidote+plagioclase), and plagioclase amphibolites (up to 50% plagioclase). Quartz, rutile, sphene, opaque minerals, and chlorite are found as minor components.

The amphibole is generally green to bluish-green; in some rocks bluish-green actinolite seems to have grown later to a brownish-green hornblende. Some amphibole grains are sieved with quartz granules or they may form poikiloblasts containing inclusions of other minerals. The plagioclase is commonly cloudy and variably saussuritized to a mixture of epidote, quartz, and turbid material. Fresh plagioclase found in some rocks may be a product of recrystallization or relics that have escaped deformation and alteration. It is commonly strained and, in some cases, marginally zoned.

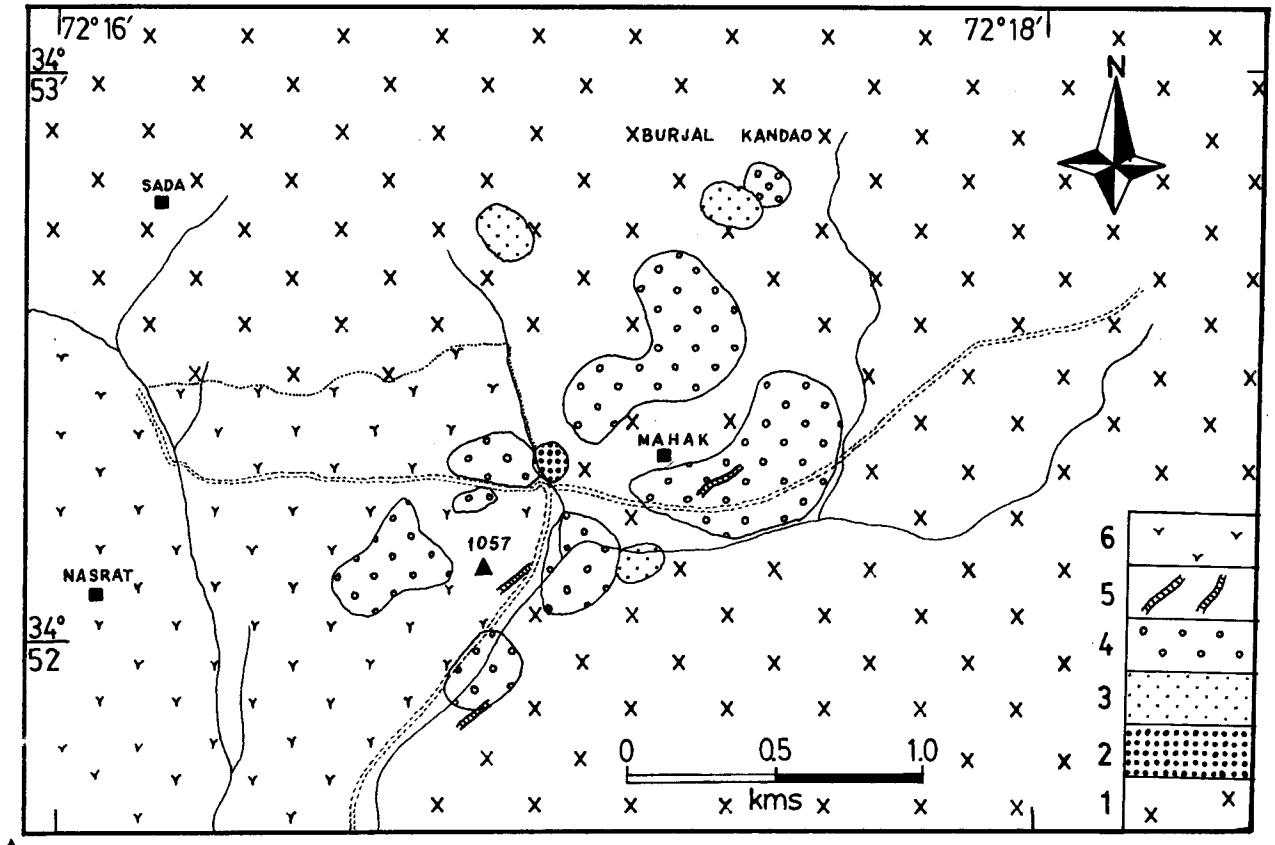

Fig. 1. Geological map of the Mahak area, Upper Swat. 1: Amphibolite; 2: Meta-pyroxenite; 3: Meta-gabbro; 4: Hornblendite; 5: Quartzo-feldspathic veins; 6: Alluvium.

Fig. 2. (Facing page) Some field features of the Mahak rocks. (A) Shear-banded and isoclinally folded amphibolites with quartzo-feldspathic and hornblendic pegmatite masses. Towards top is unsheared, homogeneous amphibolite. (B) Amphibolite with dyke-like hornblendite (centre and top), and two sets of quartzo-feldspathic veins. (C) Hornblendite in lower part passing into amphibolite upwards. (D) Hornblendite with variable grain size and patchy hornblende pegmatite.

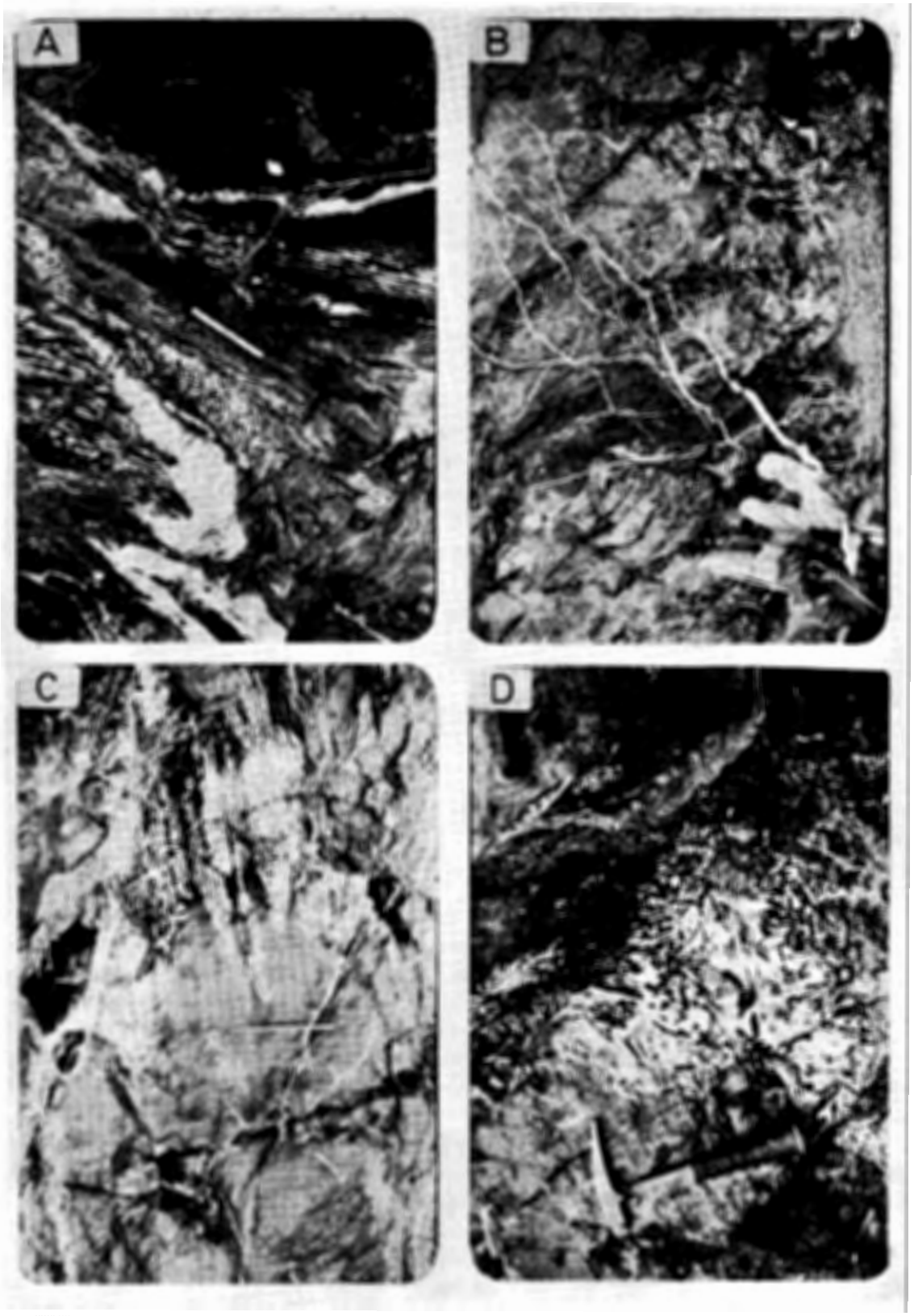
A
B
C
D

The epidote is colourless to yellowish, the latter colour probably reflecting a higher pistacite content. In some rocks, zoisite coexists with epidote, but the latter is always predominant. The epidote contains plagioclase (fresh or cloudy), quartz, rutile, sphene and, in rare cases, clinopyroxene. However, it may itself be enclosed in hornblende. The fresh plagioclase grains in epidote may suggest that the two minerals have grown at the expense of an earlier more calcic plagioclase.

Metamorphosed Gabbros and Pyroxenite

These occur as small bodies emplaced before the regional metamorphism but have escaped complete amphibolitization. Some of these may be relics, others seem to have intruded the parent rocks of the amphibolites. The metagabbros can be distinguished from the amphibolites on the basis of their igneous-looking appearance and pyroxene relics.

The metagabbros/metanorites consist of variable proportions of hornblende and one or two pyroxenes, subordinate plagioclase and accessory epidote, quartz, opaque oxide, chlorite, and rutile. In some places, however, the plagioclase content is very high and the rocks seem to be meta-anorthosites. Anorthosites are commonly associated with the gabbro-norites of the Chilas complex in Swat and Indus valleys (Jan et al., 1984; Khattak and Parvez, 1982); it is possible that these rocks and some of the amphibolites are related to the Chilas complex.

The hornblende, some poikiloblastic, may contain relics of pyroxene, vermicules of quartz and, rarely, opaque oxides and epidote. The clinopyroxene appears to be augitic in composition and partially replaced by hornblende. In some cases it is sieved with secondary hornblende granules that may be in optical continuity with the hornblende grains bordering the pyroxenes . The pyroxenes also display exsolution. Except in some cases, the plagioclase is completely saussuritized.

The metapyroxenite consists of clinopyroxene and hornblende with small amounts of sphene, chlorite, epidote, and magnetite. The clinopyroxene is medium-to coarse-grained and is partially replaced by hornblende or, rarely, chlorite. Sphene is up to 4% and its association with magnetite suggests that the two are derived from ilmenite.

Hornblendites

In addition to hornblende veins and local concentrations in the amphibolites, there are several small bodies of hornblendites concentrated around Mahak. These bodies collectively cover about one square kilometre area and the largest of these measures about 0.7 km in length. The hornblendites are massive rocks sparingly displaying a very weak parallel orientation of the hornblende grains. The contacts of these with the host amphibolites are generally gradational through plagioclase hornblendite (fig. 2).

The hornblendites are hypidioblastic to xenoblastic in mosaic, with heterogeneous grain size from very coarse - to medium-grained even within a single body. They are essentially composed of hornblende; chlorite, epidote, quartz, sphene, rutile and opaque oxides collectively form about 5%. All of these minor minerals may not occur in the same thin section and some of them are unequivocally secondary in origin. The hornblende locally displays colour zoning from brownish-green cores to bluish green margins. Twinning is rare but on a finer scale and better developed in anhedral grains. Inclusions of rutile and hornblende are common in hornblende, as noted also in Tora Tigga hornblendites (Jan et al., 1983).

Minor Dykes and Veins

Hornblende-plagioclase pegmatite (fig. 2) and medium-grained quartzo-feldspathic rocks occur as veins, patches, and thin dykes, but one quartzo-feldspathic dyke is 50m long. The

hornblendites locally contain coarse grained greenish yellow epidote veins. It was mentioned earlier on that hornblendites seldom display foliation. However, a number of quartzo-feldspathic bodies within them are deformed and show tectonic foliation. Such features were also observed in Matta hornblenditic pegmatite (Jan and Khattak, 1983).

The hornblende pegmatites, like elsewher in the amphibolite belt (Jan, 1979), show variation in the proportion of hornblende and plagioclase. The quartzofeldspathic rocks contain up to 65% plagioclase that is altered to epidote and cloudy material with only faint twinning preserved in some cases. Both plagioclase and hornblende occur in larger grains (phenocrysts or porphyroblasts), as well as in groundmass associated with quartz and epidote.

DISCUSSION

The amphibolites of the area appear to be meta-igneous, possibly plutonic, in origin. The banded variety may owe its origin to shearing rather than to inheritance from a sedimentary parentage. Chemical analyses are lacking but there is a possibility that at least some of the amphibolites are related to the metagabbros which in turn can be related to the Chilas complex. Jan (1979) has previously reported small bodies of metabasic rocks, related to the Chilas complex, occurring in the amphibolite belt. The metagabbros and pyroxenite are relictual masses that have been only partly amphibolitized.

The hornblendites do not appear to be in situ differentiates, a product of hornblendite magma or residual liquid. Their coarse-grained but variable grain-sizes, lack of chilled margins, and gradational contacts with the amphibolites suggest that they have grown during metamorphism in the presence of a fluid phase. The Mahak area may be the locale of a structural sink into which water was driven, or local chimneys along which fluid transport was active for sometime so that amphibolites were altered to hornblendites under amphibolite facies conditions. A similar origin can be proposed for the hornblende pegmatites (cf. Jan, 1979; Jan and Khattak, 1983; Jan et al., 1983).

The origin of the quartzo-feldspathic rocks is even more problematic in the absence of chemical analyses. These may be metamorphic differentiates or, more likely, a product of partial melting of deep-seated rocks during regional metamorphism.

ACKNOWLEDGEMENT

Dr. S. Hamidullah is thanked for his company in the field. NCE and Department of Geology provided funds and facilities for the field work.

REFERENCES

AHMED, Z., KHAN, R. & RAUF, A. (1980) Petrology of the Taghma area, Swat District, NWFP, Pakistan. Geol. Bull. Punjab Univ. 15. pp. 25-31.

BARD, J.P. (1983) Metamporphic evolution of an obducted island arc: Examples of Kohistan sequence (Pakistan) in the Himalayan collided range. Geol. Bull. Univ. Peshawar 16, pp. 105-184.

BANARAS, M. & GHANI, A. (1983) Petrography of the Tora Tigga complex, Munda area, Dir district. Unpubl. M.Sc. thesis. Univ. Peshawar.

COWARD, M.P., JAN, M.Q., REX, D., TARNEY, J., THIRLWALL, M. & WINDLEY, B.F. (1982) Geotectonic framework of the Himalaya of N. Pakistan Jour. Geol. Soc. London, pp. 299-308.

JAN, M.Q. (1979) Petrography of the amphibolites of Swat and Kohistan, Geol. Bull. Univ. Peshawar 11. pp. 51-64.

— & KHATTAK, M.U.K. (1983) Petrology of a hornblende-rich pegmatite and host amphibolites near Matta, Upper Swat. Geol. Bull. Univ. Peshawar 16, pp. 31-41.

— BANARAS, M., GHANI, A. & ASIF, M. (1983) The Tora Tigga ultramafic complex, Southern Dir district. Geol. Bull. Univ. Peshawar 16, pp. 11-29.

KHATTAK, M.U.K., PARAVEZ, M.K. & WINDLEY, B.F. (1984) The Chilas stratiform complex: Field and mineralogical aspects. Geol. Bull. Univ. Peshawar 17. pp. 153-69.

KHATTAK, M.U.K., PARVEZ, M.K. & WINDLEY, B.F. (1984) account of the east-central part of the Chilas Complex, Northern Pakistan. Unpubl. M.Sc. Thesis, Univ. Peshawar.

ACTA MINERALOGICA PAKISTANICA
VOLUME 1 (1985) pp. 83-89

GEOLOGY OF WARAI – JOGABUNG AREA, DISTRICT DIR TRANS HIMALAYAN ISLAND ARC, PAKISTAN

AFTAB MAHMOOD, SYED ALIM AHMAD & HAMID DAWOOD
Institute of Geology, Punjab University, Lahore–20, Pakistan.

Abstract: **A geological map covering about 45 square miles of Warai - Jogabung area of Dir district from toposheet 43 A/4 is presented. The area contains amphibolite, diorite and granite with small patches of quartzofelspathic veins, pegmatites and hornblendites. The amphibolites are the oldest rock units formed from calcareous quartzite. Diorite later on intruded as patches, veins and dykes of granitic material. Petrology of granitic rocks is presented in detail. Modal analyses and petrography of 24 selected samples are given.**

INTRODUCTION

The Warai Jogabung area lies between longitudes 72°0′ and 72°8′ E and latitudes 35°0′ and 35°5′ N. This paper describes the geological field relations, petrographic features and modal contents of various rock types exposed in the area.

GENERAL GEOLOGY

The area has been divided into following rock units: (i) Diorite (ii) Granite (iii) Amphibolite (iv) Hornblendite (v) Pegmatite.

Diorite

It covers about 27% of the investigated area. It expands in the southeast (fig. 1). In the north it pinches against the amphibolite body. In the west it strikes against the granitic body. The diorite body does not appear uniform in colour, texture and mineralogy in the field. Around the amphibolitic body diorite is rich in hornblende and quartz.

Hand specimens appear medium to coarse grained with colour indices of 20 to 50. Near the amphibolite contact the crystals show orientation. The contact of diorite with amphibolite is gradational.

Granite

Granite is in contact with diorite and amphibolite. The granite body is associated with predominant pegmatite and aplite dyke and veins. Besides the two larger outcrops, there are other granite bodies which occur as dykes, veins and patches enclosed in the northern amphibolite.

Amphibolite

It is the largest unit in the investigated area, and covers about 55% of it. The amphibolite is in contact with granites and diorites. The contact with granite is sharp. With the diorite it forms a gradational contact.

In the field, amphibolite can be classifed as follows: (i) Banded and layered amphibolite. (ii) Foliated amphibolite. (iii) Massive amphibolite.

In layered amphibolite two types of layers are present, i.e., dark coloured and light coloured layers. Thickness of the individual layer varies from 5mm to 4mm. The dark layers are rich in hornblende while the white layers are rich in quartz, feldspar and epidote. The layers are mostly parallel to each other.

The massive amphibolite do not show any alignment of hornblende or epidote prisms. It is medium to coarse grained and well jointed. Weathering colour is dark grey, and dark brown as well as reddish brown. These are medium to coarse grained rocks. Myrmekitic texture is common.

FIG 1.— GEOLOGICAL MAP OF WARAI JOGABUNG AREA, DISTRICT DIR, (N.W.F.P.) PAKISTAN

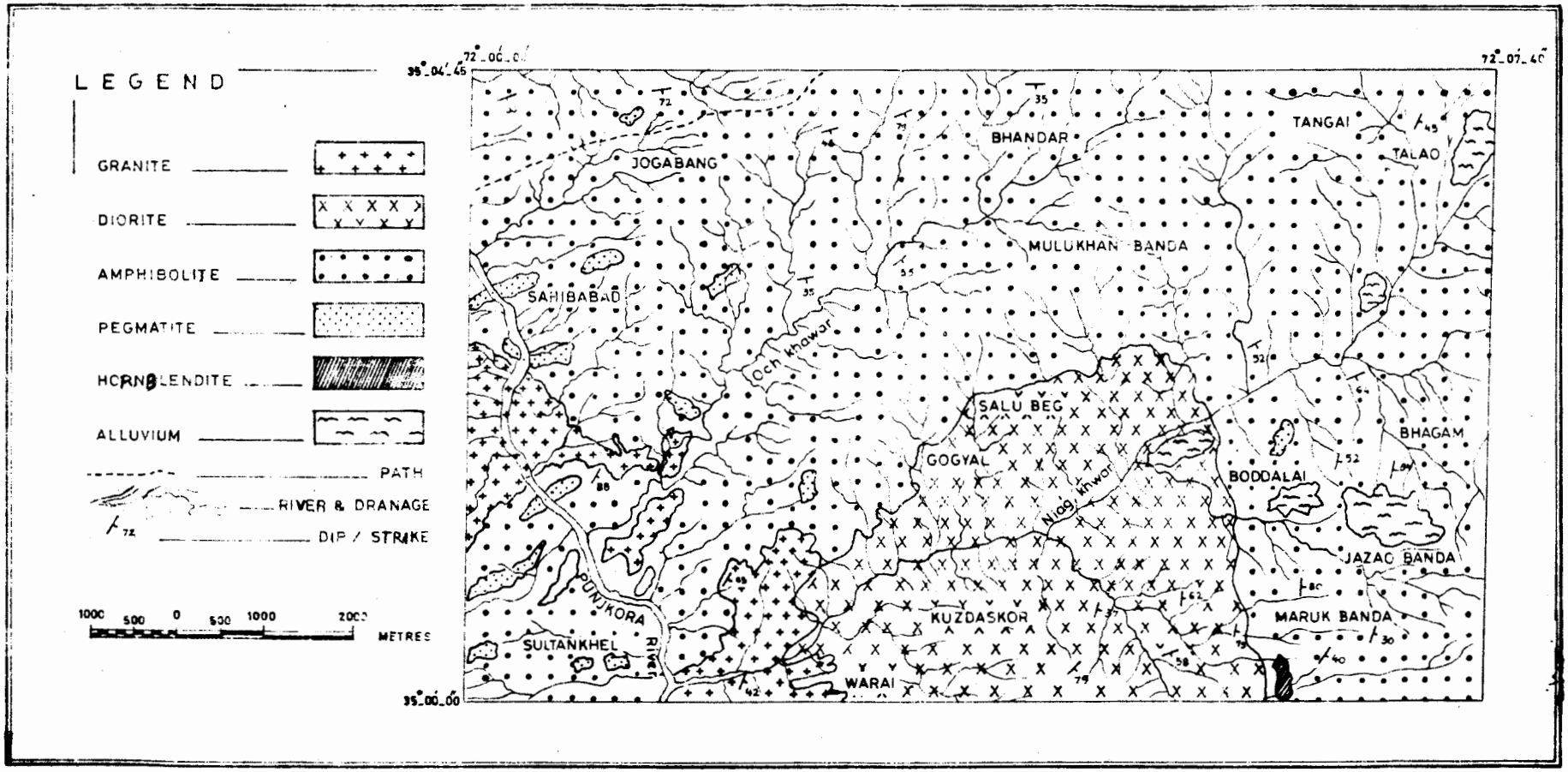

In the case of foliated amphibolites, the hornblende crystals are strongly stressed and lenses are produced giving the gneissic structure at places. Their trends are consistent with that of layered and banded amphibolite.

Pegmatites

Pegmatites are fairly common in the area. They occur as minor bodies in the form of dykes, veins and patches with commonly irregular boundaries.

Commonly graphic texture is observed. In hand specimens quartz, feldspar, mica, biotite and hornblende can easily be recognised. Plagioclase in the pegmatite is highly altered to clay minerals. The pegmatites in the area are mostly of acidic type and have sharp contacts with the host rock.

The simple pegmatites are the most common type present. Simple pegmatites include basic, intermediate as well as acidic pegmatites which have simple mineralogy, uniform texture from one end to the other, and are devoid of zoning. Complex pegmatites are also present.

PETROGRAPHY

Diorite

It is fine to coarse grained rock: porphyritic and poikilitic textures are common.

Four modal analyses are presented in table 1. Diorite consists essentially of plagioclase, hornblende, quartz chlorite and epidote. Magnetite, apatite, sphene and orthoclase are accessory minerals.

The amount of hornblende ranges from 30% to 41%. It is green to brownish pleochroic. Grains are commonly euhedral to anhedral. It is columnar, hexagonal in outline, occurring as lath shaped, prismatic crystals, partially altered to epidote and chlorite.

The amount of plagioclase ranges from 22 to 49%. It forms euhedral to subhedral equidimensional grains which are tabular and columnar in habit, and altered.

Quartz ranges from 5% to 14%. It is anhedral, fine to medium, having strained extinction, with irregular outlines, and has tiny micaceous inclusions.

Orthoclase ranges from 3% to 10%. It is medium to coarse grained, sericitized, perthitic to some extent, having irregular outlines. Clays (kaolin) ranges from 5% to 7%. It is secondary product of plagioclase. Muscovite ranges from 1% to 2%. It is flaky, scattered throughout the section. Biotite ranges from 2% to 4%. It is light brown to dark brown pleochroic. Epidote ranges from 1 to 7%. It is present as alteration product of hornblende. It is anhedral. Chlorite ranges from .05 to 3%. It is light green to dark green, pleochroic, and secondary.

Granite

It shows hypidiomorphic granular texture. Myrmekitic texture is present. The rock chiefly consists of alkali feldspar, quartz and muscovite. The rock is highly leucocratic, alkali feldspar and quartz percentage usually exceeds 50% and 12% respectively. Orthoclase ranges from 21% to 55%. It is subhedral to anhedral, having irregular boundaries, with irregular outlines. Few grains shows irregular cracks. Interference colours are grey to white of first order, with parallel extinction. Few grains show some shades of zoning. Quartz ranges from 6% to 23%. It is commonly anhedral and fractured, having strained extinction. It is fine grained. Plagioclase ranges from 14% to 36%. It is subhedral to euhedral, elongated and lath shaped. Few grains show zoning and kaolinization. Biotite ranges from 0.25% to 3%. It occurs as tabular or flaky, light brown to dark brown pleochroic grains spread throughout the section. Muscovite ranges from 0.7% to 1.9% It is of flaky habit, associated with biotite.

Epidote ranges from 0.5% to 1.6%. It is granular, colourless to faint yellowish grey, highly fractured, and appears as secondary product of hornblende. Hornblende ranges from 1%

Table 1. Representative modal analyses of diorite.

Sample No.	20159	20203	20211	20149
Plagioclase	39.0	21.4	45.0	41.1
Orthoclase	5.1	9.5	3.0	2.5
Sericite	0.6	nil	0.3	0.4
Epidote	6.6	1.4	1.1	0.6
Quartz	7.7	13.6	5.0	6.0
Hornblende	13.0	40.7	37.8	38.0
Kaolin	5.0	7.3	traces	traces
Biotite	2.1	3.8	2.3	3.4
Chlorite	0.5	0.1	1.0	1.3
Apatite	1.1	0.3	0.5	1.1
Cummingtonite	0.3	traces	traces	1.3
Muscovite	1.2	1.4	traces	3.1
Myrmekite	1.1	1.1	4.1	1.4

to 2%. It is green and brown under thin section, strongly pleochroic. Prismatic crystals are common with pseudohexagonal cross section. Kaolin ranges from 8 to 46%. It is the alteration product of feldspar. Secondary cummingtonite ranges from 5% to 1%, magnetite and hematite range from 0.3% to 1.8%. They occur as subhedral tiny grains. They are found as inclusions in biotite and hornblende but independent grains are also observed.

Amphibolite

It is medium to coarse grained when in foliated granite and fine to medium in other cases; weathering colour is dark grey, dark brown and reddish brown. Hornblende ranges from 13% to 49%. It is green, dark green to brownish green in thin sections. It is pleochroic from pale

Table 2. Representative modal analyses of granite.

Sample No.	20207	20212	20213	20215	20216	20217
Hornblende	–	1.0	–	1.6	1.6	–
Quartz	15.2	14.6	23.2	6.2	10.9	15.2
Muscovite	1.7	1.9	1.7	1.6	0.7	1.0
Cummingtonite	0.4	0.8	1.1	–	–	0.5
Biotite	2.2	2.5	2.3	1.5	0.2	0.2
Orthoclase	54.3	39.3	27.9	27.6	23.6	20.8
Plagioclase	13.6	24.1	20.9	24.6	14.4	35.9
Kaolin	38.4	8.1	20.6	34.0	45.7	23.2
Epidote	–	1.6	0.6	1.4	0.6	0.5
Chlorite	–	4.7	–	0.3	0.5	0.6
Iron Ore	0.3	1.5	1.8	1.3	1.5	1.4
Sphene	Traces	Traces	Traces	Traces	Traces	Traces

Table 3. Modal analyses of amphibolites.

	20204	20209	20214	20138	20196	20184	20178	20179	20183	20191	20197	20199
Hornblende	38.8	27.6	13.0	20.3	24.0	30.2	36.1	25.0	35.7	49.4	26.3	22.3
Quartz	24.2	10.6	1.6	10.2	17.5	7.4	15.9	8.5	10.5	21.4	12.2	11.6
Cummingtonite	0.1	28.8	8.8	0.1	17.1	0.3	1.5	6.5	–	2.9	2.2	5.6
Muscovite	0.1	–	0.1	3.7	1.1	1.6	0.8	1.4	1.4	0.3	0.5	–
Orthoclase	2.8	14.9	3.9	32.6	20.8	1.2	5.5	7.0	11.0	16.1	15.4	11.8
Plagioclase	1.2	2.1	0.4	3.9	8.0	32.9	1.2	8.7	12.2	–	6.2	10.9
Biotite	0.4	–	0.5	–	0 0	0.3	1.3	5.6	1.0	1.2	2.5	0.7
Kaolin	7.4	15.9	11.9	27.2	10.0	23.2	35.9	32.0	23.8	1.1	33.9	34.8
Epidote	23.9	–	57.7	0.4	–	0.1	1.7	3.4	1.5	4.3	0.6	1.5
Chlorite	1.1	–	1.3	0.1	1.0	0.4	–	1.1	1.9	3.3	0.1	0.1
Iron Ore	0.1	–	1.0	1.7	0.4	–	0.1	1.0	1.2	–	–	0.9

green to bluish green. It occurs as prismatic lath shaped large crystals. Some grains show twinning. Tiny quartz grains are present as inclusions. It is partially altered to chlorite. Cummingtonite ranges from 0.1% to 29%. It is light green or olive green in thin sections, strongly pleochroic, occurs as prismatic crystals. Plagioclase ranges from 0.4% to 33%. It is euhedral to subhedral, twinned, medium grained, kaolinized, carlsbad and polysynthetic twinning is present. Composition of plagioclase is mostly andesine. Epidote ranges from 0.1% to 58%. It is granular, gives typical twinning, the grains are euhedral to subhedral. Quartz ranges from 2% to 24%. It is anhderal, with rounded outlines. Chlorite ranges from 0.1% to 3%. It is secondary and occurs as vermicular crystals. Biotite ranges from 0.03% to 5.59%. It is subhedral to anhedral, brown to dark brown pleochroic, flaky in habit, spread throughout the section. Orthoclase ranges from 1.2% to 33%. It is anhedral to subhedral, altered to some extent with grains having irregular boundaries. Magnetite and haematite range from 1% to 1.7%, and are subhedral associated with hornblende.

Hornblendite

Hypidiomorphic granular texture is common. Common minerals of hornblendite are hornblende, epidote, quartz and iron ore. Hornblende varies from 50.44% to 90.60%. It is euhedral, to subhedral, prismatie and lath shaped, pleochroic from pale yellow green to light green. Epidote varies from 0.35% to 3.00%. It is anhedral, associated with hornblende along the fractures, and is alteration product of hornblende. Quartz varies from 1.37% to 2.32%. It occurs as interstitial grains in hornblende. Cummingtonite ranges from 0.73% to 21.15% associated with hornblende. Magnetite and hematite range from 0.35% to 1%, present as subhedral crystals distributed throughout the section.

Pegmatites

These are acidic. Both types, i.e., zoned and unzoned, are present. Quartz, orthoclase, plagioclase, muscovite, biotite and ore minerals are seen. Quartz ranges from 16.16% to 17.69%. It is anhedral, medium to coarse grained, having wavy extinction and irregular boundaries. Orthoclase ranges from 12.00% to 32.64%. It is subhedral to anhedral, medium to coarse grained, with irregular boundaries, partially altered; simple carlsbad twinning is observed. Plagioclase ranges from 3.77% to 18.12%. It is euhedral to subhedral, medium grained, mostly plagioclase is altered, polysynthetic, albite and pericline twinning is common. Sericitized to some extent. Muscovite ranges from 10.30% to 14.33%. Biotite ranges from 0.09% to 0.25%. It occurs as minute shreds. It is light brown to dark brown and pleochroic. Hematite ranges from 0.24% to 0.95%. It is present as subhedral minute grains.

DISCUSSION

The diorite occupies 27% of the area surveyed. It extends towards south. Towards west it makes the contact with granite and towards east it makes the contact with large body of amphibolite.

Most of the diorite is massive & jointed in the area surveyed. After its emplacement in contact with the amphibolite. It has undergone the process of metasomatism. A new equilibrium started at the contact between the amphibolite and the diorite which has resulted in a granophyric concentration in the diorite at the contact.

During the emplacement of the dioritic magma it took the pieces of the amphibolite in it which, later on, scattered irregularly throughout the body. The composition of amphibolite is more or less equivalent to the composition of the diorite. The dioritic magma dissolved inclusions of same cōmposition with which it was in equilibrium. As temperature fell, it changed the composition of itself and the inclusion.

The diorite shows a medium grained, hypidiomorphic to allotriomorphic granular texture which indicates that the magma has crystallized in an intermediate plutonic environment. Ophitic texture which is formed by the euhedral plagioclase, shows that plagioclase crystallized

earlier than the hornblende. Myrmekitic texture is due to strong reluctant short time forces produced within the magma during the process of metasomatism. In this process original equidimensional texture has slightly changed into linear texture by the development of epidote and chlorite.

The primary minerals of diorite are plagioclase (andesine) and hornblende. In the area the distribution of plagioclase, hornblende and quartz is not uniform. Due to metasomatism at the contact with the amphibolite the diorite has become rich in granophyric material. Here the percentage of quartz reaches more than 20% at various places and is named as quartz-diorite. At its northern end, the diorite becomes progressively rich in hornblende and poor in corresponding quantity of quartz. This progressive enrichment is attributed to the presence of hornblende rich amphibolite at this end. During metasomatism, hornblende of diorite tried to be concentrated with the hornblende of amphibolite but prior to this complete concentration the gradual migration ceased in the form of meladiorite.

The normal diorite occupies most of the southern part of the area surveyed. The structure as well as texture of the mineral indicate that the normal diorite is uniform throughout the area. At various places, local concentrations of quartz and feldspar have appeared in the form of dykes. Distribution of accessory minerals is uniform.

In the author's view the dioritic magma is from lower part of the semibasaltic magma, the upper part of which intruded first in the area which changed into the orthoamphibolite.

The Warai granite is an intrusive of batholithic dimensions. Its contact with the country rock is sharp and discordant. The exchange of the material is hardly appreciable. Apophyses of granite are often seen in the country rock. Petrographically the bodies are rather uniform and compact. The contact of Warai granite and amphibolite is sharp. Moreover, at the contact of granite and amphibolite, no significant chemical reaction has taken place. Such phenomena result when the intruding body and the country rock have dissimilar temperature gradients. As the attitude of the country rock is not parallel to the granite foliation so this forms discordant contact relation. Other structures developed in granite body and the country rock are also in disharmony.

This granite is a product of crystallization from hot or at least partially molten and mobile mass. It can also be inferred that the granite has formed as a result of generation of granitic magma coupled with granitization and anatexis.

Amphibolites are divided into two types:

a) Para amphibolites
b) Ortho amphibolites

Para amphibolites result from metamorphism of calcareous or dolomitic shales. Para amphibolite can be regarded as decarbonated mixture of limestone or dolomite. While orthoamphibolite is formed by the effect of metamorphism on a basic to semi-basic or a doleritic rock. The distinction between the amphibolites formed from the metamorphism of igneous rocks and the amphibolites formed from the sedimentary rocks is a difficult one. Various field, textural, structural, and chemical criteria have been proposed by various authors to distinguish between two amphibolites.

In Swat area patches of amphibolite are present in the vicinity of carbonatite. Wilcox and Poldervaart (1958) laid great emphasis on the banded nature of amphibolites as an evidence of metasedimentary origin. Heier (1962) laid a great emphasis on the association of amphibolite with marble in the field as a proof of a metasedimentary origin.

There are many evidences in the field on the basis of which it is suggested that the amphibolites have been formed as a result of progressive regional metamorphism of calcareous rocks. There is a considerable variation of both struc-

ture and texture of amphibolites. The grain size is variable. Banding and layering is fairly common. All these characteristics, though not conclusive, suggest, when looked at field evidence, a metasedimentary origin for these rocks. Whereas in the case of ortho-amphibolites, the texture and structure is generally uniform and banding is less common.

The amphibolites are composed maihly of amphibole and quartz with lesser amount of epidote, chlorite and mica. Plagioclase is also present in less amount. Magnetite is rare. Potash bearing minerals like mica, clay and orthoclase are more common than plagioclase. Cummingtonite is present in less amount. All these factors strongly suggest that these amphibolites have not been formed from gabbros, norites or diorites. The quantitative mineralogical evidence clearly suggests that these rocks have not formed by the metamorphism of igneous rocks.

ACKNOWLEDGEMENTS

The authors wish to acknowledge the guidance and encouragement of Professors F.A. Shams and Shafeeq Ahmed, and M.N. Chaudhry of Institute of Geology, Punjab University, Lahore.

REFERENCES

HEIER, K.S. (1962) The possible origin of amphibolites in an area of high metamorphic grade. Norsk. Geol. Tiddeskr. 42, pp. 152-65.

WILCOX, R.E. & POLDERVAART, A. (1958) Metadolerite dyke swarm in Bakrsville-Roan Mountain area, North Carolina. Geol. Soc. Amer. Bull. 69, pp. 1327-68.

ACTA MINERALOGICA PAKISTANICA
VOLUME 1 (1985) pp. 90-94

GEOLOGY AND PETROLOGY OF GULPATOBANDA–SAONI AREA, DIR DISTRICT, PAKISTAN.

SYED ALIM AHMAD, AFTAB MAHMOOD & A.R. KHAN
Institute of Geology, Punjab University, Lahore–20, Pakistan.

Abstract: **A geological map covering about 30 km^2 area near Gulpatobanda-Saoni in Dir District is presented. The area is composed of metasedimentary complexes with igneous intrusions. The main units in the area are calcareous quartzite, calcareous mica schist and siliceous mica schist. Detailed petrography of the major units is described. Petrogenesis of all these rocks is also presented.**

INTRODUCTION

Gulpatobanda-Saoni area is a part of Hindu-Kush Range. The area lies in the northern part of district Dir in Tehsil Kohistan of N.W.F.P. (Pakistan) between longitudes 71° 45′ and 72° 0′ E and latitudes 35° 00′ to 35° 15′ N. Gulpatobanda is a small village of Dir District situated in Kohistan valley about 80 km from Dir. The area is traversed by one unmetalled road, which connects the area both with Dir and Patrak.

The objective of the present study is to determine mineral variations in the rocks. Sampling was done extensively from all rock units to be described by petrography.

GENERAL GEOLOGY

The area has been divided into following rock units: (i) Calcareous quartzites (ii) Calcareous mica schist (iii) Siliceous mica schist (iv) Mixed zone.

Calcareous Quartzite

Thickly bedded calcareous quartzite covers about 20% of the area in the extreme southeast. The strike of these rocks is northeast, dip towards southeast. Calcite, quartz and muscovite can be easily recognised in the hand specimens. Boudinage structure is common. These are grey coloured rocks which on weathering give reddish brown colour. These are profusely cut by coarse calcitic and quartzofeldspathic veins. Garnet is also observed.

Granodiorite

Minor bodies of massive to poorly foliated granodiorite lenses and dykes are present in schistose, light brown to white, rocks.

Calcareous Mica Schist

It is highly micaceous and schistosity is well developed. A large number of coarse calcitic veins are present. The colour is green to greenish grey. It covers about 15% of the area. These rocks occur alongside the belt of calcareous quartzite and in the extreme northwest of the project area. The strike of these rocks is northeast and dip is toward southeast. Calcite, quartz, and muscovite can be easily recognised in hand specimens. These are greenish grey coloured rocks. These are also cut by quartzitic veins.

Siliceous Mica Schist

It covers an area of about 5% of the investigated area. The strike of these rock is northwest, and dip to northeast. The colour is black to greyish black and grey calcite veins are abundantly present. The intrusions of granite, diorite and granodiorite are also present.

FIG. 1 — GEOLOGICAL MAP OF GULPATO BANDA-SAONI AREA

DISTRICT DIR TEHSIL KOHISTAN

PAKISTAN

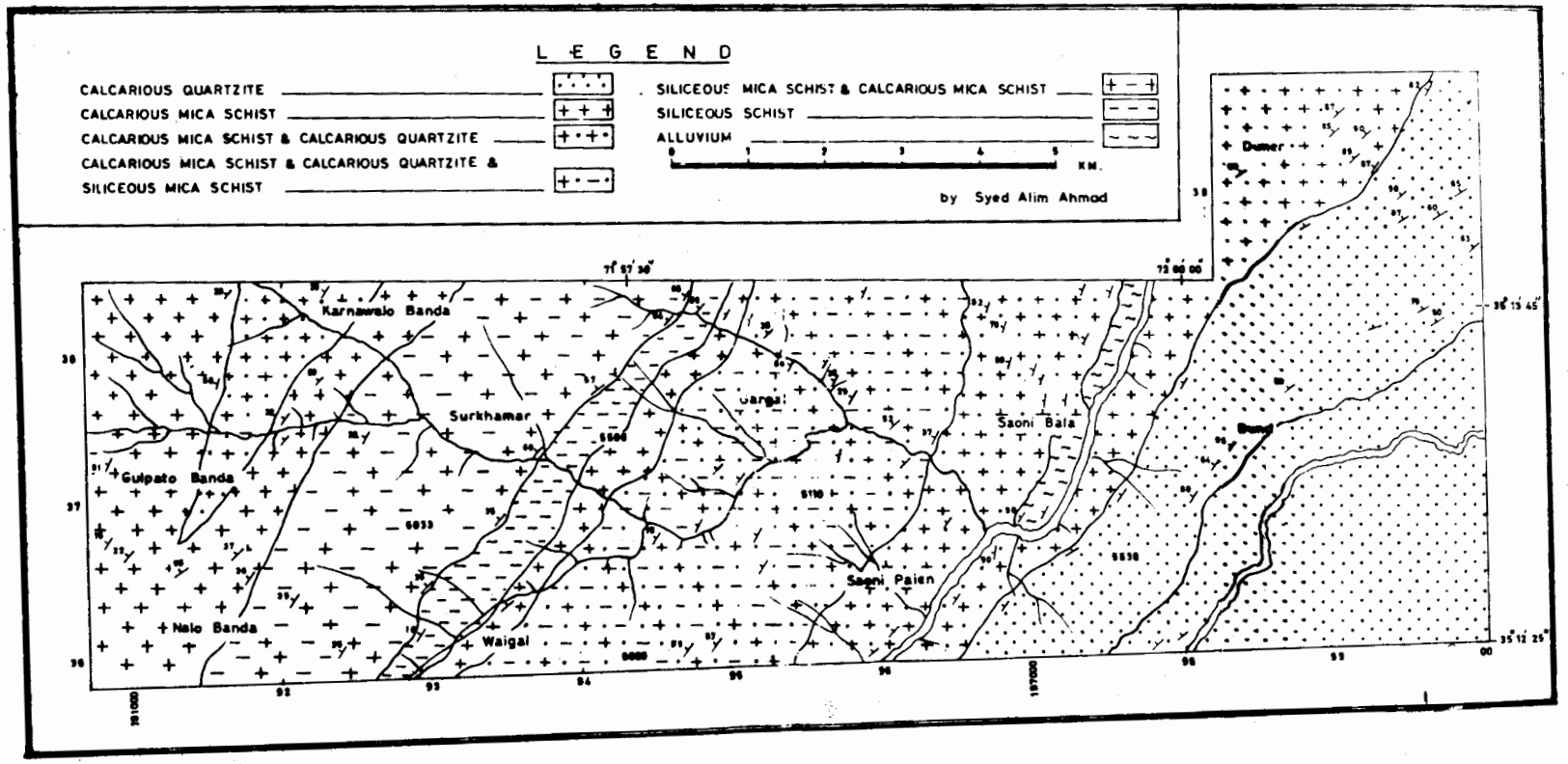

Mixed Zone

These rocks cover about 55% of the total project area. They occur towards the central area of the map. The strike of these rock is towards northeast while the dip is towards northwest. Mixed zone consists of calcareous schist, siliceous schist and calcareous quartzite which are intruded by volcanics. Veins of quartzofeldspar are also present.

PETROGRAPHY

Calcareous Schist

It is fine grained, highly schistose rock. Five modal analyses of this unit are presented in table 2. Calcite, sericite and quartz are the main constituents while sphene, muscovite, garnet, plagioclase, epidote and magnetite are the accessories. The amount of quartz varies from 20.60% to 31.74%. The grains are subhedral to anhedral and rounded in outline. Calcite inclusions are present in it. Quartz grains are stretched in the direction of schistosity.

Calcite varies from 38.40% to 49.13%. The grains are subhedral to anhedral. Very fine grained calcite is also present. The amount of sericite varies from 15.20% to 35.5%. It has fine needle-like and micaceous habit and is aligned along the schistosity.

The amount of sphene varies from 1.20% to 2.74%. The grains are anhedral and of earthy colour. The amount of epidote is 1% to 5%. It is granular, fine grained, irregularly distributed. The amount of chlorite varies from 2.55% to 5.32%. It is light green in plane polarized light and gives inky blue colour under crossed nicols.

The amount of magnetite varies from 1.00% to 2.95%. It is subhedral and powdry. The amount of clays varies from 1% to 2%. It is in the form of clusters. Traces of garnet are also present in some sections. It is anhedral and scattered throughout the section.

Calcareous Quartzite

It is fine to medium grained anhedral to subhedral and porphyritic to subporphyritic in texture. Four modal analyses are presented in table 1. Calcite and quartz are the main constituents while epidote, chlorite, sericite, muscovite, biotite, and plagioclase are the accessories. The amount of calcite varies from 45.43% to 54.66%. It is subhedral to anhedral and fine grained. Quartz is interstitial. Calcite is present as inclusions in quartz grains. Quartz varies from 24.05% to 33.74%. It is anhedral. Tiny calcitic grains are present as inclusions in it. It has strained extinction to some extent, and is found in the matrix with calcite. Sericite varies from 6.16% to 10.50%. There are fine, needles of micaceous habit. The amount of epidote varies from 1.25% to 2.55%. It is granular dispersed throughout and also present as inclusions in quartz. Muscovite varies from 1.50% to 3.45%. It is of flaky habit. Biotite varies from 1.8% to 7.3%. It is fibrous as well as flaky, pleochroic from light brown to dark brown. The amount of plagioclase varies from 2.50% to 3.50%. It is fine grained, twinned, dispersed irregularly associated with quartz. The amount of chlorite varies from 2.64% to 3.05%. It is fibrous, light green to dark green, pleochroic, with inky blue interference tints. The amount of clays is 1.00% to 3.05%. It is in the form of clusters, dispersed irregularly. The amount of epidote varies from 1.25% to 2.55%. It is granular and also present as inclusions in quartz. Magnetite varies from 1.03% to 2.14%. It occurs both as powder and as tiny anhedral grains.

Siliceous Schist

It is fine grained, highly schistose rock. Three modal analyses are presented in Table 3. Quartz and calcite are the main constituents, while biotite, epidote, iron ore, sphene, sericite and plagioclase are the accessories. The amount of quartz varies from 40.65% to 62.90%. It is anhedral, fine grained, stretched in the direction of schistosity. Calcite inclusions are present in it, with subordinate micaceous inclusions. Calcite

varies from 25.20% to 30.20%. It is subhedral to anhedral. Tiny grains are present as inclusions in quartz. The amount of sericite varies from 8.20% to 20.50%. It is of micaceous habit. The amount of plagioclases varies from 2.00% to 2.20%. It is twinned, fine grained and anhedral to subhedral. The amount of epidote varies from 8.20% to 20.50%. It is of micaceous habit. The amount of plagioclase varies from 2.00% to 2.20%. It is twinned, fine grained and anhedral to subhedral. The amount of epidote varies from 1.04% to 2.18. It is fine grained, granular, and dispersed throughout the section. Sphene varies from 1.0% to 0.9%. It is anhedral to subhedral and earthy in colour.

Table 1. Modal analyses of calcareous quartzite.

Minerals	21870	21836	21874	21832
Calcite	49.42	49.36	54.66	45.43
Quartz	26.15	24.05	30.14	33.74
Chlorite	2.64	3.05	traces	traces
Epidote	2.12	2.02	2.25	1.25
Sericite	7.65	9.28	6.16	10.50
Muscovite	3.45	3.03	traces	1.50
Biotite	4.30	3.00	1.80	traces
Plagioclase	2.07	2.05	2.50	3.50
Clay	0.06	2.12	1.00	3.05
Ore	2.14	2.01	1.49	1.03

Table 2. Modal analyses of calcareous mica-schist, totalled to 100.

Minerals	21794	21772	21825	21824	21829
Chlorite	3.02	2.55	traces	traces	5.32
Calcite	38.40	49.18	40.61	46.80	47.40
Quartz	20.60	21.85	26.90	26.99	31.74
Sphene	1.50	1.20	2.74	traces	2.15
Ores	traces	1.03	2.95	traces	traces
Garnet	nil	traces	traces	traces	traces
Biotite	nil	traces	nil	nil	traces
Epidote	1.00	traces	5.00	1.00	traces
Sericite	33.48	10.30	15.20	19.89	12.09
Plagioclase	1.00	3.89	4.60	3.82	1.25
Clay	1.00	traces	2.00	1.50	traces

Table 3. Modal analyses of siliceous mica schists, totalled to 100.

Minerals	21839	21832	21793
Quartz	55.90	40.65	61.14
Biotite	10.10	nil	traces
Calcite	20.50	28.50	22.49
Chlorite	nil	nil	traces
Ores	1.40	1.65	1.25
Epidote	traces	2.18	1.04
Sphene	1.90	2.05	traces
Sericite	8.20	20.52	12.28
Plagioclase	2.00	2.20	1.75
Clay	traces	2.25	traces

DISCUSSION

The Gulpatobanda-Saoni area represents the northern sedimentary volcanic unit. The area is composed of fairly heterogeneous and relatively rapidly deposited sequence of impure sandy shales, silty shales and calcareous quartzites. These rocks contain rather significant amounts of volcanic material and are a sedimentary volcanic sequence derived by the break-down of the northern arc and formed as a result of subduction of the Tethys. The sediments also include material derived from the oceanic plate itself. Presence of volcanic fragments of acid to intermediate compositions at certain horizons specially in quartzite lends support to this view. The calcareous quartzites contain significant amounts of feldspar. The calcareous mica schist and siliceous mica schist contain relatively higher amounts of calcite, quartz as well as sericite and sphene. The schists are not like ordinary pelites. The presence of amphibolite horizons shows metamorphism of impure calcareous quartzites with substantial amounts of volcanic material. It is therefore concluded that these sediments are, at least partly, volcanogenic arc derived.

The necessary heat and stresses were provided by the subduction and related volcanism. The metamorphism is of greenschist facies. This

fact show that the main arc with higher heat flow lay to north.

The presence of angular to subangular boulders in the paraconformity in calcareous quartzites indicates that the source area from which sediments were derived was not far away. Due to this, sandstones have not suffered much transportation. The accumulation of fossils such as Assilina, Nummulites, and Alveolina shows that the sediments were deposited in a shallow marine, benthonic environment. The sandstones were deposited by the streams and the porespaces in between them were filled by calcite cement. It is one of the commonest diagenetic changes and produce rigidity of the closing sediment by binding the grains together.

The contact of calcareous quartzites with the surrounding rocks is gradational. As we move S.E. towards amphibolite belt, the calcareous quartzites become hardened. Presence of fossils indicates that the sediments were deposited in shallow water marine environment. Quartz is medium to coarse grained.

Calcareous quartzite has porphyritic granular and poikilitic textures.

About the cementation there are two possibilities, cementation may occur with sedimentation or the cement may be introduced at any latter time. The calcite cement may be brought in solution and the calcite has undergone crystallization afterwards. The quartz grains have low sphericity and roundness. After the deposition of these sediments regional metamorphism took place. Chlorite, sericite, kaolin, limonite and calcite, are low temperature minerals. They are ready to enter into various reactions with one another and some of these reactions demand no great elevation of temperature. Calcite and kaolin react with each other to give epidote. As the grade of metamorphism increases, calcite and quartz recrystallize to give calcareous quartzites.

ACKNOWLEDGEMENTS

The author wishes to acknowledge the guidance and encouragement received from Prof. F.A. Shams, Prof. Shafeeq Ahmad, Mr. Aftab Mahmood and Dr. M.N. Choudhry of the Institute of Geology, Punjab University, Lahore.

ACTA MINERALOGICA PAKISTANICA
VOLUME 1 (1985) pp. 95-97

PETROGRAPHIC AND ENGINEERING BEHAVIOUR OF ROCKS IN THE HUB DAM AREA AND ITS BEARING ON THE SEEPAGE PROBLEM.

M. NAWAZ CHAUDHRY & ZAHID KARIM KHAN
Institute of Geology, Punjab University, Lahore–20, Pakistan.

Abstract: Petrographic and XRD studies of 19 clastic sedimentary rock samples from vicinity of Hub Dam showed the presence of gypsum, halite and sylvite in veins of fracture filling and replacement origin. The argillaceous rocks are complex admixtures of abundant illite, subordinate kaolinite and minor smectite .

INTRODUCTION

Hub dam site is located about 30 miles north-east of Karachi on Hub river. The site is about 350 yards downstream from the confluence of Hub river and Shorine Nala. The main dam is homogenous earthfill embankment (zoned type) about 15800 ft. long and 163 feet high in the river bed section. Another embankment called saddle dam across the low level area, on right abutment side has also been constructed to maintain the level of the reservoir. The catchment area is about 3,410 square miles. The capacity of live storage of the dam is 0.76 million acres foot. Uncontrolled free overfall spillway is also constructed on right abutment which is about 6012 feet long and with crest elevation of 339 SPD. About 500 cusecs capacity irrigation conduit is available at site in 6′ x 6′ section. It is mainly a water supply scheme for Karachi and its surroundings.

GEOLOGY OF THE AREA

Hub valley is a subsequent valley within the eastern limb of a big anticlinal fold and the dam axis is more or less parallel to the Hub river. Generally, the valley exhibits dendritic drainage pattern. Upper part of the valley is narrow and it widens downstream. On the whole, the valley is flat and marks various former valley floors (burried channels) on which a part of the saddle dam is founded on the right bank. Rocks present in the area belong to Nari Formation of late Oligocene age. They comprise interbedded sandstone, siltstone and mudstone with a few beds of limestone. Thickness of the overburden in the area generally ranges from 5 feet to 30 feet on left abutment and up to 65 feet on the right abutment. There is no evidence of major regional fault. Small intraformational displacements have been noted often during the field work. The strike and dip of strata are generally uniform. The beds strike N 50° E to N 67° E and dip 5° to 10° south-east. The rocks are moderately well jointed. A fairly large number of gypsum veins are present in all the rock types.

MINERALOGICAL BEHAVIOUR

Khan collected nineteen samples for petrographic and mineralogical studies from the Hub Dam and its vicinity. The samples were studied under the microscope. Modal analyses of samples were carried out by point counting. Between 3500 to 5000 points were counted for each thin section.

The types of clay minerals present were identified by optical as well as x-ray diffraction methods. The results of modal analyses are listed in table 1. Stereoscopic examination reveals streaks, patches, veins and laminae of salts. The predominant salt is gypsum, but some halite and occasional sylvite are also observed. Metasomatic introduction of these salts to small distances from the veins is observed. Salts were scratched from the veins and were chemically and optically tested. The predominance of gypsum in the veins was confirmed. Presence of subordinate rock salt and soluble K-salts were also confirmed optically as well as chemically.

Some veins of the salts are rather pure and have sharp contacts. The veins are of two types, i.e., fracture fillings and replacement veins. The petrographic types distinguished are shale, mudstone, quartz siltstone and quartz-wackes. Quartz siltstones have previously been classed as sandstones.

The shales are weakly to moderately laminated. They are unequigranular to sub-equigranular and contain both clay and silt grade particles. However the clay grade particles predominate. They contain both gypsum as well as rock salt. Gypsum is however predominant. Gypsum does not exceed 1.0% in the body of the rock itself.

Mudstones are massive looking and non-laminated to barely laminated. They are unequigranular rocks. They also, like shales, contain both silt and clay grade particles. The clay grade particles predominate. One sample of the mudstone was found to contain 12.0% carbonaceous matter. Gypsum in the body of rock does not exceed 1%.

The quartz rich siltstones are also unequigranular rocks. The grains in them are from angular to sub-rounded. However, sub-angular to sub-rounded grains predominate. They contain abundant clay matrix. The packing of grains and matrix leaves little well connected pore spaces. The rocks have previously been regarded as sandstones.

The sandstones are quartz-wackes and not arenites. They are fine grained. No medium or coarse grained varieties were present in the samples collected for studies. The rocks contain abundant clay matrix. They also contain small quantities of gypsum and halite. Soluble salts do not exceeds 0.6%. They are likely to have low permeability.

From the above the following may be concluded:

1) The rock types present are mudstone, shales, quartz siltstones with abundant clay and fine grained quartz wackes with large clay matrix.

2) The rocks show textural characteristics which would result in low primary permeability.

3) These rocks contain only small quantities of salts in the bodies of rock.

4) These rocks contain streaks, fine laminae, veins and patches of soluble salts. The predominant salt is gypsum followed by halite. The K salts are also present in very small amounts.

The primary permeability of these rocks is low. However, extensive jointing and fracturing have been noted. Many of these are filled with souble salts. The permeability is therefore mainly secondary which is likely to increase with progressive dissolution of the salts from veins, patches concertions and streaks.

The very high amounts of soluble salts being encountered in the seepage waters are not due to primary or metasomatically introduced salts in the body of the rocks themselves since such salts range from 0.1 to 1.0% of the rock. Furthermore, these rocks have low permeabilities and solutioning and seepage will be slow.

The bulk of the salts and seepage waters are derived from zones of secondary permeability, many of which are filled with soluble salts. With progressive solutioning of soluble salts from veins, streaks, patches and laminae the secondary permeability will increase. The countering effect of clay mineralogy to increasing secondary permeability is discussed in the following pages.

NATURE OF CLAYS AND THEIR ENGINEERING IMPLICATIONS

Clay minerals from shales, mudstones, quartz siltstones and quartz wackes were studied optically. The study indicates the presence of illite, kaolinite and some probable smectite. Three clay samples from mudstones were studied by x-ray diffraction. Fairly strong reflections between 9.97 and 9.99 Å indicated the

Table 1. Petrographic modal analysis.

Sample No.	Mudstone Z1	Mudstone Z2	Shale Z3	Mudstone Z4	Mudstone Z5	Shale Z6	Mudstone Z7	Mudstone Z8	Shale Z9	Mudstone Z10
Clay	90.1	82.1	78.7	75.9	74.5	72.5	72.3	70.6	64.0	62.4
Quartz	3.5	10.5	10.4	8.0	12.0	13.7	18.4	18.8	20.6	18.0
Albite	–	1.0	2.0	–	1.7	2.5	1.6	2.0	3.5	3.9
K-feldspar	–	–	1.8	–	2.1	2.0	–	1.7	2.4	2.0
Muscovite	2.0	1.8	1.6	1.3	3.6	2.9	2.6	3.3	3.0	4.6
Biotite	Tr	Tr	–	Tr	1.0	0.3	0.9	–	–	1.3
Chlorite	0.4	1.8	1.3	1.5	1.6	2.0	1.5	1.9	2.3	2.8
Hematite/Limonite	1.5	0.6	0.5	1.4	2.5	1.5	0.4	1.0	1.1	2.1
Zircon	Tr	0.3	0.4	0.3	–	0.2	0.2	–	Tr	0.3
Rutile	–	0.3	0.2	0.2	0.4	Tr	0.4	Tr	0.3	Tr
Sphene	–	Tr	–	0.3	0.1	0.3	Tr	0.4	0.2	0.4
Epidote	0.3	0.1	–	0.2	0.1	0.5	0.3	Tr	0.3	0.5
Organic matter	0.2	0.3	2.1	10.1	Tr	0.7	Tr	Tr	0.9	0.6
Glauconite	–	–	–	–	–	–	–	–	–	–
Tourmaline	Tr	0.5	–	Tr	0.2	–	0.6	0.2	0.8	0.3
Gypsum	1.2	0.5	0.7	0.5	0.2	0.8	0.6	0.1	0.5	0.8
Halite	0.8	0.2	0.3	0.3	Tr	0.1	0.2	–	0.1	Tr

	Quartz – rich siltstone			Quartz –wackes					
Sample no.	Z11	Z12	Z13	Z14	Z15	Z16	Z17	Z18	Z19
Clay	34.0	29.6	32.3	17.4	25.8	28.2	20.9	30.5	30.0
Quartz	56.5	53.2	51.0	72.0	63.9	60.3	60.0	57.8	52.7
Albite	2.0	2.4	3.5	2.0	1.7	2.0	3.1	1.9	2.6
K-Feldspar	1.5	5.2	4.0	3.6	1.5	4.5	3.7	3.0	5.3
Muscovite	2.6	3.0	3.4	1.3	2.9	3.6	4.0	2.8	3.0
Biotite	Tr	1.4	0.8	0.3	Tr	–	0.3	–	0.7
Chlorite	1.4	2.6	2.5	0.5	Tr	0.4	–	2.0	1.7
Hematite/Limonite	0.5	1.8	1.3	1.0	1.7	0.4	Tr	1.8	1.5
Zircon	0.2	0.3	0.1	Tr	0.2	0.1	–	–	0.4
Rutile	–	–	–	–	–	–	–	–	–
Sphene	0.3	Tr	0.2	0.5	0.5	Tr	–	–	–
Epidote	Tr	0.2	0.5	Tr	0.3	–	0.5	–	0.8
Oraganic matter	0.4	–	Tr	–	–	–	–	–	–
Cherty matter	–	–	–	–	–	–	6.2	–	–
Tourmaline	Tr	0.3	0.4	0.9	0.8	–	0.5	Tr	1.0
Gypsum	0.4	–	Tr	0.4	0.5	0.2	0.5	0.2	–
Halite	0.2	–	–	0.1	0.2	0.3	0.3	–	0.3

presence of illite (mainly hydromuscovite) in substantial quantities. Moderately strong reflections between 7.13 and 7.16 Å and 3.54 to 3.58 Å indicated subordinate kaolinite. Weak reflections between 14.0 - 14.15, 4.51 - 4.55 Å, 2.63 - 2.57 Å and 1.53 - 1.55 Å indicated minor smectite. The 14.0 Å reflection of smectite shifts to 18.0 Å on glycerolation. Accessory chlorite gave very weak reflections between 14.15 Å - 14.18 Å and 7.01 - 7.06 Å. From the above. It may be concluded that the clays are complex admixtures of illite (main), kaolinite (subordinate) and smectite (minor). Although the amount of smectite is small, yet it is likely to cause some expansion. Large amounts of hydromuscovite may react with high alkali cement of concrete aggregate, thereby causing some alkali-silica reaction at contact zones.

The clay mineralogy may result in some expansion and gradual healing of openings caused by the solutoning of soluble salts.

ACTA MINERALOGICA PAKISTANICA
VOLUME 1 (1985) pp. 98-115

MINERAL MICROANALYTICAL DATA ON THE DOLERITIC DYKES FROM MANSEHRA–AMB STATE AREA, HAZARA DIVISION, PAKISTAN.

ZULFIQAR AHMED

Centre of Excellence in Mineralogy, University of Baluchistan, Sariab Road, Quetta, Pakistan.

Abstract: The mineral phases present in a suite of doleritic sills and dykes cutting across the granitic-pelitic metamorphic rocks of Mansehra-Amb State area, have been analyzed by electron microprobe. Doleritic rocks represent a variety of rocks produced by magmatic differentiation, subsequent metamorphism of varying intensity and rock alteration. Plagioclase and biopyribole compositions exhibit strong variations in different doleritic samples. Sphene, epidote and hydrogrossular, found in small amounts in some samples, may indicate some auto-metasomatism. Magnetite and ilmenite are abundant among opaques, and oxidized titanomagnetite is also present. A large part of magnetite formed from pyrite and chalcopyrite.

INTRODUCTION

In the granitic-metamorphic rock area of Mansehra-Amb State, Hazara Division, Pakistan, several dykes and sills of doleritic composition occur widely scattered. They have variable thicknesses of upto 40 m, and lengths from a few metres to about half a km. The dykes and sills intrude pelitic and psammitic schists, quartzite, phenocryst-bearing Mansehra granite, tourmaline-granite of Hakale and granitic-gneiss of Susal Gali. The metamorphic rocks display typical Barrovian isograde. The doleritic rocks have been varyingly metamorphosed and range from unaltered dolerites through metadolerites and epidiorites to amphibolites and even to garnet amphibolite. A geological and mineralogical study of these dykes was conducted earlier by Shams & Ahmed (1968) in which the magmatic differentiation trend of the dolerites was demonstrated on the basis of optical data on magmatic minerals. The dykes were shown to be of tholeiitic character. The present study is a follow up of the same study, and is conducted mainly through the microprobe analyses of the mineral constituents of the dyke rocks. The mineral chemical evidence has been obtained on both the metamorphic phases and the relict igneous phases.

ANALYTICAL METHOD

Several standard thin sections and polished thin sections were made for petrographic study and mineral chemical study. The latter was conducted by employing the energy dispersive electron probe microanalyzer unit of the Department of Earth Sciences, Cambridge University, U.K. The instrument was operated at an accelerating voltage of 20 k V, with a beam current of 5 n A and a live counting time of 80 seconds for each spot analysis. Analytical procedure and processing methods used are those of Sweatman and Long (1969) and Statham (1976) respectively. A cobalt internal standard was used for calibration. Some of the samples analyzed were repeatedly analyzed at another instrument set up at the University College, London, U.K., as an accuracy check.

PETROGRAPHY

The mineral chemical data included in the present study has been obtained on 13 selected rock samples; although petrographicaily many more samples were studied. The dyke rocks vary from unaltered olivine-dolerites to quartz-dolerites and from unmetamorphosed dolerites to

Table 1. Mineral assemblages of microanalyzed mafic dyke samples.
X = Present ; A = Total absence shown by microprobe scanning.

Sample No.	ZD 1	6197	6038	7471	35	6064	6252	6196	6770	6232	7375	6022
OLIVINE	X											
PIGEONITE			X									
AUGITE	X	X	X	X	X					A	A	A
AMPHIBOLE		X			X	X	X	X	X	X	X	X
PLAGIOCLASE	X	X	X	X	X	X	X	X	X	X	X	X
QUARTZ		X					X		X			
APATITE	X										X	
CALCITE									X			
EPIDOTE							X		X			X
CHLORITE												X
BIOTITE	X	X				X	X		A	X	X	X
HYDROGROSSULAR												
SPHENE		X		X	X	X						X
ILMENITE	X	X	X	X		X	X	X		X		X
TITANOMAGNETITE	X											
MAGNETITE		A	X					X		A		
PYRITE	X											X
CHALCOPYRITE	X											

Table 2. Microprobe analyses of olivine from olivine-dolerite (ZD 1).

Anal. No.	1	2	3	Formulae to 4 oxygens:–	1	2	3
SiO_2	35.04	35.18	34.00	Si	0.991	1.022	1.018
TiO_2	0.31	0.27	0.16	Ti	0.007	0.006	0.004
FeO	39.79	43.22	47.01	Fe^{2+}	0.941	1.053	1.177
MnO	0.65	0.69	0.85	Mn	0.016	0.017	0.022
MgO	24.30	19.48	16.64	Mg	1.024	0.847	0.742
NiO	0.13	0.03	0.06	Ni	0.003	0.001	0.002
CaO	0.25	0.53	0.31	Ca	0.008	0.017	0.010
Total	100.47	99.40	99.03	Fo(%)	52.112	44.579	38.666

amphibolite grade metadolerites. Although an almandine-amphibolte is present which may be considered as medium grade metamorphic rock, majority falls in the low metamorphic grade only. Igneous textures are preserved in most dolerites, but in some samples extreme changes have occurred producing metamorphic textures. In those with intact magmatic textures such as the subophitic, ophitic and intergranular textures, igneous minerals may be partly or completely replaced by low grade metamorphic minerals. The olivine-bearing dolerites are rare compared to quartz-bearing and micropegmatite-bearing dolerites. Many are without quartz or olivine. Some dykes have finer grained chilled zones outwards from the coarse grained central zones which may contain more granophyric segregations and micropegmatite. The principal minerals are plagioclase and biopyriboles. Olivine occurs in a few dykes, and many others are quartz-bearing. Metamorphic chlorite and epidote may be abundant. Small amounts of apatite, sphene, calcite and hydrogrossular are present in some of the samples. Amongst opaque minerals ilmenite and magnetite are the most abundant; titanomagnetite is present in some sections. Pyrite is also common, and often is enveloped by magnetic. A few sections contain chalocpyrite as well. Chromite grains are absent. The rocks entirely lack the volcanic glass, although cryptocrystalline mesostasis is seen in accessory amounts. The minerals present in the samples analyzed by microprobe are shown in table 1.

MINERAL CHEMISTRY

OLIVINE

Olivine-bearing dolerites are represented by sample no. ZD1 in table 1. The olivine alteration is comparatively small, and serpentine is not seen in olivine-lacking samples. Olivine analyses in table 2, show a wide compositional range with forsterite content varying between 38.666 and 52.112% in one sample, falling in the range hortonolite-hyalosiderite which is a fairly fayalite richer and less magnesian olivine. Cr was found below the detection levels only, and Ni is also very low, MnO varies from 0.65 to 0.85% and CaQ from 0.25 to 0.53%. These values of Mn and Ca; and nil to negligible values of Cr and Ni compare well with the general behariour of such olivines from similar rocks (Deer et al., 1982, fig. 10, table 14).

PYROXENE

The pyroxenes from five samples were analyzed (table 2) with their pyroxene quadrilateral plots shown in fig. 1. Their composition can be considered in terms of four principal variables, Si, Mg, Ca and Fe. The olivine-bearing dolerite (ZD 1) contains the most magnesian of the augites, although other relatively more ferriferous grains are also present. The most clacic and segregated points are of sample 7471 which contains salite. The most spread out

Table 3. Microprobe analyses of pyroxenes with total iron oxide expressed as FeO.

Sample No.	ZD1	ZD1	ZD1	ZD1	ZD1	ZD1	ZD1	ZD1	ZD1	7471	7471	7471
Anal. No.	1	2	3	4	5	6	7	8	9	10	11	12
SiO_2	51.04	51.06	50.21	50.96	50.49	50.47	50.51	50.18	47.76	51.85	47.45	50.70
TiO_2	0.80	0.75	0.85	0.84	0.78	1.05	0.89	1.04	2.33	0.41	3.26	0.87
Al_2O_3	3.09	3.29	3.51	3.10	4.08	3.52	3.55	3.17	5.52	2.27	3.87	4.27
Cr_2O_3	0.12	0.10	0.12	0.03	0.20	0.08	0.19	0.00	n.d.	n.d.	n.d.	n.d.
FeO	9.70	7.60	8.75	9.44	7.65	10.57	9.68	11.67	8.44	8.63	9.72	0.59
MnO	0.22	0.13	0.18	0.21	0.20	0.26	0.26	0.29	0.22	0.22	0.27	0.18
MgO	16.09	15.95	15.50	15.36	15.19	15.11	14.54	14.05	13.54	12.99	12.69	13.06
NiO	0.00	0.00	0.00	0.08	0.00	0.00	0.11	0.00	0.12	0.01	0.03	0.04
CaO	18.01	19.63	18.75	18.73	19.95	18.27	18.64	18.15	21.23	21.62	20.16	20.29
Na_2O	0.45	0.59	0.63	0.24	0.49	0.65	0.55	0.58	0.44	1.08	0.79	0.73
K_2O	0.08	0.00	0.00	0.07	0.00	0.02	0.00	0.00	0.00	0.00	0.04	0.06
Total:	99.60	99.10	98.50	99.06	99.03	100.00	98.92	99.13	99.60	99.0.8	98.28	99.79
Number of ions on the basis of six oxygens.												
Si	1.903	1.903	1.890	1.910	1.886	1.885	1.901	1.898	1.797	1.953	1.821	1.896
Al^{iv}	0.097	0.097	0.110	0.090	0.114	0.115	0.099	0.102	0.203	0.047	0.175	0.104
Al^{vi}	0.039	0.047	0.046	0.047	0.066	0.040	0.058	0.041	0.042	0.054	–	0.084
Ti	0.022	0.021	0.024	0.024	0.022	0.030	0.025	0.030	0.066	0.012	0.094	0.024
Cr	0.004	0.003	0.003	0.001	0.006	0.002	0.006	0.001	n.d.	n.d.	n.d.	n.d.
Fe	0.302	0.237	0.275	0.296	0.239	0.330	0.305	0.370	0.266	0.272	0.312	0.300
Mn	0.007	0.004	0.006	0.007	0.006	0.008	0.008	0.009	0.007	0.007	0.009	0.006
Mg	0.894	0.886	0.870	0.858	0.846	0.841	0.815	0.794	0.759	0.729	0.729	0.728
Ni	0.000	0.000	0.000	0.002	0.000	0.000	0.003	0.000	0.004	<0.001	0.001	0.001
Ca	0.719	0.784	0.756	0.752	0.798	0.731	0.752	0.735	0.856	0.872	0.829	0.813
Na	0.032	0.043	0.046	0.018	0.035	0.047	0.040	0.043	0.032	0.079	0.059	0.053
K	0.004	0.000	0.003	0.003	0.000	0.001	0.000	0.000	0.000	0.000	0.002	0.003
Wo	37.546	41.112	39.769	39.454	42.379	38.433	40.171	38.705	45.508	46.556	44.403	44.161
En	46.684	46.460	45.765	45.016	44.928	44.217	43.536	41.811	40.351	38.922	39.886	39.544
Fs	15.770	12.428	14.466	15.530	12.693	17.350	16.293	19.484	14.141	14.522	16.711	16.295

points are of sample no. 6038, which shows the most ferriferous augites as well as the pigeonite of magnesian as well as intermediate compositions. The lowest Ca contents are also recorded only from this sample. Even in single grains, large variation may be noticed. For example, analysis 8 is from the rim of the same grain as analysis 2 in table 2. This shows an increase in Fe and decrease in Mg with slight decrease in Ca from core towards rim. However, such zoning is not frequent in other samples. Al_2O_3 contents are not too low and range from 2.27 to 5.52%, excluding pigeonite in which Al_2O_3 may be as low as 1.44%. TiO_2 contents are variable from 0.41 to 3.26%, including pigeonites. MnO ranges from 0.10 to 0.46%. Cr and Na are negligible and Ni was found to be almost always below the limit of detection.

The range of pyroxene compositions within individual samples in considerable; although in some samples (e.g., sp. no. 7471), the range is restricted. The presence of a wide variety of pyroxenes in these holocrystalline dykes suggests a complex cooling history. The coexistence of widely variable pyroxene in some samples

7471	35	6197	6197	6197	6197	6197	6038	6038	6038	6038	6038	6038
13	14	15	16	17	18	19	20	21	22	23	24	25
47.76	51.80	52.16	51.10	50.75	49.64	49.29	51.51	49.76	49.87	49.72	53.19	50.75
2.33	0.67	0.59	0.95	0.65	1.22	1.21	0.78	1.16	1.12	1.35	0.41	0.76
5.52	3.08	3.46	3.64	2.89	3.50	3.29	3.00	5.60	2.62	2.64	1.44	1.87
n.d.	0.23	0.21	0.06	0.45	0.08	0.01	0.05	0.22	0.12	0.07	0.06	0.05
8.44	9.29	10.50	11.90	9.14	10.37	14.35	14.02	10.60	19.46	17.42	16.99	24.76
0.22	0.15	0.38	0.23	0.10	0.29	0.33	0.37	0.14	0.45	0.33	0.33	0.46
13.54	17.01	14.83	15.59	15.60	14.46	14.14	17.55	14.80	13.05	12.65	21.95	16.42
0.12	0.00	0.17	0.12	0.00	0.05	0.00	0.06	0.00	0.01	0.00	0.01	0.10
21.23	17.11	16.24	17.03	19.60	18.56	16.00	12.85	16.34	13.45	15.73	5.48	5.68
0.44	0.55	0.54	0.74	0.05	0.81	0.84	0.31	0.38	0.63	0.49	0.13	0.05
0.00	0.00	0.00	0.00	0.02	0.03	0.05	0.02	0.12	0.06	0.00	0.00	0.00
99.60	99.89	99.05	101.36	99.25	99.01	99.51	100.46	99.12	100.84	100.40	99.99	100.85
1.797	1.913	1.951	1.886	1.901	1.878	1.877	1.909	1.861	1.901	1.897	1.960	1.930
0.203	0.087	0.049	0.114	0.099	0.122	0.123	0.091	0.139	0.99	0.103	0.040	0.070
0.042	0.047	0.104	0.044	0.028	0.034	0.025	0.040	0.108	0.019	0.016	0.023	0.14
0.066	0.019	0.016	0.026	0.018	0.035	0.035	0.022	0.032	0.32	0.039	0.011	0.022
n.d.	0.007	0.006	0.002	0.013	0.002	0.000	0.002	0.006	0.004	0.002	0.002	0.001
0.266	0.287	0.328	0.367	0.286	0.328	0.457	0.435	0.331	0.621	0.556	0.523	0.787
0.007	0.005	0.012	0.007	0.003	0.009	0.011	0.012	0.004	0.015	0.011	0.010	0.015
0.759	0.936	0.827	0.857	0.871	0.815	0.803	0.970	0.825	0.742	0.720	1.205	0.930
0.004	0.000	0.005	0.004	0.000	0.001	0.000	0.002	0.000	0.000	0.000	<0.001	0.003
0.856	0.677	0.651	0.673	0.787	0.752	0.653	0.510	0.655	0.549	0.643	0.216	0.231
0.032	0.039	0.039	0.053	0.004	0.059	0.062	0.022	0.028	0.046	0.037	0.010	0.004
0.000	0.000	0.000	0.000	0.001	0.002	0.002	0.001	0.006	0.003	0.000	0.000	0.000
45.508	35.632	36.047	35.477	40.484	39.683	34.135	26.632	36.168	28.713	33.507	11.111	11.858
40.351	49.263	45.792	45.177	44.805	43.008	41.976	50.653	45.555	38.808	37.520	61.986	47.741
14.141	15.105	18.162	19.346	14.712	17.309	23.889	22.715	18.277	32.479	28.973	26.903	40.400

(e.g., 6038) and chemical zoning, make the determination of true original pyroxene phase difficult and of limited significance. A complex petrogenetic evolution is suggested by pyroxene chemistry. In sample 6038, two pyroxenes, one Ca rich (ferroaugitic) and the other Ca-poor (ferropigeonitic) occur together. This sample also displays the highest Fe content amongst the samples analyzed.

PLAGIOCLASE

Plagioclase is ubiquitously present as is apparent from table 1. It forms laths which are upto 5 mm long in coarser grained samples. 56 plagioclase analyses reported in table 4 show an overall range from 70.727% to 17.106%. Most feldspars contain very little potash feldspar in solid solution which ranges from zero to 2.35%. Zoned crystals are quite common. Both core and rim compositions from singular grains are listed for the sample 6064 in table 4. It shows strongly zoned nature of feldspar crystals, e.g., a core with 70.727% An has a rim of 47.168% An. Strong variations are also recorded from within some rock samples,

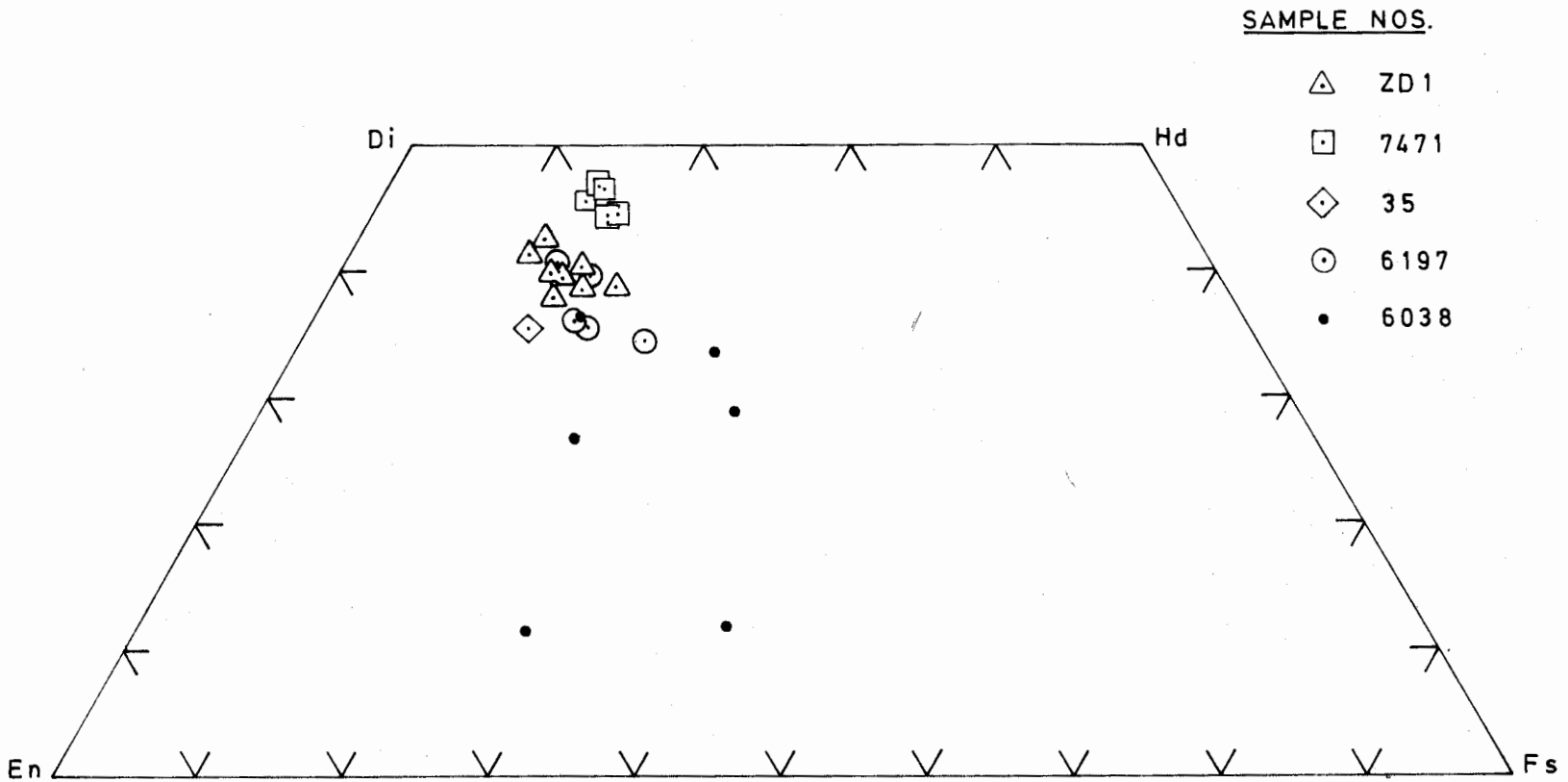

Fig.1 . Quadrilateral plots of pyroxenes from Mansehra–Amb State dolerites.

Table 4. Plagiocclase feldspar microanalyses from dolerites in which pyroxene is retained (anal. 1–22) and those from which pyroxene has disappeared. (anal. 23–52) For each sample, more calcic feldepars are listed first. Some analyses numbers are suffixed 'C' for core of agrain, 'I' for intermediate part and 'R' for rim of the same grain. The formulae are calculated to 32 oxygens. b.d = below the detection level. n.d. = not determined.

Anal. No.	Sample No.	Si	Al	Ti	Fe^{3+}	Mn	Mg	Ca	Na	K	An	Ab	Or
1.	ZD1	9.289	6.540	0.008	0.150	0.002	0.116	2.693	1.211	0.058	67.971	30.565	1.464
2.	ZD1	9.545	6.336	0.008	0.100	0.000	0.000	2.609	1.254	0.075	66.252	31.844	1.905
3.	ZD1	9.642	6.219	0.017	0.093	0.000	0.025	0.410	1.511	0.052	60.660	38.032	1.308
4.	ZD1	9.771	6.110	0.002	0.091	0.007	0.081	2.299	1.533	0.079	58.783	39.197	2.020
5.	ZD1	9.982	5.931	0.018	0.009	0.000	0.000	2.099	1.720	0.068	54.001	44.250	1.749
6.	ZD1	9.988	5.933	0.002	0.088	0.004	0.018	2.021	1.918	0.058	50.563	47.986	1.451
7.	ZD1	10.089	5.790	0.022	0.084	0.000	0.022	1.916	1.918	0.126	48.384	48.434	3.182
8.	ZD1	10.340	5.600	0.012	0.077	0.010	0.000	1.682	2.112	0.127	42.897	53.584	3.239
9.	ZD1	11.452	4.615	0.007	b.d.	0.000	0.008	0.629	3.025	0.023	17.106	82.268	0.626
10.	6197	9.543	6.358	0.019	0.097	0.001	0.013	2.547	1.288	0.073	65.174	32.958	1.868
11.	6197	9.662	6.165	0.004	0.122	0.009	0.049	2.425	1.475	0.032	61.673	37.513	0.814
12.	6197	9.658	6.211	0.010	0.093	0.000	0.042	2.347	1.561	0.011	59.888	39.832	0.281
13.	6197	9.593	6.211	0.008	0.135	0.009	0.095	2.370	1.566	0.045	59.533	39.337	1.130
14.	6038	9.536	6.271	0.018	0.087	0.000	0.143	2.502	1.409	0.048	63.198	35.590	1.212
15.	6038	9.796	6.053	0.012	0.106	0.006	0.088	2.334	1.464	0.076	60.248	37.790	1.962
16.	6038	9.855	5.987	0.012	0.090	0.015	0.090	2.271	1.667	0.082	56.492	41.468	2.040
17.	6038	9.999	5.835	0.019	0.095	0.005	0.034	2.158	1.748	0.094	53.950	43.700	2.350
18.	6038	9.954	5.854	0.017	0.086	0.005	0.088	2.161	1.764	0.085	53.890	43.990	2.120
19.	7471	8.725	5.250	0.012	0.261	0.007	0.063	1.793	1.592	0.014	52.751	46.837	0.412
20.	7471	9.943	6.011	0.004	0.038	0.000	0.092	2.025	1.808	0.023	52.516	46.888	0.596
21.	7471	9.946	5.930	0.026	0.094	0.001	0.000	2.045	1.932	0.014	51.240	48.409	0.351
22.	35	10.136	5.771	0.031	0.093	0.000	0.000	1.784	2.140	0.032	45.096	54.095	0.809
23C	6064	9.197	6.774	0.010	0.054	0.000	0.084	2.723	1.117	0.010	70.727	29.013	2.260
23I	6064	9.346	6.577	0.019	0.101	0.006	0.056	2.581	1.291	0.033	66.095	33.060	0.845
23R	6064	10.167	5.790	0.000	0.075	0.000	0.048	1.832	2.039	0.013	47.168	52.497	0.335
24C	6064	9.208	6.678	0.016	0.058	0.000	0.112	2.737	1.248	0.009	68.528	31.247	0.225
24R	6064	10.276	5.729	0.005	0.029	0.010	0.000	1.757	2.084	0.012	45.601	54.088	0.311
25C	6064	9.636	6.325	0.020	0.021	0.005	0.019	2.405	1.491	0.011	61.556	38.162	0.282
25R	6064	9.947	6.055	0.012	0.070	0.004	0.017	2.082	1.625	0.025	55.788	43.542	0.670
26C	6064	9.829	6.154	0.000	0.072	0.000	0.000	2.246	1.572	0.011	58.658	41.055	0.287
26R	6064	10.235	5.727	0.015	0.055	0.001	0.071	1.735	2.084	0.010	45.312	54.427	0.261
27.	6064	9.411	6.489	0.009	0.078	0.005	0.074	2.506	1.365	0.040	64.076	34.902	1.023
28.	6064	9.658	6.242	0.002	0.083	0.010	0.101	2.293	1.568	0.056	58.540	40.031	1.430
29.	6252	9.670	6.327	0.000	b.d.	0.006	b.d.	2.366	1.553	0.040	59.763	39.227	1.010
30.	6252	9.682	6.243	0.018	0.111	0.000	0.135	2.216	1.482	0.031	59.426	39.743	0.831
31.	6252	9.790	6.141	0.005	0.093	0.000	0.000	2.272	1.556	0.019	59.059	40.447	0.494
32.	6252	9.960	5.984	0.011	0.050	0.000	0.000	2.071	1.886	0.018	52.101	47.447	0.452
33.	6252	9.857	6.026	0.012	0.115	0.000	0.018	2.102	1.940	0.031	51.608	47.631	0.761
34.	6252	10.199	5.746	0.009	0.132	0.000	0.047	1.690	2.139	0.032	43.771	55.400	0.829
35.	6252	10.928	5.094	0.000	0.016	0.000	0.024	1.077	2.740	0.016	28.098	71.485	0.417
36.	6196	9.968	6.004	0.005	0.005	0.000	0.033	2.130	1.737	0.016	54.855	44.733	0.412
37.	6196	10.052	5.801	0.023	0.090	0.008	0.062	2.016	1.838	0.014	52.120	47.518	0.362
38.	6196	10.270	5.644	0.005	0.045	0.000	0.076	1.753	2.157	0.021	44.594	54.872	0.534
39.	6196	10.528	5.438	0.000	0.046	0.008	0.000	1.604	2.180	0.030	42.056	57.157	0.787
40.	6770	10.156	5.749	0.001	0.060	0.000	0.000	1.989	1.956	0.009	50.303	49.469	0.228
41.	6770	10.227	5.700	0.016	0.018	0.015	0.090	1.775	2.103	0.014	45.606	54.034	0.360
42.	6770	10.367	5.619	0.024	0.035	0.009	0.032	1.670	2.208	0.002	43.041	56.907	0.052
43.	6232	10.137	5.727	0.029	0.152	0.000	0.043	1.824	1.886	0.079	48.139	49.776	2.085
44.	6232	10.398	5.552	0.001	0.049	0.000	0.037	1.630	2.270	0.015	41.635	57.982	0.383
45.	6232	10.916	5.125	0.000	0.017	0.003	0.000	1.096	2.709	0.000	28.804	71.196	0.000
46.	7375	10.479	5.526	0.008	0.017	0.008	0.010	1.531	2.291	0.015	39.901	59.708	0.391
47.	7375	10.610	5.386	0.007	0.011	0.000	0.048	1.404	2.436	0.000	36.562	63.438	0.000
48.	7375	10.709	5.284	0.010	0.026	0.001	0.034	1.274	2.551	0.019	33.143	66.363	0.494
49.	7375	10.909	5.073	0.009	0.013	0.000	0.016	1.141	2.742	0.030	29.159	70.074	0.767
50.	6022	10.929	5.043	0.007	0.009	0.000	0.080	1.074	2.793	0.006	27.730	72.115	0.155
51.	6022	11.031	4.987	0.002	0.003	0.000	0.000	0.982	2.914	0.020	25.077	74.413	0.510
52.	6022	11.116	4.893	0.000	0.017	0.000	0.059	0.860	2.955	0.014	22.460	77.174	0.366

Table 5. Amphibole analyses by microprobe. All iron is expressed as Fe^{2+}

Anal. No.	1	2	3	4E	5E	6E	7E	8E	9L	10L	11L	12L	13	14	15	16
Sample No.	6197	6197	6197	6064	6064	6064	6064	6064	6064	6064	6064	6064	6252	6252	6252	6252
SiO_2	45.88	43.57	45.53	51.88	52.77	51.50	54.42	52.38	42.72	41.72	41.95	41.00	49.47	49.72	46.47	44.65
TiO_2	0.54	1.16	0.61	0.23	0.27	0.39	0.12	0.29	0.34	0.28	0.12	0.22	0.33	0.20	1.05	1.25
Al_2O_3	6.40	8.82	7.92	3.46	3.71	4.77	2.67	3.36	13.32	14.38	14.84	15.77	5.89	4.63	7.74	9.40
Cr_2O_3	0.00	0.00	0.00	0.06	0.27	0.19	0.09	0.10	0.03	0.00	0.06	n.d.	–	0.12	0.00	0.08
FeO	22.21	23.20	21.38	12.87	13.24	13.21	12.30	12.45	17.71	19.63	19.16	18.76	16.65	18.61	17.50	18.06
MnO	0.37	0.35	0.36	0.23	0.13	0.17	0.19	0.24	0.20	0.23	0.30	0.31	0.43	0.54	0.38	0.33
MgO	8.87	7.06	8.47	14.06	14.19	13.94	15.24	14.52	8.41	6.93	7.59	7.21	12.24	10.96	10.32	9.33
NiO	0.00	0.01	0.00	0.00	0.00	0.02	0.11	0.01	0.03	0.00	0.00	n.d.	0.09	0.11	0.00	0.00
CaO	10.50	10.30	11.03	12.46	11.92	12.31	12.67	12.42	11.60	11.80	12.00	11.82	11.60	11.21	11.23	11.64
Na_2O	0.42	0.68	0.58	0.28	0.26	1.06	0.46	0.18	1.12	1.50	1.43	1.37	1.02	0.64	1.15	1.38
K_2O	0.73	1.16	1.08	0.04	0.10	0.03	0.12	0.12	0.53	0.74	0.69	0.65	0.39	0.18	0.59	0.48
Total	95.92	96.31	96.96	95.57	96.86	97.59	98.39	96.07	96.01	97.21	98.14	97.11	98.11	96.92	96.43	96.60
Cations based on 23 oxygens:																
Si	7.125	6.811	6.988	7.657	7.669	7.475	7.765	7.670	6.511	6.364	6.321	6.233	7.287	7.462	7.029	6.787
Al^{IV}	0.875	1.189	1.012	0.343	0.331	0.525	0.235	0.330	1.489	1.636	1.679	1.767	0.713	0.538	0.971	1.213
Al^{VI}	0.297	0.436	0.420	0.258	0.305	0.291	0.213	0.250	0.903	0.949	0.956	1.058	0.310	0.281	0.409	0.471
Ti	0.063	0.136	0.071	0.025	0.030	0.043	0.013	0.032	0.039	0.032	0.013	0.025	0.037	0.022	0.120	0.142
Cr	0.000	0.000	0.000	0.007	0.031	0.022	0.011	0.012	0.003	0.000	0.007	n.d.	–	0.014	0.000	0.010
Fe	2.884	3.033	2.744	1.588	1.610	1.604	1.468	1.525	2.257	2.504	2.415	2.385	2.052	2.336	2.213	2.297
Mn	0.048	0.047	0.047	0.028	0.017	0.021	0.023	0.030	0.025	0.029	0.038	0.040	0.054	0.069	0.048	0.042
Mg	2.052	1.645	1.938	3.093	3.075	3.016	3.240	3.169	1.910	1.575	1.704	1.633	2.687	2.451	2.327	2.114
Ni	0.000	0.001	0.000	0.000	0.000	0.002	0.013	0.001	0.004	0.000	0.000	n.d.	0.011	0.014	0.000	0.000
Ca	1.747	1.726	1.814	1.970	1.856	1.914	1.937	1.949	1.894	1.929	1.937	1.925	1.832	1.802	1.820	1.896
Na	0.126	0.206	0.171	0.081	0.072	0.298	0.126	0.049	0.330	0.442	0.416	0.402	0.291	0.185	0.336	0.408
K	0.145	0.232	0.212	0.007	0.019	0.005	0.022	0.022	0.102	0.144	0.131	0.126	0.073	0.035	0.113	0.094
Mg/(Mg+ Fe^{2+})	41.572	35.165	41.393	66.076	65.635	65.281	68.819	67.512	45.826	38.612	41.369	40.642	56.700	51.201	51.256	47.926

e.g., the olivine dolerite sample (ZD 1) has An content from 67.971% to 17.106%; although there is a large gap between An 17.106% and 44.250%. A quartz-bearing dolerite sample 6252 has An content of 59.426% to 28.098% although again there is gap between 28.098% and 43.771% An. In some other samples, variation is not large, e.g., sample 6022, 6197, etc.

Three quartz-bearing samples contain more calcic plagioclase (e.g., An = 59.533 to 65.174% in sample 6197) as well as more sodic one (e.g., An = 43.041 to 50.303% in sample 6770).

AMPHIBOLE

Table 5 lists 32 analyses of amphiboles from various samples and serves to bring out the intra-sample and intra-granular variation in composition. Extreme variation in amphibole composition is apparent in many samples. Following the classification scheme of Leake (1978), amphiboles from different samples belong to different categories. Many of the samples contain more than one kind of amphibole. The categories present may be named as: actinolite, ferrohornblende, actinolitic hornblende ferroedinite, edinitic hornblende, ferroedinitic hornblende, hastingsite, magnesio-hornblende, magnesian hastingsitic hornblende and ferroan pargasitic hornblende. Such large variation may reflect varying degrees of alteration and metamorphism. The amphiboles of both igneous and metamorphic origin are probably present. Reviewing the published amphibole analyses from metabasites, Hynes (1982) was able to distingish between amphiboles from

17	18	19	20	21	22	23	24	25	26	27	28	29	30	31	32
6252	6252	6196	6196	6196	6770	6770	6232	6232	7375	7375	7375	6022	6022	6022	6022
42.69	42.62	49.87	48.89	46.15	39.77	38.94	42.57	41.44	44.24	45.13	44.34	42.75	42.89	41.81	41.09
0.57	2.91	0.37	0.40	0.65	0.71	0.20	0.59	0.51	0.43	0.68	0.48	0.86	0.94	0.74	0.89
11.30	11.17	3.82	4.98	7.03	14.11	17.09	11.62	12.94	12.25	11.13	12.02	10.45	11.82	12.09	12.90
0.01	0.02	0.09	0.09	0.01	n.d.	n.d.	0.00	0.08	n.d.	n.d.	0.54	0.00	0.08	0.07	0.03
19.08	17.53	18.88	18.99	22.11	22.98	23.63	19.52	20.03	12.44	12.95	12.71	16.71	17.32	17.30	17.83
0.31	0.27	0.39	0.41	0.44	0.24	0.39	0.23	0.23	0.09	0.14	0.09	0.28	0.32	0.22	0.24
8.21	8.01	11.03	10.39	8.14	4.97	4.13	8.46	7.63	12.00	12.28	11.84	10.07	9.51	9.25	9.06
0.00	0.16	0.24	0.16	0.03	0.04	0.00	0.07	0.06	0.15	0.00	0.13	0.01	0.00	0.04	0.00
11.50	12.43	12.21	11.91	11.95	11.38	10.89	11.69.	11.80	12.18	12.16	12.06	11.26	11.35	11.25	11.33
1.24	0.81	0.74	0.73	1.21	1.50	1.92	1.45	1.43	1.63	1.70	1.70	1.75	1.79	1.60	1.97
0.71	0.51	0.21	0.24	0.45	1.01	1.16	0.49	0.67	0.55	0.40	0.39	0.62	0.59	0.69	0.76
95.62	96.44	97.85	97.19	98.17	96.71	98.35	96.69	96.82	95.96	96.57	96.33	94.76	96.61	95.06	96.10
6.605	6.502	7.456	7.361	7.030	6.236	6.015	6.527	6.378	6.597	6.691	6.596	6.614	6.517	6.468	6.322
1.395	1.498	0.544	0.639	0.970	1.764	1.985	1.473	1.622	1.403	1.309	1.404	1.386	1.483	1.532	1.678
0.666	0.510	0.129	0.245	0.292	0.843	1.126	0.627	0.725	0.749	0.635	0.703	0.520	0.634	0.672	0.661
0.066	0.334	0.041	0.045	0.074	0.083	0.022	0.068	0.059	0.048	0.075	0.053	0.100	0.107	0.86	0.102
0.002	0.002	0.011	0.012	0.001	–	–	0.000	0.010	–	–	0.068	0.000	0.010	0.008	0.003
2.469	2.236	2.360	2.391	2.815	3.013	3.053	2.503	2.578	1.551	1.606	1.581	2.162	2.201	2.238	2.294
0.041	0.035	0.049	0.052	9.057	0.032	0.050	0.030	0.029	0.012	0.017	0.011	0.037	0.041	0.028	0.031
1.894	1.820	2.459	2.331	1.848	1.161	0.951	1.932	1.751	2.668	2.714	2.626	2.321	2.153	2.132	2.077
0.000	0.020	0.028	0.020	0.004	0.005	0.000	0.009	0.008	0.018	0.000	0.016	0.001	0.000	0.005	0.000
1.905	2.032	1.957	1.921	1.950	1.911	1.803	1.921	1.945	1.945	1.931	1.922	1.867	1.848	1.864	1.868
0.372	0.240	0.214	0.214	0.356	0.455	0.574	0.432	0.425	0.472	0.489	0.490	0.524	0.527	0.480	0.587
0.141	0.100	0.040	0.046	0.044	0.202	0.229	0.096	0.130	0.103	0.076	0.073	0.123	0.114	0.135	0.149
43.410	44.872	51.027	49.365	39.631	27.815	23.751	43.563	40.448	63.238	62.824	62.420	51.773	49.449	48.787	47.518

low-pressure terrains and those from medium-pressure terrains. He found that low pressure amphiboles may contain more Ti than the medium pressure amphiboles for a given extent of tschermakite substitution. Following Hynes (1982, fig. 4) the Mansehra doleritic amphiboles are plotted, in fig. 3, on the total Ti versus total Al plot, after normalization to 23 oxygens with all iron considered as Fe^{2+}. Such as plot displays resemblance with the low pressure amphiboles rather than the medium-pressure amphiboles. The Ti content varies greatly and ranges from 0.013 to 0.334 ions per formula-unit. The doleritic rocks studied include various types with or without sphene or ilmenite or both. Therefore, these rocks do not fall in the category of Hidaka Mountain metabasites which are an exception to Hynes' diagram (op. cit.).

BIOTITE

13 analyses of biotites from these dolerites are reported in table 6. The titanium content of biotite is fairly high. TiO_2 ranges between 1.43 and 5.91%, average being 3.3%. The grain with 5.91% TiO_2 occurs intergrown with a coarse grain of ilmenite. Retention of Ti in biotite shows that it is not altered. Fe and Mg contents also vary; but SiO_2, Al_2O_3 and K_2O values are not much divergent. Mole fraction of phlogopite varies from 0.293 to 0.654. Assuming the plagioclase composition as a parameter of magmatic fractionation, the plot of biotite $Mg/(Mg+Fe^{2+})$ content on a graph against the anorthite content in associated plagioclase does not show a clean

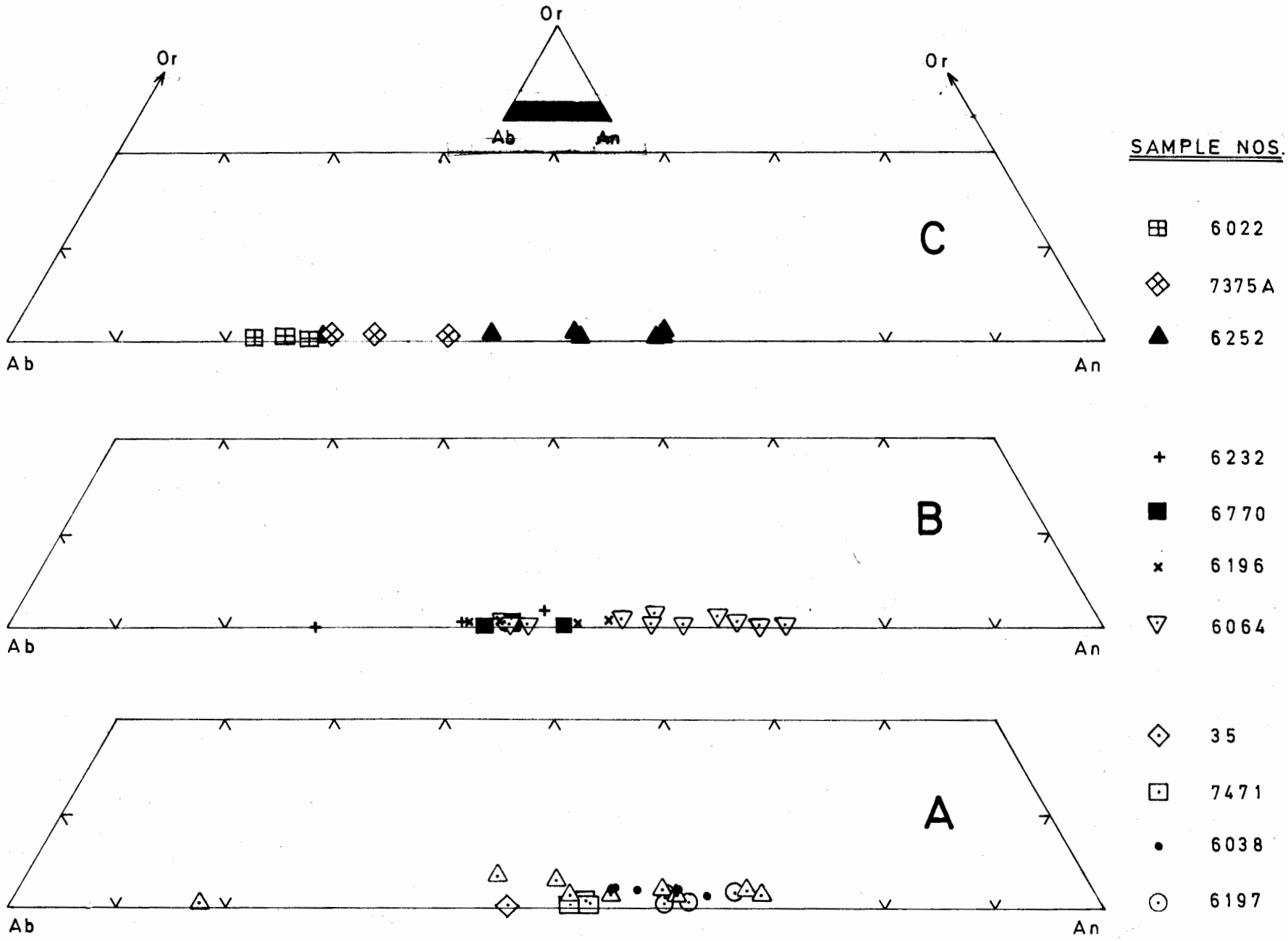

Fig. 2. Compositions of feldspars from dolerites. List of samples on right hand margin is in order of decreasing maximum An content from base upwards, separately for pyroxene-bearing dolerites (A) and pyroxene-lacking meta-dolerites (B & C).

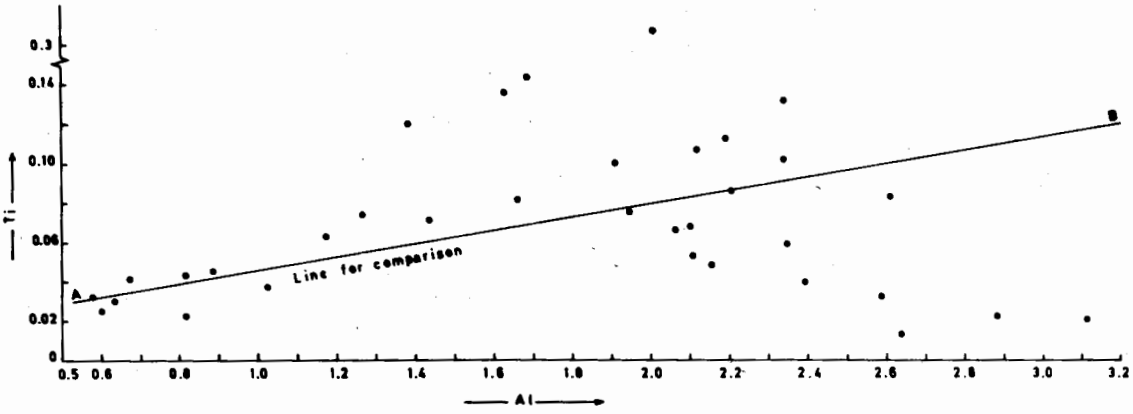

Fig.3. Plot of total Ti versus total Al in amphibole analyses of table 5, drawn after Hynes (1982, fig.4).

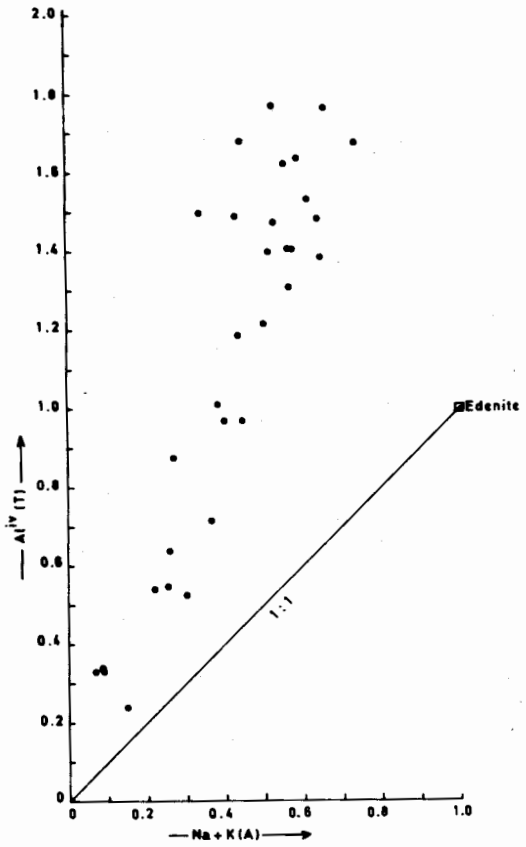

Fig.4. Al^{IV} in T site versus (Na+K) in A site; edenite substitution in the amphiboles of table 5.

Table 6. Biotite analyses. Total iron oxide is expressed as FeO.

Anal. No.	1	2	3	4	5	6	7	8	9	10	11	12	13
Sample No.	ZD1	6197	6197	6197	6040	6252	6252	6232	6232	7375	6022	6022	6022
SiO_2	36.41	35.21	34.19	34.79	35.93	36.08	32.21	37.93	37.76	37.51	36.31	35.91	36.51
TiO_2	3.53	5.89	4.86	4.28	1.43	2.35	5.91	2.10	2.42	2.52	2.72	2.45	2.47
Al_2O_3	13.03	13.70	16.45	15.00	16.81	16.32	16.05	16.13	16.40	17.29	16.09	15.12	15.92
Cr_2O_3	0.06	0.00	0.00	0.00	n.d.	0.00	b.d.	0.00	b.d.	b.d.	0.08	0.00	0.03
FeO	27.23	23.87	23.65	24.39	19.52	18.99	21.87	18.02	17.48	13.85	17.42	18.23	17.96
MnO	0.09	0.11	0.06	0.11	0.13	0.19	0.23	0.19	0.04	0.16	0.17	0.14	0.14
MgO	6.33	7.56	7.44	6.88	9.98	9.97	11.96	11.29	11.12	14.63	12.03	12.42	12.62
NiO	0.05	0.00	0.06	0.00	n.d.	0.00	0.00	0.00	0.00	0.00	0.00	0.00	0.00
CaO	0.12	0.04	0.11	0.02	0.11	0.08	0.00	0.15	0.33	0.17	0.11	0.11	0.16
Na_2O	0.31	0.00	0.07	0.00	0.00	0.13	0.29	0.30	0.50	0.11	0.17	0.43	0.37
K_2O	9.10	9.34	9.74	9.21	9.20	9.30	7.21	8.80	8.86	9.10	9.66	9.26	9.42
Total	96.26	95.72	96.63	94.68	93.11	93.41	95.73	94.91	94.91	95.25	94.76	94.07	95.60
Formulae based on 22 oxygens:													
Si	5.730	5.500	5.288	5.500	5.606	5.607	4.957	5.723	5.695	5.518	5.535	5.543	5.524
Al	2.270	2.500	2.712	2.500	2.394	2.393	2.911	2.277	2.305	2.482	2.465	2.457	2.476
Al	0.147	0.023	0.287	0.295	0.696	0.596	0.000	0.599	0.610	0.533	0.425	0.294	0.363
Ti	0.417	0.692	0.565	0.508	0.167	0.274	0.683	0.238	0.274	0.283	0.311	0.284	0.281
Cr	0.007	0.000	0.000	0.000	–	0.000	–	0.000	–	–	0.010	0.000	0.004
Fe^{2+}	3.584	3.119	3.060	3.224	2.547	2.468	2.815	2.278	2.205	1.711	2.220	2.353	2.272
Mn	0.011	0.015	0.008	0.015	0.016	0.024	0.029	0.025	0.005	0.020	0.022	0.018	.018
Mg	1.486	1.761	1.714	1.621	2.320	2.309	2.742	2.542	2.500	3.228	2.734	2.858	2.846
Ni	0.006	0.000	0.007	0.000	–	0.000	0.000	0.001	0.000	0.000	0.000	0.000	0.000
Ca	0.020	0.007	0.018	0.004	0.019	0.013	0.000	0.025	0.053	0.028	0.018	0.018	0.025
Na	0.094	0.000	0.022	0.000	0.000	0.039	0.086	0.088	0.146	0.032	0.049	0.128	0.109
K	1.827	1.862	1.922	1.856	1.831	1.843	1.415	1.698	1.705	1.703	1.879	1.822	1.818

relationship between the two parameters. However, the olivine dolerite has the least mole fraction phlogopite in its biotite. Another more magnesian sample with 60 to 65% An in its plagioclase (no. 6197) has biotite with lesser Mg. Samples 6022 and 7375 which posses the most acidic plagioclases, contain a biotite with the highest phlogopite mole fraction. This trend of increasing Mg and decreasing Fe with the progress of magmatic fractionation is against the usual trend (cf. Deer et al., 1962).

Ti in biotite has an inverse correlation with Al in the octahedral sites (Al^{vi}). In case of metapelites. Schreurs (1985) noted a trend of increasing Ti and decreasing Al^{vi} with increasing metamorphic grade. In Ti versus Al^{vi} diagram for Mansehra-Amb State doleritic rocks (fig. 5), biotites from the same sample may plot farther apart. This may be due to some biotites in a sample being metamorphic, others being relics of igneous biotite. The sum of Si and Al in the analyzed biotites (table 6) exceeds eight except one grain of biotite of sample 6252 which is intergrown with ilmenite. In tetrahedral site, Al substitutes for 2.270 to 2.911 atoms of Si in the biotites analyzed.

Table 7. Chlorite microanalyses.

Anal. No.	1	2	3	4	5	6	7
Sp. No.	6064	6770	6770	6770	6252	6022	6022
SiO_2	26.25	25.71	25.94	30.10	25.60	35.88	36.05
TiO_2	0.24	0.67	0.55	0.79	0.24	0.88	0.41
Al_2O_3	20.55	17.40	17.31	16.39	20.89	28.12	28.26
FeO	21.52	33.53	33.39	29.83	22.74	9.77	11.21
MnO	0.17	0.17	0.14	0.13	0.35	0.00	0.03
MgO	16.76	8.87	8.24	7.41	15.73	7.93	7.40
NiO	n.d.	0.07	0.05	0.10	0.00	0.00	b.d.
CaO	0.05	0.23	0.14	0.51	0.10	1.97	1.21
Na_2O	0.41	0.29	0.06	0.00	0.15	1.75	2.48
K_2O	0.00	0.06	0.20	0.92	0.09	0.06	0.07
Total	85.95	87.00	86.02	86.18	85.89	86.36	87.12
Formulae to 28 oxygens:							
Si	5.536	5.753	5.859	5.181	5.448	6.852	6.874
Al^{iv}	2.464	2.247	2.141	2.819	2.552	1.148	1.126
Al^{vi}	2.645	2.325	2.464	0.515	2.689	5.180	5.225
Ti	0.037	0.115	0.096	0.105	0.039	0.126	0.060
Fe^{2+}	3.795	6.284	6.308	4.293	4.047	1.560	1.780
Mn	0.030	0.033	0.028	0.020	0.062	0.000	0.004
Mg	5.270	2.949	2.761	1.901	4.990	2.257	2.104
Ni	–	0.012	0.009	0.014	0.000	0.000	–
Ca	0.012	0.056	0.034	0.097	0.023	0.403	0.245
Na	0.168	0.130	0.026	0.000	0.060	0.648	0.913
K	0.000	0.016	0.059	0.206	0.024	0.015	0.017

Table 8. Microprobe analyses of sphene with all iron assumed to be trivalent.

Anal. No.	1	2	3	4	Number of ions on the basis of 4 Si:–	1	2	3	4
Sp. No.	6064	6022	6022	6022					
SiO_2	31.02	30.29	29.64	30.22	Si	4.000	4.000	4.000	4.000
TiO_2	39.82	37.69	38.33	37.39	Al	0.140	0.159	0.162	0.139
Al_2O_3	0.92	1.02	1.02	0.89	Fe^{3+}	0.039	0.152	0.107	0.144
Cr_2O_3	0.00	0.05	0.00	0.07	Ti	3.861	3.743	3.890	3.721
Fe_2O_3	0.40	1.53	1.05	1.45	Cr	0.000	0.001	0.000	0.007
MnO	0.14	0.09	0.12	0.04	Mn	0.015	0.010	0.014	0.004
MgO	0.00	0.06	0.08	0.10	Mg	0.000	0.12	0.016	0.020
CaO	29.37	28.18	28.27	28.42	Ca	4.057	3.987	4.087	4.030
Na_2O	0.16	0.38	0.48	0.02	Na	0.040	0.097	0.125	0.005
K_2O	0.02	0.01	0.01	0.03	K	0.003	0.002	0.002	0.005
Total	101.85	99.30	99.00	98.63	O	20.084	20.017	20.363	19.938
					(EOCR)	0.603	0.604	0.603	0.604

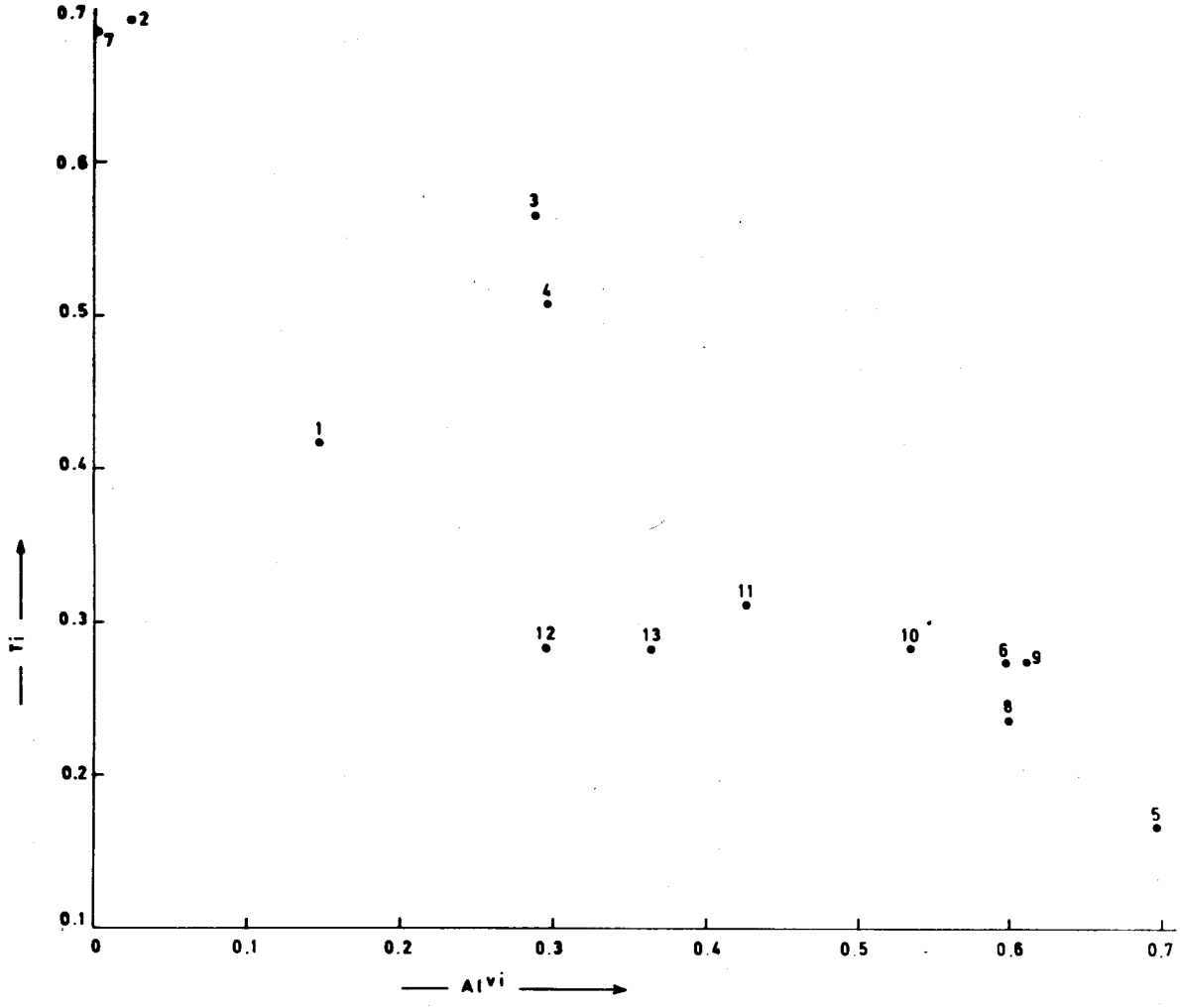

Fig. 5. Biotite compositional plot of Ti versus Al^{vi} (atoms/formula unit). Analyses numbers correspond to those in table 6.

CHLORITE

Chlorite types present in these dolerites include ripidolite, brunsvigite and penninite, as shown by the chlorite analyses reported in table 7. Overall, they are quite variable. Total Fe as FeO ranges from 9.77 to 33.53%; MgO from 7.40 to 16.76%; MnO from 0.00 to 0.35%: CaO from 0.05 to 1.97%; Al_2O_3 from 16.39 to 20.89% and SiO_2 from 25.60 to 36.05%. MnO is low overall, maximum being 0.35%. CaO is commonly much less than 1%, but in a penninite (anal. 6, 7) it is present between 1.21 and 1.97%. With lowering of Al_2O_3, FeO becomes higher.

Chemically, two different chlorite types, ripidolite and brunsvigite, are present in one sample (no. 6770). The $Mg/(Mg+Fe^{2+})$ values for coexisting chlorites and biotites match for some samples or for some grains in a sample. Probably some chlorite has formed by chloritization of biotite and the rest was formed directly or at the expense of amphibole. Al_2O_3 in the chlorite of most fractionated sample (6022) is highest and varies from 28.12% to 28.26% as against 16.39% to 20.89% Al_2O_3 in the rest of samples. The chlorite of this sample also contains relatively highest CaO and Na_2O and lowest FeO.

Table 9. Microprobe analyses of epidote. All iron calculated as Fe_2O_3. Each analysis is summed to 100 on basis of assumed H_2O^+.

			Structural formulae on the basis of 13 (O,OH):		
Anal. No.	1	2		1	2
Sp. No.	6770	6252			
SiO_2	37.83	37.87	Si	2.974	3.029
TiO_2	0.14	0.10	Al	0.026	0.000
Al_2O_3	25.56	23.29	ΣZ	3.000	3.029
Fe_2O_3	10.26	13.21	Al	2.342	2.195
MnO	0.10	0.12	Ti	0.008	0.006
MgO	0.00	0.00	Fe^{3+}	0.607	0.795
NiO	0.07	0.02	Mn	0.007	0.008
CaO	23.96	23.95			
Na_2O	0.00	0.00	Ni	0.004	0.001
K_2O	0.00	0.00	Ca	2.018	2.052
H_2O^+	2.08	1.44	OH	1.090	0.768
Total	100.00	100.00			

Table 10. Microprobe analyses of hydrogrossular from sample no. 6252.

			Ions on the basis of 24 O:		
Anal. No.	1	2		1	2
SiO_2	37.43	38.09	Si	5.901	5.940
TiO_2	0.16	0.18	Al	4.362	4.370
Al_2O_3	23.48	23.77	Ti	0.019	0.021
Cr_2O_3	0.10	0.00	Cr	0.014	0.000
FeO	11.63	11.36	Fe	1.538	1.482
MnO	0.35	0.20	Mn	0.047	0.025
MgO	0.31	0.20	Mg	0.071	0.045
NiO	0.10	0.00	Ni	0.013	0.000
CaO	23.25	23.76	Ca	3.928	3.971
Na_2O	0.00	0.00			
K_2O	0.00	0.00			
Total	96.81	97.56			

SPHENE

Table 8 lists sphene analyses in which all iron has been assumed to be trivalent and located in the Y(octahedral) site alongwith Al and Ti. There is negligible to vary small substitution of Na and Mn for Cu in the X(seven fold) site. Cr and Mg are negligible, but Fe and Al show slight substitution for Ti. The sphene does not contain appreciable amounts of REE. The sphene-bearing samples contain ilmenite, and their pyroxene has been changed totally to amphiboles. Their plagioclase is less clacic than many other samples without sphene. In fig. 6, sphene analyses are compared with the igneous, metamorphic and paragneiss-skarn sphenes after Tulloch (1979). Sphenes from the Mansehra-Amb State dolerites plot in a separated field and exhibit Al and Fe contents even lower than the igneous field sphenes.

EPIDOTE

Compositions representing the epidotes from these dolerites are given in table 9 for two quartz-dolerite samples only. Their $Fe^{3+}/(Fe^{3+} + Al)$ values correspond to 0.206 and 0.266. Presence of epidote often indicates low-grade metamorphism of doleritic rocks. Epidote forms euhedral crystals. The Ca content of epidote is apparently not derived from plagioclase; as the calcic plagioclase coexists with epidote. The epidote-bearing samples lack albite.

HYDROGROSSULAR

Garnet of hydrogrossular composition is present in a quartz-bearing dolerite (sample no. 6252) in which all pyroxene has been changed, and may have provided the Ca necessary for the constitution of hydrogrossular. The hydrogrossular contains appreciable amount of iron (table 10). Epidote is also present in the same rock. Calcic plagioclase coexists with htdrogrossular and may not have provided the Ca for

Table 11. Ilmenite analyses.

Sample No.	ZD1	7471	6197	6197	6038	6064	6064	6252	6196	6232	6232	6022	6022
SiO_2	0.27	0.33	0.41	0.26	0.42	0.72	0.30	0.25	0.46	0.18	0.34	0.26	0.17
TiO_2	51.90	48.89	54.34	53.31	51.03	53.38	53.37	51.90	54.71	53.04	52.45	47.66	48.64
Al_2O_3	0.00	0.21	0.16	0.05	0.08	0.22	0.18	0.00	0.11	0.08	0.15	0.23	0.00
FeO	45.49	48.77	45.48	46.31	47.71	41.75	42.97	44.09	44.40	46.26	46.40	49.28	48.69
MnO	0.96	0.64	1.24	1.09	0.66	2.81	2.55	2.22	1.94	1.56	1.42	1.64	1.62
MgO	0.35	0.84	0.40	0.29	0.15	0.09	0.21	0.37	0.20	0.20	0.39	0.30	0.10
CaO	0.03	0.00	0.00	0.00	0.15	0.79	0.15	0.08	0.10	0.10	0.12	0.22	0.03
Total	99.00	99.69	102.03	101.31	100.20	99.76	99.73	98.91	101.92	101.42	1o1.27	99.59	99.25
Number of cations on the basis of 6 oxygens:–													
Si	0.014	0.017	0.020	0.013	0.021	0.036	0.015	0.013	0.023	0.009	0.017	0.014	0.009
Al	0.000	0.013	0.009	0.003	0.005	0.013	0.011	0.000	0.006	0.005	0.009	0.014	0.000
Ti	1.981	1.882	2.001	1.990	1.940	1.990	2.003	1.978	2.004	1.983	1.963	1.854	1.894
Fe	1.930	2.088	1.863	1.922	2.017	1.731	1.793	1.868	1.809	1.923	1.931	2.132	2.109
Mn	0.041	0.024	0.051	0.046	0.028	0.118	0.107	0.095	0.080	0.066	0.060	0.072	0.71
Mg	0.027	9.064	0.029	0.021	0.011	0.006	0.016	0.028	0.015	0.015	0.029	0.023	0.008
Ca	0.002	0.001	0.000	0.000	0.008	0.042	0.008	0.005	0.005	0.005	0.006	0.012	9.002

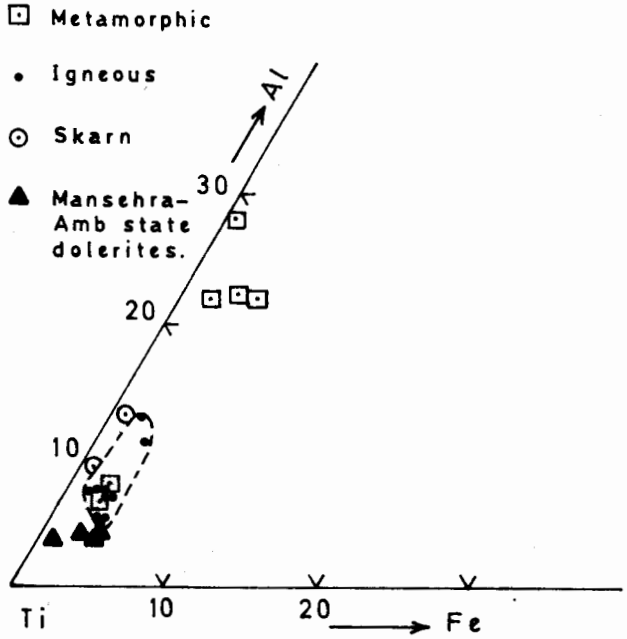

Fig.6. Atomic proportions of Al, Ti, Fe^{3+} of sphene in dolerites; and their comparison with igneous, metamorphic and skarn sphenes, after Tulloch (1979).

Table 12. Pyrite analyses from sample no. 6022

	1	2	3	4
S	53.82	53.82	53.59	53.49
Fe	47.49	46.41	46.78	47.13
Atomic percents:				
S	66.38	66.89	66.62	66.41
Fe	33.62	33.11	33.38	33.59

its formation.

OPAQUE MINERALS

Ilmenite and magnetite are the most abundant opaque minerals. Ilmenite is the principal Fe-Ti oxide mineral. Rarely titanomagnetite is seen which often displays low temperature oxidation. Titanomagnetite and ilmenite are both present in the olivine dolerite sample (ZD1) besides pyrite and chalcopyrite. Titanomagnetite being oxidized, could not be used for geothermometry. Its TiO_2 content is about 19 to 20% and Al_2O_3 is about 2 to 2.5%. Ilmenite analyses are set out in table 11. Pyrite cores are often found mantled by magnetite. Chalcopyrite may also be present. The composition of pyrite is nearly stoichiometric and shows very small variation. Pyrite from one dolerite sample was analyzed; and its Fe and S contents are given in table 12. The same pyrite grains were also analyzed for Ni, Co, Cu and Mn, but all yielded values either zero or below the detection level of analytical conditions.

DISCUSSION

Tholeiitic nature of the dolerites was indicated by the previous work on these dolerites (Shams & Ahmed, 1968). The present microanalytical work shows strong variations within most of the constituent mineral phases.

Even the most magnesian olivines and pyroxenes are considerably Fe-enriched and the most calcic plagioclase crystals are more sodic, when compared to primary tholeiites. It is probable that the magma might have either undergone extensive fractionation before emplacement, or, it had a much Fe and Na rich source. Some contamination of the magma during flow through the crustal rocks can't be ruled out, although such contamination would be restricted due to rapid crystallization at dyke walls.

The country rocks around the dolerites do not include mafic, ultramafic or even intermediate igneous rocks. Their granitic country rocks do not seem to be related to the dolerites. It seems that dolerites crystallized from their own discrete body of parent basaltic magma. The metamorphism affecting the dolerites was of low grade and of variable intensity. Many samples are unmetamorphosed; in many others the original igneous textures are intact inspite of metamorphic changes. Amphibole compositions (fig. 3), presence of epidote, and hydrogrossular, absence of almandine garnet and albite; all indicate low metamorphic intensity.

Hydrogrossular is often a product of Ca-metasomation and mostly occurs in rodingites (Deer et al., 1982) and may indicate temperatures below 420° C at kbar. The amount of hydrogrossular in these dolerites is very small, and the rodingites are not present. Other Ca-rich minerals present in these dolerites include epidote, sphene and clacite. All these are present in minor amounts only in some of the samples. All these Ca-rich minerals are found only in the dolerites in which pyroxene has disappeared. These minerals may have formed after the disappearance of clinopyroxene, retaining its Ca content.

All the dolerite samples contain plagioclase which varies from over 70% to about 17% in anorthite content. Albite is not present in any sample; and probably indicates low metamorphic grade of the dykes which might have been metamorphosed.

CONCLUSIONS

The doleritic dykes that occur cross-cutting the granitic rocks and the pelitic metamorphic country rocks of Mansehra-Amb-State area are mainly of tholeiitic character, although olivine-bearing dolerites also occur. Strong variations in chemistry of their plagioclase, biopyriboles, and other minerals are recorded and may imply a complex petrogenetic evolution of these rocks, by variously combined effects of crystal fractionation and other types of magmatic differentation, metamorphism, alteration, and assimilation. Amphibole compositions indicate low-

grade rather than medium-grade metamorphism. Olivine compositions are relatively fayalite richer. Variations in pyroxene compositions are large in some samples, not so in others.

ACKNOWLEDGEMENTS

The author wishes to thank Drs. J.V.P. Long and Peter J. Treloar for extending the microprobe facilities available at the Department of Earth Sciences, University of Cambridge, England.

REFERENCES

DEER, W. A., HOWIE, R.A. & ZUSSMAN, J. (1962) ROCK—FORMING MINERALS: Volume 3. Longmans, London, 270 p.

——(1962) ROCK—FORMING MINERALS: Volume 1A: Orthosilicates; Second Edition. Longman Group Limited, London, 919 p.

HYNES, A. (1982) A comparison of amphiboles from medium and low-pressure metabasites. Cont. Min. Pet. 81, pp. 119-25.

LEAKE, B.E., (1978) Nomenclautre of amphiboles. Min. Mag. 42, pp. 533 - 63.

SCHREURS, J. (1985) Prograde metamorphism of metapelites, garnet-biotite thermometry and prograde changes of biotite chemistry in high-grade rocks of West Uusimas, southern Finland. Lithos 18, pp. 69 - 80.

SHAMS, F.A. & AHMED, Z. (1968) Petrology of the basic minor intrusives of the Mansehra-Amb State area, northern West Pakistan. Part-I - The dolerites. Geol. Bull Punjab University 7, pp. 45 - 56.

STATHAM, P. J. (1976) A comparative study of techniques for quantitative analysis of x-ray spectra obtained with a Si (Li) detector. X-ray Spectrom. 5, pp. 16 - 28.

SWEATMAN, T.R. & LONG, J.V.P. (1969) Quantitative electron-probe microanalysis of rock-forming minerals. Jour. Pet. 10, pp. 332 - 79.

TULLOCH, A. J., (1979) Secondary Ca-Al silicates as low-grade alteration products of granitoid biotite. Cont. Min. Pet. 69, pp. 105 - 17.

ACTA MINERALOGICA PAKISTANICA
VOLUME 1(1985) pp. 116-117

SHORT COMMUNICATIONS

PETROLOGY OF THE NIAT GAH PART OF THE THAK VALLEY IGNEOUS COMPLEX, GILGIT AGENCY, PAKISTAN.

ZULFIQAR AHMED

Centre of Excellence in Mineralogy, Quetta, Pakistan.

Rocks of the "dioritic group" of the Thak Valley igneous complex (Shams, 1975) have been shown to be exposed throughout in the Niat Valley, which joins the Thak Valley near Jal, Diamir District. The lower part of Niat Gah is shown to be composed of tectonic "veined metadiorites", with widespread intrusions of acid veins, layers, and dykes. These are succeeded southwards by granodioritic to diorite rocks outcropping throughout the rest of Niat Gah and having very wide lateral and vertical extensions. (Shams, 1975, fig. 1). The geological mapping by the author on the 1 inch to a mile scale (fig. 1) shows that the dioritic rocks exposed in the Thak Gah diminish abruptly eastward in the Niat Gah, probably due to some faulting. Southward from the southern contact of "veined metadiorites", in the Niat Gah, the rock succession is as follows:–

a) At contact with the "veined diorite", a thin outcrop (fig. 1) of foliated diorite is present.

b) Southward, the foliated meta-diorite with interbeds of black graphitic schist, each 15 metres across, are present.

c) Further southwards a wide outcrop of black graphitic schists is present.

d) A similar thickness of light-coloured calcareous schists with interbedded chlorite gneisses is exposed.

e) Further south, black graphitic schists with some interbeds of chlorite schists is exposed.

Rocks mentioned under c,d, and e above belong to the Pre-Cambrian Salkhala Series, and resemble lithologically to the Salkhala rocks exposed in the Babusar area (Ahmed and Chaudhry, 1976). These have a narrow contact zone (b in the above sequence) with the foliated dioritic rocks to their north and belonging to the Thak Igneous Complex.

The geological map of Niat Gah is not compatible with previously reported (Shams 1975) great thickness of dioritic rocks with strong east-west extensions. Probably some fault zone exists in the north-south ridges making the eastern flank of Thak Gah. This may account for the absence of dioritic rocks in the Niat Gah.

REFERENCES

AHMED, ZULFIQAR & CHAUDHRY, M.N. (1976) Geology of Babusar Area, Diamir District, Gilgit, Pakistan. Geol. Bull. Punjab Univ. 12, pp. 67-78.

SHAMS, F.A. (1975) The Petrology of the Thak Valley Igneous Complex, Gilgit Agency, Northern Pakistan. Acad. Nazionale Linc. Ser. VIII. 59 (5), pp. 453-464.

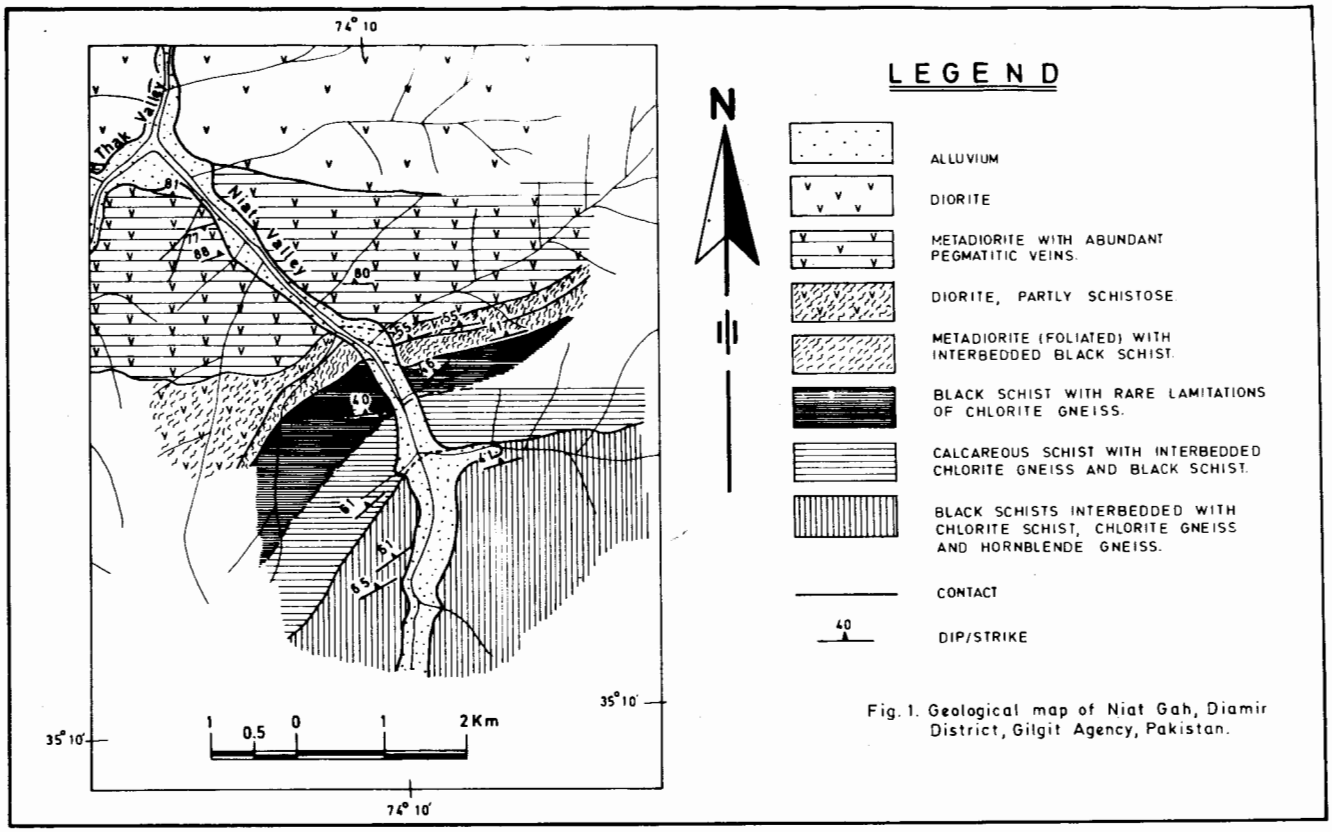

Fig. 1. Geological map of Niat Gah, Diamir District, Gilgit Agency, Pakistan.

ACTA MINERALOGICA PAKISTANICA
VOLUME (1985) p. 118

BASIC PEGMATITE FROM NEAR CHILAS, DIAMIR DISTRICT, PAKISTAN.

ZULFIQAR AHMED
Centre of Excellence in Mineralogy, Quetta, Pakistan.

An ultramafic-mafic igneous complex is exposed near Chilas in Gilgit Agency, at the junction of Thak Valley with the Indus valley, and was named as Thak Valley Igneous Complex by Shams (1975). Further upstream along the right bank of the Indus Valley, Desio (1974) mentions the occurrence of a norite composed of a well-twinned labradiorite, hypersthene and some pyrite. Shams (1975) recognized the following rock units making his "noritic group" norite, olivine corona gabbro, hornblende gabbro, hypersthene diorite, anorthosite, dunite, peridotite, pyroxenite and hornblendite.

Within the rocks of noritic or gabbroic compositions, their coarser grained pegmatitic varieties are sporadically developed. These pegmatites are composed mainly of feldspar (70-80%), which is partly a plagioclase (An_{32}) showing poorly developed twinning; and a greenish brown, strongly pleochroic hornblende. Anhedral magnetite also occurs, but there is no pyrite as reported from the associated noritic rocks by Desio (1974). By alteration, some biotite is produced from hornblende, and sericite or epidote from plagioclase. The chemical and modal analyses of one sample gave the following results:–

Weight percentages

SiO_2	50.92	MnO	0.22
TiO_2	1.13	P_2O_5	0.15
Al_2O_3	20.70	Na_2O	4.50
CaO	10.44	K_2O	0.30
MgO	3.24	H_2O^+	1.73
Fe_2O_3	3.81	H_2O^-	0.16
FeO	3.01	Total	100.28

C.I.P.W.Norm

Q	0.12	Sal/Fem	= 3.35
or	1.67	Q/F	= 0.0016
ab	37.73	Alk/CaO	= 0.59
an	35.31	K_2O/Na_2O	= 0.041
di	12.45		
hy	2.18		
mt	5.55		
il	2.13		
Σ	97.14		

The plots in the FeO - MgO - ($Na_2O + K_2O$) and CaO - Na_2O - K_2O triangular diagrams show that the pegmatite falls in the overall area delineated by Shams (1975, fig. 1). It shows that these pegmatites crystallized simultaneously with the enclosing noritic rocks, from the same parent melt.

However, its plagioclase composition (An_{32}) is considerably sodic than that reported from noritic mass (An_{46-50}) by Shams (op. cit.) The chemical analysis of a similar rock from near Singal in Thak Valley (Shams, op. cit.), gives a little higher SiO_2, FeO, Na_2O and K_2O and lower CaO, MgO and H_2O^+ contents. The ab in the norm is similar in both the rocks.

REFERENCES

DESIO, A. (1974) Geological reconnaissance in the middle Indus Valley between Chilas and Besham Qila (Pakistan). Boll. Soc. Geol. Ital. **93**, pp. 345-68.

SHAMS, F.A. (1975) The Petrology of the Thak Valley Igneous Complex, Gilgit Agency, Northern Pakistan. Acad, Nazionale d. Lincei, Serie VIII, **59(5)**, pp. 453-64.

ACTA MINERALOGICA PAKISTANICA
VOLUME 1(1985) pp. 119-120

BOOK REVIEW

GRANITES OF HIMALAYAS, KARAKORUM AND HINDU KUSH By F.A. SHAMS (EDITOR) Institute of Geology, Punjab University, Lahore, Pakistan (1983) xxv+427 p. Price Rs. 400.00 or US$ 50.00.

This is a well-produced volume dedicated to Professor Ardito Desio in recognition of his pioneering researches in these mountain ranges, particularly the Karakorum Range. It is a befitting publication to commemorate the centenary celebrations of the University of the Punjab–the oldest seat of higher education in Pakistan. Professor Shams' long experience of working with the granitic rocks of Himalayas has obviously played an important role in the planning and publication of this truely international volume. These are 24 papers full of valuable data contributed by 32 scientists from nine different countries.

The papers deal with field aspects, petrography, and geochemistry of granitic rocks, their age and stratigraphic position, origin and evolution in the light of current plate tectonic models related to the Himalaya, Karakorum and Hindu Kush Ranges. Such a broad spectrum of data is expected to be of value not only to those interested in the three ranges, but also to those working on granites elsewhere. A brief account of the contents of the book is serially described in this review.

Following a background of the knowledge on Himalayan granite till seventies (N.E. Odell, pp. 1-10), Sharma (pp. 11-37) describes nine liner granitic belts in the Himalayas. These span about 2000 m.y. but those actually related to the Himalayan orogeny are confined only to the Indus suture zone and the Vaikrita thrust sheet of Higher Himalaya. Valdiya (pp. 39-53) discusses these in relation to four tectonically distinct and stratigraphically diverse settings.

In the light of geochemical data, Rao (pp. 55-74) considers the pre- and syn-tectonic granitic rocks of the Himalayas as metasomatic and the post-tectonic granites as the product of anatexis. A similar geochemical approach has been followed by Shams (pp. 75-121) in his exhaustive review of the granitoids of Pakistan Himalayas. Ashraf (pp. 123-141) describes the acid minor bodies of Mansehra in detail. Complexes of the Peshawar Plain Alkaline Igneous Province are reviewed by Kempe (pp. 143-169) who regards them to have originated from a quartz trachyte magma produced in a rift zone due to rebound relief tension or compression release following collision. With the help of geochemical data, Chaudhry and Shams (pp. 171-181) postulate that the Shahbazgarhi porphyries of the alkaline province were emplaced in a zone that underwent alternate episodes of tension and compression. Fernandez (pp. 183-199) records that the Mansehra granites show collision-related increasing deformation towards the Indus suture to the north.

Kumar et al. (pp. 201-216) review the radiometric ages of the western Kumaon and eastern Ladakh granitoids in the light of structural-stratigraphic data on the 2300 m.y. emplacement history of these rocks. Powar (pp. 217-234) presents petrographic and geochemical data on the sheet-like bodies of granites in the central crystalline zone of eastern Kumaon. He postulates them to be S-type crustal anatexites that were emplaced in three distinct phases.

In an important paper, Le Fort et al. (pp. 235-255) regard the Simchal plutons of central Nepal Himalayas as belonging to a lower Palaeozoic belt of granite plutons extending for 1600 km

along the Lesser Himalaya and beyond in Afghanistan. They might represent a thermal corridor originating from crustal strike-slip faulting. This zone might also be a thinned crust with simultaneous arching, giving rise to magma generation from the heated base. They also hypothesize that this event had occurred in the Gondwana crust at a very large scale, extending even to Australia.

Bartolomi et al. (pp. 257-270) describe the basement-derived Early Cambrian granites and post-metamorphic tourmaline granites occurring south of Mt. Everest. The problem of reverse metamorphism in metapelites from Kumaon and Nepal is tackled by Maruo and Kizaki (pp. 271-286).

There are three papers on granite-related mineralization in the Himalayas. Mitchel et al. (pp. 287-297), in a S-N section across Central Himalayas, discuss the mineral potential of granitic rocks in relation to their tectonic settings. Shams (pp. 299-307) proposes a plate tectonic model for the Himalayas and the prospects for uranium mineralization, and Butt (pp. 309-326) presents detailed data on Pb-Zn-Mo and U mineralization associated with Lahor (Kohistan) granites and pegmatites.

Thakur (pp. 327-339) analyzes the structural framework, tectonics and geochronological data on the granites of eastern Kumaon and western Himalaya. The pre-Himalayan granitic activity is related to three magmatic phases in the Indian craton. He suggests the involvement of the Indo-Pak crustal plate in the Himalayan orogen. The Ladakh batholith is considered to be a product of the melting together of oceanic crust and sediments and the Karakorum batholith only of the sediments. Sharma (pp. 341-354) arrives at a more or less similar conclusion regarding the Ladakh and Karakorum batholiths. The former is thought to be derived from melting of the subducted oceanic crust and the latter from melting of a continental crust. Jan and Asif (pp. 355-376) describe the geochemistry of quartz-diorites and tonalites of the Ladakh-Kohistan plutonic belt in Swat Kohistan and consider them as the products of independent pulses of magma produced either by the partial melting of subducted oceanic crust or obducted upper mantle wedge. Some of the younger granites of Kohistan, according to their model, are the product of crustal anatexis. Le Fort et al. (pp. 377-387) date the emplacement age of the Karakorum batholith at 95 ± 6^4 m.y. and trace out the emplacement and tectonic history. The geodynamics of the region are restored during Cretaceous on the basis of similarity of these granitoids with those of eastern Hindukush and central Afghanistan. Using deep seismic soundings and gravity profiles, the Late Marussi (pp. 389-392) proposes that the S-N oriented Nanga Parbat-Haramosh massif is related to the E-W extending Karakorum and might represent a large diapir structure.

Sheng and Wei (pp. 393-406) suggest that granite plutonism in Gangdesi and Nyainqentanglha mountains in Xizang, China, took place in three episodes. These episodes can be related to compressive events transformed from an active island arc (150-100 m.y. b.p) through an active continental margin (90-50 m.y) to, finally, into a young orogen (40-10 m.y). All granitoids belong to two series, an intermediate-acidic I-type and an acidic S-type arising from anatexis in different levels of the crust. Debon et al. (pp. 407-423) present the geochemistry of the Badakhshan plutonic belt in western Hindukush, Afghanistan. The 17 plutons they studied are light-and dark-coloured, typically cafemic and calc-alkaline magmatic association similar to those in volcanic arcs and involving some continental crust during Late Hercynian-Early Kimmerian.

As can be judged, the volume offers something for every geologist. This useful collection of papers by leading experts covers 427 pages and contains dozens of figures, tables, and a coloured geological map of Nepal. In a world gripped by inflation, this book is modestly priced at Rs. 400 (50 US$). The general get-up, printing and binding are of good quality and Professor Shams has done an excellent job as editor. It is a valuable source of reference and is highly recommended for libraries, researchers and advanced students of petrology.

Dr. R.A. Khan Tahirkheli
Vice Chancellor,
University of Peshawar,
Peshawar, Pakistan.

ANNUAL REPORT OF THE CENTRE OF EXCELLENCE IN MINERALOGY, QUETTA (1985)

STAFF AND STUDENTS

ACADEMIC STAFF

	Date of joining C.E.M.
Professor and Director	
ZULFIQAR AHMED Ph.D. (London), P.D.M.P. (Austria), M.Sc. & B.Sc. Hons. (Punjab).	25.8.1984
Asistant Professor	
MOHAMMAD MUMTAZUDDIN M.Sc. (McGill), B.Sc. (Aligarh).	1.04.1974
Lecturer	
MOHAMMAD MUNIR M.Sc. (Baluchistan)	1.10.1976
JAWED AHMED M.Sc. (Karachi).	1.04.1980
Research officer	
QAISER MAHMOOD M.Sc. (Punjab).	2.08.1985
Visiting professor	
DUANE M. MOORE Ph.D. (Illinois).	1.09.1984 to 1.07.1985

GENERAL STAFF.

Accounts Officer	
MIRZA MANZOOR AHMED B.Com. (Karachi).	7.05.1980
Administrative Officer	
S. SHAHABUDDIN M.Sc. (Baluchistan).	21.05.1977
Technician	
KHUSHNOOD AHMED SIDDIQUI Dipl. Assoc. Engr. (Hyderabad).	13.07.1976
Photographer	
HUSSAINUD DIN	16.06.1981
Assistant Librarian	
ABDUL GHAFOOR M.L.S. (Bluchistan).	2.05.1985
Draftsman	
AHMED KHAN MANGI B.A. (Sind) Cert. Drawing	1.07.1981
Steno-typist	
GHALIB SHAHEEN	17.07.1985
Assistant (Office)	
LAL MOHAMMAD DURRANI	12.05.1973

Store Keeper	
MUSA KHAN	20.80.1977
Senior Clerk	
MOHAMMAD ANWAR	18.09.1973
Junior Clerk	
GHULAM QASIM	3.10.1983
Cashier-cum-Clerk	
JUMA KHAN	11.06.1985
Laboratory Assistant	
SHER HASSAN	22.08.1977
Rock Cutter	
FAREED KHAN	8.04.1985
Junior Mechanic	
ABDUL QADIR	21.08.1977
Driver	
ALI MOHAMMAD	17.07.1984
Loader	
RAWAT KHAN	2.07.1977
Laboratory Attendants	
GHULAM RASOOL	20.08.1977
MEHRAB KHAN	21.08.1977
Peons (Naib Qasid)	
SIKANDAR KHAN	30.04.1976
MOHAMMAD RAFIQ	12.10.1978
Cleaner	
NAZIR MASIH	1.04.1977

POST GRADUATE STUDENTS

M. PHIL. CANDIDATES (SESSION 1983-85).

Abdul Salam, M.Sc.
Mohammad Munir, M.Sc.
Wazir Khan, M.Sc.

(SESSION 1984—86)

Abdul Tawab, M.Sc.
Hussan Khan Kharoti, M.Sc.
Joozer Marzban, M.Sc.
Hassan Shaheed, M.Sc.
Shamim Ahmed Siddiqui, M.Sc
Jawed Ahmed, M.Sc.

(SESSION 1985—87)

Abdul Waheed Tareen
Muhammad Ahmed Farooqui.
Masood Iqbal.*
Muhammad Arshad Rashid.*
Nazarul Islam.*
Ferozeud Din.*
Zubair Butt.
Qaiser Mahmood.
Mehrab Khan.
Khalid Mahmood.
Rehanul Haque.*

*Registration not confirmed.

ACADEMIC ACTIVITIES

In May, 1985, a week long intensive study and practicals workshop on "X-ray analysis and identification of clay minerals" was organized and conducted by the Fulbright Professor at the Centre, Duane M. Moore, of the Knox College, Illinois, USA. Geological Survey of Pakistan, (G.S.P.) Quetta, provided part of their laboratory facilities to the thirty participating geologists.

A special lecture on the "Mesozoic Stratigraphy of Baluchistan" was delivered on 29th September, 1985, at the Centre, by Dr. A.N. Fatmi of G.S.P.

The Centre started work on many new research projects while continuing further work on projects started in 1984. This issue contains part of the results. The Centre was able to make modest start on clay minerals research by starting work on the clay minerals associated with the coal bearing Ghazij (Shale) Formation of lower Eocene age. Duane M. Moore guided the work of Jawed Ahmed in this field. Three of the Ghazij Formation sections exposed at Mangi Kach, Sor Range-Degari, and Mardan-Nala were measured and sampled in 1985. X-ray diffraction and differential thermal analyses were done on samples. The project is to continue in 1986 through sampling of one another section, and completion of XRD and DTA work. One aim is the identification of a startigraphic horizon of potential value in coal exploration. The work on the Pakistan Science Foundation sponsored research project entitled "Geology and mineralogy of selected Pakistani ophiolites" was begun by field mapping and sampling of a section of the Bela ophiolite which is the biggest ophiolite of Pakistan, and least understood so far. The field work located many mining locations for metallurgical grade chromite and magnesite. Bela ophiolite is the most complete ophiolite of Pakistan in terms of its stratigraphic sequence which includes tectonite harzburgite with minor dunite bodies and chromitite; dunitic and wehrlitic cumulates, with segregated chromite bodies; pyroxenite forming a mapable horizon, in addition to rarely found satellitic pyroxenite dykes; widespread gabbro outcrops, dolerite dyke swarms in addition to the sheeted dyke complex; a zone rich in rodingite dykes, granophyric concentrates reaching the composition of typical granite; pillow lavas and chert horizons. It is hoped that the samples collected will yield significant information. A review article on the Pakistani ophiolites and related mineral deposits was prepared, and contributed to IGCP, 197.

Mapping on 1:10,000 scale of the south western extremity of the Zhob Valley ophiolite exposed in the Kach-Khanozai area was begun by Zulfiqar Ahmed and Mohammad Munir. The mapping revealed new outcrops of mafic, volcanic and pyroclastic rocks. Gabbro contains accessory chromite and is considered a part of the Zhob Valley ophiolitic sequence.

Shamim Ahmed Siddiqui under guidance of Zulfiqar Ahmed carried out field work in January, 1985, in the Gunga and Shekran areas of Khuzdar District. The plan includes understanding the genesis and controls of mineralization of zinc-lead-iron sulphides and barite deposits found in the region. Samples have been collected from different outcrops of gossan and associated zinc-lead bearing horizons.

Abdul Tawab and Hassan Khan Kharoti have carried out field mapping of a small part of Khuzdar-Nal road section where ophiolitic rocks including gabbro, dunite, serpentinite, mélange occur in a structurally complicated manner. Petrographic work is to continue in 1986.

Qaiser Mahmood and Zubair Butt mapped on 1:10,000 scale another portion of the ophiolitic rocks dominated by rodingite dykes and a sheeted dyke complex, which outcrops south of Wadh in Khuzdar District. Their work concerns mainly with the attitudes of dykes.

1985 PAPERS OF REGIONAL INTEREST FROM OTHER JOURNALS

TECTONICS VOL. 4 No. 1 (January, 1985)

COOLING HISTORY OF THE NW HIMALAYA, PAKISTAN.

BY PETER K. ZEITLER pp. 127 to 151.

GEOLOGICAL SOCIETY OF AMERICA BULLETIN VOL. (April 1985)

THE MAGNETOSTRATIGRAPHY, FISSION–TRACK DATING, AND STRATIGRAPHIC EVOLUTION OF THE PESHAWAR INTERMONTANE BASIN, NORTHERN PAKISTAN.

BY DOUGLAS W. BURBANK & R.A. KHAN THAIRKHELI pp. 539 to 552.

GEOLOGY VOL. 13, No. 6 (June, 1985)

THRUST TECTONICS AND THE DEEP STRUCTURE OF THE PAKISTAN HAMALAYA.

BY M.P. COWARD & R.W.H. BUTLER pp. 417 to 420.

GEOLOGY VOL. 13, No. 7 (July, 1985)

LARGE SCALE SEDIMENT UNDERPLATING IN THE MAKRAN ACCRETIONARY PRISM, SOUTHWEST PAKISTAN.

BY J.P. PLATT, J.K. LEGGET, J. YOUNG, HILAL RAZA & S. ALAM pp. 507 to 511.

ECONOMIC GEOLOGY VOL. 80 (1985)

THE WAZIRISTAN OPHIOLITE, PAKISTAN: GENERAL GEOLOGY AND CHEMISTRY OF CHROMITE AND ASSOCIATED PHASES.

BY M. QASIM JAN, BRIAN F. WINDLEY & ASHRAF KHAN pp. 294 to 306.

ANNOUNCEMENT

Articles are invited for Volume 2 of the ACTA MINERALOGICA PAKISTANICA which will include a thematic set of articles on the geology of Saindak region, Pakistan, and porphyry copper deposits. For inclusion, the manuscripts may reach the Editor before 30th September, 1986.

INFORMATION FOR AUTHORS

ACTA MINERALOGICA PAKISTANICA publishes annually the results of original scientific research in the multi-faceted field of mineral sciences, covering mineralogy, petrology, crystallography, geochemistry, economic geology, isotope minerlogy, petrography, petrogenesis, mineral chemistry and related disciplines. Review articles and short notes are also considered for publication.

Authors of the articles submitted for publication in ACTA MINERALOGICA PAKISTANICA should send two complete copies of the manuscript, typed double-spaced on one side of the paper only. Copies of tables should be in final format. As far as possible, tables and figures should be prepared for reduction to the single column size or to the page size (204mmX278mm). Use of mineral symbols by Kretz (The American Mineralogist, 1983, Volume 68, pp. 277–279) is recommended for superscripts, subscripts, equations, figures and tables.

Only articles not previously published and not about to be published, wholly or in part, in either Pakistani or foreign journals, are considered for publication. Publication is subject to the discretion of the Editor. Accepted papers become copyright of the Centre of Excellence in Mineralogy, Quetta. Authors alone are responsible for the accuracy of the contents and views expressed in their respective papers. Fifty off-prints of each published paper will be sent to authors free of charge. Additional copies may be ordered just after receiving the acceptance letter from the Editor. Manuscripts should be sent to: Acta Mineralogica Pakistanica C/O Centre of Excellence in Mineralogy, University of Baluchistan, Sariab Road, Quetta, Pakistan.

ACTA MINERALOGICA PAKISTANICA VOLUME 1, 1985.

CONTENTS